

MECHANOSENSITIVE AND FcγRIIa-
MEDIATED PLATELET CALCIUM
ENTRY MECHANISMS

Thesis submitted for the degree of
Doctor of Philosophy
at the
University of Leicester

by
Zeki Ilkan BSc MRes

Department of Molecular and Cell Biology
University of Leicester

2017

Abstract

Mechanosensitive and FcγRIIa-mediated Platelet Calcium Entry Mechanisms

Zeki Ilkan

Elevation of intracellular Ca^{2+} ($[\text{Ca}^{2+}]_i$) is essential for platelet function. Despite the established role of shear stress in haemostasis and thrombosis, the possible contribution of mechanosensitive (MS) Ca^{2+} -permeable ion channels to platelet activation remains unknown. One well-established Ca^{2+} -permeable ion channel which enhances platelet responses at high shear is the ATP-gated P2X1 channel. The relative contribution of this channel to platelet function was studied following the activation of the FcγRIIa immune receptor.

qRT-PCR and Western blotting revealed that human platelets and a megakaryocytic cell line, Meg-01, express the MS cation channel Piezo1. To investigate Ca^{2+} -permeable MS channel activity, single platelets and Meg-01 cells were loaded with the Ca^{2+} indicator Fluo-3, and exposed to arterial shear in flow chambers which induced increases in $[\text{Ca}^{2+}]_i$ in both cell types in physiological salines. The MS channel blocker GsMTx-4 inhibited these responses and reduced thrombus formation over collagen, whereas Piezo1 channel agonist Yoda1 potentiated platelet shear-induced Ca^{2+} transients. In Fura-2-loaded platelet suspensions, the GsMTx-4-sensitive shear-evoked responses were shown to be independent of P2X1, Orai1 and TRPC6.

FcγRIIa-mediated $[\text{Ca}^{2+}]_i$ elevations and aggregation were monitored using ratiometric $[\text{Ca}^{2+}]_i$ measurements and light transmission, respectively. The contribution of P2X1 channels was assessed following inhibition by NF449, and inactivation by pre-addition of α,β -meATP or apyrase exclusion. These treatments significantly reduced antibody- or bacteria-induced FcγRIIa-mediated responses, indicating a significant P2X1 channel contribution. Phosphorylation assays indicated that P2X1 amplifies FcγRIIa-mediated responses via direct Ca^{2+} influx, rather than via a feedforward effect on early tyrosine phosphorylation.

In conclusion, this thesis provides evidence that platelets express functional MS Piezo1 channels which can provide a direct route for Ca^{2+} entry under normal and pathological arterial shear, and contribute to thrombus formation. Additionally, P2X1 channels were shown to amplify FcγRIIa-mediated platelet Ca^{2+} signalling and aggregation, which can contribute to platelet activation under shear in infective endocarditis.

Publications and presentations arising from this thesis

Publications

- Ilkan Z, Wright JR, Francescut L, Goodall AH, Mahaut-Smith MP (2015) Thrombus Formation Under Flow is Inhibited by the Mechanosensitive Cation Channel Blockers GsMTx-4 peptide and Gadolinium Chloride. *Circulation*, 132: A11593 [Abstract]
- Ilkan Z, Wright JR, Goodall AH, Gibbins JM, Jones CI, Mahaut-Smith MP (2017) Evidence for shear-mediated Ca²⁺ entry through mechanosensitive cation channels in human platelets and a megakaryocytic cell line. *J Biol Chem* [Under review].
- Ilkan Z, Watson S, Watson SP, Mahaut-Smith MP. Role for P2X1 channels in FcγRIIa induced Ca²⁺ entry in human platelets [Manuscript in preparation].

Oral communications

- Ilkan Z, Wright JR, Francescut L, Goodall AH, Mahaut-Smith MP (2015) Thrombus Formation Under Flow is Inhibited by the Mechanosensitive Cation Channel Blockers GsMTx-4 peptide and Gadolinium Chloride. **American Heart Association Scientific Sessions; Orlando, Florida, USA (November 2015).**
- Ilkan Z, Francescut L, Watson S, Watson SP, Mahaut-Smith MP (2016) Role for P2X1 receptors in FcγRIIa induced Ca²⁺ entry in human platelets. **Joint British Society for Haemostasis & Thrombosis (BSHT), Anticoagulation in Practice (AiP) and UK Platelet Group meeting; Leeds, United Kingdom (November 2016).**

Poster communications

- Ilkan Z, Wright JR, Goodall AH, Gibbins JM, Jones CI, Mahaut-Smith MP (2016) Role for the mechanosensitive ion channel Piezo1 in human platelet shear-dependent calcium entry and thrombus formation. **3rd European Platelet Network (EUPLAN) Conference; Bad Homburg vor der Höhe, Germany (September 2016).**
- Ilkan Z, Watson S, Watson SP, Mahaut-Smith MP. Role for P2X1 receptors in FcγRIIa induced calcium entry in human platelets. **Joint British Society for Haemostasis & Thrombosis (BSHT), Anticoagulation in Practice (AiP) and UK Platelet Group meeting; Leeds, United Kingdom (November 2016).**

Travel grants and other awards

- British Society for Haemostasis & Thrombosis (BSHT) Scientist in Training Award (August 2016).
- British Pharmacological Society (BPS) Travel Bursary (November 2015).
- ATVB Travel Award for Young Investigators (Council on Atherosclerosis, Thrombosis and Vascular Biology) – American Heart Association (September 2015).
- 2015 Leicester-Nara Research Exchange Scholarship – NWU, Japan (February 2015).

Acknowledgements

First of all, I would like to express my sincerest gratitude to my supervisor Prof Martyn P. Mahaut-Smith for recognising my passion for scientific research and the field of cardiovascular research by recruiting me to his laboratory as a PhD student. His support, patience and guidance were immense throughout the entire duration of my project, and I am very thankful to him for all the advice he provided both on a daily basis and generally in support of my development as a proactive and creative scientist. I also would like to extend special thanks to my co-supervisor Prof Alison H. Goodall for overseeing my progress and providing expert advice whenever possible.

I acknowledge Medical Research Council (UK) for awarding me a Doctoral Training Grant which covered the costs of my research activities and provided living allowance. Many thanks also to American Heart Association (AHA) and British Pharmacological Society (BPS) for the generous ATVB Travel Award for Young Investigators and the BPS Travel Grant to support my participation at the AHA Scientific Sessions in Orlando, Florida, USA in November 2015.

I would like to thank very much Dr Joy R. Wright for helping me get started with my project, academic advice and technical help. I express my deep gratitude to Dr Lorenza Francescut for providing excellent technical help and support in multiple aspects of my project, and for the maintenance and smooth running of our laboratory. Special thanks also go to my colleagues Dr Sangar Osman, Ms Tayyaba Iftikhar and Ms Chelsea Morgan for their support and company, and the members of our department Prof Richard J. Evans, Dr John S. Mitcheson and Dr Catherine Vial, Dr Elena Dubinina and Mr Tom Richards. I am thankful to Prof Jon M. Gibbins and Dr Chris I. Jones (Reading) for their advice on single platelet attachment for calcium imaging, and Prof Steve P. Watson (Birmingham) and his group members, Stef, Alex and Chiara, for establishing a fruitful collaboration with me. I owe many thanks to a long list of volunteers who donated their platelets to help me answer many scientific questions, which allowed me to expand the boundaries of what we know about human platelet physiology and their contribution to cardiovascular disease.

Last but not least, I would like to express my warmest regards and affection to my parents, grandparents and sister, who always encouraged me and demonstrated extraordinary support, patience and love throughout my studies. This work would not have been accomplished without their constant reassurance and support.

Dedication

This thesis is dedicated to my late grandfather M. Zeki Beyaz, whose name and ambitious soul I carry. He always appreciated my enthusiasm and has been a true source of inspiration throughout my studies. He will always be greatly remembered.

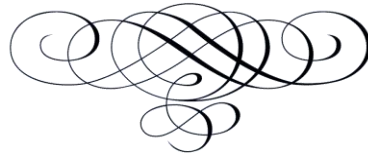


Table of Contents

| | |
|--|-----|
| Abstract..... | i |
| Publications and presentations arising from this thesis | ii |
| Acknowledgements..... | iii |
| Table of Contents..... | v |
| List of Tables | ix |
| List of Figures..... | x |
| Abbreviations..... | xiv |
| Chapter 1 Introduction..... | 1 |
| 1.1 Platelets: Historical perspective and background | 1 |
| 1.2 Haemostasis and the role of platelets in cardiovascular disease | 2 |
| 1.3 Calcium signalling in platelets | 7 |
| 1.4 Rheology, shear stress and platelet function | 10 |
| 1.5 Platelet ion channels and their potential role as therapeutic targets..... | 15 |
| 1.6 Mechanosensitive ion channels: recent advances | 17 |
| 1.7 Immune function of platelets and the unique role of P2X1 channels | 21 |
| 1.8 Aims and Objectives | 24 |
| Chapter 2 Materials and Methods..... | 27 |
| 2.1 Salines and materials..... | 27 |
| 2.1.1 Salines..... | 27 |
| 2.1.2 Materials | 28 |
| 2.2 Cell culture and attachment..... | 29 |
| 2.2.1 Meg-01 and HUVECs | 29 |
| 2.2.2 Bacterial culture..... | 29 |
| 2.3 Phlebotomy and washed platelet preparation..... | 31 |
| 2.3.1 Phlebotomy..... | 31 |

| | |
|---|----|
| 2.3.2 Preparation of washed platelets and Meg-01 cells for dye loading..... | 31 |
| 2.4 Fluorescence imaging..... | 32 |
| 2.5 Thrombus formation under flow | 32 |
| 2.6 Intracellular Ca ²⁺ imaging in Meg-01 cells under flow..... | 33 |
| 2.7 Intracellular Ca ²⁺ imaging in Meg-01 cells mechanically stimulated with a glass probe..... | 33 |
| 2.8 Imaging of Ca ²⁺ transients in single platelets under flow | 35 |
| 2.9 In vitro light transmission aggregometry and ATP secretion assay..... | 36 |
| 2.9.1 In vitro light transmission aggregometry | 36 |
| 2.9.2 ATP secretion assay | 37 |
| 2.10 Fura-2 ratiometric Ca ²⁺ measurements | 39 |
| 2.10.1 Fluorescence measurements | 39 |
| 2.10.2 Fura-2 dye calibration..... | 39 |
| 2.10.3 Data processing | 40 |
| 2.11 Quantitative real-time polymerase chain reaction (qRT-PCR)..... | 41 |
| 2.11.1 mRNA extraction..... | 41 |
| 2.11.2 Reverse transcription and qRT-PCR | 42 |
| 2.11.3 Agarose gel electrophoresis..... | 43 |
| 2.12 Western blot analysis and phosphorylation assay..... | 44 |
| 2.12.1 Cell lysate preparation | 44 |
| 2.12.2 Bradford Assay | 45 |
| 2.12.3 SDS-PAGE and Western blotting | 46 |
| 2.13 Sample preparation for Sanger sequencing..... | 48 |
| 2.14 Data analysis and statistics..... | 48 |
| Chapter 3 Identification of mechanosensitive ion channels in platelets and Meg-01 cell line and a biophysical study of their contribution to function | 50 |
| 3.1 Introduction | 50 |
| 3.2 Results..... | 52 |

| | |
|--|-----|
| 3.2.1 Human platelets and Meg-01 cells express Piezo1 mRNA and protein..... | 52 |
| 3.2.2 Meg-01 cells attached on poly-D-lysine-coated surfaces are suitable for Ca ²⁺ imaging under arterial flow | 56 |
| 3.2.3 Meg-01 cells display GsMTx-4-sensitive fluid shear stress-dependent [Ca ²⁺] _i increases | 60 |
| 3.2.4 HUVECs display GsMTx-4-sensitive fluid shear stress-dependent [Ca ²⁺] _i increases | 64 |
| 3.2.5 Hypotonic challenge does not induce observable [Ca ²⁺] _i increases in platelets and Meg-01 cells | 67 |
| 3.2.6 Meg-01 cells display [Ca ²⁺] _i increases in response to mechanical stimulation with a glass probe | 69 |
| 3.2.7 The Piezo1 agonist Yoda1 induces increases in [Ca ²⁺] _i in Meg-01 cell suspensions | 71 |
| 3.3 Discussion | 73 |
| Chapter 4 Evidence for a contribution of mechanosensitive Piezo1 channel activity to human platelet shear-dependent calcium entry and thrombus formation | 77 |
| 4.1 Introduction | 77 |
| 4.2 Results | 79 |
| 4.2.1 Evidence for Piezo1 channel activity in single platelets under arterial shear stress | 79 |
| 4.2.2 Mechanosensitive Ca ²⁺ events in platelets are independent of purinergic GPCR stimulation..... | 88 |
| 4.2.3 Effect of GsMTx-4 on previously identified Ca ²⁺ entry pathways of human platelets..... | 95 |
| 4.2.4 Collagen-induced thrombus formation but not platelet aggregation is inhibited by GsMTx-4 | 99 |
| 4.2.5 GsMTx-4 inhibits thrombus formation by blocking P2X1 as well as mechanosensitive cation channels | 102 |
| 4.3 Discussion | 104 |

| | |
|--|-----|
| Chapter 5 Role for P2X1 channels in FcγRIIa-induced calcium entry and functional responses in human platelets..... | 108 |
| 5.1 Introduction | 108 |
| 5.2 Results | 110 |
| 5.2.1 FcγRIIa receptor activation induces Ca ²⁺ entry through P2X1 channels | 110 |
| 5.2.2 P2X1 channel desensitisation inhibits Ca ²⁺ entry induced by a range of concentrations of the cross-linker IgG F(ab') ₂ antibody | 115 |
| 5.2.3 FcγRIIa-mediated Ca ²⁺ responses are partially resistant to apyrase and NO, but are abolished by PGI ₂ | 118 |
| 5.2.4 Antibody or bacteria-induced FcγRIIa activation causes ATP secretion, and platelet aggregation responses which are partially inhibited by P2X1 desensitisation | 122 |
| 5.2.5 FcγRIIa receptor stimulation by antibody cross-linking induces P2X1-independent tyrosine phosphorylation events | 124 |
| 5.2.6 Thrombus formation under normal arterial shear stress over <i>Streptococcus sanguinis</i> is independent of P2X1 channel activity | 126 |
| 5.3 Discussion | 129 |
| Chapter 6 General discussion and future work | 133 |
| 6.1 Recapitulation of main findings | 133 |
| 6.2 Physiological and clinical implications..... | 136 |
| 6.2.1 Potential roles for Piezo1 in haemostasis and thrombosis..... | 136 |
| 6.2.2 Novel role for P2X1 in platelet immune responses..... | 138 |
| 6.3 Limitations and future directions | 139 |
| 6.4 Conclusions | 142 |
| Bibliography | 144 |

List of Tables

| | |
|--|----|
| Table 2.1 The flow rates used in Vena8 TM biochips (Cellix) and parallel-plate flow chambers, and their corresponding calculated shear rates used in shear stress assays. ... | 35 |
| Table 2.2 A list of QuantiTect pre-designed primers (Qiagen) used to detect mRNA expression in platelets and Meg-01 cells. | 43 |
| Table 2.3 The antibodies used in protein detection and phosphorylation assays. | 47 |
| Table 2.4 The forward (F) and reverse (R) primers designed to target Piezo1 and Piezo2 channels in Meg-01 cells for Sanger sequencing..... | 49 |
| Table 3.1 Various coating materials used to attach Meg-01 cells and the qualitative observations made in cell morphology and strength of cell attachment under arterial shear stress. | 57 |

List of Figures

| | |
|--|----|
| Figure 1.1 Platelet size and ultrastructure..... | 2 |
| Figure 1.2 A simplified illustration of primary haemostasis showing platelet activation and aggregation in response to endothelial damage. | 4 |
| Figure 1.3 Calcium cycling and signalling in platelets..... | 8 |
| Figure 1.4 Virchow's triad and local haemodynamic changes at an atherosclerotic plaque..... | 12 |
| Figure 1.5 Shear stress profiles in vitro and in vivo. | 13 |
| Figure 1.6 Representations of the Piezo1 and P2X1 structures..... | 20 |
| Figure 1.7 FcγRIIa signalling following receptor clustering in human platelets..... | 22 |
| Figure 2.1 Representative growth curve for the bacterial strain <i>S. sanguinis</i> 133-79. ... | 30 |
| Figure 2.2 Cartoon representations of the flow systems used in thrombus formation and shear stress assays..... | 34 |
| Figure 2.3 A cartoon representation of single platelet attachment to anti-PECAM-1 antibody coated biochip surface via the Ig domains 1 and 2 of the platelet PECAM-1 for the imaging of Ca ²⁺ transients under shear stress. | 36 |
| Figure 2.4 Representative luminescence traces obtained by ATP addition to saline, and a concentration-response standard curve. | 38 |
| Figure 2.5 Representative primer efficiency curve for Piezo1 QuantiTect primer pair. | 44 |
| Figure 2.6 A representative Bradford assay standard curve of absorbance at 595nm against a series of known bovine serum albumin (BSA) concentrations. | 47 |
| Figure 3.1 Most commonly used methods of mechanical stimulation in the studies of Piezo channel function..... | 51 |
| Figure 3.2 Mechanosensitive ion channel mRNA expression in human platelets and the Meg-01 cell line. | 53 |
| Figure 3.3 PCR amplification products obtained using in-house designed primer pairs of known sequence, and the sequence alignment following Sanger sequencing..... | 54 |
| Figure 3.4 Western blots for Piezo1 and Piezo2 in Meg-01 and human platelet lysates. | 55 |
| Figure 3.5 Representative bright field images of Meg-01 cells attached on various coating materials. | 58 |
| Figure 3.6 Monitor of Ca ²⁺ mobilisation in attached Meg-01 cells..... | 59 |

| | |
|---|----|
| Figure 3.7 Fluid shear stress-dependent Ca^{2+} influx in Meg-01 cells is inhibited by GsMTx-4 and chelation of extracellular Ca^{2+} | 61 |
| Figure 3.8 Fluid shear stress-dependent Ca^{2+} influx in Meg-01 cells is inhibited by GsMTx-4 and chelation of extracellular Ca^{2+} | 62 |
| Figure 3.9 Fluid shear stress induces incremental cytosolic Ca^{2+} increases in Meg-01 cells which are inhibited by GsMTx-4 and chelation of extracellular Ca^{2+} | 63 |
| Figure 3.10 Fluid shear stress-dependent Ca^{2+} influx in HUVECs is inhibited by GsMTx-4..... | 65 |
| Figure 3.11 Shear stress induced increases in $[\text{Ca}^{2+}]_i$ in HUVECs are inhibited by GsMTx-4..... | 66 |
| Figure 3.12 Hypotonic challenge does not induce GsMTx-4-sensitive Ca^{2+} influx in Meg-01 or platelet cell suspensions..... | 68 |
| Figure 3.13 Mechanical stimulation of Meg-01 cell with a glass probe results in $[\text{Ca}^{2+}]_i$ elevations. | 70 |
| Figure 3.14 The Piezo1 selective agonist Yoda1 induced $[\text{Ca}^{2+}]_i$ increases in Meg-01 cells. | 72 |
| Figure 4.1 Fluid shear stress induces Ca^{2+} transients in single platelets. | 82 |
| Figure 4.2 Fluid shear stress-induced Ca^{2+} transients in single platelets are inhibited by GsMTx-4 and chelation of extracellular Ca^{2+} | 83 |
| Figure 4.3 Fluid shear stress-induced average Ca^{2+} increases in single platelets are inhibited by GsMTx-4 and chelation of extracellular Ca^{2+} | 84 |
| Figure 4.4 Stenotic levels of shear stress induced relatively more significant average Ca^{2+} increases in single platelets..... | 85 |
| Figure 4.5 The Piezo1 selective agonist Yoda1 induced $[\text{Ca}^{2+}]_i$ increases in washed platelets. | 86 |
| Figure 4.6 The Piezo1 selective agonist Yoda1 induced increases in $[\text{Ca}^{2+}]_i$ in singly attached platelets..... | 87 |
| Figure 4.7 The effect of addition of a series of ADP concentrations on $[\text{Ca}^{2+}]_i$ in washed platelet suspensions..... | 90 |
| Figure 4.8 Stimulation of P2Y1 and P2Y12 receptors with a near-threshold concentration of ADP did not cause an observable change to the Ca^{2+} transient profile in singly attached platelets under shear. | 91 |
| Figure 4.9 Fluid shear stress-induced average Ca^{2+} increases in single platelets remain unchanged by the inclusion of a low concentration of ADP in the extracellular saline. 92 | |

| | |
|---|-----|
| Figure 4.10 Pre-treatment with ADP concentrations higher than 0.1 μ M reduce maximum $[Ca^{2+}]_i$ | 93 |
| Figure 4.11 Monitoring of ADP-induced Ca^{2+} response activity over a period of 100 minutes..... | 94 |
| Figure 4.12 Effect of GsMTx-4 on Ca^{2+} entry via TRPC6, P2X1 and store-operated channels in platelets. | 96 |
| Figure 4.13 P2X1 activity was monitored throughout the experiments where P2X1 responses were measured..... | 97 |
| Figure 4.14 Fura-2-loaded Meg-01 suspensions do not display $[Ca^{2+}]_i$ increases following α,β -meATP treatment..... | 98 |
| Figure 4.15 Collagen-induced thrombus formation is inhibited by GsMTx-4. | 100 |
| Figure 4.16 Collagen-induced platelet aggregation is not inhibited by GsMTx-4. | 101 |
| Figure 4.17 GsMTx-4 inhibits thrombus formation by blocking P2X1 as well as mechanosensitive cation channels. | 103 |
| Figure 5.1 Cross-linked mAb IV.3-evoked Fc γ RIIa receptor activation induces Ca^{2+} entry through P2X1 channels..... | 112 |
| Figure 5.2 Ca^{2+} entry through P2X1 channels can be fully inhibited by the selective antagonist NF449 or by channel desensitization. | 113 |
| Figure 5.3 Fc γ RIIa receptor activation induced by <i>S. sanguinis</i> results in an early P2X1-dependent Ca^{2+} event. | 114 |
| Figure 5.4 P2X1 receptor desensitization inhibits Ca^{2+} entry through P2X1 channels induced by a range of cross-linker IgG F(ab') ₂ antibody concentrations. | 117 |
| Figure 5.5 P2X1-mediated Ca^{2+} responses to Fc γ RIIa receptor activation are resistant to NO and elevated apyrase levels, but are abolished by PGI ₂ | 119 |
| Figure 5.6 Average $\Delta[Ca^{2+}]_i$ responses to Fc γ RIIa receptor activation by cross-linking mAb IV.3, in the presence of endothelium-derived inhibitors. | 120 |
| Figure 5.7 PGI ₂ inhibits ATP secretion induced by Fc γ RIIa receptor activation..... | 120 |
| Figure 5.8 Optimisation of PGI ₂ concentration and preparation conditions..... | 121 |
| Figure 5.9 P2X1 channels contribute to Fc γ RIIa-induced platelet aggregation achieved by <i>S. sanguinis</i> or cross-linking of mAb IV.3 with IgG F(ab') ₂ in washed platelets, accompanied by P2X1-independent dense granule secretion. | 123 |
| Figure 5.10 Fc γ RIIa receptor stimulation by cross-linking of mAb IV.3 induces phosphorylation events downstream of the Fc γ RIIa signalling pathway regardless of P2X1 channel desensitization. | 125 |

Figure 5.11 Inhibition of P2X1 channels with 1 μ M NF449 does not alter thrombus formation on immobilised *S. sanguinis* under normal arterial shear stress conditions (1002.6s⁻¹)..... 127

Abbreviations

| | |
|----------------------------------|---|
| [Ca ²⁺] _i | Intracellular Ca ²⁺ |
| 5-HT | 5-Hydroxytryptamine |
| ACD | Acid-Citrate-Dextrose |
| ADP | Adenosine diphosphate |
| AF | Atrial fibrillation |
| AMPA | α -amino-3-hydroxy-5-methyl-4-isoxazolepropionic acid receptor |
| ANOVA | Analysis of variance |
| ATP | Adenosine triphosphate |
| B.P. | Base pairs |
| BSA | Bovine serum albumin |
| DAG | Diacylglycerol |
| ddH ₂ O | Double-distilled H ₂ O |
| DiOC ₆ | 3,3'-Dihexyloxycarbocyanine iodide |
| DMSO | Dimethyl sulfoxide |
| EGTA | Ethylene glycol-bis(β -aminoethyl ether)-N,N,N',N'- tetraacetic acid |
| EP ₃ | Prostaglandin E ₂ receptor 3 |
| ER | Endoplasmic Reticulum |
| FDA | Food and Drug Administration |
| GAPDH | Glyceraldehyde 3-phosphate dehydrogenase |
| GP | Glycoprotein |
| GPCR | G-protein coupled receptor |
| GsMTx-4 | <i>Grammostola spatulata</i> mechanotoxin-4 |
| HBSS | Hanks' balanced salt solution |
| hIgG | Human immunoglobulin G |
| HUVEC | Human Umbilical Vein Endothelial Cells |

| | |
|------------------|--|
| IE | Infective endocarditis |
| IP ₃ | Inositol triphosphate |
| ITAM | Immunoreceptor tyrosine-based activation motif |
| kDa | Kilodaltons |
| KO | Knockout |
| LAT | Linker for activation of T cells |
| mAb | Monoclonal antibody |
| MPC | Magnetic particle concentrator [®] |
| MS | Mechanosensitive |
| NCBI | National Center for Biotechnology Information |
| NMDA | N-methyl-D-aspartate receptor |
| NO | Nitric Oxide |
| OAG | 1-oleoyl-2-acetyl-sn-glycerol |
| OCS | Open Canalicular System |
| pAb | Polyclonal antibody |
| PAR | Protease-activated receptor |
| PBS | Phosphate-buffered saline |
| PCR | Polymerase chain reaction |
| PECAM-1 | Platelet endothelial cell adhesion molecule |
| PGI ₂ | Prostaglandin I ₂ |
| PKC | Protein kinase C |
| PLC | Phospholipase C |
| PMCA | Plasma membrane Ca ²⁺ ATPase |
| PNACL | Protein Nucleic Acid Chemistry Laboratory |
| RIPA | Radioimmunoprecipitation assay |
| SERCA | Sarco/endoplasmic reticulum Ca ²⁺ -ATPase |
| sNO | Spermine NONOate |

| | |
|------------------|--|
| SOCE | Store-operated Ca ²⁺ entry |
| TG | Thapsigargin |
| TLR2/1 | Toll-like 2/1 receptors |
| TMC1/2 | Transmembrane channel-like protein 1/2 |
| TRPC6 | Transient receptor potential cation channel, subfamily C, member 6 |
| TxA ₂ | Thromboxane A ₂ |
| V _{max} | Maximum velocity |
| vWF | von Willebrand Factor |
| WBC | White blood cell |

Chapter 1

Introduction

1.1 Platelets: Historical perspective and background

Platelets (*or* thrombocytes) were identified and comprehensively studied for the first time by the Italian professor of pathology, Giulio Bizzozero, in the late 19th century. In addition to red blood cells and white blood cells, Bizzozero identified “a constant blood particle... which has been suspected by several authors...”, and named these particles ‘*piastrine*’ (the Italian word for ‘small plates’) (Mazzarello *et al.*, 2001; Bizzozero, 1881). These particles later on became known as ‘platelets’ in English, and are currently described as small, discoid, anucleate blood cells (~2-3µm in diameter) which constantly circulate within the cardiovascular system together with the other cellular components of the blood, the erythrocytes and leukocytes (Figure 1.1 A). Like other blood cells, platelets arise as a result of a process called haematopoiesis within the bone marrow, where haematopoietic stem cells develop into mature blood cells (Fernandez & de Alarcon, 2013). All blood cells arise from common myeloid progenitor cells which, for platelet production, give rise to the platelet precursor cells, megakaryocytes (Fernandez & de Alarcon, 2013; Machlus & Italiano, 2013; Hartwig & Italiano, 2003).

Megakaryocytes, which usually make up <1% of the bone marrow cell population, reside within close proximity to the blood vessels during the process of thrombopoiesis (Nakeff & Maat, 1974). As part of this process, they extend projections into vascular sinusoids, releasing large megakaryocytic fragments called ‘preplatelets’ and ‘proplatelets’ (Machlus & Italiano, 2013). Once in the bloodstream, these extensions of megakaryocytes fragment into barbell-shaped proplatelets which become further cleaved into individual platelets with the aid of blood flow (Machlus & Italiano, 2013; Thon *et al.*, 2012; Junt *et al.*, 2007). This continuous platelet production mechanism ensures constant renewal of circulating platelets which are known to survive in the body for approximately 10 days after production (Davi & Patrono, 2007). The newly formed platelets retain many structural and biochemical features of their precursor cells, however, some differences between the two cell types exist (Pease, 1956). Although platelets do not possess nuclei, they carry residual genetic material in the form of messenger RNA (mRNA) from the megakaryocytes and are able to

synthesise proteins *de novo* (Weyrich *et al.*, 2009). In addition to structures normally exhibited by many other cell types, such as plasma membrane, mitochondria, endoplasmic reticulum (ER), and cytoskeleton, platelets possess additional features such as open canalicular systems (OCS), and alpha (α) granules and delta (δ)/dense granules. The OCS enable the secretion of α and δ -granules during activation, which contain important biochemicals that mediate platelet activation and aggregation, such as coagulation factors, ATP, ADP, serotonin, fibrinogen, von Willebrand Factor (vWF), *etc* (Whiteheart, 2011; Escolar & White, 1991) (Figure 1.1 B, *see* Section 1.2).

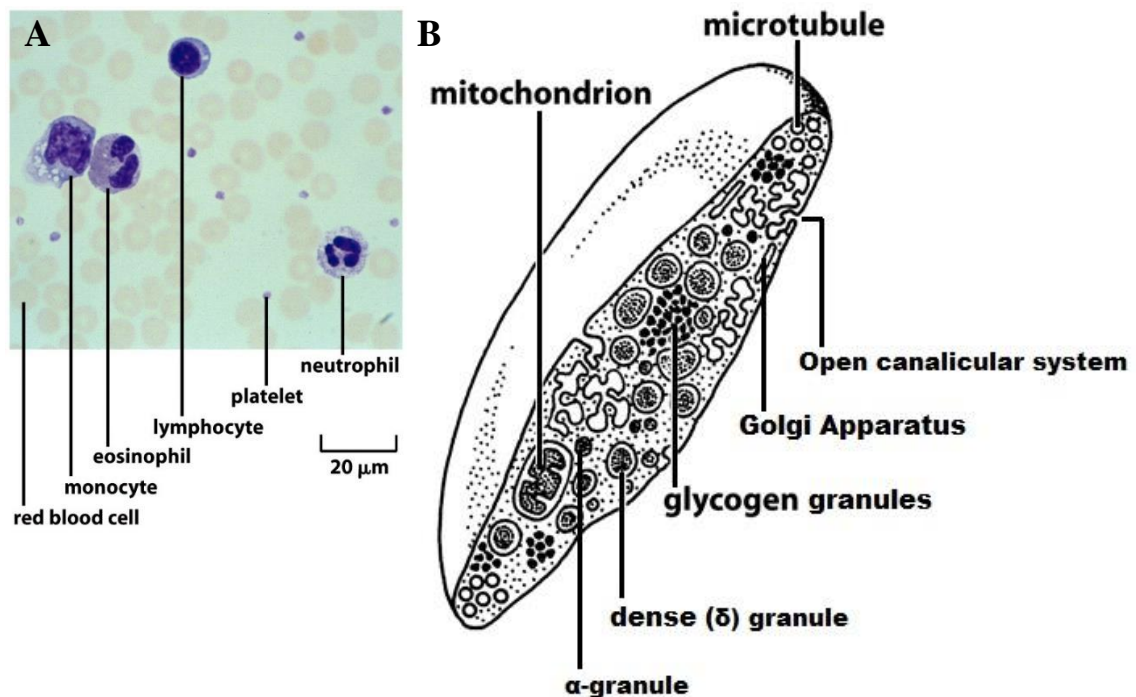


Figure 1.1 Platelet size and ultrastructure. (A) A light micrograph of blood cells showing the small size of platelets in comparison with the other blood cells. (B) A labelled representation of platelet ultrastructure. The open canalicular systems (OCS) provide routes for substance transport in and out of the platelets, and enable α and δ -granule secretion. [Figures were modified from Alberts *et al.* 2009]

1.2 Haemostasis and the role of platelets in cardiovascular disease

The important role of platelets in blood clotting and thrombus formation was discovered for the first time by Bizzozero in guinea pigs, using *in vivo* microscopy techniques (Brewer, 2006; Bizzozero, 1882). Today, platelets are known to play an established vital role in the process of haemostasis, which is an on-going biochemical mechanism that helps maintain the integrity of the vascular system and prevent blood

loss in response to injury through blood clotting (Clemetson, 2012). Under normal conditions, platelets are in their 'resting' or 'inactive' state as they travel within the healthy blood vessels. The right balance between anti-coagulant and pro-coagulant factors such as nitric oxide (NO) and prothrombin is maintained under normal conditions (Wolberg *et al.*, 2012). As a result of tissue damage, the integrity of the endothelial cell layer of the blood vessels becomes disrupted, causing the exposure of the pro-coagulant extracellular matrix components, such as collagen, to the circulation. This initial interaction between the circulating platelets and the injury site initiates the haemostatic response. The process of haemostasis can be divided into primary and secondary phases (Gale, 2011). The initial processes of platelet attachment, activation, aggregation and formation of the haemostatic plug constitute primary haemostasis (Figure 1.2). On the other hand, the stabilisation of the haemostatic plug via the formation of a fibrin mesh through the action of serine proteases and other coagulation factors is collectively known as secondary haemostasis, which is also referred to as the coagulation cascade (Gale, 2011; Andrews & Berndt, 2004).

The first physical interaction between platelets and the injury site under arterial blood flow takes place when vWF binds to and forms a bridge between the exposed collagen strands of the injury site and platelet receptors glycoprotein (GP) Ib (Clemetson, 2012; De Meyer *et al.*, 2009). This interaction slows down travelling platelets and docks them to the injury site (Figure 1.2). vWF is always present in the plasma through constitutive release by endothelial cells, and is also secreted from platelet α -granules upon activation (De Meyer *et al.*, 2009; Ruggeri, 2007). The A3 domain of the vWF binds exposed collagen strands, and the rest of the molecule unfolds by undergoing conformational changes under high shear forces of the circulation to reveal and extend the A1 domain, which recruits platelets by binding to their GPIb α receptors (De Meyer *et al.*, 2009; Lankhof *et al.*, 1996). The binding of specific amino acid residues (GPO: glycine-proline-hydroxyproline) located on exposed sub-endothelial collagen to platelet GPVI receptors also accompanies the initial GPIb-vWF interactions, (Clemetson, 2012; Smethurst *et al.*, 2007). The collagen-GPVI interaction is a key event which commences signalling events leading to platelet activation.

Signalling through GPVI is believed to be supported by the interaction of platelet integrin $\alpha_2\beta_1$ with specific sites on collagen, which brings about the immunoreceptor tyrosine-based activation motif (ITAM)-dependent signalling downstream of GPVI upon collagen binding (Watson & Gibbins, 1998). Activation of

this signalling pathway significantly contributes to shape change and platelet activation through the rearrangement of the cytoskeletal network, α - and δ -granule secretion, and an elevation of the intracellular Ca^{2+} concentration ($[\text{Ca}^{2+}]_i$) (Roberts *et al.*, 2004). Following the initial collagen-mediated events, the next phase of platelet activation is mainly driven by the activation of G-protein coupled receptors (GPCRs) by a number of agonists which include δ -granule releasates such as adenosine diphosphate (ADP), adenosine triphosphate (ATP) and serotonin (5-hydroxytryptamine or 5-HT) (Figure 1.2).

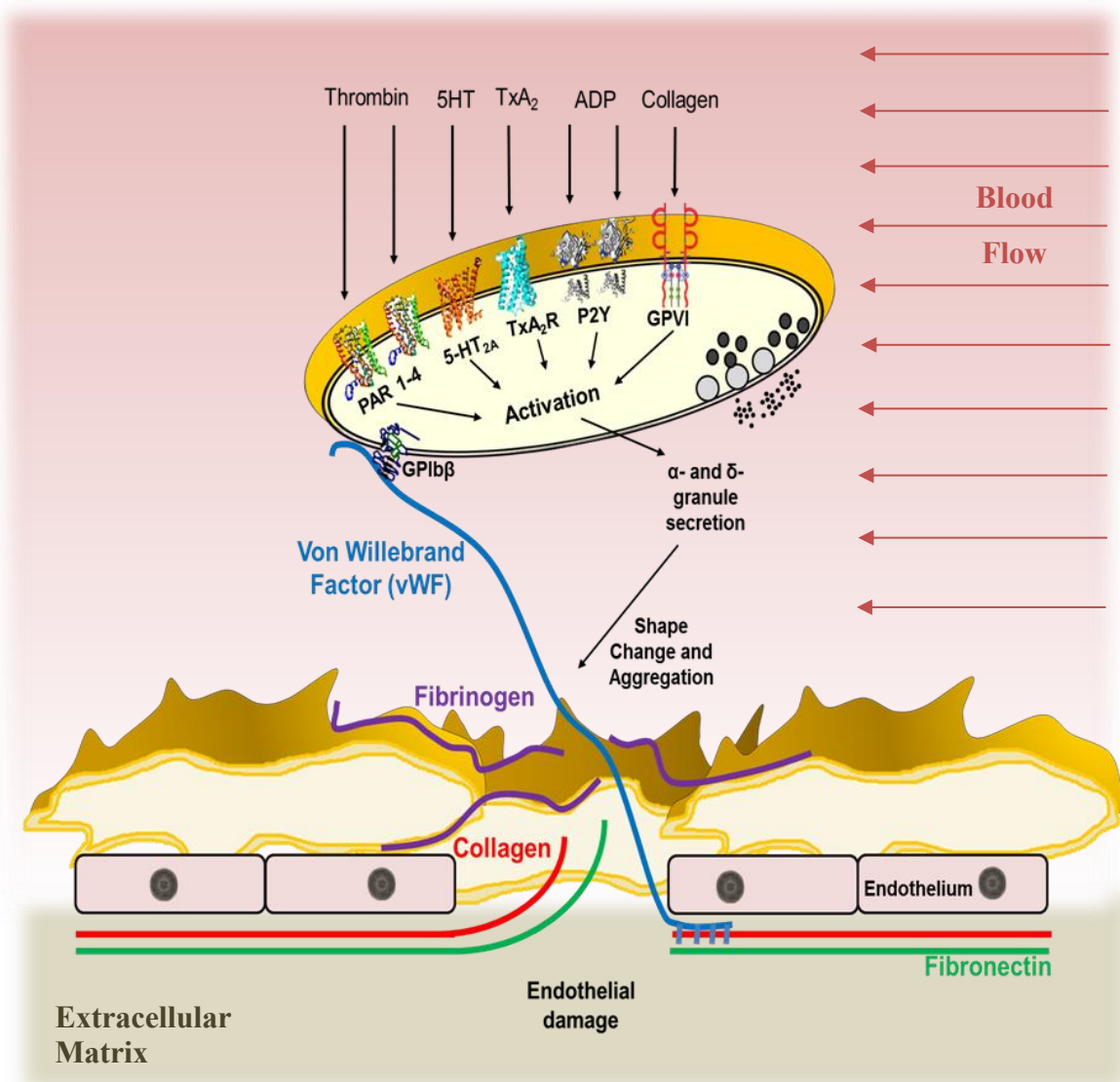


Figure 1.2 A simplified illustration of primary haemostasis showing platelet activation and aggregation in response to endothelial damage. Under blood flow, the initial interaction between platelets and the injury site is mediated by the vWF, which tethers circulating platelets to the injury site by forming a bridge between the platelet GPIb receptor and exposed collagen. This is followed by more stable adhesion by collagen and GPIIb/IIIa interactions which initiate signalling events. This results ...

(...) in the secretion of α - and δ - granules which release thrombin, 5-HT, ADP, and TxA_2 , that act on G-protein coupled receptors (GPCRs) in an autocrine and paracrine manner, resulting in further activation, shape change, and more platelet recruitment to the injury site. Aggregation is mainly mediated by fibrinogen which cross-links the $\alpha_{\text{IIb}}\beta_3$ integrins on different platelets to help form a plug to prevent blood loss from the injury site (secondary haemostasis). Fibronectin interaction provides additional stabilisation for the plug.

Secretion and *de novo* synthesis of the pro-coagulant molecule TxA_2 by cyclooxygenases also takes place which reinforces platelet activation (Hanasaki & Arita, 1988). Another powerful platelet agonist is the serine protease, thrombin, which is produced by the coagulation cascade and links primary and secondary haemostasis (Coughlin, 2000). The cleavage of extracellular N-terminal domains of the protease-activated receptors 1 and 4 (PAR 1-4) by thrombin results in the activation of receptor signalling through intramolecular ligation (Coughlin, 2000; Vu *et al.*, 1991). Signalling through this mechanism contributes to platelet activation through shape change, granule secretion and integrin activation. The agonists secreted throughout the process of primary haemostasis play an important role in stimulating platelets that become incorporated in aggregate formation, through a paracrine mode of action (Oury *et al.*, 2006b). Signalling events following platelet recruitment lead to ‘inside-out’ activation of the integrins $\alpha_{\text{IIb}}\beta_3$ which involve their transition from a low-affinity state to a high-affinity state (Shattil *et al.*, 2010). Activated $\alpha_{\text{IIb}}\beta_3$ can be bound by fibrinogen which mediates platelet aggregation through the cross-linking of $\alpha_{\text{IIb}}\beta_3$ integrins between different platelets, or vWF which help stabilise platelet adhesion (Li *et al.*, 2010). Binding of ligands to activated $\alpha_{\text{IIb}}\beta_3$ integrins results in further signalling events called ‘outside-in’ signalling, which bring about secretion of granules, platelet spreading and clot retraction (Shattil & Newman, 2004).

Thrombin production from prothrombin takes place through a complex series of coagulation cascade reactions initiated with tissue factor (TF) that is expressed on various cells at a vascular injury site (McVey, 2016). The process of coagulation is a series of reactions categorised into ‘extrinsic’ and ‘intrinsic’ pathways, initiated when TF activates another coagulation factor (factor X), resulting in thrombin production and activation of coagulation through a positive feedback mechanism (Palta *et al.*, 2014; Gale, 2011). Thrombin generation is mediated by the formation of the enzyme

complexes, prothrombinase and tenase, on activated platelet membranes (Palta *et al.*, 2014). In addition to its contribution to platelet activation via its action on PARs, thrombin also cleaves fibrinogen into insoluble fibrin, which forms a protective mesh around the haemostatic plaque to increase its strength (Gale, 2011). In healthy individuals, the process of coagulation is tightly regulated by a number of inhibitors which limit the growth of a thrombus. These molecules include the serine protease inhibitor, antithrombin, which binds to and inhibits the coagulation factors thrombin and factor X (Palta *et al.*, 2014; Previtali *et al.*, 2011). Finally, as part of the wound healing process, tightly-controlled fibrinolytic mechanisms dissolve fibrin into fibrin degradation products through the action of several serine proteases (Chapin & Hajjar, 2015). The primary serine protease which dissolves fibrin is plasmin, which is generated from the hepatic zymogen plasminogen, with the aid of ‘tissue plasminogen activator’ and ‘urokinase plasminogen activator’ enzymes (Chapin & Hajjar, 2015; Palta *et al.*, 2014). Similar to coagulation, fibrinolysis is also tightly-regulated by several plasmin or plasminogen inhibitors, such as α 2-antiplasmin, that prevent excessive fibrinolysis (Palta *et al.*, 2014; Cesarman-Maus & Hajjar, 2005).

If the feedback mechanisms which control thrombus formation malfunction, or if the tightly-regulated balance between the production of anti-coagulant and pro-coagulant factors becomes disrupted, haemostasis can become pathological which is termed thrombosis (Clemetson, 2012). In such situations where platelets can activate spontaneously or excessively, they can cause or exacerbate a number of cardiovascular diseases, including myocardial infarction and strokes, through contributing to atherosclerosis or formation of thromboembolisms, respectively. Arterial thrombosis has been established as primarily a platelet-driven disorder, whereas venous thrombosis is known to be caused by stasis and hypercoagulability, and mainly mediated by erythrocytes and fibrin (Previtali *et al.*, 2011; Prandoni, 2009). Therefore, it is generally accepted that platelets play a more prominent role in the development of arterial rather than venous disorders (Previtali *et al.*, 2011). Ischaemic heart disease and stroke remain the top causes of death in the world, and account for 17% of avoidable deaths in the United Kingdom (World Health Organization, 2014; Office for National Statistics, 2013). It has been shown that the pathological mechanism responsible for the majority of ischaemic heart diseases and strokes is arterial thrombosis (ISTH Steering Committee for World Thrombosis Day, 2014).

The roles of platelets in the development of atherosclerosis have been clearly defined. In diseased arteries, platelets recognise the site of an atherosclerotic lesion and form aggregates, facilitating atherothrombotic events (Badimon *et al.*, 2012). This can potentially lead to reduced blood supply to organs such as the heart, resulting in myocardial infarction (Badimon *et al.*, 2012; Ross, 1999). Furthermore, it has been demonstrated in mice that biochemical events associated with platelet activation play a key role in atherosclerotic plaque development (Massberg *et al.*, 2002; Ruggeri, 2002; Pratico *et al.*, 2001; Ross, 1999). Upon the fusion of α -granules with the platelet plasma membrane during activation, the exposure of the adhesive P-selectin proteins on platelets aggregating on atherosclerotic lesions were shown to mediate leukocyte recruitment which exacerbates plaque development (Badimon *et al.*, 2012; Ruggeri, 2002; Ramos *et al.*, 1999).

Formation of dangerous circulating thromboembolisms is usually a result of risk factors such as atrial fibrillation (AF)-related endothelial damage or stasis, or endothelial dysfunction that causes impaired production of endothelium-derived anti-platelet factors such as NO or PGI₂ (Iwasaki *et al.*, 2011; Migliacci *et al.*, 2007). Circulating emboli can travel to vital organs such as the brain, where they can potentially clog the arteries which supply blood to the tissues, giving rise to stroke via ischaemia.

1.3 Calcium signalling in platelets

In many cell types, intracellular Ca²⁺ plays a central role as a second messenger in the regulation of a wide variety of cellular processes; for instance in the heart, calcium-induced calcium release controls cardiomyocyte function (Berridge *et al.*, 2003). An increase in intracellular Ca²⁺ levels ([Ca²⁺]_i) is a pivotal signalling event that is essential for most major functional events during platelet activation which eventually lead to platelet aggregation. Ca²⁺-dependent events include cytoskeletal rearrangements and integrin inside-out signalling, and activation of protein kinase C, calmodulin and Ca²⁺-dependent proteases (Li *et al.*, 2010; Varga-Szabo *et al.*, 2009; Hathaway & Adelstein, 1979). Several studies highlighted the essential role Ca²⁺ signalling plays in the regulation of platelet activation, shape change, and thrombus formation (Gilio *et al.*, 2010; Hartwig, 1992). Furthermore, platelets and megakaryocytes were shown to express the intracellular signalling molecule CalDAG-GEFI, which possesses domains

that bind to Ca^{2+} and DAG, leading to integrin activation, granule secretion and synthesis of TxA_2 (Bergmeier & Stefanini, 2009; Crittenden *et al.*, 2004). Sustained elevations in $[\text{Ca}^{2+}]_i$ also play an important role in reinforcing platelet activation and aggregation by inducing phosphatidylserine (PS) exposure on the plasma membrane, through the stimulation of scramblase activity (Freysinet & Toti, 2010; Ramstrom *et al.*, 2003).

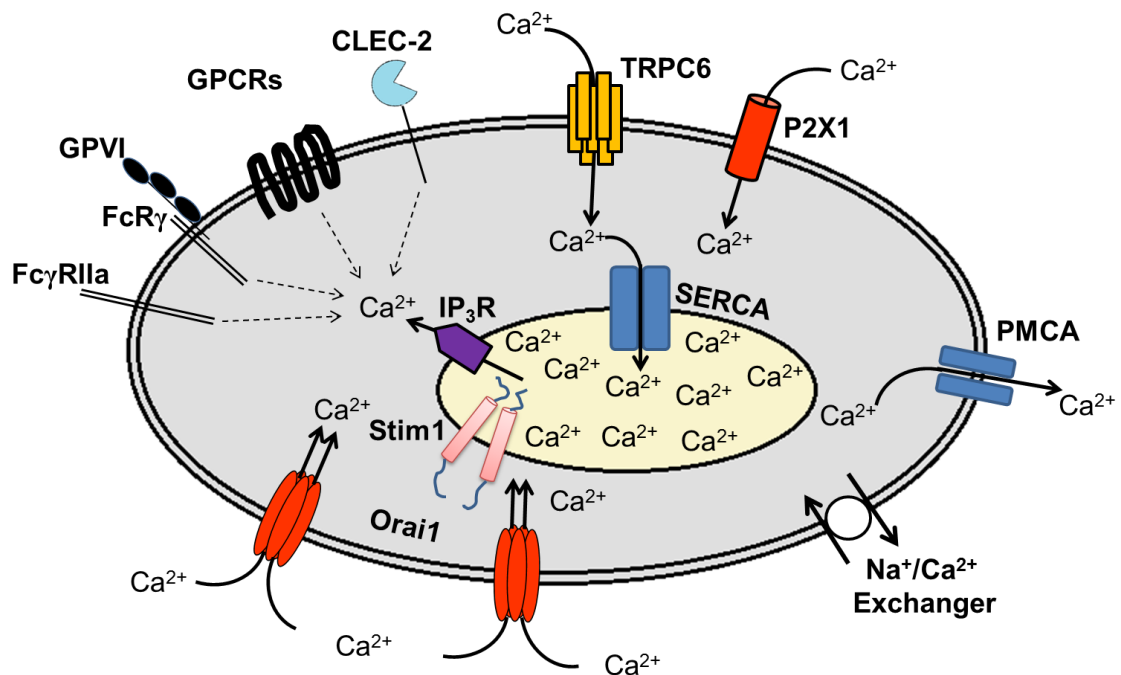


Figure 1.3 Calcium cycling and signalling in platelets. Stimulation of GPCRs, GPVI, and the immune receptors CLEC-2, $\text{FcR}\gamma$ and $\text{Fc}\gamma\text{RIIIa}$ by agonist binding activates intracellular signalling cascades (dashed arrow). These converge to result in the hydrolysis of PIP_2 to release IP_3 and DAG, which are involved in the mobilization of Ca^{2+} from the ER through IP_3R , and activation of PKC and TRPC6, respectively. The reduction of ER Ca^{2+} content is detected by Stim1, which in turn activates Ca^{2+} entry through plasma membrane Orai1 channels (store-operated Ca^{2+} entry/SOCE). The ATP-gated P2X1 channels allow Ca^{2+} entry following extracellular ATP binding. The mechanisms which reduce $[\text{Ca}^{2+}]_i$ include plasma membrane Ca^{2+} ATPases (PMCA) and sarco/endoplasmic reticulum Ca^{2+} ATPases (SERCA) which pump Ca^{2+} outside the platelet and into the ER, respectively (Varga-Szabo *et al.*, 2009). The $\text{Na}^+/\text{Ca}^{2+}$ exchanger can also extrude Ca^{2+} , but following Na^+ entry through P2X1 and TRPC6 can operate in reverse mode and amplify $[\text{Ca}^{2+}]_i$ elevation during activation.

Under both normal and thrombotic conditions, the exposure of negatively charged PS is known to enhance the formation of thrombin from prothrombin, and thus regulate coagulation (Lentz, 2003). There are several pathways via which Ca^{2+} can enter the platelet cytosol. Ca^{2+} can either be released from the intracellular stores (endoplasmic reticulum, ER), also called the dense tubular system, or enter from the extracellular milieu through ion channels (Figure 1.3).

Ca^{2+} entry from the extracellular medium is mediated by a number of receptor- or store- operated ion channels (Mahaut-Smith, 2012; Li *et al.*, 2010; Varga-Szabo *et al.*, 2009) (Figure 1.3). Ca^{2+} entry through Orai1 channels via store-operated Ca^{2+} entry (SOCE) and the purinergic P2X1 channels represent the two major Ca^{2+} entry mechanisms into the platelet from the cell exterior (*see* Sections 1.5 and 1.7 for more information). In addition, it was shown that the transient receptor potential channel 6 (TRPC6) becomes activated by thrombin through the formation of DAG (Hassock *et al.*, 2002). TRPC6 channel activity was revealed to be independent of SOCE and the phosphorylation of cyclic AMP-dependent protein kinases which are known for mediating powerful inhibitory effects in platelets (Smolenski, 2012; Hassock *et al.*, 2002). Interestingly, it has also been demonstrated that Ca^{2+} -entry through TRPC6 channels tends to take place at relatively higher thrombin concentrations, and thus may contribute to platelet function at varying levels depending on the degree of stimulation (Mahaut-Smith, 2012; Harper & Poole, 2011).

The release of Ca^{2+} sequestered in the ER can be achieved by the stimulation of a number of receptors on the plasma membrane by their respective ligands (Li *et al.*, 2010; Varga-Szabo *et al.*, 2009) (Figure 1.3). The stimulation of G_q -coupled receptors such as P2Y1 by ADP, PARs 1 and 4 by thrombin, 5-HT_{2A} by serotonin (5-HT) and TxA₂R by thromboxane (TxA₂) are some of the main events which initiate GPCR-dependent activation of the PLC isoform PLC β (Varga-Szabo *et al.*, 2009). The activation of PLC β by GPCRs, and PLC γ 2 by GPVI, CLEC-2, Fc γ RIIa and integrins such as $\alpha_{\text{IIb}}\beta_{\text{III}}$ are dependent on G_q activation, although the latter PLC isoform can also be regulated by G_i via PI₃K (Varga-Szabo *et al.*, 2009; Suzuki-Inoue *et al.*, 2006; Offermanns, 2006; Blake *et al.*, 1994). Activated PLC isoforms hydrolyse PIP₂ into IP₃ and DAG, whereby the former binds to IP₃R on the ER causing the release of Ca^{2+} from the intracellular stores. The latter mediates SOCE-independent Ca^{2+} entry through the TRPC6 ion channels (Berridge *et al.*, 2003; Hassock *et al.*, 2002). In addition to the main Ca^{2+} store in platelets, the ER, other Ca^{2+} stores such as acidic organelles exist

whose contribution to platelet function is thought to be less important, and have been less thoroughly studied (Mahaut-Smith, 2012; Varga-Szabo *et al.*, 2009).

According to previous studies, the baseline levels of $[Ca^{2+}]_i$ in resting human platelets vary between approximately 50 and 75nM (Vicari *et al.*, 1994). Elevations in $[Ca^{2+}]_i$ as small as ~50nM have been demonstrated to be sufficient to give rise to responses such as shape change associated with platelet activation (Rolf *et al.*, 2001). Therefore, in the circulation it is of extreme importance to maintain stable levels of $[Ca^{2+}]_i$ to prevent unnecessary activation of platelets (Varga-Szabo *et al.*, 2009). For this reason, platelets express ATPases which reduce $[Ca^{2+}]_i$ by removing Ca^{2+} from the cytosol (Figure 1.3). Two main ATPases remove Ca^{2+} from the cytosol: sarco/endoplasmic reticulum Ca^{2+} ATPases (SERCAs) and plasma membrane Ca^{2+} ATPases (PMCAs). The latter remove Ca^{2+} by pumping it to the cell exterior, whereas the former pump Ca^{2+} back into the ER (Enyedi *et al.*, 1986). Furthermore, the plasma membrane Na^+/Ca^{2+} exchanger also contributes to the removal of cytosolic Ca^{2+} when the $[Ca^{2+}]_i$ is high, and thereby also helps prevent unnecessary platelet activation (Valant *et al.*, 1992).

1.4 Rheology, shear stress and platelet function

The vasculature is under constant exposure to mechanical stress due to continuous blood flow throughout the cardiovascular system, originating from the supply of pressure from the heart. As a result of this, blood vessel walls are subject to two main types of haemodynamic forces: cyclical strain and shear stress (Ballermann *et al.*, 1998). Cyclical strain refers to the mechanical forces which act perpendicular to vessel walls, causing changes in the circumference of the vessels due to either expansion or contraction of the diameter of the lumen, and thus is responsible for blood pressure (Traub & Berk, 1998; Kroll *et al.*, 1996). This is made possible by tensile stress, which can stretch the endothelial lining of the vessels and influence vascular pathophysiology (Gimbrone *et al.*, 1999; Kroll *et al.*, 1996). On the other hand, shear stress is a force exerted in the direction of blood flow, acting parallel to the apical surface of the endothelial cells (Ballermann *et al.*, 1998; Kroll *et al.*, 1996). Circulating blood flows in infinite numbers of parallel layers known as ‘laminae’, each of which

flow with varying velocities and thus create frictional forces between the layers as they slide past each other (Figure 1.5 B) (Bird *et al.*, 2002). Maximum velocity (V_{\max}) is reached towards the centre of the vessel lumen, which represents the region of minimum shear stress, whereas minimum velocity is observed closer to the vessel walls where maximal shear stress is detected (Kroll *et al.*, 1996). Owing to their small size, platelets tend to travel closer to the vessel walls due to collisions with erythrocytes, and therefore experience maximal shear stress in the circulation (Uijttewaal *et al.*, 1993; Tangelder *et al.*, 1985). Shear stress is defined as “the force per unit area between laminae”, and is the most important environmental factor in platelet function and thrombosis (Bird *et al.*, 2002; Kroll *et al.*, 1996).

The crucial role of shear stress in haemostasis and thrombosis is well-established, and was first reported in the 19th century by Rudolf Virchow (Kumar *et al.*, 2010). Virchow’s Triad explains the vital role of haemodynamic variations in blood flow (rheology), endothelial damage and hypercoagulability (due to variations in blood composition) as the main thrombotic risk factors (Wolberg *et al.*, 2012) (Figure 1.4 A). Of importance, arterial thrombosis is associated with increased shear stress levels at regions of vessel narrowing (stenosis), such as at the sites of atherosclerotic plaque development. In such cases, platelet-rich occlusive thrombi can form following plaque rupture at the distal end of the plaque, where local elevations in shear stress are observed (Wolberg *et al.*, 2012; Bark & Ku, 2010) (Figure 1.4 B).

There are a number of differences between shear stress generated within standard *in vitro* model systems and those experienced by blood cells *in vivo*. Traditionally, *in vitro* shear stress apparatus are designed to apply uniform shear stress patterns, both spatially and temporally, by the application of a continuous flow (White & Frangos, 2007). The laminar flow pattern achieved by such *in vitro* approaches is termed ‘mean positive shear stress’ (White & Frangos, 2007). Nevertheless, arterial shear stress *in vivo* is both pulsatile due to the nature of cardiac function, resulting in temporal shear stress gradients, and at some regions is spatially non-uniform mainly because of the existence of anatomical features such as bifurcations (Ku *et al.*, 1985) (Figure 1.5 A and C). Despite this, at regions other than such bifurcations or stenosis, blood flow remains uniform and one-directional, similar to that achieved using an *in vitro* apparatus (White & Frangos, 2007). Fluid flow through blood vessels can be described by Poiseuille’s Law (Papaioannou & Stefanadis, 2005; Bird *et al.*, 2002). Assuming that blood flow through an inelastic cylindrical conduit is laminar, and that

blood is a Newtonian fluid (i.e. its viscosity is unaffected by shear stress), shear stress is directly proportional to flow rate, but inversely proportional to vessel diameter (Papaioannou & Stefanadis, 2005).

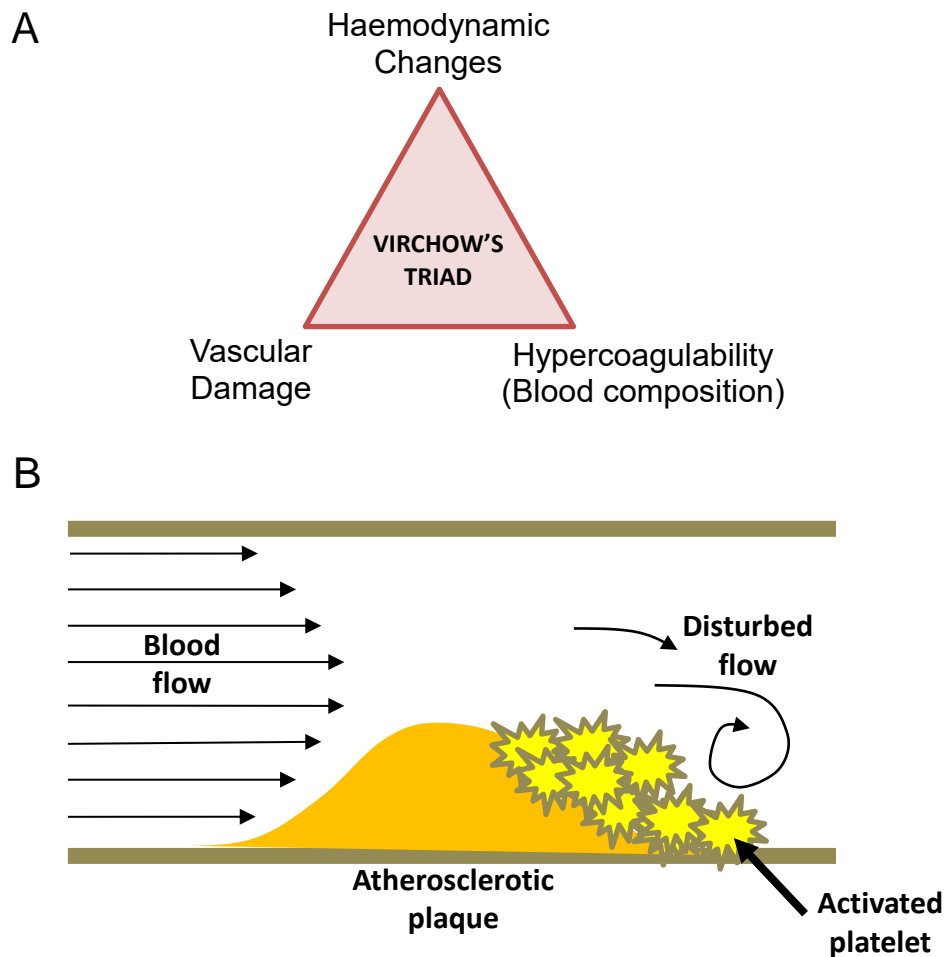


Figure 1.4 Virchow's triad and local haemodynamic changes at an atherosclerotic plaque. (A) The three main thrombotic risk factors. Abnormalities in blood flow alter the normal laminar flow and associated levels of shear in the arteries. (B) Arterial thrombosis may be associated with thrombus formation at the distal end of an atherosclerotic plaque, where pathologically high levels of shear stress ($3000\text{-}250000\text{s}^{-1}$) are experienced due to severe stenosis (Bark & Ku, 2010; Shih-Hsin & McIntire, 1998).

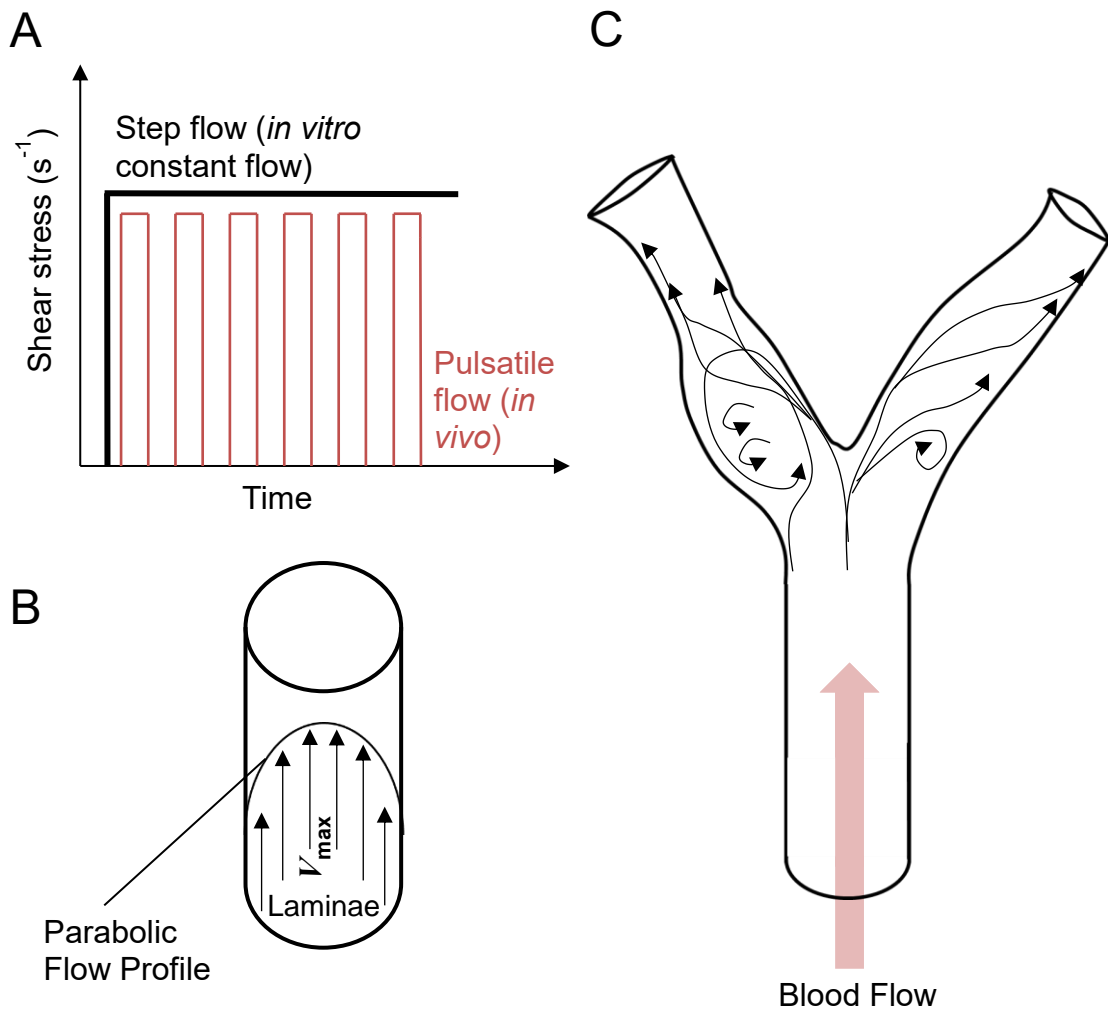


Figure 1.5 Shear stress profiles in vitro and in vivo. (a) Elements which make up continuous shear stress in traditional in vitro flow chambers (step flow), and in vivo (pulsatile), both of which result in the exposure of same levels of shear stress with different temporal flow profiles. (b) A representation of blood laminae which flow at maximal velocity (V_{max}) as the lumen of the vessel is approached during uniform flow in vivo and in vitro. (c) Variations in blood flow, and hence shear stress, at the regions of anatomical bifurcations, causing departures from 'mean positive shear stress' observed at the regions of uniform blood flow. [Re-created from (Ku et al., 1985)].

In the circulation, shear stress on platelets exerted by laminar blood flow is regarded as a vital environmental factor leading to platelet activation in both normal and pathological situations. For example, shear stress is required at the early stages of the haemostatic machinery where it unfolds von Willebrand Factor (vWF) to reveal its binding domains to Glycoprotein Ib (GPIb) and thus allow attachment to collagen exposed at an injury site (Schneider *et al.*, 2007; Siedlecki *et al.*, 1996) (*see* Section 1.2). Since the 1970s, many studies have demonstrated that increased pathological levels of shear stress and abnormal flow patterns such as recirculation at the sites of vessel bifurcations can directly induce platelet activation (known as shear-induced platelet activation), and hence aggregation and thrombus formation (Raz *et al.*, 2007; Einav & Bluestein, 2004; Bluestein *et al.*, 1999; Bluestein *et al.*, 1997; Holme *et al.*, 1997; O'Brien, 1990; Stein & Sabbah, 1974). Although no previous report has provided a clear molecular or physiological mechanism behind the effects observed under shear, the presence of a Ca²⁺ entry pathway has been suggested in earlier studies (Chow *et al.*, 1992; Levenson *et al.*, 1990). Using an approach to monitor [Ca²⁺]_i within a cone-and-plate viscometer, Kroll and colleagues demonstrated a transmembrane Ca²⁺ influx in response to arterial or higher levels of shear (Chow *et al.*, 1992). In addition, Simon and co-workers report a link between transmembrane Ca²⁺ flux and hemodynamic shear stress from studies of hypertensive patients (Levenson *et al.*, 1990). However, the physiological events underlying the stimulatory effects of shear stress on platelets, especially Ca²⁺ mobilisation, remain unclear.

1.5 Platelet ion channels and their potential role as therapeutic targets

Ion channels are indispensable for the functioning of all cell types. The plasma membrane is a barrier between the cytoplasm and the extracellular space, thereby maintaining an isolated environment within the cell. ATP-driven pumps establish a concentration gradient for a number of ions such as Na^+ , K^+ and Ca^{2+} across the plasma membrane, in addition to a potential difference due to selective permeability to these ions (Aidley & Stanfield, 1996). For instance, at rest most cells (including platelets) have a high K^+ permeability and therefore a resting potential nearer the K^+ equilibrium potential (-90mV) than that of other ions. With the aid of ion channels and these electrochemical gradients, cells can control ionic fluxes across the cell membrane which can modify a number of molecular and physiological processes.

Several types of ion channels contribute significantly to the processes of haemostasis and thrombosis, and hence can play a determining role in the development of a wide range of platelet-related disorders (Mahaut-Smith, 2012; Smyth *et al.*, 2009). Perhaps, the most important group of ion channels studied hitherto in platelets are those which mediate Ca^{2+} mobilisation in response to various types of stimuli. As discussed in more detail in Section 1.3, there are various well-known Ca^{2+} entry mechanisms into the platelet, amongst which P2X1 channels, which operate by ATP binding, represent the fastest and the only Ca^{2+} entry mechanism following ATP release from a vascular injury site (Mahaut-Smith, 2012; Mahaut-Smith *et al.*, 2011; Born & Kratzer, 1984) (*see* Section 1.7 for some examples of detailed roles). Other Ca^{2+} -impermeable ionotropic receptor types operate in platelets, such as NMDA, AMPA and kainate receptors which have been reported to contribute to platelet function to varying degrees, and increase the risk of thrombosis in patients with a history of stroke (Sun *et al.*, 2009; Morrell *et al.*, 2008; Franconi *et al.*, 1996). In addition to Ca^{2+} -permeable ion channels and ionotropic receptors, several studies have demonstrated emerging roles for voltage-gated and Ca^{2+} -activated K^+ channels in platelets (Schmidt *et al.*, 2011; McCloskey *et al.*, 2010; Wolfs *et al.*, 2006; Mahaut-Smith *et al.*, 1990). Furthermore, there is evidence for the involvement of gap junction channels such as connexins and the related transmembrane protein pannexin-1 in enhancement of platelet activation, thrombosis, and thus represent novel therapeutic targets (Molica *et al.*, 2015; Vaiyapuri *et al.*, 2015; Taylor *et al.*, 2014; Vaiyapuri *et al.*, 2012).

Ion channels attracted considerable attention as targets for novel therapies for decades (Bagal *et al.*, 2013) due to their critical role in cellular physiology and the regulation of a broad spectrum of biological processes including muscle contraction, sensory transduction, and generation of action potentials in neurons. An increasing number of diseases related to mutations in ion channel genes (channelopathies) are also being studied in various fields. It has been shown that about 13.4% of known FDA-approved drugs to date target ion channels, which make them the second largest class of therapeutic targets after GPCRs (Overington *et al.*, 2006). Well-known examples include Verapamil and Diltiazem which block L-type Ca^{2+} channels for the treatment of cardiac arrhythmias, angina pectoris and hypertension (Clare, 2010). Current anti-platelet therapies do not target any ion channels, although there is an increasing awareness that platelet ion channels, especially those which mediate Ca^{2+} mobilisation, could be potential therapeutic targets. Development of novel therapeutic approaches targeting such channels could help eliminate the issues with effectiveness and safety that are associated with the current anti-thrombotic therapies (Mahaut-Smith, 2012; Varga-Szabo *et al.*, 2009; Barrett *et al.*, 2008). Importantly, *in vivo* inhibition of several ligand-gated Ca^{2+} permeable ion channels in murine models provide effective anti-thrombotic effects, while at the same time maintaining relatively intact haemostatic responses (Mahaut-Smith, 2012; Varga-Szabo *et al.*, 2009; Braun *et al.*, 2009). Two prominent candidates have been proposed as therapeutic ion channel targets in platelets: the SOCE component Orai1 and the ATP-gated P2X1 channel (*see* Figure 1.3) (van Kruchten *et al.*, 2012; Hu & Hoylaerts, 2010). The essential roles for Stim1 and Orai1 in thapsigargin-induced SOCE were demonstrated using Stim1^{-/-} and Orai1^{-/-} murine platelets, which displayed reduced thrombus formation *in vivo*, whereas bleeding times were only slightly longer (Varga-Szabo *et al.*, 2009). P2X1 channels were also shown to significantly contribute to arterial thrombosis *in vivo* (Oury *et al.*, 2006a; Hechler *et al.*, 2005; Hechler *et al.*, 2003), and hence were proposed as valuable therapeutic target in the prevention of thrombosis (Mahaut-Smith *et al.*, 2011).

Platelet ion channels are certainly not limited to those whose contribution to platelet function have been studied and reviewed above and elsewhere. A recent study by our laboratory has screened for more than 400 ion channel mRNA transcripts in human platelets and several megakaryocytic cell lines, generating the first platelet ‘channelome’ database (Wright *et al.*, 2016). This comprehensive study reveals that human platelets abundantly express twenty different ion channels, whose contribution to

platelet function and possible roles in the development of cardiovascular diseases remain unknown. It is important to note that this database only provides information about expression levels of detected ion channels at the mRNA level, and further studies are required to determine the expression levels of the corresponding proteins. Furthermore, regardless of the relative expression levels of each of the ion channels detected, their contribution to platelet function may still be significant, even though the expression levels are not very abundant. For instance, every platelet is thought to express between 150-300 P2X1 channels, in comparison to more than 50,000 copies of the integrin $\alpha_{IIb}\beta_3$ per platelet, highlighting the important contribution to thrombosis that ion channels can make at expression levels relatively lower than other important integrins (Wright *et al.*, 2016; Quinn *et al.*, 1999; MacKenzie *et al.*, 1996). On the other hand, the detected ion channels may have no contribution to platelet function and be present as a carry-over from expression in the megakaryocyte where they play a role in the processes of megakaryocyte maturation within the bone marrow (megakaryopoiesis) and/or platelet production (thrombopoiesis) (Mahaut-Smith, 2012).

1.6 Mechanosensitive ion channels: recent advances

All organisms have evolved specialised mechanisms to sense physical as well as chemical changes that occur around or inside them, and to respond accordingly. The detection of physical stimuli such as shear stress, sound, temperature, gravity, osmotic pressure, membrane tension, and stretch, and their conversion into biological signals by specialised mechanisms is called mechanotransduction. This allows the healthy growth, development, survival and correct functioning of cells, and thus of tissues and organisms. Mechanosensitive (MS) ion channels, whose open probability is dependent on the mechanical stress exerted on the surrounding membrane, are regarded as the most well-characterised biological mechanosensors (Martinac, 2012; Morris, 1990). There are many types of MS ion channels, differing in the type of mechanical stimulus that activates them, and hence they cannot be classified as members of a homologous ion channel family (Sachs & Morris, 1998). Generally, either one of the two models of gating mechanisms are thought to be responsible for channel opening: in the first, mechanical perturbations in the surrounding membrane are conveyed to the channel along the bilayer thereby changing the protein conformation, whilst in the second, links which anchor the channel to the cell cytoskeleton are responsible for opening the

channel. Compared to signalling via second messengers following ligand binding to a receptor, MS ion channels provide a more direct and thus more rapid route of signal amplification by allowing a large quantities of ions into the cells (Gillespie & Walker, 2001). In eukaryotes, MS ion channels mediate mechanotransduction of stimuli during the processes of hearing, touch, and cell volume regulation (turgor control) (Martinac, 2012). Examples include the non-selective cation channels, transmembrane channel-like proteins 1 and 2 (TMC1 and TMC2), which are essential for the conversion of stimuli such as sound and gravity into electrical signals in inner ear hair cells (Kawashima *et al.*, 2011). Several MS ion channels have also been described in the cardiovascular system which are involved in physiological processes of cardiac and vascular cells, such as blood pressure regulation, and pathophysiological conditions such as functional remodelling in cardiomyocytes associated with heart failure (Stiber *et al.*, 2009). For instance, it was demonstrated that the MS ion channels of the baroreceptor neurons innervating rodent aorta generate $[Ca^{2+}]_i$ increases in response to mechanical stimulation, and contribute to the regulation of arterial blood pressure (Sullivan *et al.*, 1997).

The recent identification of the Piezo family of MS cation channels in eukaryotes has attracted considerable interest from various fields of research. The mechanosensory roles of the channels belonging to this family in vertebrates, Piezo1 and Piezo2, were first studied in the mouse Neuro2A glial tumour cell line (Coste *et al.*, 2010). Since then, their functional roles in various tissues and their contributions to disease mechanisms have been reported within an ever-growing number of studies (Cahalan *et al.*, 2015; Ranade *et al.*, 2014a; Li *et al.*, 2014). Piezo1 and 2 proteins are encoded by the Fam38A and Fam38B genes, respectively, and are multipass transmembrane pore-forming subunits which assemble to form mechanically activated cation channels (Coste *et al.*, 2010). Astonishingly, the functional Piezo1 complex (as a homo-oligomer) is regarded as the largest plasma membrane ion channel identified to date, and is estimated to be approximately 1.2 million Daltons (Coste *et al.*, 2012). Reconstitution of Piezo proteins in lipid bilayers resulted in distinct mechanically activated tetrameric cation channel complexes which could be inhibited by the generic mechanosensitive ion channel blocker ruthenium red, and also by the specific inhibitor of MS cation channels, GsMTx4 (*Grammostola spatulata* mechanotoxin 4) (Coste *et al.*, 2012; Bae *et al.*, 2011; Coste *et al.*, 2010). It was shown that Piezo channels are permeable to both monovalent and divalent cations, whilst anion permeability was not

reported (Gnanasambandam *et al.*, 2015; Coste *et al.*, 2010). However, there was a strong preference for Ca²⁺ permeation from the external medium upon stretching the plasma membrane by a patch pipette (Coste *et al.*, 2010). More recently, cryo-electron microscopy has revealed that Piezo1 proteins actually form homotrimers, where each monomer resembles a propeller, and the extracellular domains of this whole structure act as the mechanosensors that control ion gating through the core in the center via the C-terminus (Ge *et al.*, 2015; Coste *et al.*, 2015) (Figure 1.6 A). Moreover, using cytoskeleton-free artificially generated blebs, Cox and colleagues have revealed that Piezo1 is gated by bilayer tension, rather than via a link to the cytoskeleton (Cox *et al.*, 2016). The very first physiological role for Piezo protein (known as DmPiezo in *Drosophila melanogaster*) *in vivo* was found to be in the sensing of noxious stimuli in *D. melanogaster* (Kim *et al.*, 2012). Also, when DmPiezo was expressed in human cells, the cells displayed MS currents resembling those observed in mouse and rat cells (Kim *et al.*, 2012; Coste *et al.*, 2010).

Even though Piezo1 and Piezo2 amino acid sequences resemble each other, and they are both very different from the ion channels belonging to other families or protein classes, differences do exist between these two homologs in terms of their expression and function (Ge *et al.*, 2015). Using Piezo2 conditional KO mice, gene deletion approaches and other electrophysiological methods, Piezo2 channels were shown to be mediators of light touch sensation in birds, rodents and humans (Schrenk-Siemens *et al.*, 2015; Ranade *et al.*, 2014b; Schneider *et al.*, 2014). On the contrary, Piezo1 channels were studied more extensively due to their crucial involvement in a wider variety of physiological processes and disease phenotypes in humans. Loss-of-function and gain-of-function mutations in the Piezo1 gene were revealed to be linked to hereditary diseases of dehydrated stomatocytosis (xerocytosis) in red blood cells and lymphatic dysplasia, respectively (Lukacs *et al.*, 2015; Albuisson *et al.*, 2013; Andolfo *et al.*, 2013; Zarychanski *et al.*, 2012). Of relevance to the focus of this thesis, evidence shows the vital role of Piezo1 in the sensation of shear stress in flowing blood, vascular development, red blood cell volume homeostasis, and the control of cell differentiation (Cahalan *et al.*, 2015; Ranade *et al.*, 2014a; Faucherre *et al.*, 2014; Pathak *et al.*, 2014; Li *et al.*, 2014). Further roles for this ion channel in different organs were reported, including sensation of renal epithelial cell stretching and compression, which becomes impaired as a result of the dysregulation of its function, that is thought to be associated with polycystic kidney disease (Peyronnet *et al.*, 2013). Similarly, urothelial Piezo1 was

shown to sense bladder extension and mediate the release of the signalling molecule ATP that regulates micturition reflex, and its inhibition was suggested as a novel treatment for overactive bladder (Miyamoto *et al.*, 2014; Wang *et al.*, 2005). Elucidation of these MS roles for Piezo1 channel have, in part, relied upon pharmacological reagents such as the inhibitor GsMTx-4 (Li *et al.*, 2014; Coste *et al.*, 2012; Bae *et al.*, 2011) and the recently developed selective agonist Yoda1 (Syeda *et al.*, 2015; Lukacs *et al.*, 2015).

In a recent screen of the platelet channelome using quantitative PCR, transcripts for the Fam38A gene were detected (Wright *et al.*, 2016). Platelet proteomic and transcriptomic studies also indicate Piezo1 expression in human platelets (Boyanova *et al.*, 2012; Burkhart *et al.*, 2012). Despite the close association between platelet function and the mechanical forces of shear stress which they are constantly exposed to, hitherto the functional relevance of such MS ion channels have not been studied in these blood cells.

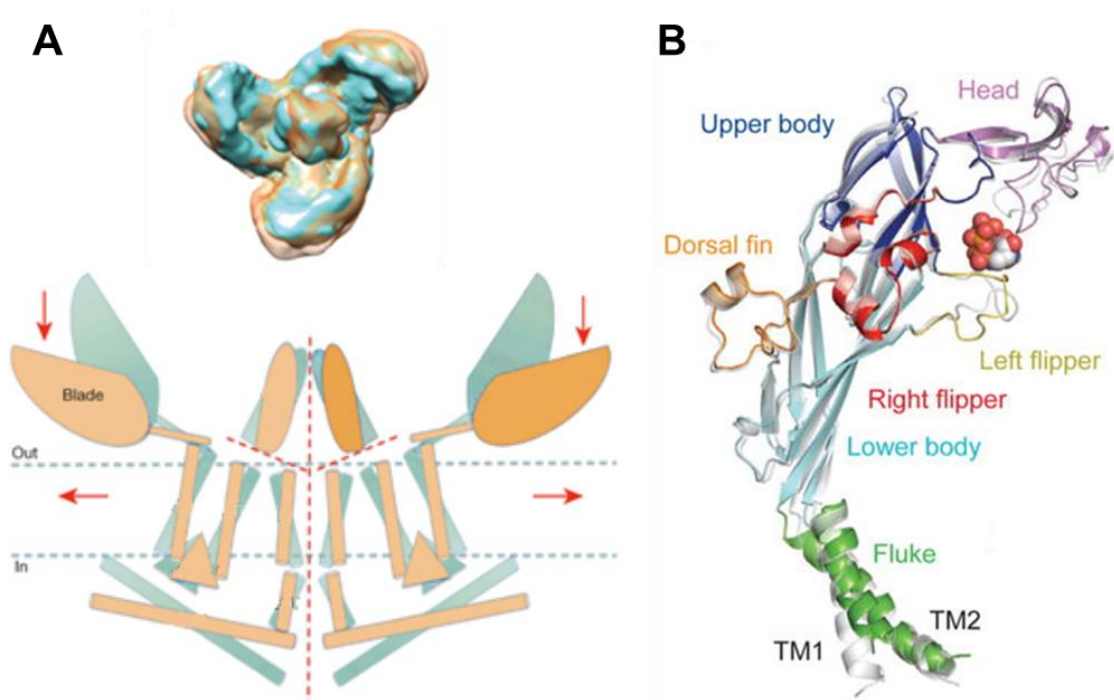


Figure 1.6 Representations of the Piezo1 and P2X1 structures. (A) Upper figure shows Piezo1 structure viewed from the top, illustrating the three propeller-like blades which reside on the extracellular domain and detect mechanical stimuli. The lower figure ...

(...) shows a representation of the proposed working model of *Piezo1*, where the blue figure represents the closed conformation and the orange figure represents the open conformation of the channel. (B) A structural representation of a *P2X* subunit resembling the shape of a dolphin, whereby ATP binding induces conformational changes in the dorsal fin, left flipper and head regions, which is transmitted to the transmembrane regions (TM1 and TM2) resulting in the opening of the channel for ion movement. Representations were adapted from Ge *et al.*, 2015 and Hattori & Gouaux, 2012.

1.7 Immune function of platelets and the unique role of P2X1 channels

In addition to their essential role in the process of haemostasis and thrombosis, platelets play important roles in immunity through the interaction of their immune receptors with invading pathogens. Platelets are increasingly recognised as crucial components of the innate immune system, whereby they accelerate the removal of the invading pathogens (Cox *et al.*, 2011). Following pathogen-induced activation, platelets secrete antimicrobial chemicals such as β -defensin which fights against pathogens, and cytokines and chemokines such as interleukin 1 beta that recruit leukocytes to the site of infection (Cox *et al.*, 2011; Coppinger *et al.*, 2004). Human platelets express the low affinity receptor for immunoglobulin (Ig) G, Fc γ RIIa (CD32a), which recognises the IgG that opsonizes the invading pathogens in the circulation (Arman & Krauel, 2015). Cross-linking of Fc γ RIIa receptors results in the activation of a signal transduction pathway through a single immunoreceptor tyrosine-based activation motif (ITAM), in a similar manner to the stimulation of the collagen receptor GPVI (Watson & Gibbins, 1998; Blake *et al.*, 1994) (Figure 1.7). The interaction between bacteria and platelets has also been shown to lead to formation of dangerous circulating or localised thrombi such as in infective endocarditis (IE) (Fitzgerald *et al.*, 2006).

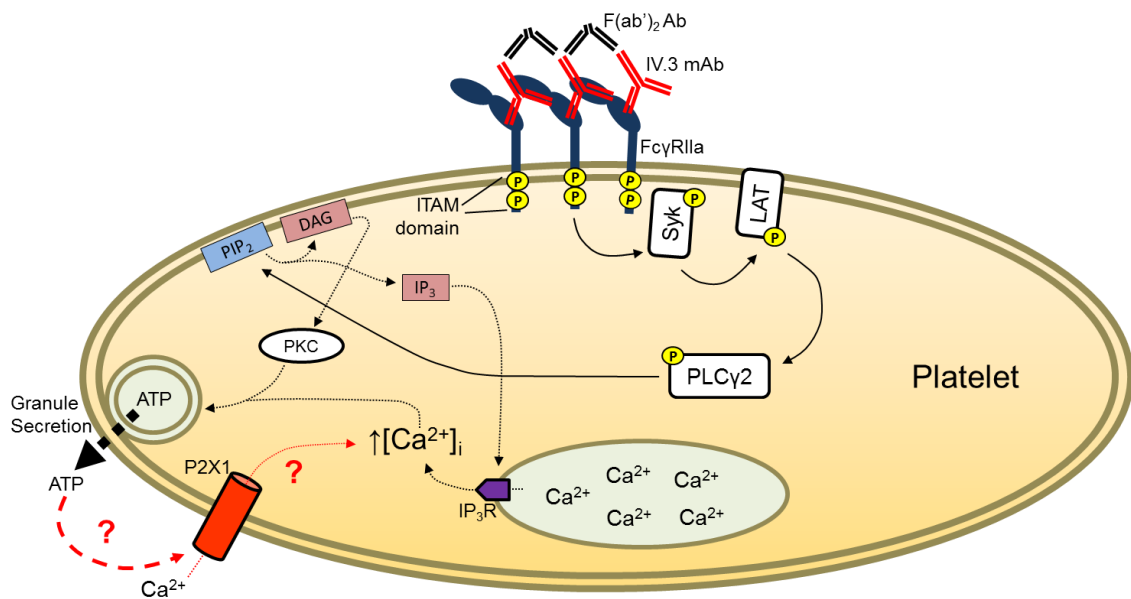


Figure 1.7 *FcγRIIa* signalling following receptor clustering in human platelets. Cross-linking of the anti-*FcγRIIa* antibody (IV.3 mAb) activates the *FcγRIIa* receptors which involves the phosphorylation of the two tyrosines within the ITAM domains in the cytoplasmic region, creating a docking site for Syk tyrosine kinase. Syk phosphorylation initiates the signalling pathway, resulting in the phosphorylation of PLCγ2 which leads to the production of DAG and IP₃. IP₃ binds IP₃R on the ER membrane, which mediates Ca²⁺ release from the stores. DAG activates PKC, which mediates ATP release through dense granule secretion (Arman & Krauel, 2015) Possible contribution of P2X1 to *FcγRIIa*-mediated increase in [Ca²⁺]_i through ATP release remains unclear, and is addressed in this thesis.

The vital role of *FcγRIIa* receptor in platelet aggregation and thrombus formation has been established by a number of *in vitro* and *in vivo* studies (Arman *et al.*, 2014; Zhi *et al.*, 2013; Kerrigan *et al.*, 2008). Despite this, our knowledge of the physiological effects induced by *FcγRIIa* receptor involvement in platelet function is still rudimentary. The possible co-operation between platelet immune receptors such as *FcγRIIa* and purinergic receptors were postulated by a study (Klarstrom Engstrom *et al.*, 2014), however, such a synergy has not been extensively studied and the mechanism of contribution of P2X1 channels to *FcγRIIa* receptor activation remains unclear (Figure 1.7).

P2X1 channels (or P2X1 receptors) are ionotropic receptors which belong to a family of purinergic ATP-gated ion channels that has several receptor subunits in a

variety of mammalian cells (P2X1-7) (Oury *et al.*, 2014; North, 2002). Structurally, each P2X subunit is made up of two transmembrane domains, and subunits can either assemble into homotrimeric or heterotrimeric ion channels (Oury *et al.*, 2014). The operational mechanism of P2X subunits have been described by analogy to the shape of a dolphin, whereby ATP binding induces conformational changes in the dorsal fin, left flipper and head regions, which is transmitted to the transmembrane regions resulting in the opening of the channel for ion movement (Hattori & Gouaux, 2012) (Figure 1.6 B). Amongst the seven different P2X receptor subunits, the homotrimeric P2X1 receptors are the only receptors expressed in platelets and megakaryocytes, which provide significant Ca^{2+} entry routes into cells (Mahaut-Smith, 2012; Wang *et al.*, 2003). Importantly, P2X1 channels have been described as the only ATP-gated ion channels in platelets that provide the fastest Ca^{2+} entry route following ATP release from an injury site (Mahaut-Smith, 2012). It has been shown that platelet shape change and granule secretion are achieved through the activation of a PKC-dependent ERK2 signalling pathway that leads to the phosphorylation of the myosin light chain, following P2X1-mediated increases in $[\text{Ca}^{2+}]_i$ (Oury *et al.*, 2002). Thrombin-dependent P2X1 activity was shown to persist in platelets treated with one of the most commonly used anti-platelet drugs, aspirin (Grenegard *et al.*, 2008). This makes studies indicating P2X1 as a novel therapeutic target even more appealing.

The significance of P2X1 receptor signalling in early Ca^{2+} mobilisation has been demonstrated following the stimulation of platelet immune receptors (TLR2/1), in addition to major platelet GPCRs and tyrosine kinase-coupled receptors (Jones *et al.*, 2014b; FUNG *et al.*, 2007). Ratiometric $[\text{Ca}^{2+}]_i$ measurements in human platelets have demonstrated that selective inhibition or desensitisation of P2X1 receptors leads to significant reductions in $[\text{Ca}^{2+}]_i$ elevations following the stimulation of GPVI, TxA_2 , PAR and P2Y receptors with their corresponding agonists, highlighting the vital role of ATP as a secondary platelet agonist, alongside with ADP and TxA_2 (FUNG *et al.*, 2007; Fung *et al.*, 2005). Particularly, the synergy between P2X1 and P2Y1 receptors have been suggested to fortify platelet attachment to an injury site and thus exacerbate arterial thrombosis (Mahaut-Smith *et al.*, 2004). Similar experimental approaches have been useful in the discovery of the important contribution of P2X1 channels to $[\text{Ca}^{2+}]_i$ increases triggered by TLR2/1, in the presence of endothelium-derived inhibitory molecules such as NO and PGI_2 , suggesting a role for P2X1 in immune-dependent platelet activation (Fung *et al.*, 2012). It has also been suggested that due to the

relatively early onset of P2X1 responses, the main mechanism of P2X1 activation by a variety of agonists is via an autocrine mode of action of ATP that is released from the dense granules (FUNG *et al.*, 2007). Given the important contribution of P2X1 channels in TLR2/1-induced $[Ca^{2+}]_i$ elevations in platelets, it is plausible to suggest that these channels could amplify other immune receptor $[Ca^{2+}]_i$ responses as well.

Relevant to the mechanosensation theme of the majority of this thesis, it is also worth mentioning the important role of shear stress in P2X1 channel-mediated thrombus formation (Erhardt *et al.*, 2006; Mahaut-Smith *et al.*, 2004; Hechler *et al.*, 2003; Oury *et al.*, 2003). Using whole blood from P2X1^{-/-} mice, it was initially shown *in vitro* that P2X1 does not play a significant role in thrombus formation on collagen at normal levels of shear stress in large arteries ($\sim 800s^{-1}$), however, at higher shear levels in the smaller arterioles ($\sim 6000s^{-1}$) the contribution was highly significant (Hechler *et al.*, 2003). *In vivo*, P2X1^{-/-} mice were shown to exhibit reduced sizes of thrombus formation compared to healthy mice using laser-induced vessel wall injury (Hechler *et al.*, 2003). This indicates the vital contribution of P2X1 receptors under the relatively high arterial forces of shear stress (Hechler *et al.*, 2003). Supporting these observations, perfusing blood from transgenic mice overexpressing P2X1 receptors over collagen *in vitro* resulted in enhanced platelet aggregation and PS exposure under normal arterial shear, potentially mediated by the ERK2 signalling pathway (Oury *et al.*, 2003).

1.8 Aims and Objectives

Calcium mobilisation plays a central role both in normal haemostatic platelet function and in thrombosis. Our knowledge of the identities and the functioning of the platelet ion channels which mediate the major Ca^{2+} mobilisation events underlying platelet activation has been limited to mainly ligand-gated or store-operated ion channels, although evidence exists for the presence of MS Piezo1 and Piezo2 channels in platelets and megakaryocytes (Wright *et al.*, 2016; Boyanova *et al.*, 2012; Burkhart *et al.*, 2012). In spite of the well-established imperative links between platelet function and shear stress under normal and pathological conditions, and the evidence for a shear-stress-dependent Ca^{2+} entry pathway of unknown identity (Chow *et al.*, 1992), the expression and functional relevance of MS ion channels in platelets remain unclear. Therefore, the first hypothesis of this thesis is that:

-
- Human platelets express the MS Ca^{2+} channels Piezo1 and/or Piezo2, which contribute to $[\text{Ca}^{2+}]_i$ elevations under arterial shear stress, and thrombus formation.

To date, the main Ca^{2+} -permeable ion channel identified to contribute to platelet activation under conditions of high shear is the ATP-gated P2X1 channel. This enhances thrombus formation in small arteries *in vivo* (Erhardt *et al.*, 2006; Hechler *et al.*, 2003; Oury *et al.*, 2003). *In vitro*, P2X1 contributes to Ca^{2+} responses and platelet function following stimulation by a range of agonists. This contribution is particularly important for tyrosine kinase-coupled receptors GPVI and TLR2/1 since both secretion of ATP by these stimuli and P2X1 channels themselves are resistant to inhibition. One receptor which has not been studied in terms of its P2X1 contribution is Fc γ RIIIa, which is tyrosine kinase-linked and involved in innate immune responses. Considering that immune responses and platelets both contribute to development of atherosclerosis or thrombosis, Ca^{2+} influx mechanisms downstream of Fc γ RIIIa may form a unique input during plaque formation or atherothrombosis. The second hypothesis of this thesis is therefore that:

- P2X1 channels contribute to $[\text{Ca}^{2+}]_i$ increases following Fc γ RIIIa receptor activation in human platelets, and shear stress determines the extent to which P2X1 channels contribute to Fc γ RIIIa-dependent thrombus formation.

To address the hypotheses above, this thesis will specifically aim to achieve the following:

1. To determine the expression levels of MS cation channels in human platelets and the megakaryocytic cell line, Meg-01 at the RNA and protein levels;
2. To develop a novel assay of shear-induced Ca^{2+} responses in which platelets (and Meg-01 cells) are attached to glass coverslips without the use of adhesive ligands;
3. To study the effect(s) of the MS cation channel inhibitor GsMTx-4 and the specific Piezo1 agonist Yoda1 on Ca^{2+} influx, other well-known Ca^{2+} entry routes, and thrombus formation over collagen;

-
4. To investigate the possible synergy between P2X1 channels and FcγRIIIa receptors in contributing to $[Ca^{2+}]_i$ elevations, platelet aggregation and thrombus formation under arterial shear;
 5. To assess the sensitivity of FcγRIIIa-induced P2X1 signalling to the endothelium-derived physiological inhibitors;
 6. To identify the molecular mechanism underlying the synergy between P2X1 channels and FcγRIIIa receptors.

Chapter 2

Materials and Methods

2.1 Salines and materials

2.1.1 Salines

Salines were made using ultrapure double-distilled water (ddH₂O) from Elga Purewater[®] Classic system (18.2M Ω .cm at a temperature of 24.1°C). Hanks' balanced salt solution (HBSS) contained (in mM): 5.33 KCl, 0.44 KH₂PO₄, 137.93 NaCl, 4.17 NaHCO₃, 0.34 Na₂HPO₄, 5.56 D-glucose, 5.00 HEPES, 0.49 MgCl₂, 0.41 MgSO₄·7H₂O, and 1.26 CaCl₂ (pH titrated to 7.35). To prepare washed platelets (WP) for Ca²⁺ measurements, whole blood was collected into the anticoagulant acid-citrate-dextrose (ACD) solution which contained (in mM): 85 trisodium citrate, 78 citric acid, 111 glucose. For thrombus formation, blood was collected into 40 μ M Phe-Pro-Arg-cmk.2HCl (PPACK) (HTI, VT, USA).

WP were prepared in nominally Ca²⁺-free saline (in mM: 145 NaCl, 5 KCl, 1 MgCl₂, 10 HEPES, 10 glucose; pH titrated to 7.35) that also contained 0.32U/mL apyrase grade VII from potatoes (Sigma, Poole, UK) for experiments when P2X1 receptor responses were being studied. In thrombus formation under flow assays, HEPES-buffered saline (HBS) solution (in mM: 150 NaCl, 5 KCl, 1 MgSO₄, 10 HEPES; pH titrated to 7.4) was used to fill and wash through the flow system before and after introducing whole blood.

For Western blot analysis, cell lysis was achieved by the addition of 1x (for protein detection) or 2x (for phosphorylation assays) radioimmunoprecipitation assay (RIPA) buffer (for 1x: 150mM NaCl, 50mM Trizma hydrochloride, 0.5% sodium deoxycholate, 0.1% SDS, 1% Triton X-100; pH titrated to 8.0), in which 1x Roche EDTA-free protease inhibitor cocktail tablet (cOmplete[™] Mini, Roche, Switzerland) was dissolved (per 10mL of RIPA). To inhibit phosphatase activity in lysates to be used in phosphorylation assays, RIPA also contained 4mM sodium orthovanadate and 20mM sodium fluoride. For western blotting the buffers used were: 1x Tris/Glycine transfer buffer (in mM: 192 glycine, 25 Tris base, 10% (v/w) methanol), 1x Tris-buffered saline with Tween 20 (TBS-T; in mM: 13.7mM NaCl, 2mM Tris base, 0.1% (v/w) Tween-20,

pH titrated to 7.4), and 1x Tris/Glycine/SDS running buffer (National Diagnostics, Atlanta, GA, USA).

For mRNA extraction from ultra-purified platelets, the platelet inhibitor cocktail was prepared by mixing 7.5mL ACD, 100 μ M prostaglandin E₁ (PGE₁), 0.5M ethylenediaminetetraacetic acid (EDTA), and 30mM acetylsalicylic acid (aspirin). The Lysis/Binding buffer contained (in mM): 100 Trizma HCl (pH titrated to 8.0), 500 LiCl, 10 EDTA, and 5 dithiothreitol (DTT), and 1% lithium dodecyl sulphate (LiDS). Wash buffers A and B contained (in mM): 10 Trizma HCl (pH 8.0), 0.15 LiCl, 1 EDTA, and 0.1% LiDS; and 10 Trizma HCl (pH 8.0), 0.15 LiCl, 1 EDTA, respectively.

2.1.2 Materials

The MS ion channel inhibitor GsMTx-4 peptide (STG-100) was from Alomone Labs (Jerusalem, Israel), and the specific activator of Piezo1, Yoda1, was from Tocris Bioscience (Bristol, UK). Fura-2 AM and Fluo-3 AM were from Invitrogen (Paisley, UK). PECAM-1 (WM59) (MCA1738T) for platelet attachment was purchased from AbD Serotec (Kidlington, UK). Native equine tendon Horm[®] collagen (type I) was purchased from Takeda (Linz, Austria). Anti-Fc γ RIIa monoclonal antibody (mAb) IV.3 was purified from a hybridoma in the laboratory of Prof Steve P. Watson (University of Birmingham, UK). Goat anti-mouse IgG F(ab')₂ was purchased from Fisher Scientific UK. The NO donor, Spermine NONOate was from Enzo Life Sciences Ltd (Exeter, UK). The glycoprotein (GP) IIa/IIIb inhibitor eptifibatide (integrilin) was from Source Bioscience (Nottingham, UK). Extracellular ATP measurements were performed using the Chrono-lume[™] reagent kit (#395; Chrono-log Corporation, Havertown, PA, USA). Rabbit anti-human phospho-Syk (Tyr525/526) mAb and rabbit anti-human phospho-PLC γ 2 (Tyr1217) polyclonal antibody (pAb) were from Cell Signaling Technology (Danvers, MA, USA). Rabbit anti-human phospho Y200 (Anti-LAT) mAb was from Abcam (Cambridge, UK). Mouse anti-human anti-phosphotyrosine (clone 4G10) mAb was from Millipore UK Ltd (Watford, UK). Unless otherwise stated, all other materials were from Sigma-Aldrich (Poole, UK).

2.2 Cell culture and attachment

2.2.1 *Meg-01 and HUVECs*

Meg-01 cells were obtained from the European Collection of Cell Cultures (ECACC, Salisbury, UK) and grown in RPMI1640 supplemented with 10% foetal bovine serum (FBS) (Invitrogen, Paisley, UK) and 100U/mL Penicillin-Streptomycin (P/S). Cells were split every 2-3 days. For attachment of Meg-01 cells, sterilised glass coverslips (24mm×50mm, thickness №1; VWR International, Darmstadt, Germany) were coated with 0.1mg/mL Poly-D-lysine hydrobromide (MW>300,000) for 15 minutes. The slides were then rinsed with sterile water and dried for 2 hours. Meg-01 cells in medium were added to the coated slides and incubated at 37°C for 15 minutes to promote attachment. Attached cells were then treated with 2µM Fluo-3 AM at room temperature for 45 minutes. After washing in HBSS, slides were immediately inserted in a parallel-plate flow chamber for experimentation (Figure 2.2 A). Meg-01 cells used in experiments were from passage numbers 1-14. Pooled primary human umbilical vein endothelial cells (HUVECs) (PromoCell GmbH, Heidelberg, Germany) were supplied by courtesy of Professor Nicholas P.J. Brindle at the Department of Cardiovascular Sciences at the University of Leicester. HUVECs were cultured on glass coverslips (24mm×50mm, thickness №1) coated with a mixture of 2% gelatin and 0.1mg/mL Poly-D-lysine hydrobromide (MW>300,000) (coated at room temperature for 1 hour) in Medium 200 supplemented with low serum growth supplement (LSGS), 10% FBS and 100U/mL P/S. HUVECs used in experiments were from passage numbers 6-8. Meg-01 and HUVECs were both cultured at 37°C in a 95% air/5% CO₂ atmosphere.

2.2.2 *Bacterial culture*

The bacterial strain *Streptococcus sanguinis* (133-79) was provided by Professor Mark Harzberg (University of Minnesota). For each experiment, bacteria were cultured in 20mL Brain Heart Infusion Broth (BHI) under anaerobic conditions at 37°C, overnight. Exponential growth profiles for the strain were constructed by recording the optical densities (OD) at 600nm at regular time intervals (Figure 2.1). For experimentation, the OD of the cultures were measured between 15 and 16 hours after inoculation, and were adjusted to 1.6, which corresponds to 6x10⁸ CFU/mL as previously shown (Arman *et al.*, 2014). The optical density adjustment was carried out as follows: after measurements, required volumes of bacterial culture were centrifuged

twice at 2500g for 10 minutes and re-suspended in phosphate-buffered saline (PBS). Bacterial suspensions were brought to room temperature before experimentation. For thrombus formation under flow, 1mL of *Streptococcus sanguinis* (133-79) suspension in BHI was placed on a heat-sterilised glass coverslip (24mm×50mm, thickness №1) and incubated at room temperature for 2 hours. Uniform coating was confirmed with a phase-contrast microscope, and slides were washed thrice in PBS to remove unbound bacteria. Slides were blocked by incubating with 1% bovine serum albumin (BSA) for 1 hour at 37°C before insertion into the parallel-plate flow chamber for experimentation.

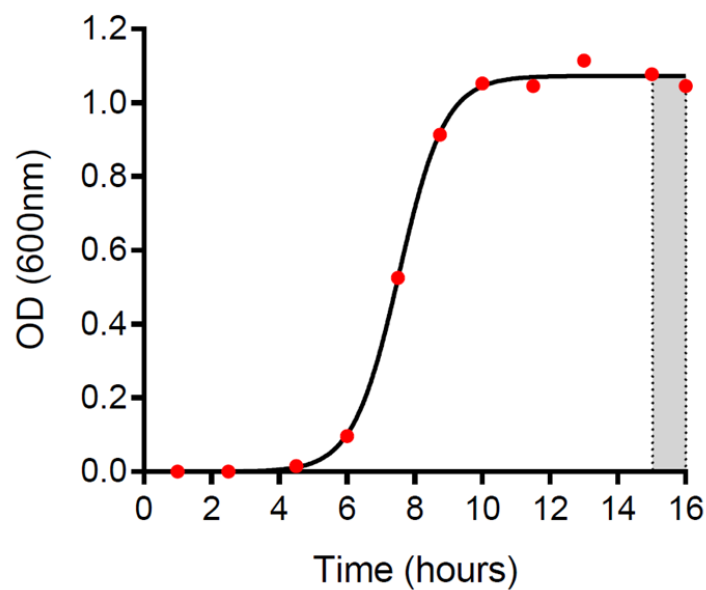


Figure 2.1 Representative growth curve for the bacterial strain *S. sanguinis* 133-79. OD=optical density. The grey-shaded region indicates the time interval during which bacteria were collected and washed for use in the experiments.

2.3 Phlebotomy and washed platelet preparation

2.3.1 Phlebotomy

The study was approved by the University of Leicester Committee for Research Ethics concerning human subjects (non-NHS). Blood was collected in accordance with the Declaration of Helsinki from informed consenting volunteers of either gender who had not taken any medication that can affect platelet function for at least two weeks. Blood was collected from a vein in the antecubital region using a Surflo[®] 21G Butterfly Winged Infusion Set (Terumo, UK) into 20mL or 60mL syringes by application of negative pressure. Before blood collection, either of the following anticoagulants were added to the syringe: ACD at a ratio of 6:1 (blood:ACD), or PPACK at a final concentration of 40 μ M.

2.3.2 Preparation of washed platelets and Meg-01 cells for dye loading

Platelet rich plasma (PRP) was prepared by centrifuging the whole blood at 150g for 20 minutes for mRNA extraction (*see* Section 2.11.1), 100g for 20 minutes for aggregometry, or 700g for 5 minutes for other experiments. For $[Ca^{2+}]_i$ measurements, PRP was incubated at room temperature for 15 minutes with 100 μ M aspirin and 0.32U/mL apyrase (Type VII, Sigma), then incubated with either 2 μ M Fura-2 AM (for 45 minutes at 37°C, with regular gentle inversions of the tube) or 5 μ M Fluo-3 AM (for 45 minutes on a rotor at room temperature). The PRP was then centrifuged at 350g for 20 minutes and platelets re-suspended in an equal volume of nominally Ca^{2+} -free saline (which also contained 0.32U/mL apyrase for experiments when P2X1 receptor responses were being studied). Immediately prior to Fura-2 measurements in cuvettes or before introducing Fluo-3-loaded platelets to biochips for attachment, the platelet suspension was diluted 1:1 with Ca^{2+} -free saline. For light transmission aggregometry, washed platelets (WP) were prepared as described for $[Ca^{2+}]_i$ measurements. Aspirin was excluded when bacteria were used to stimulate aggregation. WP were re-suspended in a volume of saline equivalent to that of the original PRP.

20mL of Meg-01 cells in RPMI1640 medium (20mL) were harvested and treated with aspirin and apyrase as described for platelets and washed twice in apyrase-containing nominally Ca^{2+} -free saline by centrifugation at 200g for 5 minutes. Cells were loaded with Fura-2 as described for platelets above. For Fluo-3 loading protocol into attached Meg-01 cells, *see* Section 2.2.1.

2.4 Fluorescence imaging

Imaging of thrombus formation and $[Ca^{2+}]_i$ recordings from single platelets or Meg-01 cells were carried out on an Olympus IX81 inverted confocal microscope with a FV1000 laser scanning module (Olympus, UK), at 60x, 1.35 NA oil immersion lens (UPLSAPO). The confocal aperture was set for optimal optical slicing (1 Airy unit, slice thickness $\approx 1.25\mu\text{m}$). Fluo-3 fluorescence images were captured at a rate of 1.74Hz for platelets, and 0.37Hz for Meg-01 cells and HUVECs.

2.5 Thrombus formation under flow

Glass coverslips (24mm \times 50mm, thickness №1) were coated with collagen (100 $\mu\text{g}/\text{mL}$) overnight in a humidified chamber at 4°C. Whole blood was stained with 1 μM DiOC₆ on a rotor at room temperature for 30 minutes before use. A programmable AL-1000 syringe pump (World Precision Instruments, Sarasota, Florida, USA) attached to a parallel-plate flow chamber (Figure 2.2a) was used to initially introduce HBS solution (in mM: 150 NaCl, 5 KCl, 1 MgSO₄, 10 HEPES) to remove air bubbles. 1mL whole blood was then introduced into the system for a period of 5 minutes at the required shear level before perfusing HBS to clear the components unbound to the collagen surface. The blood flow rate required to generate a specified level of shear in each assay (Table 2.1) was calculated according to the following equation, where Q= flow rate (mL/s), w= microslide lumen width in cm for Vena8™ biochip or parallel-plate chamber (0.08 or 0.15, respectively); h= microslide lumen height in cm for Vena8™ biochip or parallel-plate chamber, (0.008 or 0.0125, respectively); t= shear stress (Pa); μ = viscosity of whole blood (0.003Pa/s) or water (0.001002 Pa/s):

$$Q = \frac{wh^2 t}{6\mu}$$

Finally, to calculate the shear rate (s^{-1}), t was divided by μ .

Time series scans were performed during thrombus formation, and subsequent Z-stack analyses of stable thrombi were carried out within 15 minutes of their formation using step changes (ΔZ) of $0.69\mu\text{m}$. Data represent an average of at least 4 randomly chosen fields per experiment. Analysis and 3D reconstruction of Z-stacks were performed with ImageJ 1.49 Volume Viewer 2.0 plugin (National Institutes of Health, USA). Surface coverage and thrombus volume were calculated according to the Cavalieri principle as previously described (Pugh *et al.*, 2010; Prakash *et al.*, 1994). The heights of the thrombi were calculated by dividing the total thrombus volume by the area of the field.

2.6 Intracellular Ca^{2+} imaging in Meg-01 cells under flow

Fluo-3-loaded Meg-01 cells attached to slides were treated with $2.5\mu\text{M}$ GsMTx-4 for 1 minute or vehicle (HBSS) as necessary before inserting the slides into the parallel-plate flow chamber. To apply fluid shear stress, the reservoir was filled with either HBSS, Ca^{2+} -free HBSS containing 1mM ethylene glycol tetraacetic acid (EGTA), or HBSS containing $2.5\mu\text{M}$ GsMTx-4 as appropriate, and the syringe pump was set to draw fluid through the system at the shear rates of 1002.6s^{-1} , 2282.7s^{-1} and 3989.2s^{-1} , which represent shear conditions in normal arteries, moderately stenotic arteries and severely stenotic arteries, respectively (*see* Table 2.1). Images were analysed on ImageJ 1.47v (Schneider *et al.*, 2012) using the Time Series Analyzer V2.0 plugin to obtain the Ca^{2+} traces. The fluorescent signals were background corrected and fluorescence levels (F) were normalised against the pre-stimulus fluorescence level (F_0) to yield F/F_0 ratios.

2.7 Intracellular Ca^{2+} imaging in Meg-01 cells mechanically stimulated with a glass probe

Meg-01 cells were attached onto poly-D lysine-coated coverslips and loaded with Fluo-3 as described in Section 2.2.1. Mechanical stimulation was performed manually using a glass pipette with a blunt tip attached to a Luigs & Neumann mini/combi manipulator (Ratingen, Germany). The glass pipette was pulled on a Narishige PP-830 two-stage patch puller (Tokyo, Japan), and had a final tip diameter of approximately $1\text{-}2\mu\text{m}$ after fire-polishing. Images were obtained and analysed as described in Sections 2.4 and 2.6.

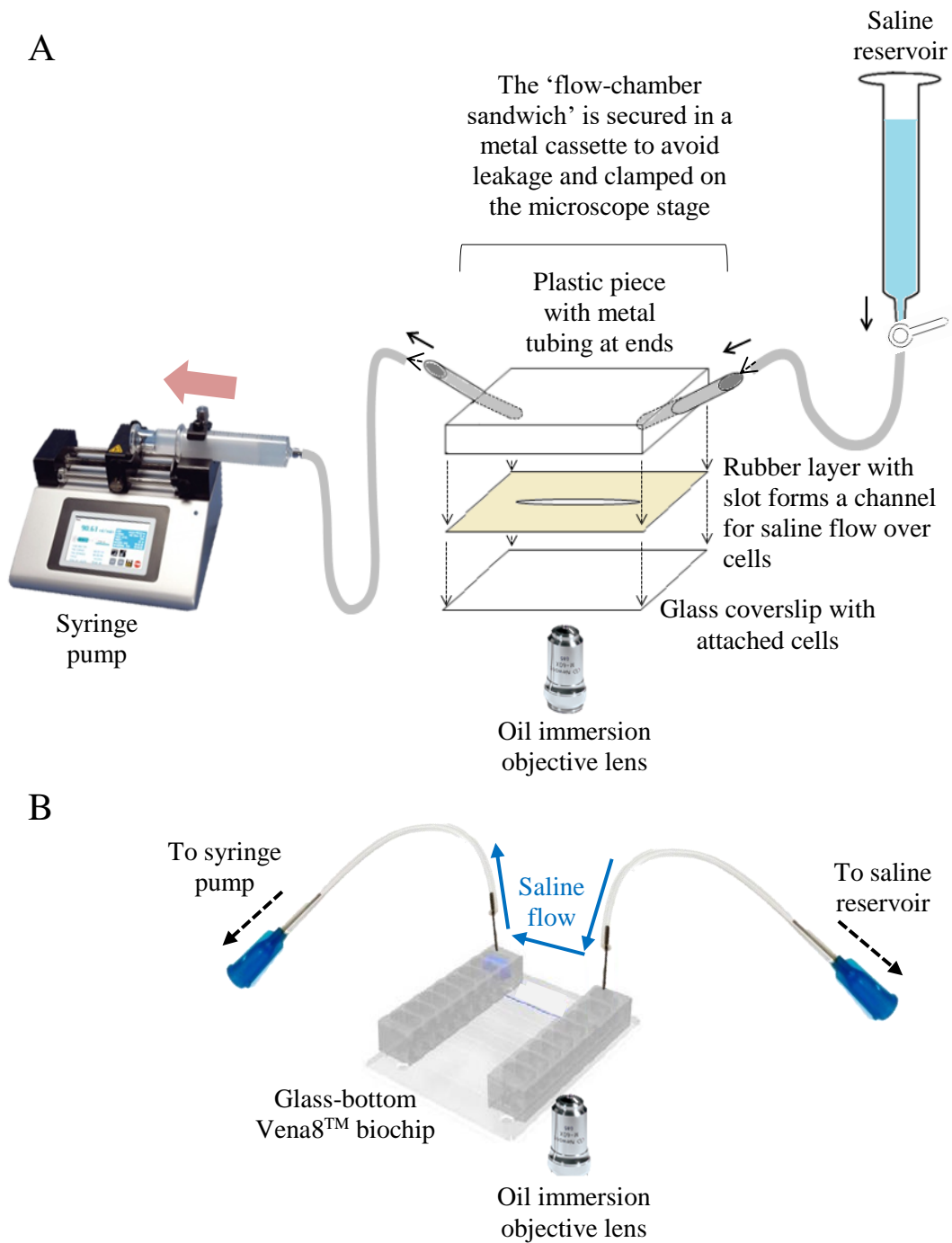


Figure 2.2 *Cartoon representations of the flow systems used in thrombus formation and shear stress assays. (A) The parallel-plate flow chamber used for studies of thrombus formation and shear stress-induced Ca^{2+} increases in Meg-01 cells. To study shear-induced increases in $[Ca^{2+}]_i$ in the Meg-01 cell line, cells were attached to poly-D-lysine coated coverslips, loaded with Fluo-3, and HBSS perfused through the passage under control of the syringe pump to achieve specific shear rates (see Table 2.1). To study thrombus formation, the glass coverslip was coated with collagen and the reservoir was filled with DiOC₆-stained whole blood containing PPACK. ...*

... (B) The assembly of a glass-bottom Vena8TM biochip to study Ca²⁺ transients in single platelets under shear stress. The 'flow chamber sandwich' in A is replaced by the biochip, in which Fluo-3-loaded platelets are attached to PECAM-1 antibody-coated micro-channels (shown with a blue line on the biochip) before experimentation.

| Physiological Condition | Flow rate (mL/min) [Vena8 TM biochip] | Flow rate (mL/min) [Parallel-plate] | Shear rate (s ⁻¹) |
|--------------------------|--|-------------------------------------|-------------------------------|
| Normal Arterial | 0.051 | 0.235 | 1002.6 |
| Stenotic Arterial (Low) | 0.117 | 0.535 | 2282.7 |
| Stenotic Arterial (High) | 0.204 | 0.935 | 3989.2 |

Table 2.1 The flow rates used in Vena8TM biochips (Cellix) and parallel-plate flow chambers, and their corresponding calculated shear rates used in shear stress assays. Physiological conditions indicate the equivalent arterial flow conditions in vivo for each shear rate (Shih-Hsin & Mcintire, 1998; Kroll et al., 1996).

2.8 Imaging of Ca²⁺ transients in single platelets under flow

For attachment of platelets, biochips were coated with monoclonal mouse anti-human PECAM-1 (CD31) antibody by incubation at 37°C for 1 hour. Excess antibody was removed and non-specific sites blocked with 2% BSA at 37°C for 1 hour. Immediately prior to each experiment, Fluo-3 loaded platelets were introduced into the biochip channel and incubated at 37°C for 10 minutes with occasional gentle shaking to promote attachment (Figure 2.3). The biochip was then mounted on the microscope stage (Figure 2.2 B) and HBSS introduced into the channel under gravity. Pharmacological reagents (2.5µM GsMTx-4 or 25µM Yoda1) were introduced at a very low shear rate (410.16s⁻¹) prior to the experimental recording. Captured time-series images were analysed on ImageJ 1.47v (Schneider *et al.*, 2012) using the Time Series Analyzer V2.0 plugin, to obtain the Ca²⁺ traces. F/F₀ values were calculated after background and F₀ correction and values were transferred to GraphPad Prism 6.0 (La Jolla, CA, USA) software for quantification of the F/F₀ integral over 4 minutes (F/F₀.4min). The baseline was set manually and peaks more than 1 point above baseline were included within the calculation of a Ca²⁺ increase.

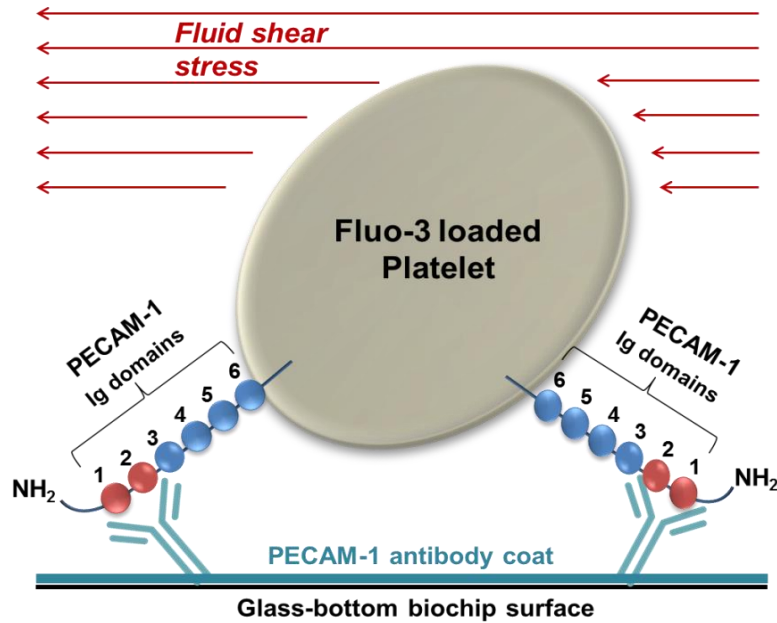


Figure 2.3 A cartoon representation of single platelet attachment to anti-PECAM-1 antibody coated biochip surface via the Ig domains 1 and 2 of the platelet PECAM-1 for the imaging of Ca^{2+} transients under shear stress.

2.9 *In vitro* light transmission aggregometry and ATP secretion assay

2.9.1 *In vitro* light transmission aggregometry

Platelet aggregation and ATP secretion were monitored in a Chronolog 400 lumi-aggregometer (Chrono-Log Corporation, Havertown, PA, USA), at 37°C. To test the effect of GsMTx-4 on collagen-induced platelet aggregation, WP were added into siliconized glass cuvettes (Chrono-Log Corporation, Havertown, PA, USA) containing Chrono-log #311 stir bars and 100µg/mL fibrinogen, and 2mM $CaCl_2$ was added before the start of each experiment. The platelets were then incubated at 37°C for 3 minutes before experimentation. 500µL of saline was placed in the reference well and maximum transmission (aggregation) was set before the start of each recording. Each cuvette was incubated with 2.5µM GsMTx-4 or vehicle (Ca^{2+} -free saline) for 30 seconds, before addition of collagen to stimulate aggregation. Where necessary, aggregation was inhibited by the inclusion of 9µM integrilin 3 minutes before experimentation. In all experiments, the cuvette volume was maintained at 500µL after the final stimulation.

The ABF files obtained from the Axoscope Software (Molecular Devices, Sunnyvale, CA, USA) were processed by Origin 2015 Sr2 for Windows (OriginLab Corporation, Northampton, MA, USA) to acquire the raw transmission values. Percentage light transmission (or aggregation) values were calculated using the following formula, where average baseline is the mean of the pre-stimulation raw transmission values:

$$\% \text{ Light transmission (aggregation)} = \frac{\text{Raw transmission value} - \text{Average baseline}}{\text{Average baseline} \times 100}$$

In Figure 4.16, the % aggregation values displayed on the bar chart were further processed by normalising the vehicle light transmission response to 100% aggregation.

2.9.2 ATP secretion assay

Detection of ATP secretion was performed using the Chrono-Lume luciferin-luciferase assay kit (Chrono-Log Corporation, Havertown, PA, USA). Chrono-Lume reagent (50 μ L per tube) was added to 450 μ L of platelet suspension 3 minutes before stimulation with an agonist. The mixture also contained fibrinogen (100 μ g/mL) and pooled human hIgGs (0.1mg/mL) when bacteria were used to induce secretion. In experiments where P2X1 channel desensitisation was required, 600nM α,β -meATP was added 60 seconds prior to 2mM CaCl₂. Fc γ RIIa stimulation by antibody-induced cross-linking was achieved by the addition of mAb IV.3 (1 μ g/mL), followed by the required concentration of the cross-linking IgG F(ab')₂. ATP secretion was assessed in the presence of 0.32U/mL apyrase using the luminescence detection channel of the Chrono-log lumi-aggregometer. For each batch of luciferin-luciferase, a concentration-response standard curve was constructed using the background-corrected peak signal (mV) detected in normal platelet saline across a range of known ATP concentrations (nM) (Figure 2.4). These curves allowed the conversion of the peak voltage output change values (ΔV , mV) obtained after stimulation of the platelets into corresponding ATP concentrations.

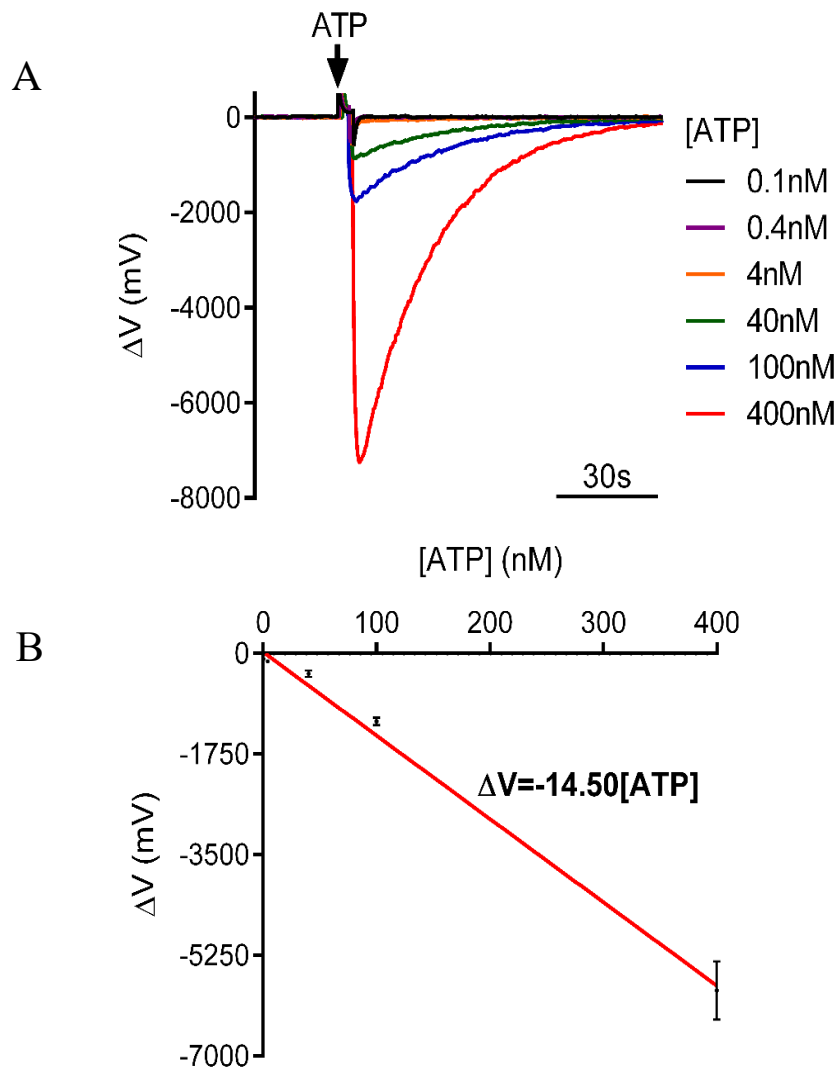


Figure 2.4 Representative luminescence traces obtained by ATP addition to saline, and a concentration-response standard curve. (A) The background-corrected luminescence traces of voltage output (mV) against a series of known ATP concentrations. (B) The standard curve of baseline-corrected maximum ΔV values obtained using a range of known ATP concentrations ($n=3$). The resulting equation shown next to the curve was used to convert voltage output values to ATP concentrations.

2.10 Fura-2 ratiometric Ca²⁺ measurements

2.10.1 Fluorescence measurements

Fura-2 ratiometric Ca²⁺ measurements were performed in stirred cell suspensions using a Cairn spectrofluorimeter system (Cairn Research Ltd, Faversham, Kent, UK) at 37°C. After loading with Fura-2, cells were re-suspended in nominally Ca²⁺-free saline. In all experiments, Fura-2-loaded platelet suspensions were diluted with nominally Ca²⁺-free saline in a 1:1 ratio, and 2mL of diluted cell suspension was added in each cuvette. Each cuvette was added a magnetic stirrer and warmed up by placing inside a 37°C chamber for 3 minutes prior to experimentation. Where necessary, 2mM CaCl₂ was added to individual cuvettes 30s before stimulation with an agonist. Wherever P2X1 channel contribution was studied, the saline included 0.32U/mL apyrase. In experiments where bacteria were added to stimulate FcγRIIIa receptors, hIgGs (0.1mg/mL) and fibrinogen (100µg/mL) were also included in each cuvette prior to stimulation. FcγRIIIa stimulation by antibody cross-linking was achieved by pre-incubating the platelets with mAb IV.3 (1µg/mL) for 2 minutes before addition of a required concentration of IgG F(ab')₂. A 75W xenon arc lamp was used to provide the excitation light, which was filtered by a 6-position filter rotating at 45 rotations per minute. The light travelled to the cuvette holder through a liquid light guide, and light emitted from the samples were collected by a photomultiplier tube (PMT) located at a right angle to the light guide. The PMT output was digitised and stored using the Cairn proprietary software (Cairn Research Ltd, Faversham, Kent, UK).

2.10.2 Fura-2 dye calibration

Fura-2 ratiometric fluorescence signals at 340 and 380nm excitation and ≈490-600nm emission were background corrected (using saline as background), and expressed as [Ca²⁺]_i (nM) after calibration. For calibration, Fura-2-loaded platelet plasma membranes were permeabilised using 50µM digitonin, and added 1mM CaCl₂ and 10mM EGTA, which yielded maximum and minimum Ca²⁺ fluorescence values, respectively, at 340nm and 380nm. R_{min} and R_{max} values were calculated using the background-corrected fluorescence values, where they represent the signal ratios in Ca²⁺-free and maximum Ca²⁺ availability conditions, respectively. To correct for the

effect of the cytoplasmic environment of the dye, a viscosity correction factor of 0.85 was applied (Poenie, 1990). Using a dissociation constant (K_d) for Ca^{2+} of 224nM as described previously (Rolf *et al.*, 2001), the background-corrected 340/380nm signal ratios (R) were converted to $[Ca^{2+}]_i$, using the Grynkiewicz equation (Grynkiewicz *et al.*, 1985):

$$[Ca^{2+}]_i = K_d \times \frac{F_{380 \max}}{F_{380 \min}} \times \frac{(R - R_{\min})}{(R_{\max} - R)}$$

where $F_{380 \max}$ and $F_{380 \min}$ are the maximum and minimum fluorescence signals at 380nm wavelength. Throughout this thesis, the peak $[Ca^{2+}]_i$ responses (i.e. $\Delta[Ca^{2+}]_i$ values) represent the increase in $[Ca^{2+}]_i$ above the pre-stimulus concentration.

2.10.3 Data processing

The binary data files obtained from the Cairn spectrofluorimeter system software (Cairn Research Ltd, Faversham, Kent, UK) were converted to ASCII files using Analyse Software Version 1.00a (Cairn Research Ltd, Faversham, Kent, UK). The background-corrected values were then converted to $[Ca^{2+}]_i$ according to the Grynkiewicz equation and measured calibration constants (Section 2.10.2) using a macro script written within Origin[®] 2015 Sr2 (OriginLab Corporation, Northampton, MA, USA). Traces of $[Ca^{2+}]_i$ against time were then plotted on GraphPad Prism 6.0 software (La Jolla, CA, USA) for presentation.

2.11 Quantitative real-time polymerase chain reaction (qRT-PCR)

2.11.1 mRNA extraction

For isolation of platelets from whole blood, CD45 and CD42b antibody-coated magnetic beads were prepared initially as follows: Equal volumes of Dynabeads® Pan Mouse IgG slurry (Invitrogen, Paisley, UK) and PBS were mixed, and washed beads were collected by immunomagnetic depletion, on a magnetic particle concentrator® (MPC) (Invitrogen). Beads were washed again with PBS, and CD45 (BD PHarMingen, UK) and CD42b (BD PHarMingen, UK) antibodies were added into different batches of washed IgG suspensions in a ratio of 3:100 and 4:100 (antibody:bead), respectively. The mixtures were incubated for 10 minutes on a rotor at 4°C to allow binding of antibodies to beads. Platelet inhibitor cocktail (1.5mL) was added per 10mL whole blood and gently mixed by inversion. After centrifugation at 150g for 20 minutes, the upper 80% fraction of the PRP layer was transferred to microcentrifuge tubes with screw caps in 1.5mL aliquots. 100µL of CD45 antibody-coated beads was added to each aliquot to negatively select white blood cells (WBC) and WBC-platelet aggregates by incubation on a rotor for 20 minutes at room temperature. Samples were then placed on a MPC, and WBC-free PRP was transferred into clean tubes. 200µL of CD42b antibody-coated beads were then added in each PRP sample, and incubated for 20 minutes on a rotor at room temperature to positively select platelets. The tubes were placed on the MPC and the supernatant was discarded. Platelets bound to the CD42b coated beads were washed with PBS and 1mL of Lysis/Binding buffer added to detach platelets from the beads and lyse the platelets. The beads were removed from the lysate by placing the tubes on the MPC, and transferring the lysates to clean tubes on ice.

For isolation of mRNA from the platelet lysates, Dynabeads® Oligo (dT)₂₅ (Life Technologies, CA, USA) (100µL per 1mL sample) were washed and re-suspended in an equivalent volume of Lysis/Binding buffer, using the MPC to remove the supernatant. The Oligo (dT)₂₅ beads were incubated with the samples on a rotor at room temperature for 5 minutes. The samples were placed on the MPC and supernatant was removed. The mRNA-bound beads were washed twice in 1mL wash buffer A and once in wash buffer B. The mRNA-bound beads were re-suspended in 20µL RNase-free water and stored at -80°C.

For mRNA extraction from Meg-01 cells, 20mL of Meg-01 cells in RPMI1640 medium were harvested and added 1.5mL platelet inhibitor cocktail (per 10mL cell

suspension) and gently mixed by inversion. Cells were then washed twice in PBS by centrifugation at 200g for 5 minutes and cell lysis was achieved by the addition of 1mL Lysis/Binding buffer. Isolation of mRNA and preparation of cDNA were performed as described for the platelet samples above.

2.11.2 Reverse transcription and qRT-PCR

The reverse transcription reaction mixtures were prepared in 0.2mL PCR tubes, containing 5µL of the mRNA sample, 2µL of 10mM dNTP mix (Promega, UK) and 6µL RNase-free water each. The mix was incubated at 65°C for 5 minutes then placed on ice to denature the secondary structure of RNA. Into each reaction mixture, 4µL 5x cDNA synthesis buffer (Invitrogen, Paisley, UK), 1µL 0.1M DTT (Invitrogen), 1µL RNase inhibitor (Promega, Madison, WI, USA), and 1µL Cloned AMV-Reverse Transcriptase (15 U/µL; Invitrogen) were added and the mixtures were incubated at 45°C for 60 minutes followed by 85°C for 5 minutes in a thermal cycler. The cDNA samples were stored at -20°C.

For PCR amplification, reaction master mixes were prepared by mixing together 12.5µL 2x QuantiFast SYBR Green Master Mix (Qiagen, Hilden, Germany), 2.5µL pre-designed QuantiTect primer solution (Qiagen) for the gene of interest (Table 2.2), and 8µL RNase-free water, per well of a 96-well plate. In each well, 23µL of reaction master mix was added and mixed with 2µL of cDNA. The following cycling conditions were set to run on an MJ-Research PTC-200 Peltier Thermal Cycler (GMI Inc, Ramsey, MN, USA): 50°C (2min), 95°C (5min), 40x [95°C (10sec), 60°C (30sec)], 95°C (15sec), 60°C (15sec), 95°C (15sec). All primers were run in duplicates for each cell type and the mean Ct values were calculated for analysis. The reaction end-products were stored at -20°C for visualisation with agarose gel electrophoresis. The relative expression of each gene compared to the housekeeping gene glyceraldehyde 3-phosphate dehydrogenase (GAPDH) was calculated using the following formula (Amisten, 2012):

$$\text{Relative expression} = \frac{E_{\text{gene of interest}}^{-\text{Ct gene of interest}}}{E_{\text{housekeeping gene}}^{-\text{Ct housekeeping gene}}}$$

, where E represents the amplification efficiency of a primer pair, and Ct represents the cycle threshold values obtained after the qRT-PCR experiment. The E value for each primer pair was calculated using the following equation (Amisten, 2012):

$$E = 10^{(-\frac{1}{k})}$$

, where k is the gradient of the primer efficiency curve of Ct values against the -log of a cDNA dilution range (Figure 2.5).

| Gene | Catalogue № |
|-----------------|-------------|
| Fam38A (Piezo1) | QT00088403 |
| Fam38B (Piezo2) | QT02359623 |
| P2RX1 (P2X1) | QT00009240 |
| TRPC6 | QT00037660 |
| GAPDH | QT01192646 |

Table 2.2 A list of *QuantiTect* pre-designed primers (*Qiagen*) used to detect mRNA expression in platelets and *Meg-01* cells.

2.11.3 Agarose gel electrophoresis

Agarose gels (1.8%) were made by dissolving 2.7g of agarose (Melford, Ipswich, UK) with 1x TAE buffer (Invitrogen, Paisley, UK), by heating in a microwave and swirling before pouring into the tank. Each qRT-PCR end-product (10µL) was mixed with 2µL of 5x DNA loading buffer (Bioline, London, UK), and 10µL was loaded into each well of the gel to visualise the amplification products. Gels were run for 60 minutes at 110V supply and stained with 10mg/mL ethidium bromide (EtBr) solution (Invitrogen, Paisley, UK) in 1x TAE buffer for 15 minutes on a rocker. Imaging of the gels were performed in a UVIDoc gel documentation system (UVItec Ltd., Cambridge, UK) after washing off excess EtBr with ddH₂O for 5 minutes.

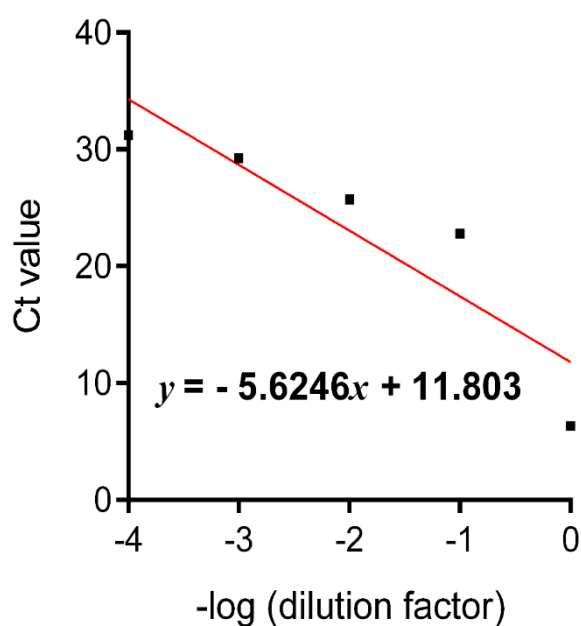


Figure 2.5 Representative primer efficiency curve for Piezo1 QuantiTect primer pair. Following qRT-PCR amplification of a serial dilution of a platelet cDNA sample (dilution factors: 1, 10, 100, 1000 and 10000), the Ct values obtained were plotted against $-\log$ transformed dilution factors to yield the equation displayed. Using the equation $E=10^{(-1/k)}$, the efficiency (E) for this primer pair is 1.51.

2.12 Western blot analysis and phosphorylation assay

2.12.1 Cell lysate preparation

For platelet lysate preparation for Western blot analysis, the washed platelet preparation protocol for $[Ca^{2+}]_i$ measurements (see Section 2.3.2) was performed without the second wash step, dye addition and loading steps for 45 minutes at 37°C. After the PRP was centrifuged, the platelet poor plasma (PPP) was discarded and the platelet pellet was lysed by the addition of 1xRIPA buffer and pipetting to disrupt the pellet. The tube was placed on ice for 1 hour during which the contents were mixed rigorously every 10 minutes using a vortex mixer. For Meg-01 cell lysate preparation,

20mL of Meg-01 cells in RPMI1640 medium were harvested and washed twice in PBS by centrifugation at 200g for 5 minutes. After the second wash, the Meg-01 cell pellet was lysed in 1xRIPA buffer as described for platelets above. After lysis, the lysates were centrifuged at 20000g at 4°C for 10 minutes and the supernatant was stored at -80°C for analysis.

For phosphorylation assays, platelet FcγRIIa receptors were stimulated in a Chronolog 400 lumi-aggregometer (Chrono-Log Corporation, Havertown, PA, USA), at 37°C. WP were prepared as described as for $[Ca^{2+}]_i$ measurements (see Section 2.3.2), without the dye addition and loading steps for 45 minutes at 37°C, and platelets were re-suspended in 2-4mL of 0.32U/mL apyrase-containing nominally Ca^{2+} -free saline. Platelets were counted manually in a haemocytometer, and the cell counts of the platelet suspensions varied between 4.0×10^8 and 1.5×10^{12} platelets/mL. 500μL of platelets were warmed up in glass cuvettes to 37°C, and were added 9μM eptifibatide (integrilin) to prevent platelet aggregation. Lysis was performed at 60 seconds or 90 seconds after FcγRIIa stimulation (by cross-linking using 1μg/mL mAb IV.3 and 15μg/mL IgG F(ab')₂), by the addition of an equal volume of ice-cold 2x RIPA buffer (including 1x Roche protease inhibitor tablet, 4mM Sodium orthovanadate and 20mM Sodium fluoride). In samples where P2X1 channels were desensitised, 600nM α,β -meATP was added for 90 seconds before stimulation. $CaCl_2$ (2mM) was added to each cuvette at the beginning of each experiment, except for the samples in which P2X1 desensitisation was induced (in which case, $CaCl_2$ was added 60 seconds after α,β -meATP addition).

2.12.2 Bradford Assay

Protein quantification in the cell lysates was performed by a Bradford assay. A series of bovine serum albumin (BSA) concentrations (in mg/mL: 10, 8, 5, 2.5, 1.25, 0.625) were prepared in 1xRIPA buffer and 5μL of BSA or cell lysate was added in each well of a 96-well plate, with each sample assessed in triplicates. 250μL Bradford Reagent was then added to each well and incubated for 10 minutes on a rocking mixer, at room temperature. Absorbance values were measured at 595nm in an Infinite® M200 Plate Reader (Tecan, Switzerland), and the background-corrected mean absorbance values for each BSA concentration were used to construct a Bradford assay standard curve (Figure 2.6). The equation of the line of best fit was used to calculate the protein concentration in the lysates, corresponding to the mean absorbance values obtained for each lysate.

2.12.3 SDS-PAGE and Western blotting

Cell lysates were added an equal volume of 2x Laemmli sample buffer (Sigma) and heated up to 70°C in a heating block for 10 minutes, after the necessary protein concentration adjustment. For the detection of MS ion channels, 20µg of lysate was added in each well of a 7% polyacrylamide gel. For the phosphorylation assays, 20µg of lysate was added in each well of a 12-well Bolt™ 4-12% Bis-Tris Plus Gel (Invitrogen, Paisley, UK). Each gel included at least one lane of 10µL of Dual Color Precision Plus Protein™ Standard (10-250kDa, Bio-Rad, Hertfordshire, UK). Gels were run at 100V for 90 minutes, and for MS ion channel detection, the separated proteins were transferred onto a PVDF (polyvinylidene fluoride) membrane (Fisher Scientific, Loughborough, UK) by wet transfer technique in 1x Tris/Glycine transfer buffer at 100V for 60 minutes. For phosphorylation assays, semi-dry transfers onto PVDF membranes were performed using a Trans-Blot® Turbo™ Transfer System and Trans-Blot® Turbo™ RTA Mini LF PVDF Transfer Kit (Bio-Rad). After transfer, bands were visualised by staining with Ponceau-S solution to make sure the transfer was successful. Membranes were washed thoroughly in TBS-T, and blocked in 5% (w/v) skimmed milk prepared in TBS-T (Premier Foods, London, UK) on a roller mixer for 60 minutes at room temperature. Primary antibodies against the proteins of interest were prepared in TBS-T (Table 2.3), and added in 50mL falcon tubes with the membranes, and incubated at 4°C on a roller mixer overnight. The membranes were washed 3-6 times (5 minutes each) in 1xTBS-T to remove excess antibody and incubated with horseradish peroxidase (HRP)-conjugated secondary antibodies for 60 minutes at room temperature. Membranes were washed again 3-6 times (5 minutes each) in 1x TBS-T, and were treated with the Amersham™ Enhanced Chemiluminescence (ECL™) Prime kit (GE Healthcare, Buckinghamshire, UK) according to manufacturer's instructions. The membranes were assembled between two clean acetate sheets for imaging. The sheets containing the membranes were placed in a hyperfilm cassette, and hyperfilms (GE Healthcare, Buckinghamshire, UK) were exposed to the membranes in a dark room. Films were developed in a hyperfilm processor (GE Healthcare, Buckinghamshire, UK) and scanned for analysis.

| Antibody | Source | Type | Dilution and stock concentration | Company |
|----------------------------------|--------|------------|----------------------------------|------------------------------------|
| FAM38A (Piezo1) | Rabbit | Polyclonal | 1:2000 360µg/mL | Proteintech, Manchester, UK |
| FAM38B (Piezo2) | Rabbit | Polyclonal | 1:200 100µg/mL | Santa Cruz, Heidelberg, Germany |
| Anti-P2X1 | Rabbit | Polyclonal | 1:1000 800µg/mL | Alomone Labs, Jerusalem, Israel |
| Anti- α -tubulin | Mouse | Monoclonal | 1:1000 100µg/mL | Merck Millipore, Hertfordshire, UK |
| Anti-Phosphotyrosine, clone 4G10 | Mouse | Monoclonal | 1:1000 1mg/mL | Merck Millipore, Hertfordshire, UK |
| Phospho-Syk (Tyr525/526) | Rabbit | Monoclonal | 1:500 † | Cell Signaling, Danvers, MA, USA |
| Anti-LAT (Phospho Y200) | Rabbit | Monoclonal | 1:1000 † | Abcam, Cambridge, UK |
| Phospho-PLC γ 2 (Tyr1217) | Rabbit | Polyclonal | 1:250 † | Cell Signaling, Danvers, MA, USA |
| Anti-Rabbit HRP | Swine | Polyclonal | 1:10000 340µg/mL | Dako, Ely, UK |
| Anti-Mouse HRP | Goat | Polyclonal | 1:10000 1mg/mL | Dako, Ely, UK |

Table 2.3 The antibodies used in protein detection and phosphorylation assays.

† The antibodies were a gift from Prof Steve P Watson and only the working dilutions were provided.

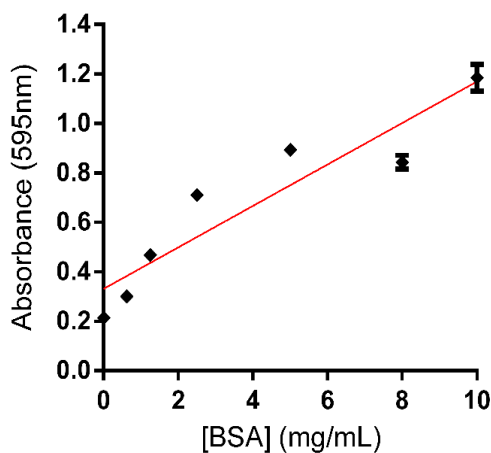


Figure 2.6 A representative Bradford assay standard curve of absorbance at 595nm against a series of known bovine serum albumin (BSA) concentrations. Data represent mean \pm SEM of 3 replicates for each concentration.

2.13 Sample preparation for Sanger sequencing

Primers were designed for Piezo1 and Piezo2 genes using the National Center for Biotechnology Information (NCBI) database primer design tool (Bethesda, MD, USA) (Table 2.4). Conventional end-point polymerase chain reaction (PCR) was carried out by preparing master mixes for each gene to be screened using 2x PuReTaq Ready-To-Go™ PCR Beads (GE Healthcare, Amersham, UK) dissolved in 12.5µL sterile water and 0.5µL of each of the forward and reverse primers. 11.5µL of master mix was added 1µL Meg-01 cDNA and the reaction was started under the following cycling conditions: 94°C (10min), 94°C (30sec), 35x [60°C (30sec)], 72°C (30sec), 72°C (10min) and final hold at 4°C. 1.8% agarose gel electrophoresis was performed as described in Section 2.11.3. EtBr-stained gels were placed in a UVItec ultraviolet (UV) transilluminator (UVItec Ltd., Cambridge, UK) to visualise the DNA and bands were excised from the gel with a scalpel and amplified DNA was purified using MinElute® Gel Extraction Kit (Qiagen, Hilden, Germany) according to manufacturer's protocol. Purified DNA was quantified using a Thermo Scientific NanoDrop™ 1000 Spectrophotometer (Waltham, MA, USA) and Sanger sequencing was carried out by the University of Leicester Protein Nucleic Acid Chemistry Laboratory (PNAACL) facility, using a high-throughput Applied Biosystems 3730 Genetic Analyser (Waltham, MA, USA). The sequences provided by the PNAACL facility have been accessed using the ChromasLite 2.1.1 software (Technelsiyum, South Brisbane, Australia), and the reverse complemented sequences have been exported in FASTA format into the Basic Local Alignment Search Tool (BLAST) available on the NCBI website (Bethesda, MD, USA) for alignment analysis with the original mRNA sequence obtained from the NCBI library. Alignment has been performed using the University of Virginia FASTA server available at <http://fasta.bioch.virginia.edu> (Pearson *et al.*, 1997).

2.14 Data analysis and statistics

All statistical analyses were performed using GraphPad Prism 6.0 software (La Jolla, California, USA). Ratiometric $[Ca^{2+}]_i$ measurements, platelet aggregation and ATP secretion raw data were processed on Origin 2015 Sr2 for Windows (OriginLab Corporation, Northampton, MA, USA), as described in Sections 2.9 and 2.10.3. In Chapters 3 and 4, one-way analysis of variance (ANOVA) followed by Tukey's *post*

hoc multiple comparison analyses or, paired Student's t-tests (two-tailed) were performed as appropriate. In Chapter 5, one-way ANOVA followed by Holm-Sidak's *post hoc* multiple comparisons, two-way ANOVA followed by Bonferroni's multiple comparisons tests, and paired Student's t-tests (two-tailed) were performed. All results are shown as the mean \pm standard error of the mean (SEM). In all experiments data represent 3-7 donors or cell line passages. P values of P<0.05 (*), P<0.01 (**), P<0.001 (***), and P<0.0001 (****) were considered statistically significant, whereas P>0.05 (ns) indicate no statistical significance.

| Gene | Ion channel | Primer Sequence (5'-3') | Product Size |
|--------|-------------|---|--------------|
| Fam38A | Piezo1 | F:TCGGCGCGGTCCTGT R:GTGTGACCTTGGAGGCCG | 150 |
| Fam38B | Piezo2 | F:GGCAGTAGCATGTGCATTCCG R:CTTCAAGGCTCACCAACGTG | 200 |

Table 2.4 *The forward (F) and reverse (R) primers designed to target Piezo1 and Piezo2 channels in Meg-01 cells for Sanger sequencing. The product sizes are given in base pairs.*

Chapter 3

Identification of mechanosensitive ion channels in platelets and Meg-01 cell line and a biophysical study of their contribution to function

3.1 Introduction

The crucial roles of MS ion channels have been well-established in biological systems where mechanical stimuli, such as shear stress and stretch, need to be detected and converted into biological signals. Of particular importance, MS ion channels are expressed on cells and tissues which come in direct contact with such physical stimuli, such as endothelial cells and the vasculature (Wang *et al.*, 2016; Allison, 2016; Ranade *et al.*, 2014a; Li *et al.*, 2014). Despite platelets being exposed to mechanical forces of shear within the circulation, and the molecular mechanisms behind platelet adhesion and activation are shear-stress reliant (Schneider *et al.*, 2007), there is no evidence for MS ion channel expression and function in human platelets. Preliminary proteomic and transcriptomic studies have revealed Piezo1 and Piezo2 cation channels as the only MS ion channel candidates in the human platelets and megakaryocytic cell lines (Wright *et al.*, 2016; Boyanova *et al.*, 2012; Burkhart *et al.*, 2012). In addition, the thrombin and OAG-activated Ca²⁺-permeable ion channel TRPC6 was demonstrated to be functional in human platelets and responsive to membrane stretch in smooth muscle cells (Spasova *et al.*, 2006; Hassock *et al.*, 2002). Potentially, the involvement of such ion channels in the process of platelet activation could provide a mechanism for more direct mechanical activation of platelet signalling events (Kroll *et al.*, 1996).

The study of ion channels function in platelets have, in part, relied upon surrogate patch-clamp recordings from megakaryocytic cells (Mahaut-Smith, 2012). Piezo1 ion channel transcripts were detected in both human platelets and the Meg-01 cell line. The experimental results described in this chapter aim to engineer a novel approach which would allow the study of the contribution of MS cation channels to [Ca²⁺]_i in Meg-01 cells initially, which were used as an alternative system for studies of platelet signalling events (Mahaut-Smith, 2012; Ogura *et al.*, 1985). Using microfluidic flow chambers to apply fluid shear stress, it was shown that Piezo1 MS channels can operate in response to this type of shear stress in HUVECs (Li *et al.*, 2014). Other types of assays most commonly used to mechanically stimulate Piezo channels in cell-based assays and patch-clamp studies include osmotic (hypotonic) challenge or silicone stret-

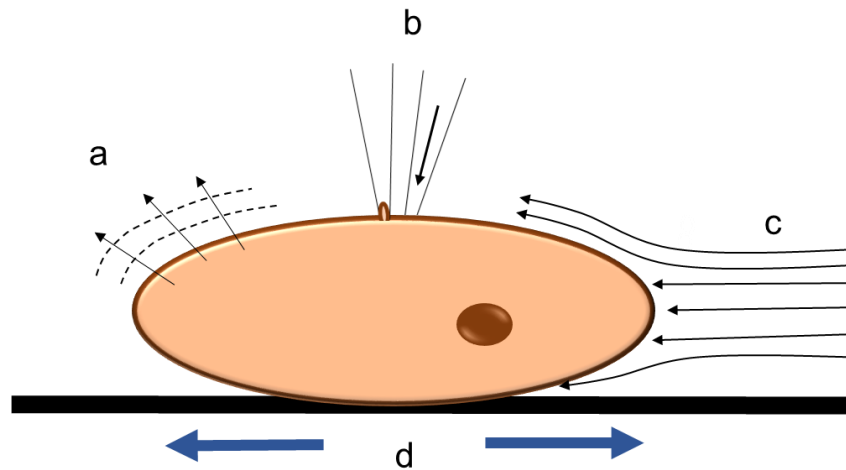


Figure 3.1 Most commonly used methods of mechanical stimulation in the studies of Piezo channel function. (a) Hypotonic swelling; (b) whole-cell patch recording during application of membrane deformation with a probe; (c) fluid shear stress; (d) stretch of cells seeded on a silicon surface. [Adapted from (Delmas *et al.*, 2011)]

ch chambers to induce membrane stretch, or the use of piezo-electrically driven glass probes to induce membrane deformation during whole cell patch-clamp recording (Figure 3.1) (Schrenk-Siemens *et al.*, 2015; Miyamoto *et al.*, 2014; Coste *et al.*, 2010). Provided the physiological link between platelet function and fluid shear stress in the circulation, and the evidence that Piezo1 plays a key role in cell volume regulation in red blood cells which arise from a common myeloid progenitor cell as platelets (Cahalan *et al.*, 2015; Faucherre *et al.*, 2014; Zarychanski *et al.*, 2012), this study will attempt to test and incorporate fluid shear stress and hypotonic challenge approaches to stimulate MS ion channels in different cell-based assays.

This chapter will confirm the identity and assess the expression levels of the previously detected MS cation channels in human platelets and the Meg-01 cell line at the mRNA and protein levels. A suitable adhesion protocol will be devised that would allow the application of shear stress over Meg-01 cells loaded with the Ca^{2+} indicator dye, Fluo-3, within a flow chamber to monitor shear stress-dependent Ca^{2+} entry. In these assays, Meg-01 cells will be treated with the MS cation channel inhibitor, GsMTx-4, to study MS cation channel function. Furthermore, alternative mechanical stimulation techniques will be investigated in the study of MS ion channel function in Meg-01 cells and human platelets.

3.2 Results

3.2.1 Human platelets and Meg-01 cells express Piezo1 mRNA and protein

Within a transcriptomic screen of human platelets for all known ion channels, Piezo1 (Fam38A) and TRPC6 were the only MS cation channels detected (Wright *et al.*, 2016). Piezo1 was detected at trace levels in this recent study, thus the qRT-PCR assay was repeated using a larger sample volume. In these purified platelet samples, quantifiable levels of Fam38A were detected, but not the related family member Fam38B, encoding Piezo2 (Figure 3.2 A). In agreement with the previous study, Meg-01 cells were found to express higher levels of Fam38A transcripts compared to platelets and to also express Fam38B (Figure 3.2 A). Agarose gel electrophoresis performed using the qRT-PCR end products confirmed that these target genes were the only ones amplified. Band intensities obtained confirm that Piezo1 mRNA is expressed at higher levels in Meg-01 cells than in platelets, and Piezo2 mRNA is abundantly expressed in Meg-01 cells but not in platelets (Figure 3.2 B). In contrast, TRPC6 mRNA was not detected in Meg-01 cells although it was present in platelets as reported previously (Hassock *et al.*, 2002) (Figure 3.2 A).

To further assess the identity of the channels detected with QuantiTect primers for Piezo1 and 2, Sanger sequencing was performed on the amplified PCR products. New primers were designed targeting Piezo1 and Piezo2 genes because the sequences of the bioinformatically-validated QuantiTect Primer pairs used in the qRT-PCR experiments were not provided by the producer. This was because primer sequence information was required by the PNAOL facility in order to perform sequencing. The new primers successfully detected Piezo1 and Piezo2 mRNA in the Meg-01 cells but failed to do so in platelets (Figure 3.3 A). This was possibly due to the lower efficiency of the newly designed primers in detecting the target genes which are expressed at very low levels in platelets. Therefore, Sanger sequencing could only be performed on the bands obtained in Meg-01 cells. Obtained sequences for Piezo1 and Piezo2 were aligned with the known sequences stored on the NCBI library and % sequence identity for each gene was provided (95.3% and 96.2%, respectively) (Figure 3.3 B). The % sequence identities were less than 100% because of scrambled signals observed at the beginning and the end of the sequences obtained, arising mainly due to the non-stringent nature of the analysis.

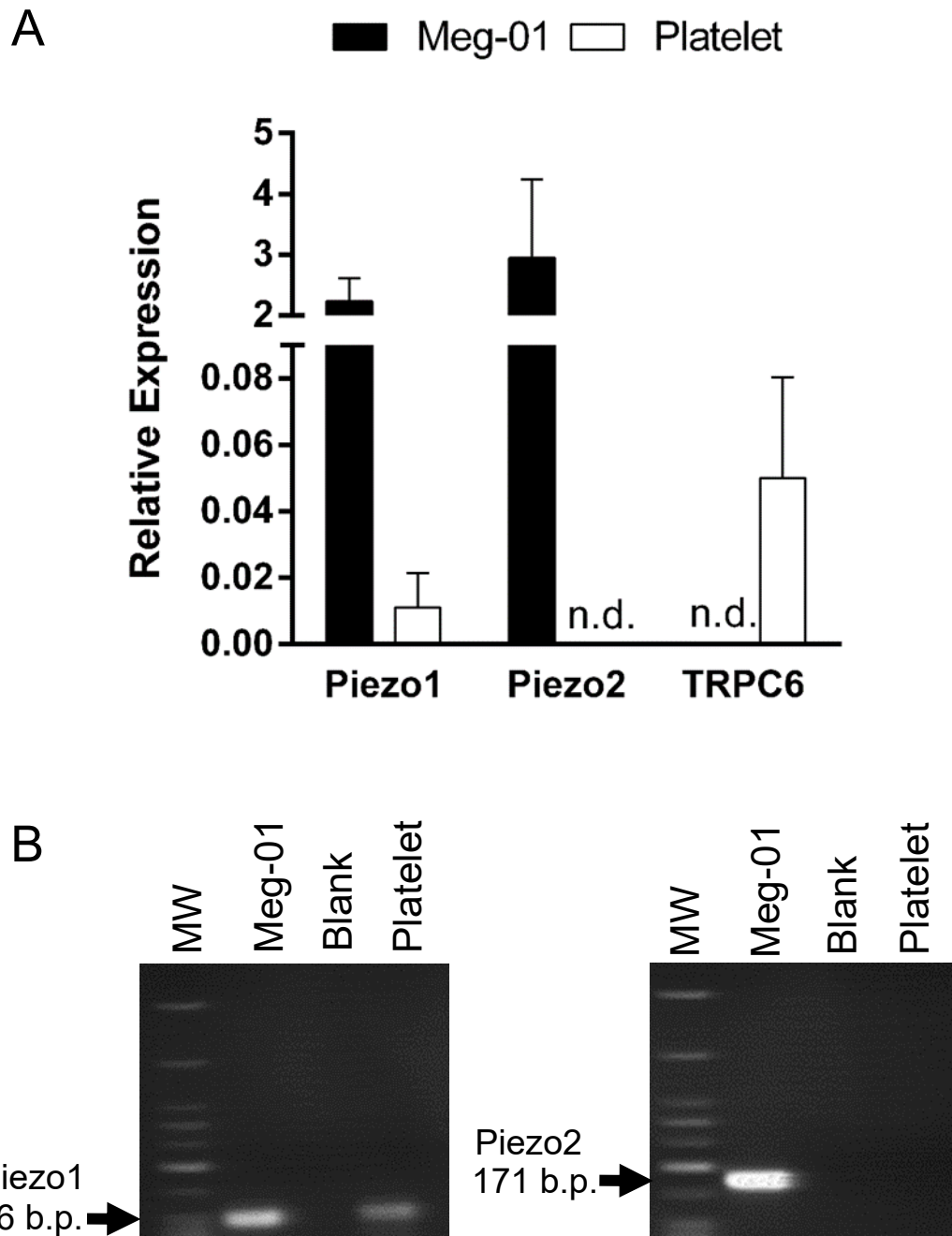


Figure 3.2 *Mechanosensitive ion channel mRNA expression in human platelets and the Meg-01 cell line.* (A) Relative expression of mRNA transcripts for three MS cation channels (Piezo1, Piezo2 and TRPC6) in human platelets and the Meg-01 cell line, relative to GAPDH. n.d. = not detected. (B) The qRT-PCR reaction end products visualised by agarose gel electrophoresis. The blank lanes lacked mRNA during amplification. b.p.= base pairs. In each image, 'Meg-01' and 'Platelet' refer to qRT-PCR experiments performed using a Meg-01 passage or a platelet donor, representative of experiments using three passages or donors. MW: molecular weight marker. Data represents mean \pm SEM ($n=3$ individual donors).

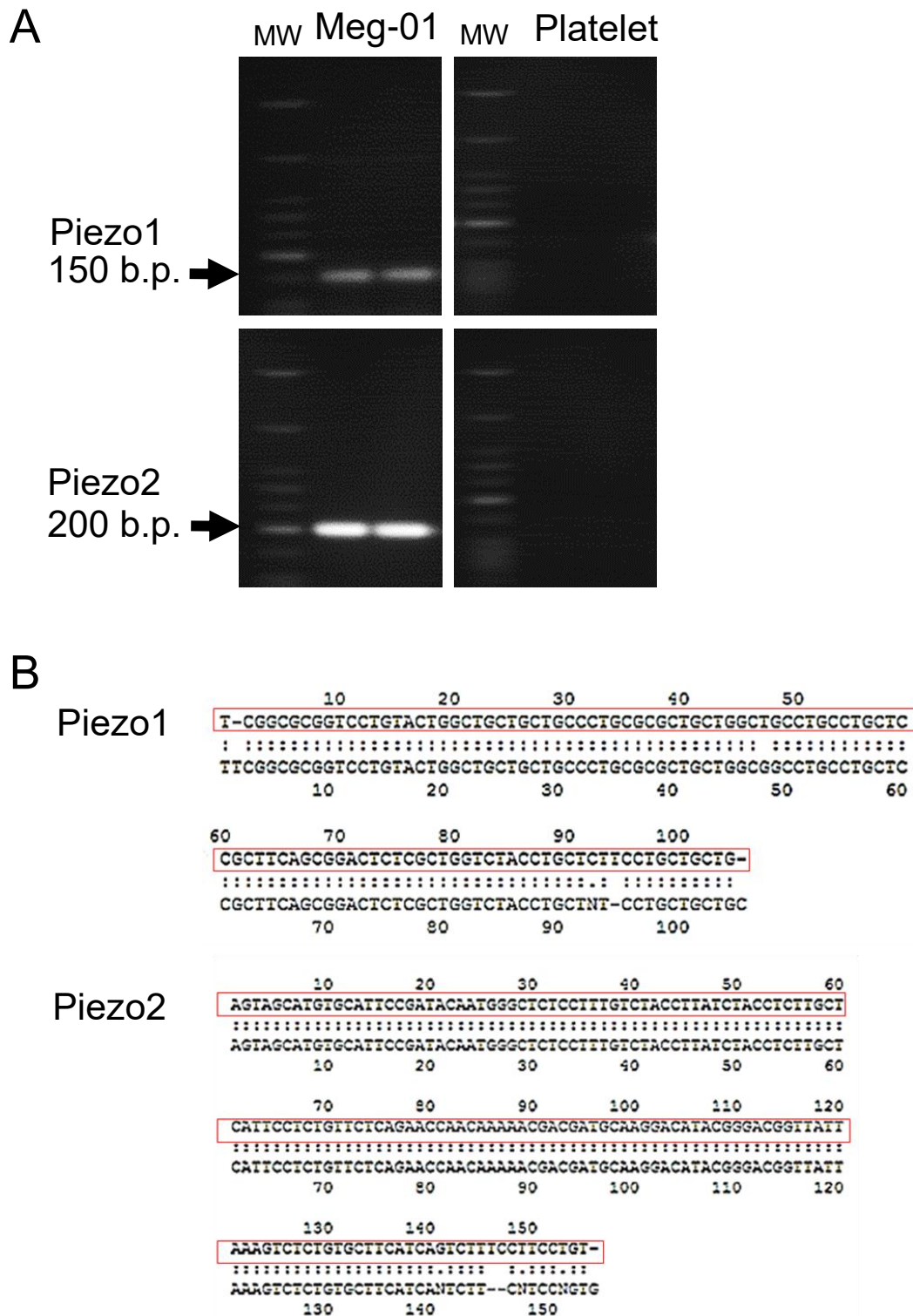


Figure 3.3 PCR amplification products obtained using in-house designed primer pairs of known sequence, and the sequence alignment following Sanger sequencing. (A) The PCR reaction end products visualised by agarose gel electrophoresis were excised from the gels and sequenced. b.p.= base pairs. No product was detected in platelet samples. The end products were run in duplicates. (B) The comparison of the original mRNA sequence from NCBI (enclosed in red) with obtained sequences for Piezo1 and Piezo2 in Meg-01 samples. MW: molecular weight marker.

(...) approximate sizes of the bands obtained by comparing against the molecular weight marker lane in each blot (not shown).

Piezo1 protein was also detected using Western blotting in both cell types and this further suggested a lower level of expression in platelets compared to Meg-01 (Figure 3.4 A). The opposite order of expression was observed for P2X1 protein in the two cell types, which was included as a positive control ion channel target in platelet lysates (Figure 3.4 A). Although three alternatively spliced forms of Piezo2 protein were detected in Meg-01 cells, no bands were detected in platelet lysates (Figure 3.4 B) in agreement with the lack of Piezo2 mRNA (Figure 3.2 A).

3.2.2 Meg-01 cells attached on poly-D-lysine-coated surfaces are suitable for Ca²⁺ imaging under arterial flow

Fluid shear stress is the most physiologically relevant method to mechanically stimulate MS cation channels on human platelets. The development of a fluid shear stress assay suitable for monitoring changes in [Ca²⁺]_i in Meg-01 cells under shear involves the attachment of cultured Meg-01 cells onto glass coverslips using a suitable surface coating. Two main criteria were considered when selecting the best coating material to use:

1. Cell adhesion should be sufficiently strong to withstand high levels of fluid flow within the arterial shear stress range (1002.6 - 3989.2 s⁻¹) for the duration of an experiment (~8 minutes).
2. The coating material should not result in intracellular signalling, cause Ca²⁺ mobilisation, or shape change/spreading upon cell attachment.

Materials most commonly used in cell adhesion studies (poly-L lysine, poly-D-lysine, collagen, fibronectin, and gelatin) were used to coat glass coverslips (Heino, 2007; Li *et al.*, 2005; Carlsson *et al.*, 1981; Mazia *et al.*, 1975), and the strength of attachment was tested by exposing the attached cells to high levels of arterial shear stress (3989.2 s⁻¹) for 8 minutes. Qualitative observations were recorded (Table 3.1) and representative

images of attached cells were captured (Figure 3.5). Meg-01 cells grow in suspension and are non-adherent in nature (Ogura *et al.*, 1985), thus it is not surprising that no coating material provided optimal attachment conditions which could support attachment of a large number of cells. However, poly-D-lysine (0.1%; mw >300,000) was found to be the most suitable coating compared to lower molecular weight types or poly-L-lysine, since it provided sufficiently firm attachment for a small percentage of cells compared to lower molecular weight types or poly-L-lysine, and caused no observable morphological changes in the attached cells (Table 3.1 and Figure 3.5 C). 100µg/mL of collagen (Horm) or fibronectin caused significant morphological changes, and hence were not studied further (Figure 3.5 A, B).

| Coating | Observation |
|--|---|
| 0.1% Poly-L-lysine hydrobromide (70,000-150,000) | Less than ~20% attach weakly, which detach upon flow. |
| 0.1% Poly-D-lysine hydrobromide (70,000-150,000) | Less than ~20% attach weakly, which detach upon flow. |
| 0.1% Poly-D-lysine hydrobromide (≥300,000) | Less than ~25% attach weakly, most of which detach upon flow (Figure 3.5 C). |
| 0.1% Poly-D-lysine hydrobromide (70,000-150,000) + 1 mg/mL Laminin | Less than ~20% attach weakly, which detach upon flow. |
| 100µg/mL Collagen (Horm) | Morphological changes: lamellipodia formation and extensive spreading (Figure 3.5 A). |
| 100µg/mL Fibronectin | Morphological changes: lamellipodia formation and extensive spreading (Figure 3.5 B). |
| 0.02% Gelatin | No attached cells observed. |

Table 3.1 Various coating materials used to attach Meg-01 cells and the qualitative observations made in cell morphology and strength of cell attachment under arterial shear stress. The row highlighted in green indicates the best attachment material for Meg-01 cells, and hence was used in the rest of the experiments presented in this chapter.

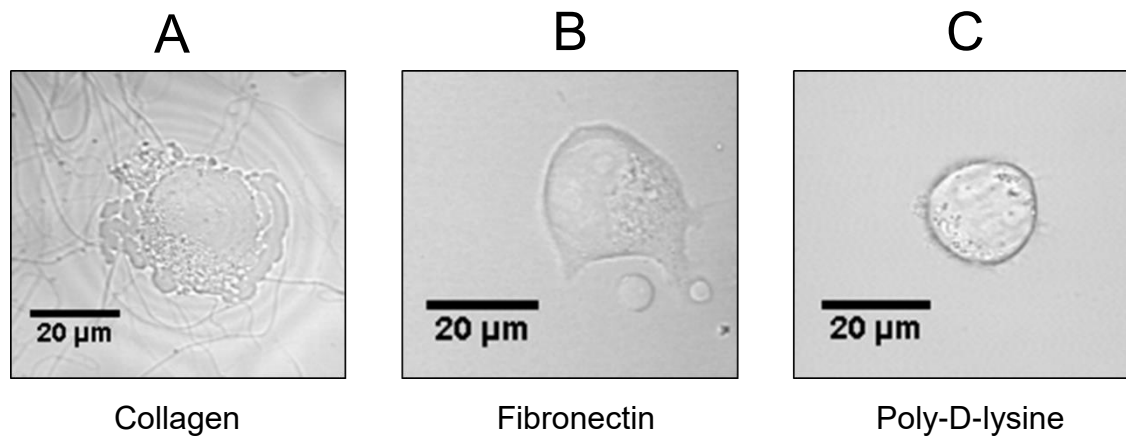


Figure 3.5 Representative bright field images of Meg-01 cells attached on various coating materials. Attachment on 100µg/mL collagen (A), or 100µg/mL fibronectin (B) caused substantial morphological changes such as blebbing and formation of lamellipodia. (C) 0.1% poly-D-lysine hydrobromide ($\geq 300,000$) caused no observable morphological changes.

Poly-lysine (L and D) is known to provide a positively charged surface and promotes cell attachment via interaction with the negatively charged components of the cell membrane. In order to test whether this method of cell attachment is still compatible with the study of Ca^{2+} mobilisation events, Fluo-3-loaded Meg-01 cells were attached to poly-D-lysine-coated glass coverslips and changes in Fluo-3 signal were monitored before and after the addition of the ionophore, ionomycin (1µM) to facilitate Ca^{2+} influx (Figure 3.6). Attachment to poly-D-lysine caused no Ca^{2+} mobilisation during the first 3 minutes of the experiment and the F/F_0 value was stable at background levels (1.0 ± 0.0) (Figure 3.6 B). After 3 minutes (at 180s), the introduction of ionomycin into the chamber via trituration and mixing by gentle pipetting resulted in a sharp increase in the Fluo-3 signal (Figure 3.6 A, B). The results of this experiment indicated that Meg-01 attachment to poly-D-lysine *per se* does not induce Ca^{2+} mobilisation, and Ca^{2+} mobilisation can be accurately monitored in attached cells.

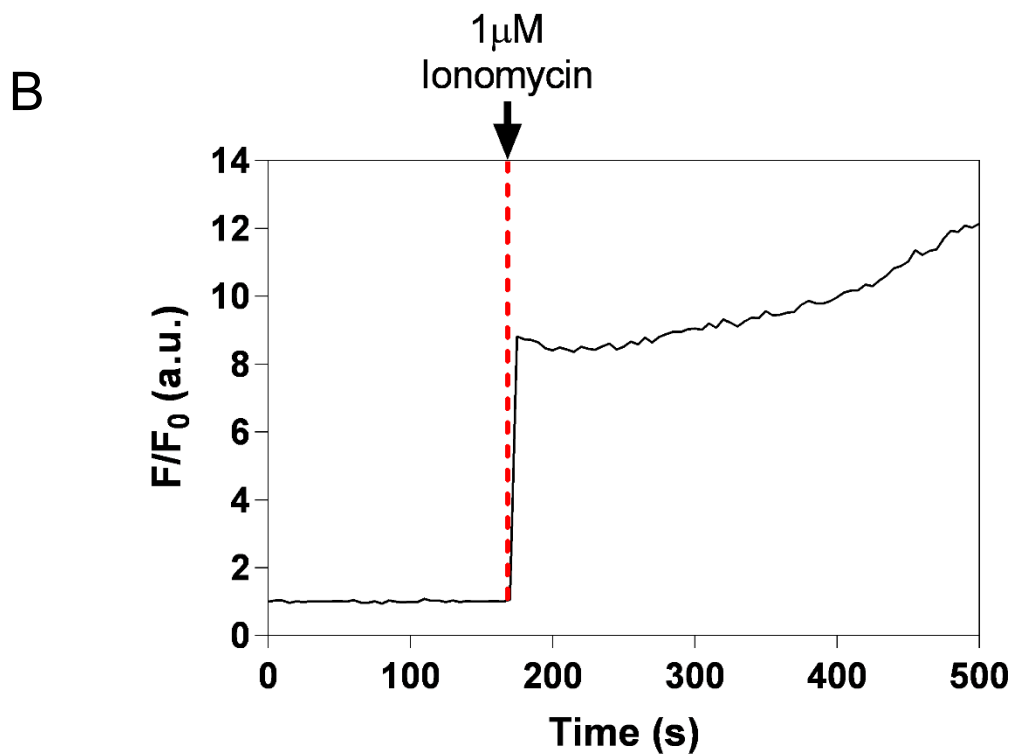
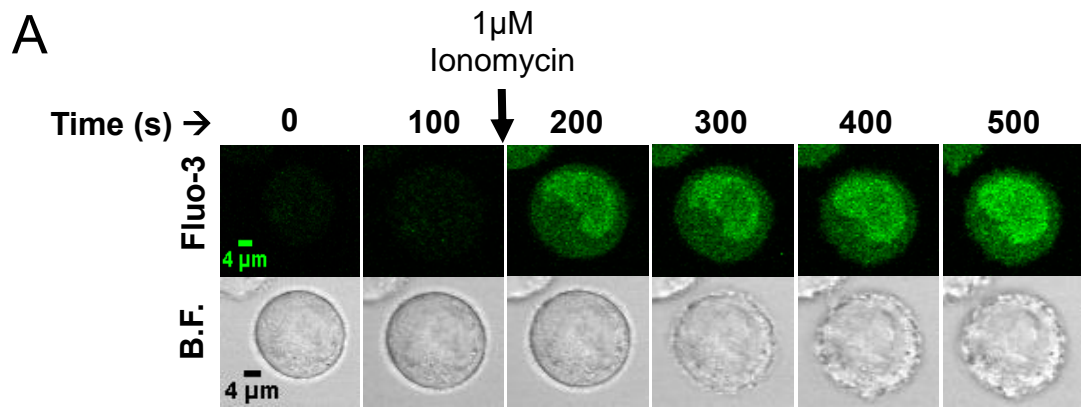


Figure 3.6 Monitor of Ca^{2+} mobilisation in attached Meg-01 cells. Representative images (A) and F/F_0 fluorescence recording (B) of single Meg-01 cells attached to poly-D-lysine, before and after ionomycin-induced Ca^{2+} entry. Attachment to poly-D-lysine does not induce Ca^{2+} mobilisation per se, however, Ca^{2+} entry following ionomycin treatment can be monitored in attached Fluo-3-loaded cells.

3.2.3 *Meg-01 cells display GsMTx-4-sensitive fluid shear stress-dependent $[Ca^{2+}]_i$ increases*

Meg-01 cells express several platelet lineage surface markers and have been used as a model for signalling in megakaryocytes and platelets (Mahaut-Smith, 2012; Ogura *et al.*, 1985). The outcomes of the cell attachment optimisation experiments explained in Section 3.2.2 provided a suitable protocol for Meg-01 cells attachment for the monitoring of $[Ca^{2+}]_i$ under arterial flow conditions. Therefore, this section investigated the effect of applied shear stress on $[Ca^{2+}]_i$ in this megakaryoblastic cell line as a first step to address the hypothesis that MS cation channels contribute to platelet responses. When 1.26mM Ca^{2+} -containing saline (HBSS) was applied at increasing arterial shear rates to Meg-01 cells attached to a glass coverslip, increases in the Fluo-3 signal were observed of a magnitude that correlated with the size of the shear force applied (Figure 3.7 A and 3.8 A): F/F_0 increased from 1.0 ± 0.0 at no shear ($0.0s^{-1}$), to 1.1 ± 0.0 , 1.2 ± 0.0 , and 1.4 ± 0.1 at normal arterial ($1002.6s^{-1}$), stenotic (low) ($2282.7s^{-1}$), and stenotic (high) ($3989.3s^{-1}$) shear rates, respectively (Figure 3.9 A).

In the absence of extracellular Ca^{2+} ($0 Ca^{2+}$, 1mM EGTA saline) shear-dependent increases in the Fluo-3 signal were abolished except for a small, residual response ($F/F_0=1.12 \pm 0.06$) at the highest flow rate (Figure 3.7 B and 3.8 B middle panels, and 3.9 B). Pre-treating the attached Meg-01 cells with $2.5\mu M$ GsMTx-4 and the inclusion of GsMTx-4 in the applied saline abolished all increases in Fluo-3 signal in response to applied shear stress (Figure 3.7 C and 3.8 C, and 3.9 B). These findings suggest that Meg-01 cells possess MS cation channels on their plasma membrane, which sense and respond to fluid shear stress by mediating Ca^{2+} influx from the extracellular environment.

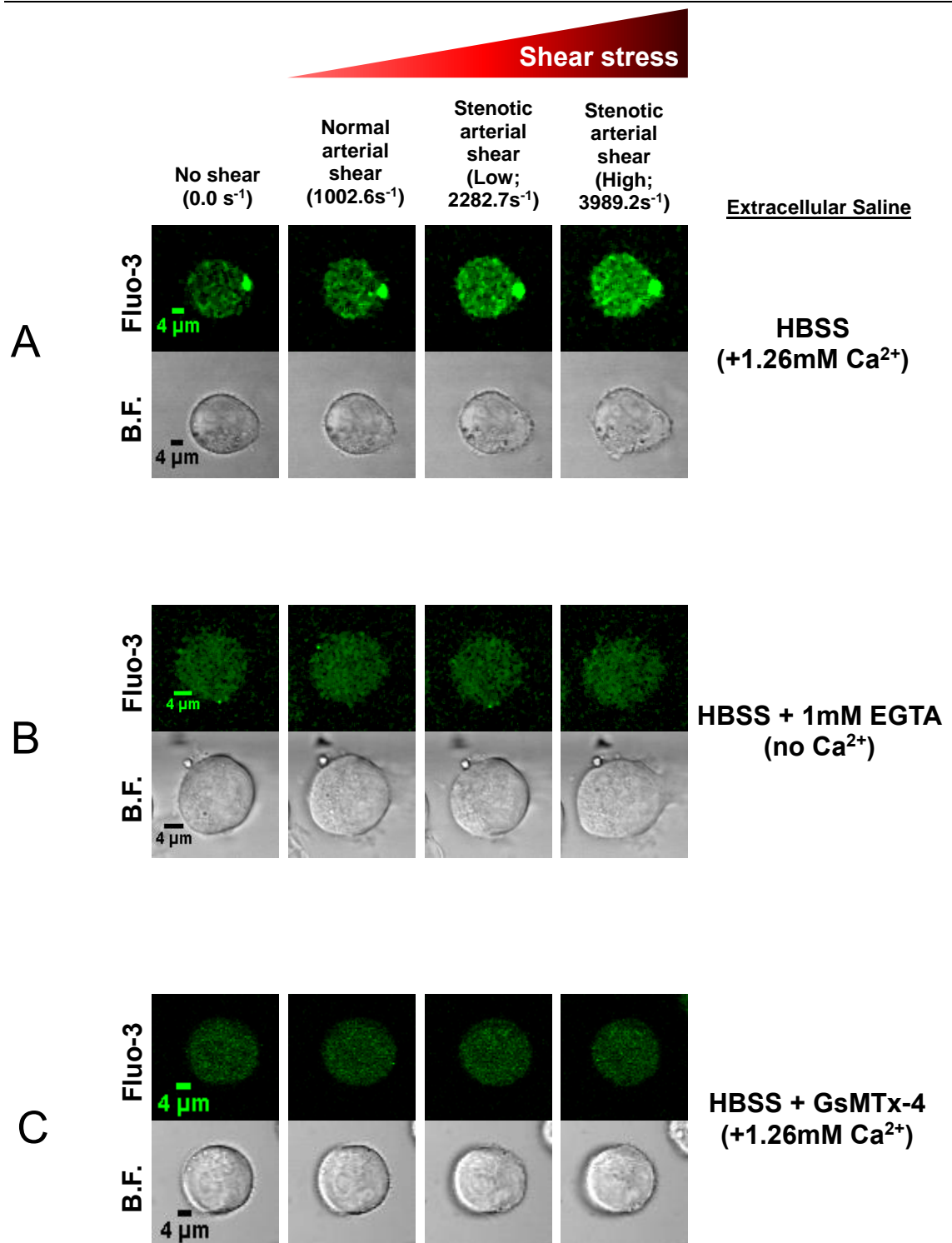


Figure 3.7 Fluid shear stress-dependent Ca^{2+} influx in Meg-01 cells is inhibited by GsMTx-4 and chelation of extracellular Ca^{2+} . Representative images of single Meg-01 cells exposed to normal arterial and two levels of stenotic shear in Hanks' balanced salt solution (HBSS) with Ca^{2+} (A), without Ca^{2+} (EGTA) (B), and with GsMTx-4 ($2.5\mu\text{M}$) in the presence of Ca^{2+} (C). F/F_0 traces obtained for the representative cells are shown in Figure 3.8.

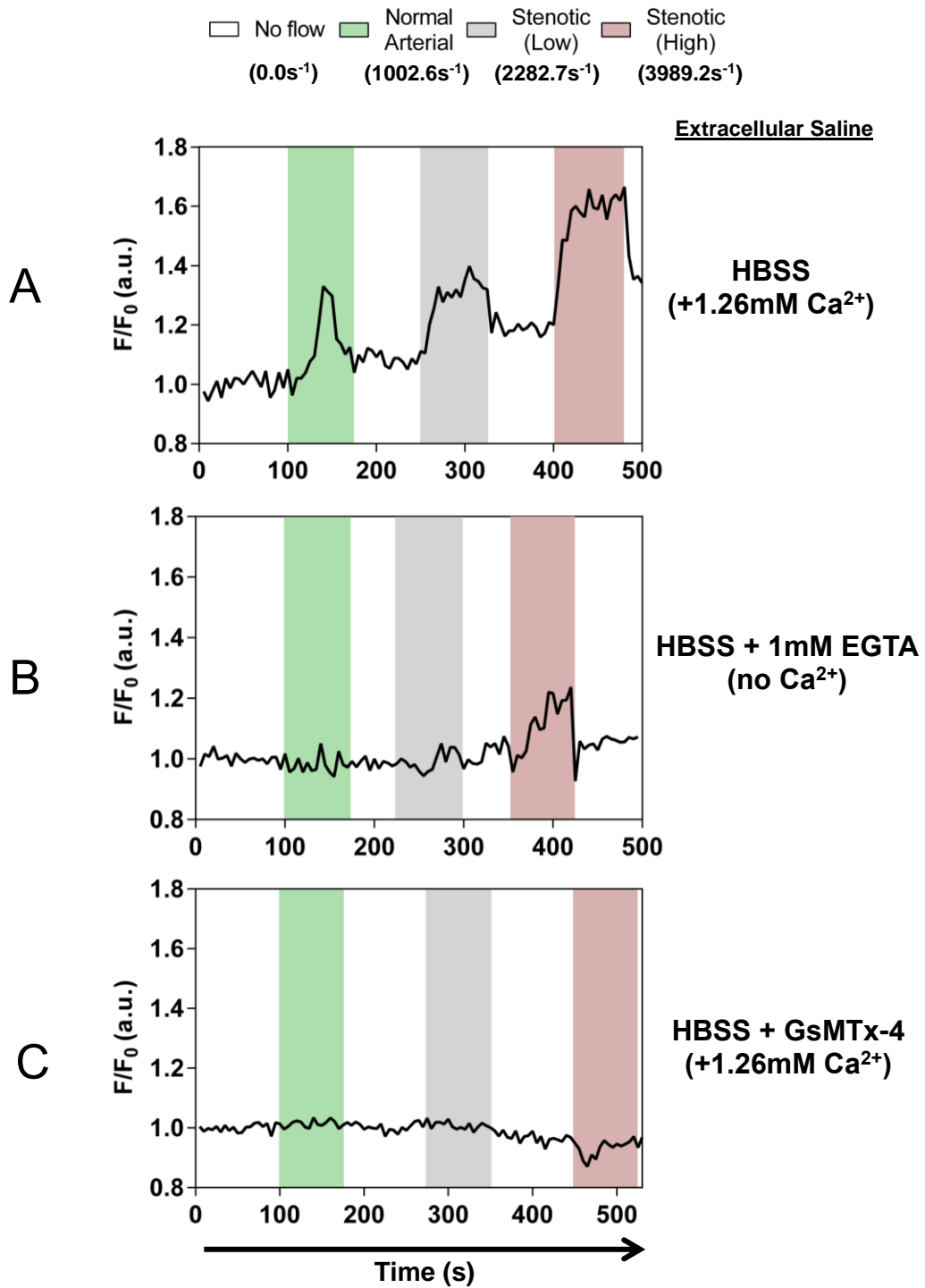


Figure 3.8 Fluid shear stress-dependent Ca²⁺ influx in Meg-01 cells is inhibited by GsMTx-4 and chelation of extracellular Ca²⁺. Representative F/F₀ fluorescence recordings of single Meg-01 cells (shown in Figure 3.7) exposed to normal arterial and two levels of stenotic shear in Hanks' balanced salt solution (HBSS) with Ca²⁺ (A), without Ca²⁺ (EGTA) (B), and with GsMTx-4 (2.5μM) in the presence of Ca²⁺ (C).

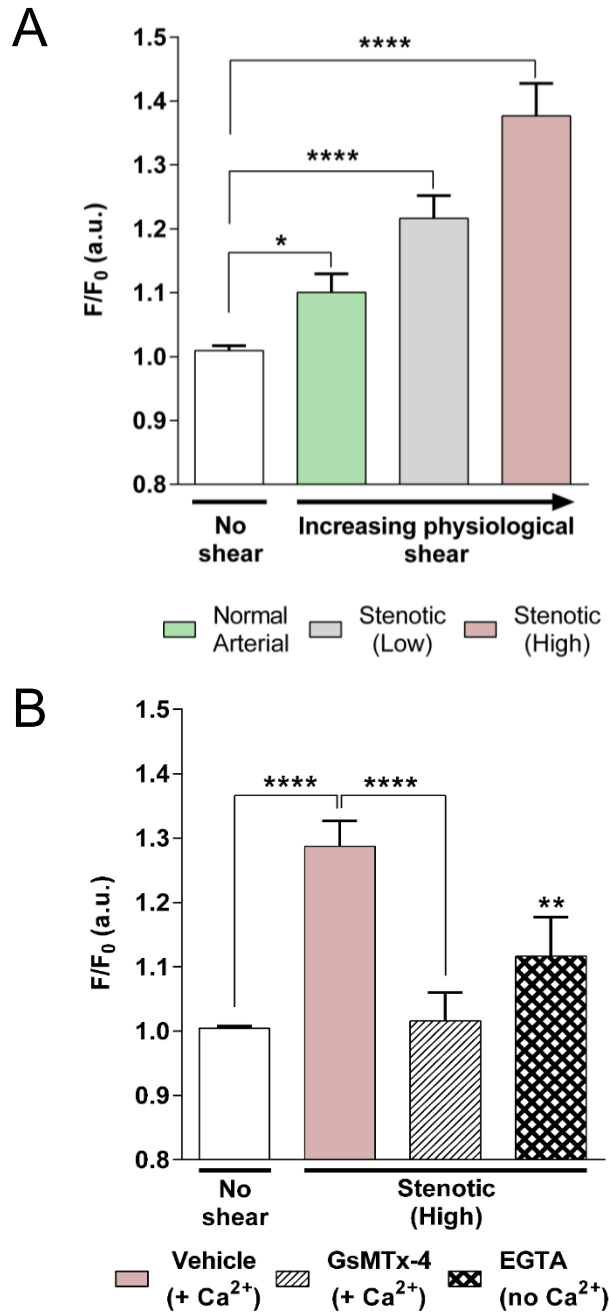


Figure 3.9 Fluid shear stress induces incremental cytosolic Ca²⁺ increases in Meg-01 cells which are inhibited by GsMTx-4 and chelation of extracellular Ca²⁺. (A) Average peak F/F₀ increases (n=53 cells) in response to increasing arterial shear levels in the presence of 1.26mM extracellular Ca²⁺. (B) Average peak F/F₀ increases under no flow conditions and at the high stenotic shear rate with and without extracellular Ca²⁺, and with 2.5μM GsMTx-4 in the presence of Ca²⁺ (n=51 cells); *P<0.05; **P<0.01 (compared to vehicle treated high stenotic levels); ****P<0.0001. Data represent mean ± SEM.

3.2.4 HUVECs display GsMTx-4-sensitive fluid shear stress-dependent $[Ca^{2+}]_i$ increases

Microfluidic flow chambers have been used to demonstrate that Piezo1 channels mediate Ca^{2+} entry in HUVECs in response to fluid shear stress within the normal arterial range (10-15 dynes/cm²) (Li *et al.*, 2014; Mongrain & Rodes-Cabau, 2006). Application of increasing levels of arterial shear stress to HUVECs within the same flow chamber system as that used to study MS Ca^{2+} influx in Meg-01 cells (*see above*) also induced elevations in $[Ca^{2+}]_i$, which were abolished by GsMTx-4 (Figure 3.10, and Figure 3.11 A upper panel). In 1.26mM Ca^{2+} -containing saline (HBSS), the F/F_0 of HUVECs increased from 1.0 ± 0.0 at no shear ($0.0s^{-1}$), to 1.8 ± 0.3 at the stenotic (high) ($3989.3s^{-1}$) shear rate (Figure 3.11 B). The $[Ca^{2+}]_i$ response to stenotic (high) shear was completely blocked 2.5 μ M GsMTx-4 (F/F_0 of 1.0 ± 0.1 ; Figure 3.11 B). Therefore, fluid shear stress-dependent elevations in $[Ca^{2+}]_i$ are observed in both HUVECs and Meg-01 cells, which are both known to express Piezo1 channels and these responses are similarly inhibited by the MS ion channel inhibitor, GsMTx-4.

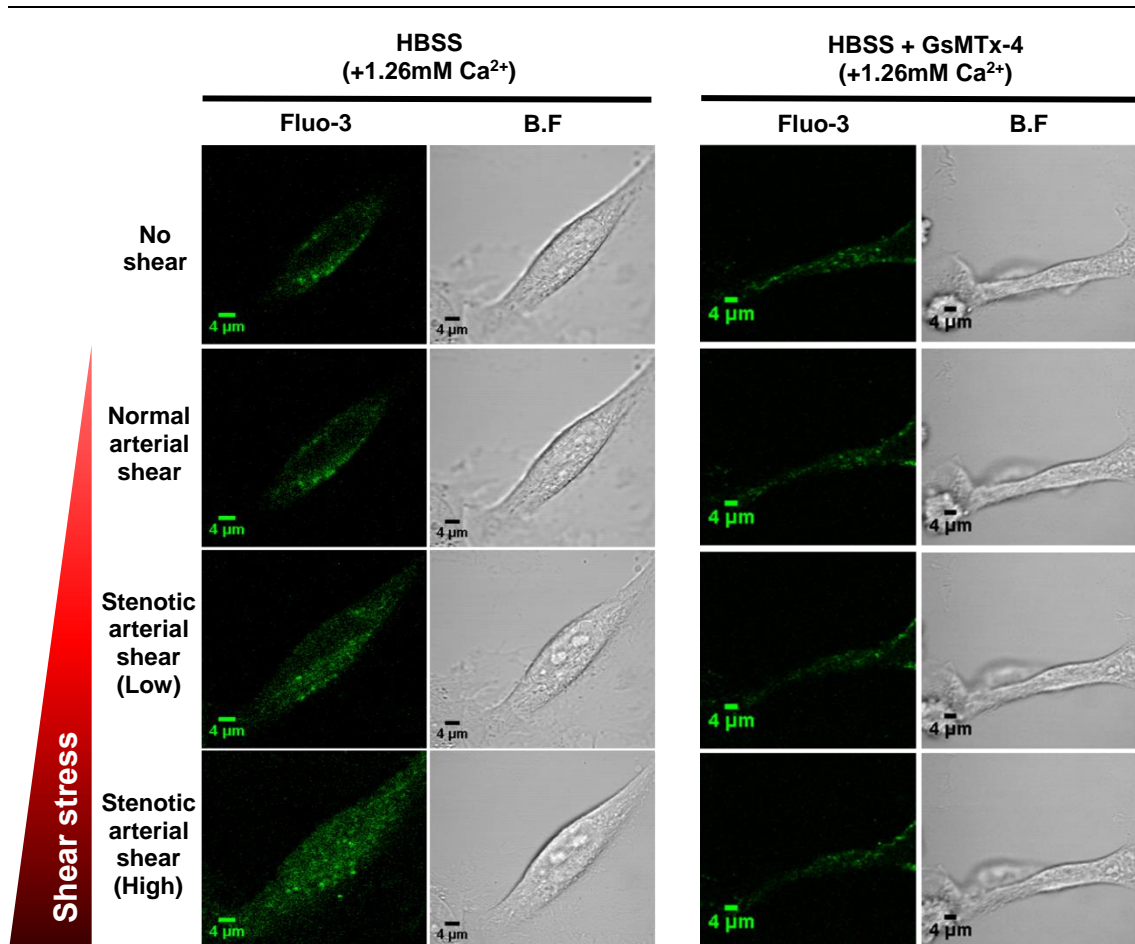


Figure 3.10 Fluid shear stress-dependent Ca²⁺ influx in HUVECs is inhibited by GsMTx-4. Representative images of single HUVECs exposed to normal arterial and two levels of stenotic shear in Hanks' balanced salt solution (HBSS) with Ca²⁺ (left panel), and with 2.5μM GsMTx-4 in the presence of 1.26mM Ca²⁺ (right panel).

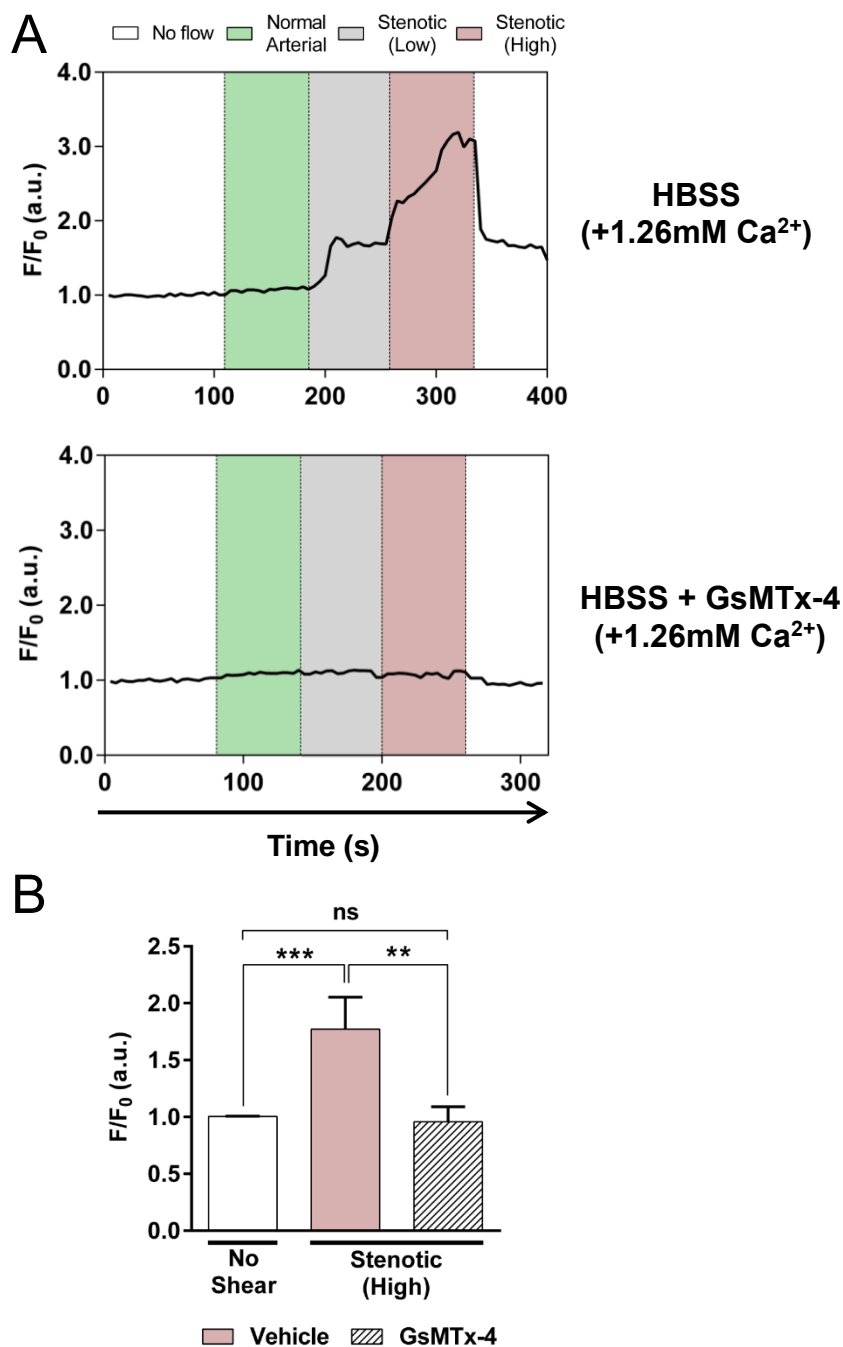


Figure 3.11 Shear stress induced increases in $[Ca^{2+}]_i$ in HUVECs are inhibited by GsMTx-4. (A) Representative F/F_0 recordings from single Fluo-3-loaded HUVECs in HBSS containing 1.26mmol/L Ca^{2+} , in the absence (top panel) and presence (lower panel) of 2.5 μ M GsMTx-4. (B) Average F/F_0 increases induced by high stenotic shear rate in the presence and absence of 2.5 μ M GsMTx-4 compared to no flow conditions (Data represent mean \pm SEM; $n=14-28$ cells for each condition measured in 3 different HUVEC cultures); *** $P < 0.001$; ** $P < 0.01$; ns (not significant).

3.2.5 Hypotonic challenge does not induce observable $[Ca^{2+}]_i$ increases in platelets and Meg-01 cells

Previous studies have provided the evidence that Piezo1 plays a key role in cell volume regulation in red blood cells (Cahalan *et al.*, 2015; Faucherre *et al.*, 2014; Zarychanski *et al.*, 2012). Therefore, this section tests the hypothesis that hypotonic swelling (Figure 3.1 a) in Meg-01 cells or platelets can operate MS ion channels through plasma membrane stretch (Figure 3.12 A). Platelet hypotonic shock responses were studied previously, where hypotonic stress was induced by the addition of an equivalent volume of ddH₂O into platelet suspensions (Farrugia *et al.*, 1989). Therefore, $[Ca^{2+}]_i$ were monitored by ratiometric Ca^{2+} measurements in Fura-2-loaded Meg-01, as well as platelet cell suspensions during exposure to a hypotonic challenge by the addition of ddH₂O. The addition of 2mL ddH₂O into 2mL cell suspensions containing Ca^{2+} resulted in a small transient increase in $[Ca^{2+}]_i$ in Meg-01 cells which was not abolished by GsMTx-4 pre-treatment (Figure 3.12 B). Interestingly, no clear hypotonically-activated elevation in $[Ca^{2+}]_i$ was observed in platelet suspensions (Figure 3.12 C). In all Meg-01 and platelet experiments, there was a slow and gradual rise in the $[Ca^{2+}]_i$ signal, which was abolished by the chelation of extracellular Ca^{2+} by 4mM EGTA, indicating Fura-2 dye leakage from the loaded cells which interacted with extracellular Ca^{2+} (Figure 3.12 B and C). Chelation of Ca^{2+} by EGTA will lead to proton release (Riley & Pfeiffer, 1986), thus 4mM Tris-Base was added in the cuvettes at the end to prevent acidic shifts in pH. No pH-dependent change in Ca^{2+} responses were observed (Figure 3.12 B and C).

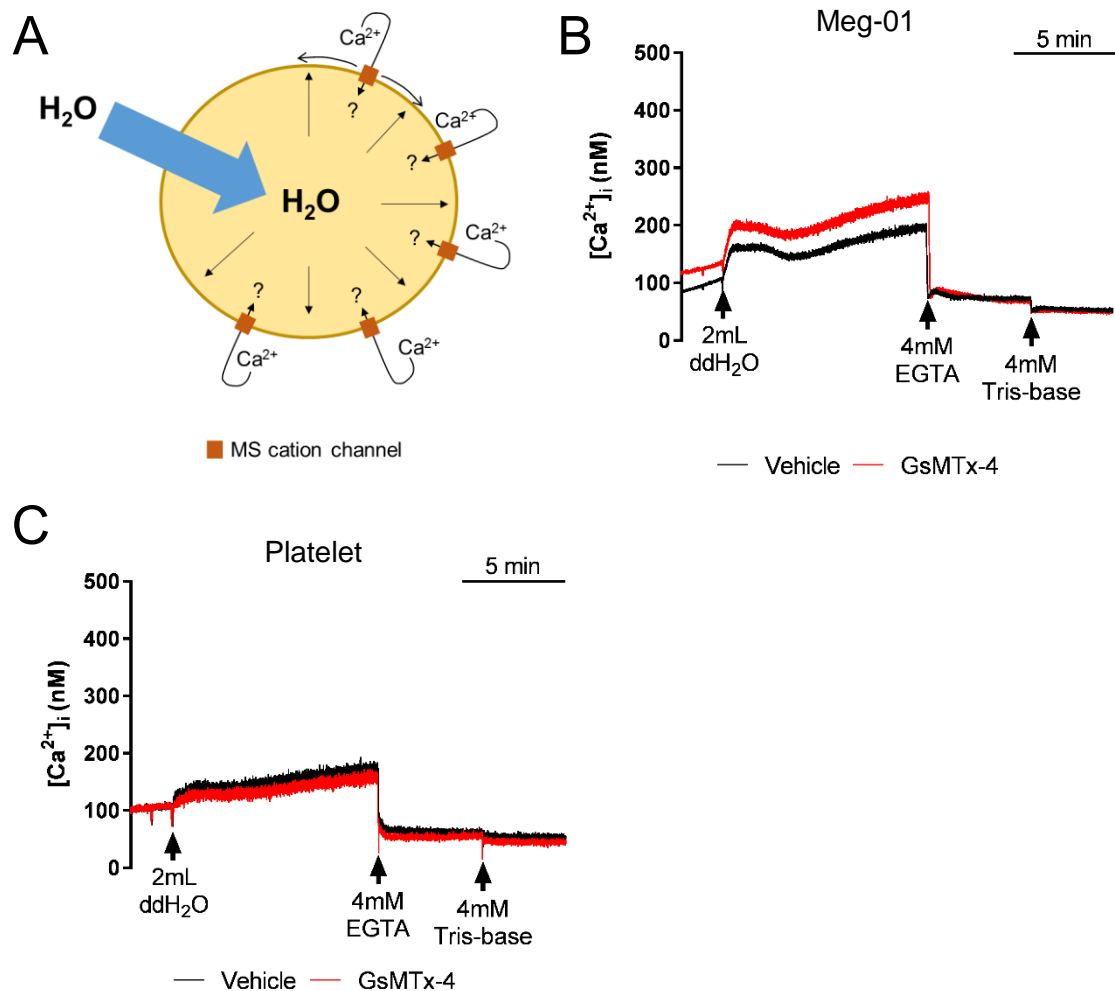


Figure 3.12 Hypotonic challenge does not induce GsMTx-4-sensitive Ca^{2+} influx in Meg-01 or platelet cell suspensions. (A) Cartoon representation of a hypothetical mechanism via which hypotonic challenge may cause platelet membrane stretch and thus the opening of the MS cation channels which allow Ca^{2+} entry. Representative $[Ca^{2+}]_i$ recordings of Meg-01 (B) and platelet (C) suspensions exposed to hypotonic challenge by the addition of an equivalent volume of ddH₂O, in the presence or absence of GsMTx-4 pre-treatment. In both (B) and (C) EGTA was added in the end to chelate Ca^{2+} in the extracellular which gave rise to a background increase in the ratiometric signal due to dye leakage.

3.2.6 *Meg-01 cells display $[Ca^{2+}]_i$ increases in response to mechanical stimulation with a glass probe*

Since their identification, the functional study of Piezo channels involved the use of a glass probe to mechanically stimulate channel opening in human and rodent cell lines (Cox *et al.*, 2016; Syeda *et al.*, 2015; Coste *et al.*, 2010). Patapoutian and his colleagues obtained transient $[Ca^{2+}]_i$ elevations in human embryonic kidney (HEK)-293T cells transfected with Piezo1 upon deformation of the plasma membrane using a piezoelectric motor-controlled glass probe (Syeda *et al.*, 2015). Similarly, in this section, increases in $[Ca^{2+}]_i$ were observed in Fluo-3 loaded Meg-01 cells when the blunt tip of a glass pipette was used to depress the surface of a Meg-01 cell as an alternative mechanical stimulus to shear stress (Figure 3.13 A and B). The glass pipette was manually controlled with a manipulator rather than with a piezoelectric motor, and hence the distance travelled by the probe could not be easily measured. However, the top of the cell was monitored by eye to ensure that the cell had not been punctured or permanently damaged by the glass probe. In the rest of this work, shear forces applied by fluid flow as a more physiological mechanical stimulus for blood cells were used.

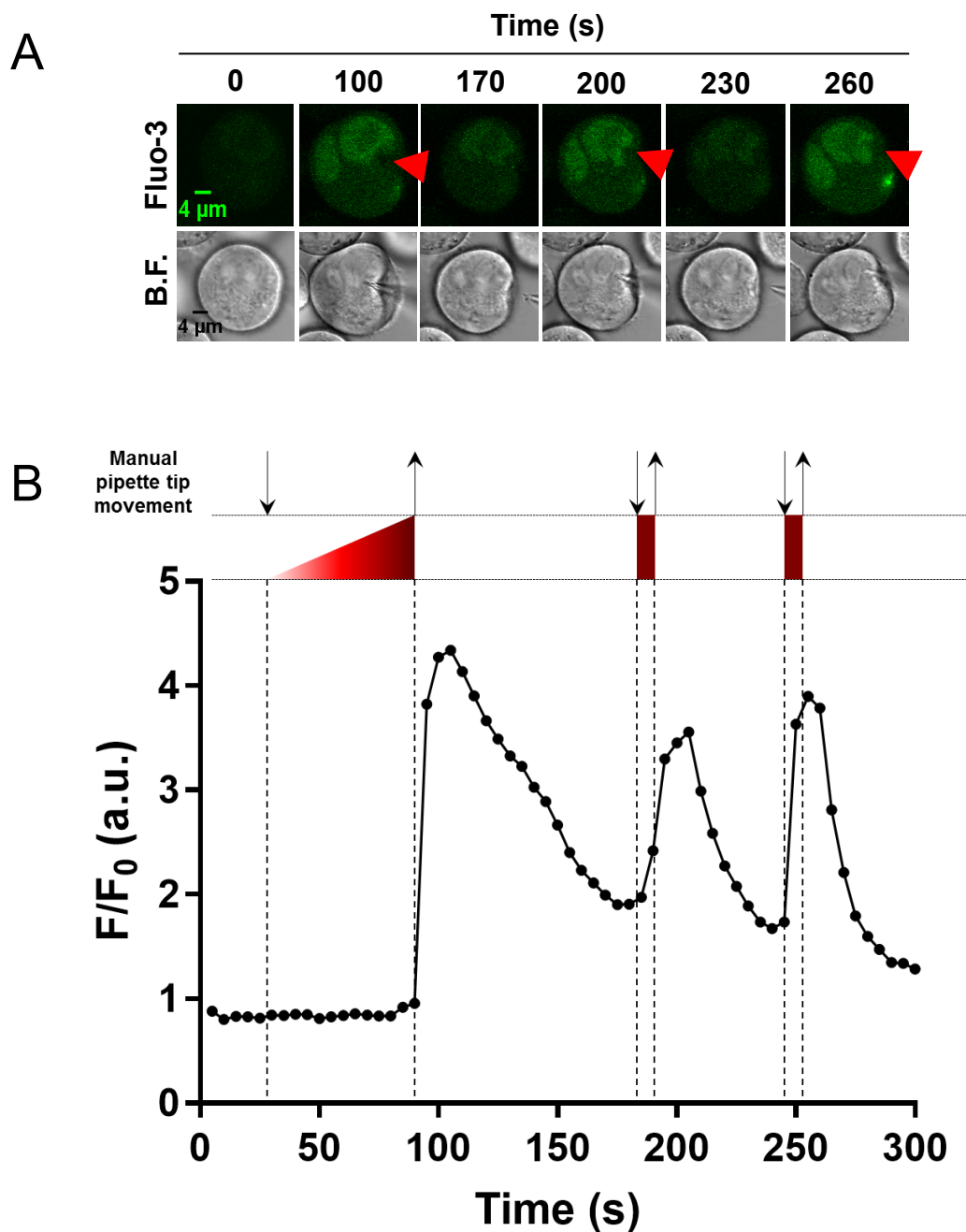


Figure 3.13 Mechanical stimulation of Meg-01 cell with a glass probe results in $[Ca^{2+}]_i$ elevations. (A) Representative images of a Fluo-3-loaded Meg-01 cell at time points before and during $[Ca^{2+}]_i$ elevations stimulated by depression of the plasma membrane. The extracellular saline (HBSS) contained 1.26mM Ca^{2+} . The red arrowheads indicate the position and the direction in which the glass probe was applied. Similar responses were obtained from 14 Meg-01 cells from different cultures. (B) The F/F_0 fluorescence recording of the Meg-01 cell shown in A. The downward arrows indicate when a push was applied onto the cell, and upward arrows indicate release of push. The regions enclosed with dashed lines represent the duration of a mechanical push by the glass probe.

3.2.7 The Piezo1 agonist Yoda1 induces increases in $[Ca^{2+}]_i$ in Meg-01 cell suspensions

Ever-increasing numbers of studies on Piezo1 channel structure and function eventually led to the identification of the first Piezo1 agonist, Yoda1 (Ge *et al.*, 2015; Syeda *et al.*, 2015). It has been revealed that this synthetic molecule modulates Piezo1 currents by stabilising the open conformation of the channel, and activates Piezo1 channels even in the absence of mechanical stimulation, without the need of any other cellular components other than the plasma membrane (Syeda *et al.*, 2015). Since then, Yoda1 has been used in various physiological studies to show that it results in Ca^{2+} influx in red blood cells followed by dehydration, and can mimic the influence of fluid shear stress on endothelial cells (Wang *et al.*, 2016; Cahalan *et al.*, 2015).

As an alternative to fluid shear stress, and as a way of confirming the identity of MS Ca^{2+} channels responsible for the physiological effects observed within this chapter, the effect of 25 μ M Yoda1 was tested on stirred Fura-2-loaded Meg-01 cell suspensions in ratiometric Ca^{2+} measurements. Fast and sharp increases in $[Ca^{2+}]_i$ were observed following the addition of Yoda1, compared to vehicle (DMSO)-treated samples (Figure 3.14 A, C). Chelation of extracellular Ca^{2+} using EGTA (1mM) completely abolished the responses to Yoda1 (Figure 3.14 B, C), indicating that Yoda1 activates plasma membrane ion channels which mediate flux of Ca^{2+} from the extracellular environment to the cytoplasm.

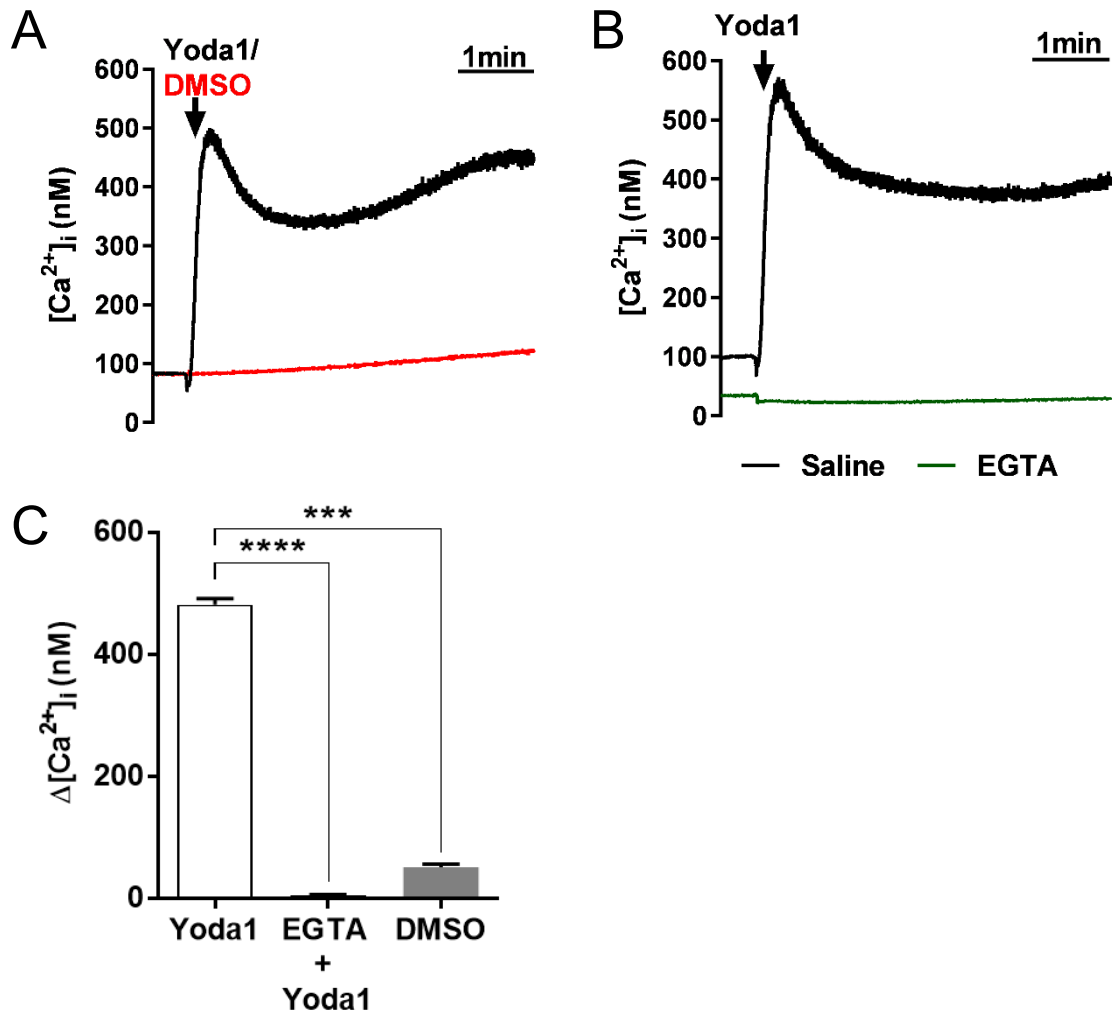


Figure 3.14 The *Piezo1* selective agonist *Yoda1* induced $[Ca^{2+}]_i$ increases in *Meg-01* cells. Representative $[Ca^{2+}]_i$ responses to *Yoda1* (25 μ M) assessed in stirred Fura-2-loaded suspensions of *Meg-01* compared to vehicle control (DMSO), in the presence of extracellular Ca^{2+} (A), and following the removal of extracellular Ca^{2+} (EGTA) (B). (C) The average peak $[Ca^{2+}]_i$ increases following *Yoda1* addition, in the presence of extracellular Ca^{2+} compared to its vehicle control (DMSO) and following removal of external Ca^{2+} (EGTA). Data represent mean \pm SEM (n=4). ****P<0.0001; ***P<0.001.

3.3 Discussion

This chapter demonstrates that human platelets and the megakaryocytic cell line Meg-01 express the MS cation channel Piezo1, which likely mediates Ca^{2+} entry into Meg-01 cells under arterial shear stress levels. The study of the MS roles for Piezo1 channel have often relied upon the use of pharmacological reagents such as the inhibitor GsMTx-4, and the selective agonist Yoda1, in specialised assays which allow mechanical stimulation of such channels (Li *et al.*, 2014; Bae *et al.*, 2011; Coste *et al.*, 2010). *In vitro*, Piezo ion channels can be activated by several distinct types of mechanical force targeting the plasma membrane (Schrenk-Siemens *et al.*, 2015; Miyamoto *et al.*, 2014; Li *et al.*, 2014; Coste *et al.*, 2010). In this chapter, three different mechanical stimulation methods which create membrane tension were investigated. Application of fluid shear stress at levels equivalent to physiological shear rates in arteries was the focal point of this thesis, due to the relevance of this type of mechanical force to platelet function in the circulation and thrombus formation. Meg-01 cells have often been used as a model for signalling in platelets and megakaryocytes (Mahaut-Smith, 2012; Ogura *et al.*, 1985). Therefore, using pharmacological tools to study MS channel function in fluid shear stress assays, this chapter not only provides evidence for functional MS Piezo1 channels in the Meg-01 cell line, but from a technical standpoint, also serves as the foundation of the study of MS cation channels in human platelets which is the focus of the next chapter (Chapter 4).

Several pieces of evidence support the conclusion that Meg-01 cells possess MS Ca^{2+} influx mechanisms that are activated by flow, and thus shear forces, and that the underlying pathway is Piezo1. Firstly, expression of mRNA transcripts and protein for Piezo1 was detected in both platelets and Meg-01 cells (Wright *et al.*, 2016) (Figures 3.2 and 3.4). Secondly, Meg-01 cells that were attached to a poly-D-lysine-coated surface displayed $[\text{Ca}^{2+}]_i$ responses upon exposure to arterial levels of shear that were inhibited by the MS channel blocker GsMTx-4, or removal of external Ca^{2+} . Thirdly, a recently described selective chemical agonist of Piezo1, Yoda1 (Syeda *et al.*, 2015), directly stimulated Ca^{2+} entry into Meg-01 cells in the absence of shear. In agreement with these data, Patapoutian and colleagues demonstrated that Yoda1 can induce Piezo1 activation in the absence of mechanical stimulation and also increase channel sensitivity to mechanical activation (Syeda *et al.*, 2015). Although GsMTx-4 is a generic MS ion channel blocker, it has been the main inhibitor used in the studies of Piezo1 function

(Copp *et al.*, 2016; Li *et al.*, 2015; Pathak *et al.*, 2014; Miyamoto *et al.*, 2014; Bae *et al.*, 2011). The toxin acts through insertion into the lipid bilayer and modification of the lipid:channel interface (Suchyna *et al.*, 2004), hence may influence a number of ion channels. This issue is addressed later in the study (*see* Chapter 4).

Since the contribution of MS channels to platelet or megakaryocyte function had not been studied hitherto, no shear stress assay had been described which allowed specifically the study of such channels in these cell types. A suitable protocol was generated and optimised in this chapter, which allowed the monitor of changes in $[Ca^{2+}]_i$ of Meg-01 cells under shear stress as a first step. Attachment to 0.1% poly-D-lysine ($\geq 300,000$)-coated coverslips provided the best possible approach to both stably attach Meg-01 cells without causing Ca^{2+} mobilisation. Within the bone marrow niche, megakaryocytes are not normally exposed to fluid shear stress, although other types of mechanical stimuli may exist (*see* below). Megakaryocytic cell lines serve as more convenient alternatives to human platelets in physiological studies, which are easy to produce and handle, and yet are suitable models that provide useful insights into platelet function (Mahaut-Smith, 2012; Schmitt *et al.*, 2001; Ogura *et al.*, 1985). Therefore, this chapter presents the first data using a novel shear stress assay generated to allow the study of MS channel function in the Meg-01 cell line. Platelets are constantly exposed to fluid shear stress in the circulation, and rely upon molecular mechanisms which utilise these mechanical forces in their surroundings to carry out their function in haemostasis (Schneider *et al.*, 2007; Siedlecki *et al.*, 1996; Chow *et al.*, 1992; Levenson *et al.*, 1990). As observed in HUVECs, which are known to express functional Piezo1 channels, arterial shear resulted in shear rate dependent elevations in $[Ca^{2+}]_i$ that were eliminated by the inhibition of MS cation channels using GsMTx-4, or by elimination of extracellular Ca^{2+} . Interestingly, under the conditions of absence of extracellular Ca^{2+} , many of the Meg-01 cells studied displayed residual $[Ca^{2+}]_i$ elevations (Figure 3.8 B). This potentially indicates MS Ca^{2+} channel expression on intracellular membranes that can mediate Ca^{2+} entry into the cytosol from the stores, which were not inhibited by the GsMTx-4 pre-treatment. Similar residual responses were observed by other studies where the possibility of intracellular Piezo1 was suspected (Syeda *et al.*, 2015). This could also potentially indicate the activity of MS channels or MS Ca^{2+} mobilising events not inhibited by GsMTx4.

Piezo1 function in other cell types has been demonstrated using alternative approaches to mechanically induce Piezo1 channel activation (Figure 3.1) (Schrenk-

Siemens *et al.*, 2015; Delmas *et al.*, 2011; Coste *et al.*, 2010). Indeed, different types of mechanical forces play important roles in megakaryocyte maturation, function, platelet production and interaction with osteoblasts within the bone marrow (Soves *et al.*, 2014; Jiang *et al.*, 2014; Machlus & Italiano, 2013; Junt *et al.*, 2007). Provided the role of Piezo1 in Ca²⁺ influx-mediated dehydration in red blood cells, this chapter also attempted to monitor changes in [Ca²⁺]_i levels following hypotonic challenge. Platelet suspensions did not produce a clear Ca²⁺ response to hypotonic challenge, indicating no prominent MS pathway involved in detecting changes in cell volume. The small GsMTx-4-independent Ca²⁺ peak in Meg-01 cells indicate possible involvement of MS cation channel-independent Ca²⁺ entry routes in response to hypotonic challenge. On the other hand, robust Ca²⁺ peaks were recorded following membrane depression with a glass probe, providing evidence for a MS Ca²⁺ entry pathway in Meg-01 cells (Figure 3.13), similar to responses obtained in other cell types in previous reports (Syeda *et al.*, 2015). However, due to technical difficulties in the quantification of the distance travelled by the glass probe, and hence the degree of mechanical stimulation, and frequent cell detachment because of probe movement, this method of MS channel activation was not preferred.

In addition to the implications of this study in MS cation channel function in platelets, the findings presented in this chapter also raise the possibility that Piezo1 may contribute to megakaryocyte function. For example, shear forces are important during thrombopoiesis by promoting platelet release from proplatelet extensions within the venous sinusoids (Thon *et al.*, 2012; Junt *et al.*, 2007). In addition, megakaryocytes have been postulated as active participants in the mechanosensitivity of the marrow environment that regulates the bone mass, likely through interactions with osteoblasts (Soves *et al.*, 2014). Furthermore, it is known that megakaryocyte gene expression of both native murine megakaryocytes and megakaryocytic cell lines is modulated by mechanical forces, including shear stress (Soves *et al.*, 2014). Piezo1 represents a possible candidate for the mechanosensors in these previous studies.

In conclusion, this chapter reveals for the first time that the human megakaryocytic cell line Meg-01 expresses MS cation channels which mediate Ca²⁺ entry into the cytoplasm under arterial levels of shear stress. The effect of Yoda1 in ratiometric [Ca²⁺]_i measurements demonstrate that Piezo1 is the possible identity of these channels. The use of a novel shear stress assay where Fluo-3-loaded Meg-01 cells are individually attached onto glass coverslips provides evidence that MS cation

channels mediate Ca^{2+} movement from the extracellular to cell interior in a shear-rate dependent manner. Highest levels of Ca^{2+} entry are achieved at shear rates equivalent to pathologically high levels of arterial shear stress *in vivo*, such as regions of vessel narrowing resulting from stenosis or atherosclerosis, implying a possible key role for these channels in platelets. In addition to pointing towards a possible role for Piezo1-mediated Ca^{2+} entry in platelets, the findings presented in this chapter indicate Piezo1 as a candidate for possible mechanosensors involved in megakaryocyte function within the bone marrow or in thrombopoiesis. Finally, this chapter presents a novel approach of monitoring changes in $[\text{Ca}^{2+}]_i$ in attached Meg-01 cells under fluid flow, which may be adapted to investigate MS channels function in attached platelets (Chapter 4).

Chapter 4

Evidence for a contribution of mechanosensitive Piezo1 channel activity to human platelet shear-dependent calcium entry and thrombus formation

4.1 Introduction

In the circulation, platelets are continuously exposed to fluid shear stress exerted by laminar flow of blood. This physiological force is regarded as a vital environmental factor leading to platelet activation in both normal and pathological situations. For instance, shear stress was demonstrated to enhance the engagement between vWF and GPIb receptors on the platelet surface, an interaction which would result in a PKC activation-dependent intracellular Ca^{2+} mobilisation (Nesbitt *et al.*, 2002; Siedlecki *et al.*, 1996; Kroll *et al.*, 1991). The mechanisms for more direct mechanical activation of platelet signalling events, however, have not been identified (Kroll *et al.*, 1996).

In the last half-century, a number of studies demonstrated important links between elevated levels of pathological shear stress and thrombus formation (Raz *et al.*, 2007; Einav & Bluestein, 2004; Bluestein *et al.*, 1999; Bluestein *et al.*, 1997; Holme *et al.*, 1997; Stein & Sabbah, 1974). Despite this, our knowledge of the molecular or physiological mechanisms responsible for the relationship between platelet activation and shear stress is still rudimentary. Nevertheless, the presence of a Ca^{2+} entry pathway induced by shear stress has been suggested in earlier studies (Chow *et al.*, 1992; Levenson *et al.*, 1990).

An increase in $[\text{Ca}^{2+}]_i$ is a critical signalling event that is essential for many functional events during platelet activation, including cytoskeletal rearrangements and integrin inside-out signalling (Li *et al.*, 2010; Varga-Szabo *et al.*, 2009). Despite the established link between fluid shear stress and platelet activation, MS Ca^{2+} channel activity in platelets has never been reported previously. Data presented in Chapter 3 provide evidence for shear-stress driven direct Ca^{2+} entry into a human megakaryocytic cell line through MS cation channels. Moreover, data imply that in platelets the MS Ca^{2+} channel Piezo1 could potentially mediate a shear stress-dependent mechanism of Ca^{2+} influx within the circulation. Potentially, the involvement of such ion channels in the process of platelet activation would provide a shear-stress driven mechanism underlying a faster and more direct pathway for Ca^{2+} entry.

Primarily, this chapter will modify and extend the use of the shear stress assay employed in Chapter 3 to allow the investigation of shear stress-dependent Ca^{2+} events in freshly isolated, Fluo-3-loaded single human platelets. A novel approach was developed, using PECAM-1 antibodies, to adhere platelets to glass-bottom biochips without inducing spontaneous activation and thereby permit the study of shear-induced Ca^{2+} responses in individual platelets. MS ion channel function will be studied using the MS cation channel inhibitor GsMTx-4 and the selective Piezo1 agonist Yoda1, and the effect of both normal and stenotic arterial levels of shear stress will be tested on platelet MS channel function. Possible contribution from other potentially MS receptors, such as the GPCRs P2Y1 and P2Y12, will also be addressed using the same approach. Finally, the effect of GsMTx-4 on other Ca^{2+} entry routes will be assessed, and thrombus formation under arterial flow will be investigated in order to provide a link to functional responses.

4.2 Results

4.2.1 Evidence for Piezo1 channel activity in single platelets under arterial shear stress

The shear-induced Ca^{2+} entry observed in Meg-01 cells led to the development of a method to examine whether a similar pathway exists in human platelets. Previous measurements of Ca^{2+} responses under arterial shear in single platelets have used glass coverslips coated with adhesive receptor ligands such as fibrinogen, collagen or synthetic peptides mimicking their binding domain (Mazzucato *et al.*, 2002; Yap *et al.*, 2002; Nesbitt *et al.*, 2002); however, this approach would generate activation signals including Ca^{2+} mobilisation independently of the mechanical stimulus. Therefore, this study used an antibody against the receptor PECAM-1, which is inhibitory to platelet function, in order to immobilise platelets on glass coverslips. PECAM-1 normally plays a role in homophilic interactions between Ig domains 1 and 2 of the molecules on nearby platelets (Sun *et al.*, 1996). The PECAM-1 antibody used in this assay (clone WM59) binds to Ig domains 1 and 2 hence inhibiting homophilic binding between platelets. It therefore provides a coat onto which platelets can attach and become immobilised without being activated by the glass surface (Jones *et al.*, 2014a; Jones *et al.*, 2012) (*see* Chapter 2, Figure 2.3).

Exposure of attached unstimulated platelets to normal arterial shear stress (1002.6s^{-1}) resulted in multiple transient increases in cytosolic Ca^{2+} after a delay of 1-2 min (Figure 4.1 A, B). Subsequent arrest of flow led to a reduction but not complete inhibition of this Ca^{2+} response, although a second application of arterial shear caused a further increase in the number of Ca^{2+} transients (Figure 4.1 B). The Ca^{2+} responses were quantified using the F/F_0 integral for a total of 4 min ($F/F_{0,4\text{min}}$). Prior to application of flow, this value was 0.4 ± 0.1 due to the presence of occasional Ca^{2+} transients, and increased significantly to 1.9 ± 0.3 during normal arterial shear ($P < 0.001$, $n=46$ cells) (Figure 4.3 A). In every platelet sample, a proportion of attached platelets did not show increased Ca^{2+} transients in response to arterial shear. However, in the platelets that displayed relatively constant resting levels of $[\text{Ca}^{2+}]_i$ in the absence of shear and also responded to shear, the F/F_0 integrals during a first and second exposure to arterial shear were not significantly different (Figure 4.3 B). This allowed the effects of GsMTx-4 and removal of extracellular Ca^{2+} to be assessed during the second cycle of shear.

The shear-induced Ca^{2+} transients were significantly reduced by either the addition of $2.5\mu\text{M}$ GsMTx-4 to the extracellular saline ($F/F_{0.4\text{min}}$ value of 0.6 ± 0.1 , which is 31.8% of control; $P<0.001$, $n=23$ cells); or removal of extracellular Ca^{2+} ($F/F_{0.4\text{min}}$ value of 0.7 ± 0.2 , which is 38.5% of control; $P<0.05$, $n=14$ cells) (Figures 4.2 A, B and 4.3 A). A higher arterial shear (3989.3s^{-1}), equivalent to the situation when stenosis or narrowing occurs in the arteries, induced a larger and more significant increase ($F/F_{0.4\text{min}}$ value of 2.1 ± 0.3 ; $P<0.0001$, $n=38$) above pre-stimulus (no flow) levels when compared to normal arterial shear (Figure 4.4 A) and was also inhibited by GsMTx-4 ($F/F_{0.4\text{min}}$ value of 0.6 ± 0.1 ; $P<0.05$, $n=13$). As observed in the experiments where normal arterial levels of shear stress was applied, F/F_0 integrals during a first and second exposure to stenotic shear were not significantly different (Figure 4.4 B).

Together these results suggest that platelets, like Meg-01 cells, possess a MS Ca^{2+} influx pathway induced by physiological levels of shear. The major difference between the response in these two cell types was the longer delay between stimulus application and the $[\text{Ca}^{2+}]_i$ increase in platelets compared to Meg-01 cells. This may result from the greater rigidity of platelet surface membranes, a consequence of the extensive cortical cytoskeleton which will resist deformation and thus activation of MS ion channels (Mahaut-Smith, 2004; Hartwig, 1992).

To further assess the contribution of Piezo1 channels to platelet signalling and functional events, the recently characterised Piezo1 agonist, Yoda1, was used (Syeda *et al.*, 2015). In Fura-2 ratiometric measurements from stirred suspensions, Yoda1 caused a substantial, immediate and sustained elevation of $[\text{Ca}^{2+}]_i$ in platelets, as observed in Meg-01 cells in Chapter 3, when Ca^{2+} was present in the extracellular milieu (Figure 4.5 A). Most or all of this response was lost in Ca^{2+} -free external saline [decrease of 63% from $99.4\pm 9.7\text{nM}$ to $37.0\pm 5.6\text{nM}$ in platelets ($P<0.05$; $n=4$), and by 99% from $481.3\pm 9.8\text{nM}$ to $5.2\pm 0.5\text{nM}$ in Meg-01 ($P<0.0001$; $n=4$)], as expected if the predominant location of Piezo1 channels is on the surface membrane (Figures 4.5 B, C and *see* 3.14). The residual response to Yoda1 in platelets in Ca^{2+} -free medium can be explained by the suggested presence of Piezo1 channels on membranes of the intracellular stores (Syeda *et al.*, 2015). These experiments were conducted in apyrase-free medium to abolish P2X1 receptor activity, which was confirmed by the absence of responses to $\alpha,\beta\text{-meATP}$ (*see* Chapter 5, Figure 5.2 C).

Yoda1 also enhanced intracellular Ca^{2+} transients in platelets attached to glass-bottom biochips via PECAM-1 (Figure 4.6 A). Yoda1 increased the occurrence of Ca^{2+}

transients in both the absence of flow, and upon application of shear (Figure 4.6 A, compare with Figure 4.1 B). Under static conditions, the F/F_0 integral increased more than 3-fold from $F/F_{0.4\text{min}}$ value of 0.3 ± 0.1 to 1.2 ± 0.1 ($P<0.01$, $n=35$ cells). Under normal arterial flow, in the absence of Yoda1 the $F/F_{0.4\text{min}}$ value was 1.2 ± 0.1 , which showed a 1.7-fold increase to 2.1 ± 0.2 in the presence of the Piezo1 agonist ($P<0.01$, $n=35$ cells) (Figure 4.6 B).

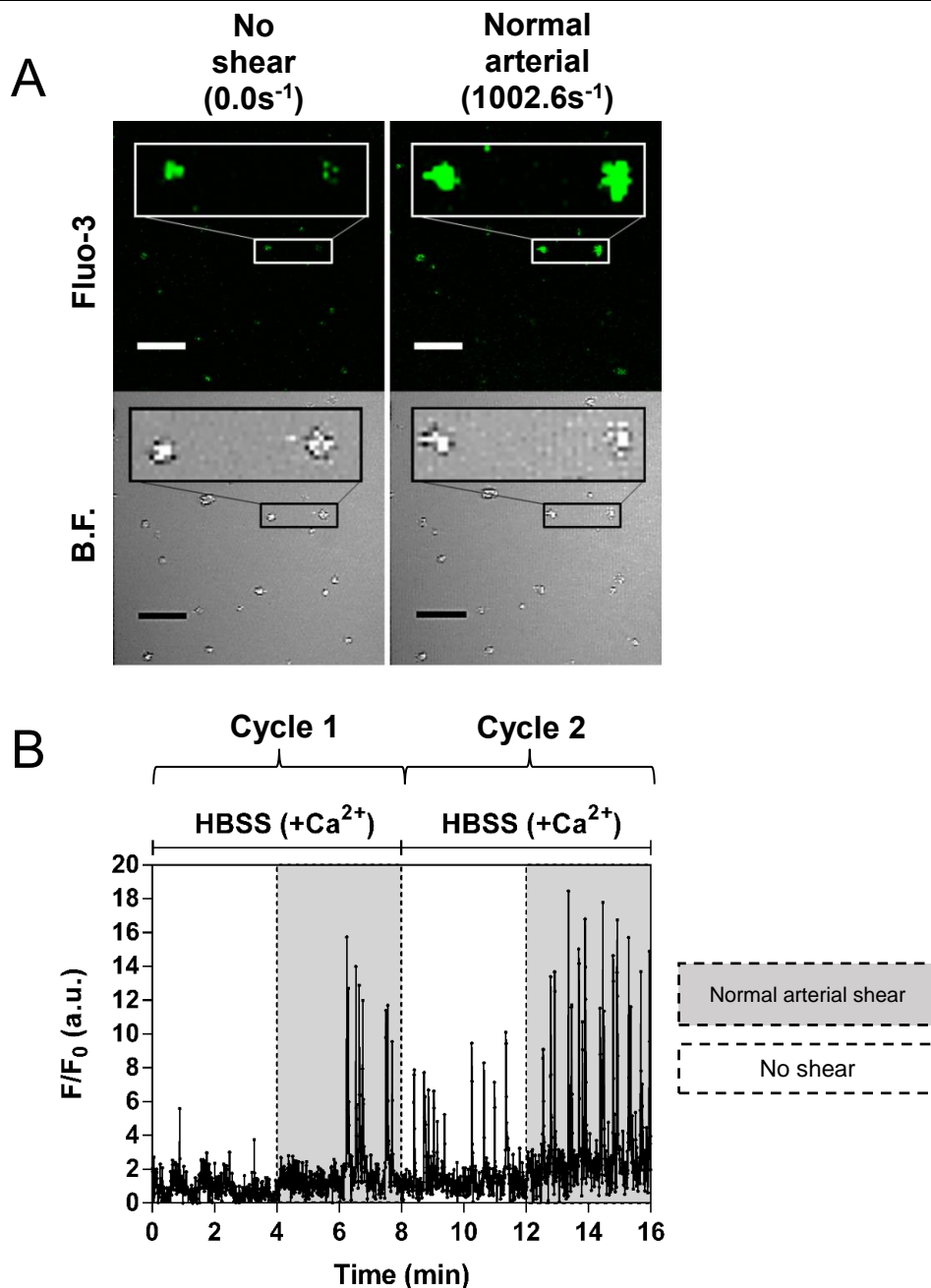


Figure 4.1 Fluid shear stress induces Ca^{2+} transients in single platelets. (A) Representative Fluo-3 fluorescence and bright field (B.F.) images of individual Fluo-3-loaded attached platelets before and during exposure to arterial shear. Scale bars = 20 μ m; the magnified rectangular sections have been zoomed threefold. (B) Representative F/F_0 Fluo-3 recordings in single platelets during no applied shear stress and normal arterial shear. Two successive cycles of 4 minutes without shear followed by 4 minutes of arterial shear were applied using Ca^{2+} -containing saline (HBSS+ Ca^{2+}). Apyrase was omitted from the extracellular saline to avoid P2X1 receptor responses.

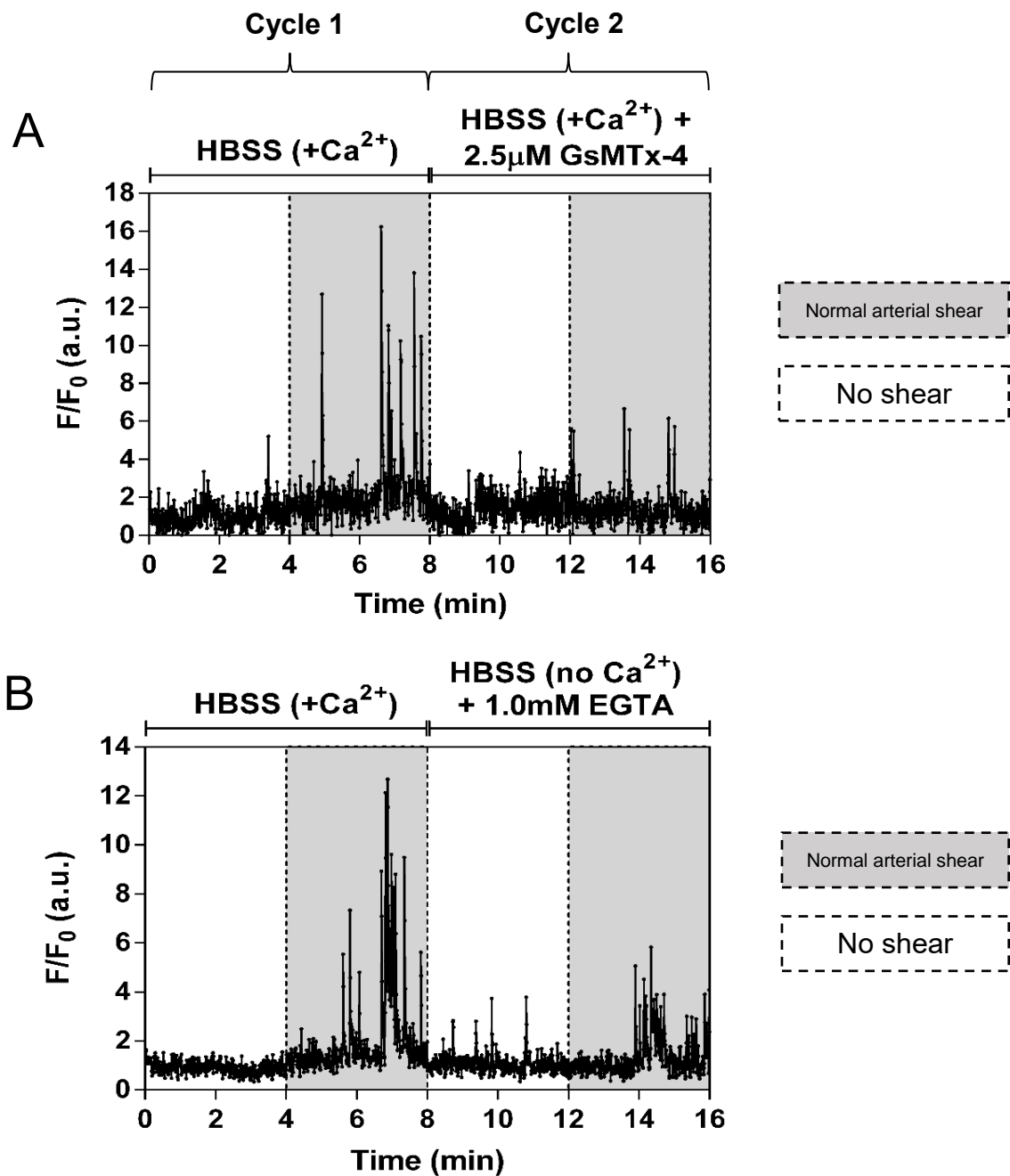


Figure 4.2 Fluid shear stress-induced Ca²⁺ transients in single platelets are inhibited by GsMTx-4 and chelation of extracellular Ca²⁺. Representative F/F₀ Fluo-3 recordings in single platelets, in which the second cycle (cycle 2) was used to compare the control conditions (i.e. HBSS+Ca²⁺ only) (Figure 4.1 B), with the effect of GsMTx-4 (A), or removal of extracellular Ca²⁺ (B). Apyrase was omitted from the extracellular saline to avoid P2X1 receptor responses.

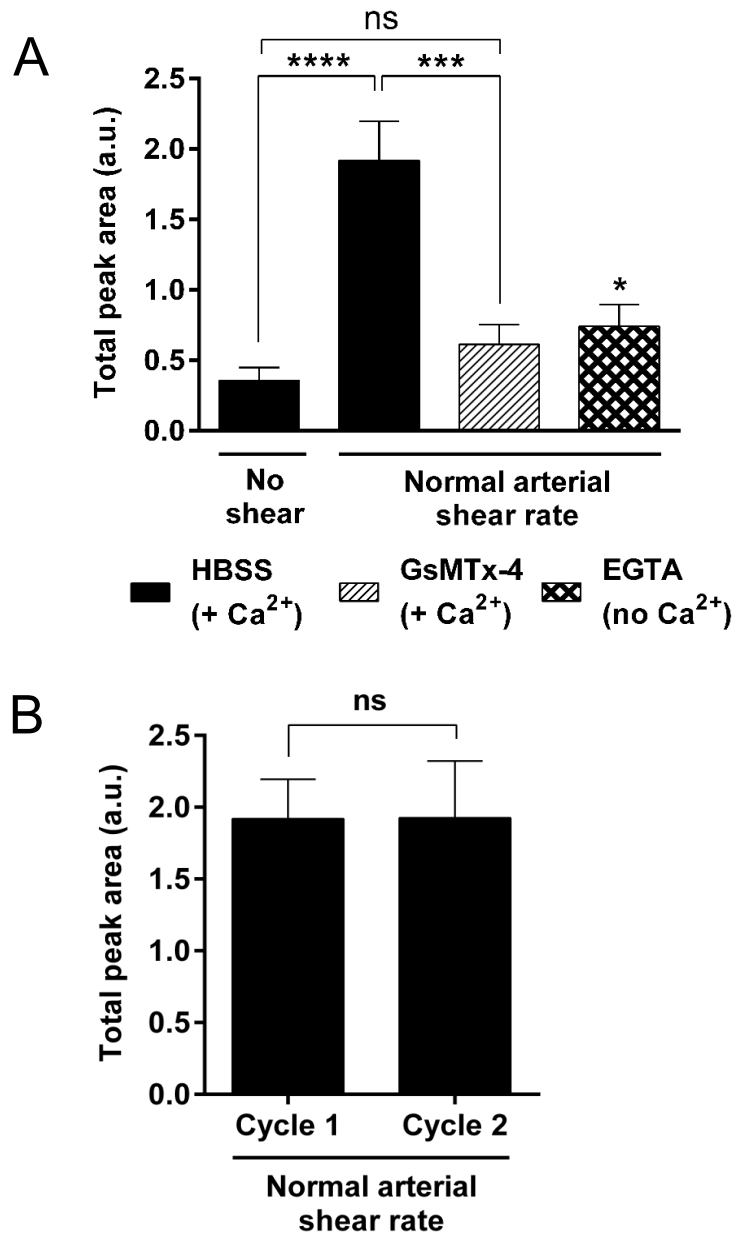


Figure 4.3 Fluid shear stress-induced average Ca^{2+} increases in single platelets are inhibited by GsMTx-4 and chelation of extracellular Ca^{2+} . Average Ca^{2+} increases were calculated as the 4 min F/F_0 integral of all $[Ca^{2+}]_i$ transients. (A) Responses in the absence of shear and during arterial shear, in the presence of extracellular Ca^{2+} with and without GsMTx-4 ($2.5\mu M$), and in the absence of extracellular Ca^{2+} ($n=46, 46, 23, 14$ cells in no shear, HBSS, GsMTx-4 and EGTA, respectively); $*P<0.05$, compared to HBSS only control under shear. (B) Comparison of Ca^{2+} responses during cycles 1 and 2 of normal arterial flow with Ca^{2+} -containing HBSS only ($n=46$ and 13 cells, respectively). No significant difference was found between F/F_0 integrals of the calcium transients from cycles 1 and 2. $****P<0.0001$; $***P<0.001$; ns =not statistically significant. Data represent mean \pm SEM of 7 individual donors.

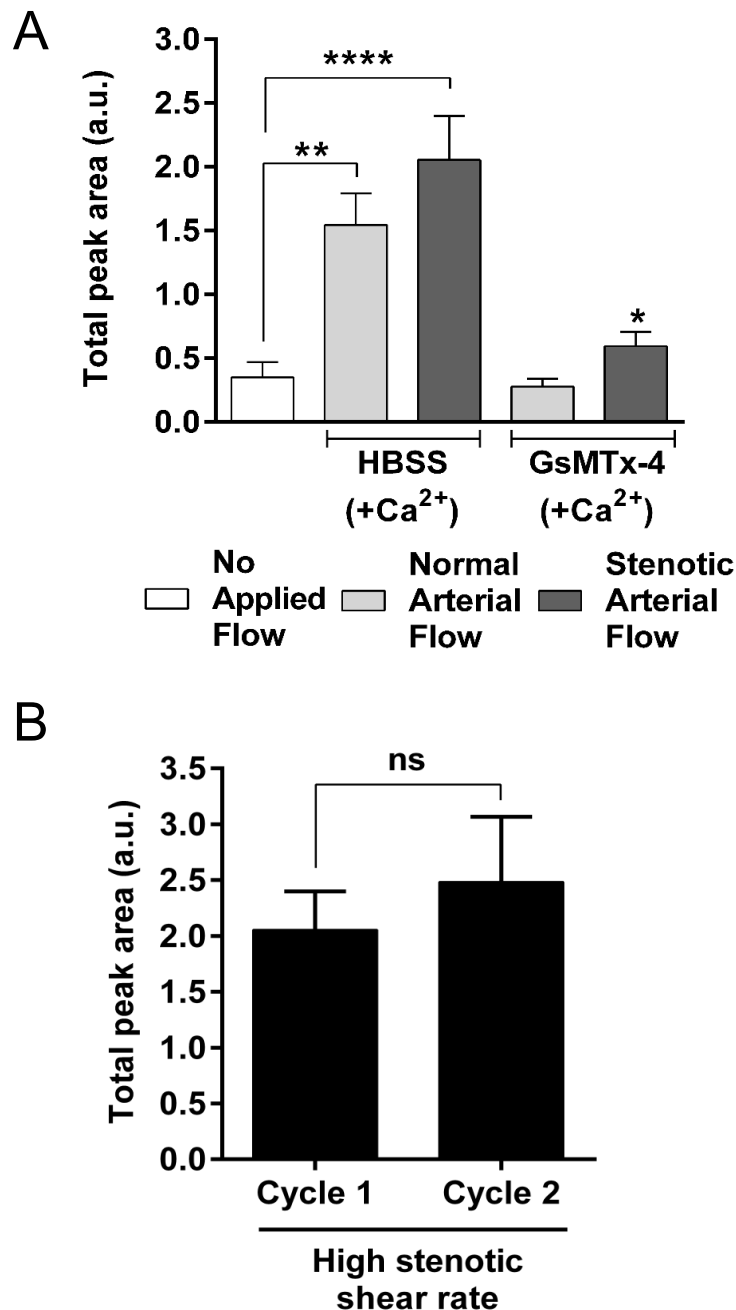


Figure 4.4 Stenotic levels of shear stress induced relatively more significant average Ca^{2+} increases in single platelets. (A) Ca^{2+} responses in Ca^{2+} -containing HBSS in the absence of shear (no applied flow), and during normal and stenotic arterial shear, with and without GsMTx-4 ($n=36, 36, 38, 13$ and 13 cells in no applied flow, HBSS normal arterial, HBSS stenotic arterial, GsMTx-4 normal arterial and GsMTx-4 stenotic arterial flow conditions, respectively); * $P<0.05$, compared to HBSS only control under stenotic shear. (B) No significant difference was found between F/F_0 integrals of the calcium transients from cycles 1 and 2 of stenotic arterial flow, using Ca^{2+} -containing HBSS only ($n=38$ and 20 cells, respectively). **** $P<0.0001$; ** $P<0.01$; ns=not statistically significant. Data represent mean \pm SEM of 6 individual donors.

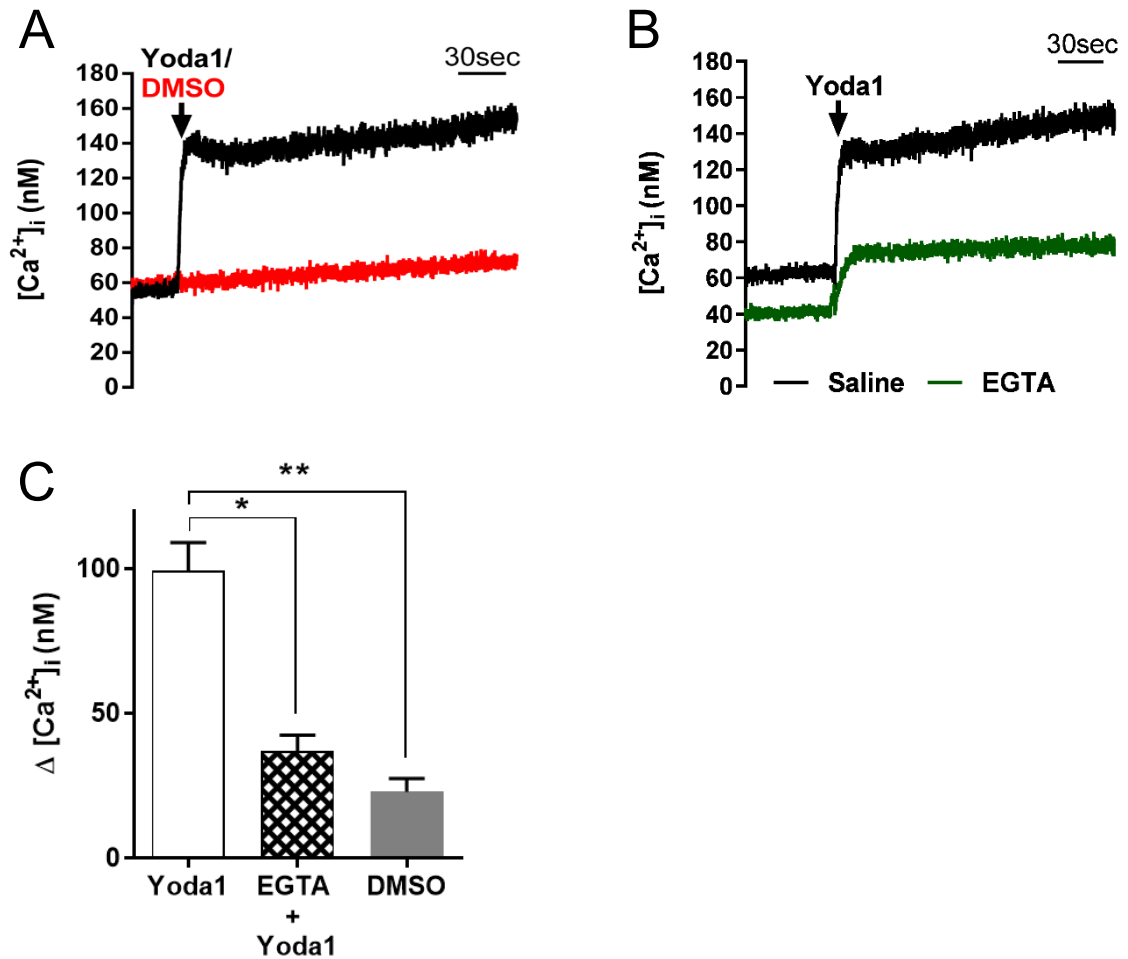


Figure 4.5 The Piezo1 selective agonist Yoda1 induced $[Ca^{2+}]_i$ increases in washed platelets. Representative $[Ca^{2+}]_i$ responses to Yoda1 (25 μ M) assessed in stirred Fura-2-loaded suspensions of washed platelets compared to vehicle control (DMSO), in the presence of extracellular Ca^{2+} (A), and following the removal of extracellular Ca^{2+} (EGTA) (B). (C) The average peak $[Ca^{2+}]_i$ following Yoda1 addition, in the presence of extracellular Ca^{2+} compared to its vehicle control (DMSO) and following removal of external Ca^{2+} (EGTA). ** $P < 0.01$; * $P < 0.05$. Apyrase was omitted from the extracellular saline to avoid P2X1 receptor responses. Data represent mean \pm SEM ($n = 4$ individual donors).

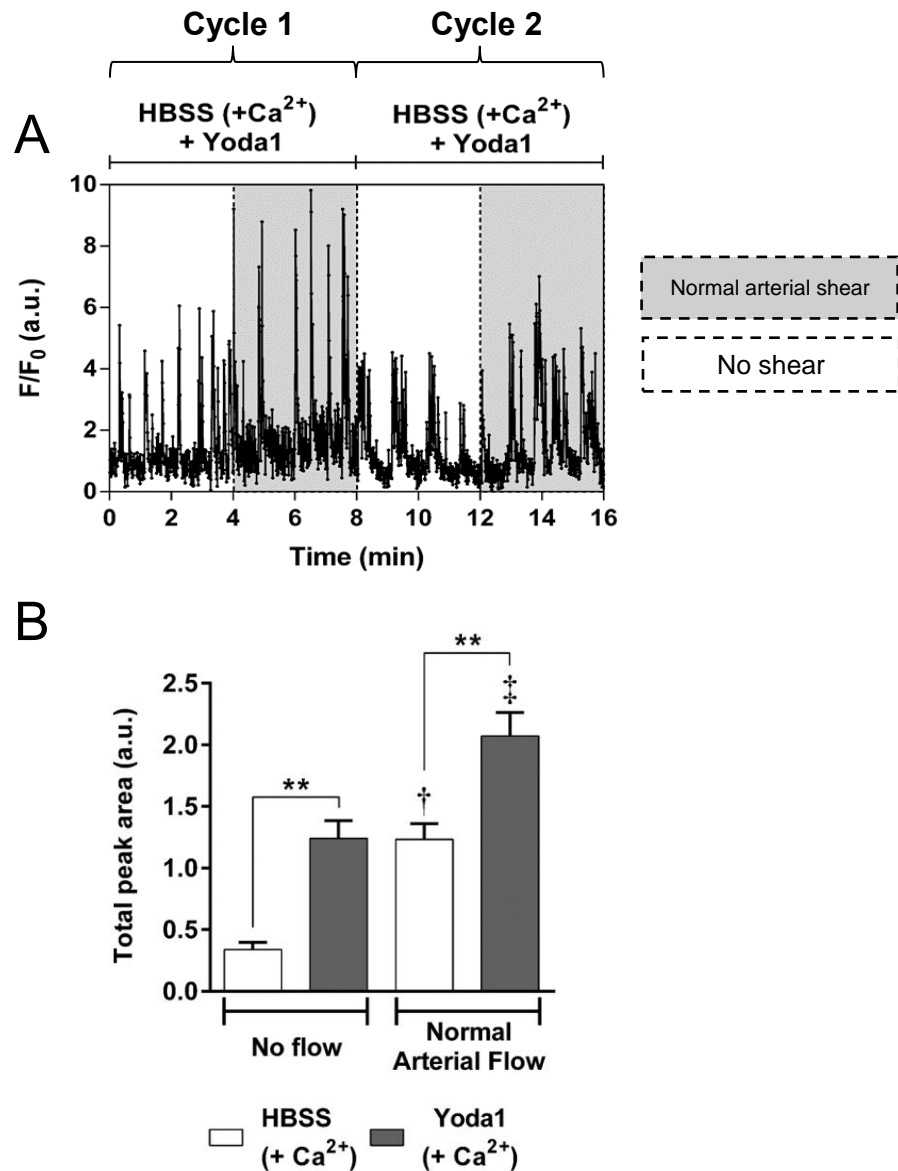


Figure 4.6 The Piezo1 selective agonist Yoda1 induced increases in $[Ca^{2+}]_i$ in singly attached platelets. (A) Representative F/F_0 Fluo-3 recordings in single platelets attached to a PECAM-1-coated coverslip in the presence of Yoda1 and exposed to 2 cycles of no flow and arterial shear. See Figure 4.1 B for the control trace. (B) Average Ca^{2+} increases above baseline ($F/F_{0.4min}$) in the presence and absence of Yoda1, under conditions of no flow and normal arterial shear ($n= 20, 35, 20$ and 35 cells in HBSS no flow, Yoda1 no flow, HBSS normal arterial and Yoda1 normal arterial conditions, respectively). ** $P < 0.01$; † $P < 0.01$ compared to no flow, in presence of HBSS; ‡ $P < 0.001$ compared to no flow in presence of Yoda1. Apyrase was omitted from the extracellular saline to avoid P2X1 receptor responses. Data represent mean \pm SEM of 7 individual donors).

4.2.2 Mechanosensitive Ca^{2+} events in platelets are independent of purinergic GPCR stimulation

In Section 4.2.1, it was observed that the chelation of extracellular Ca^{2+} by EGTA results in a less significant ($P < 0.05$) reduction in the average $F/F_{0.4min}$ value than using GsMTx-4 ($P < 0.001$) under normal arterial shear rate, compared to control conditions (Figure 4.3 A). In addition, the removal of extracellular Ca^{2+} in Fura-2-loaded washed platelet suspensions did not fully eliminate the Yoda1-induced increase in $[Ca^{2+}]_i$, although the responses were substantially reduced (Figure 4.5). These observations indicate that a mechanism whereby MS Ca^{2+} release from the intracellular stores potentially could accompany the shear- or Yoda-1-induced $[Ca^{2+}]_i$ elevations, which could account for the residual responses still obtained in the absence of extracellular Ca^{2+} . An alternative explanation for these residual Ca^{2+} responses under shear stress could be the possibility of other stretch-activated proteins on the plasma membrane. In addition to MS ion channels, there is increasing evidence that a number of GPCRs can be activated by mechanical stimulation, including fluid shear stress (Storch *et al.*, 2012; Yasuda *et al.*, 2008; Mederos y Schnitzler *et al.*, 2008; Zou *et al.*, 2004).

Under normal physiological conditions, secretion of secondary agonists such as ADP and formation of TxA_2 follow the activation of platelets by potent agonists such as collagen or thrombin. Platelets possess a number of GPCRs including P2Y1 and P2Y12 which ADP stimulates, in addition to PAR1, PAR4, TxA_2R , EP_3 *etc.* It has been shown that P2Y1 and 12 receptors are responsible for the Ca^{2+} responses in response to ADP, and also that MS ion channel responses can be modulated by P2Y receptor activation (Linan-Rico *et al.*, 2013; Inoue *et al.*, 2009; Song *et al.*, 2009; Fernandes *et al.*, 2008; Fox *et al.*, 2004; Hardy *et al.*, 2004; Baurand *et al.*, 2001; Sage *et al.*, 2000; Leon *et al.*, 1999; Jin *et al.*, 1998; Cattaneo *et al.*, 1997). Previously, synergistic mechanisms between agonist- and mechanical-induction of GPCR activation and ion channel function have been investigated (Scholz *et al.*, 2015; Storch *et al.*, 2012; Kauffenstein *et al.*, 2012; Anfinogenova *et al.*, 2011). Provided the evidence for G-protein and P2Y receptor involvement in mechanosensation in other cells types, this section aims to investigate the influence of P2Y receptor activation on shear stress-mediated Ca^{2+} transient formation in singly attached platelets. In order to achieve this, initially the optimal ADP concentration to use in shear stress assays was assessed by $[Ca^{2+}]_i$

measurements in Fura-2-loaded platelet suspensions. Using a range of ADP concentrations similar to those previously used to activate P2Y receptors in Ca^{2+} measurements (Hardy *et al.*, 2005), $[\text{Ca}^{2+}]_i$ elevations were recorded after direct addition of ADP, and a concentration-effect curve was constructed (Figure 4.7 A, B). Based on this curve, a threshold ADP concentration was selected ($0.1\mu\text{M}$), which produced a small $[\text{Ca}^{2+}]_i$ response in most platelets samples (Figure 4.7 A). This concentration of ADP was used to achieve activation (EC_{10}) of P2Y receptors and still permit detection of any amplification by mechanical events. Inclusion of this threshold ADP concentration in the extracellular saline in shear stress assays did not enhance shear-induced Ca^{2+} spiking (Figures 4.8 A and 4.9 A). In ratiometric $[\text{Ca}^{2+}]_i$ recordings, pre-exposure to a threshold ADP concentration before maximal P2Y receptor stimulation with $10\mu\text{M}$ ADP also had no significant effect on the maximal ADP-evoked Ca^{2+} response, although the trend of the responses suggested that $0.1\mu\text{M}$ ADP causes a slight desensitisation of P2Y receptors (Figure 4.10 A, B). Since this low concentration only caused a slight elevation in $[\text{Ca}^{2+}]_i$ of a portion of platelet samples when directly added (Figure 4.7 A), the lack of an enhancement in Ca^{2+} spiking could have been due to its desensitising effect. To further address this issue, a concentration closer to the EC_{50} value ($0.3\mu\text{M}$) was selected (Figure 4.7 B) but this also failed to have a significant effect on shear-induced Ca^{2+} spiking in singly attached platelets (Figures 4.8 B and 4.9 B). Parallel measurements of ADP-evoked $[\text{Ca}^{2+}]_i$ responses in Fura-2-loaded suspensions of platelets from the same batch of blood indicated minimal time-dependent loss of P2Y receptor responses (Figure 4.11).

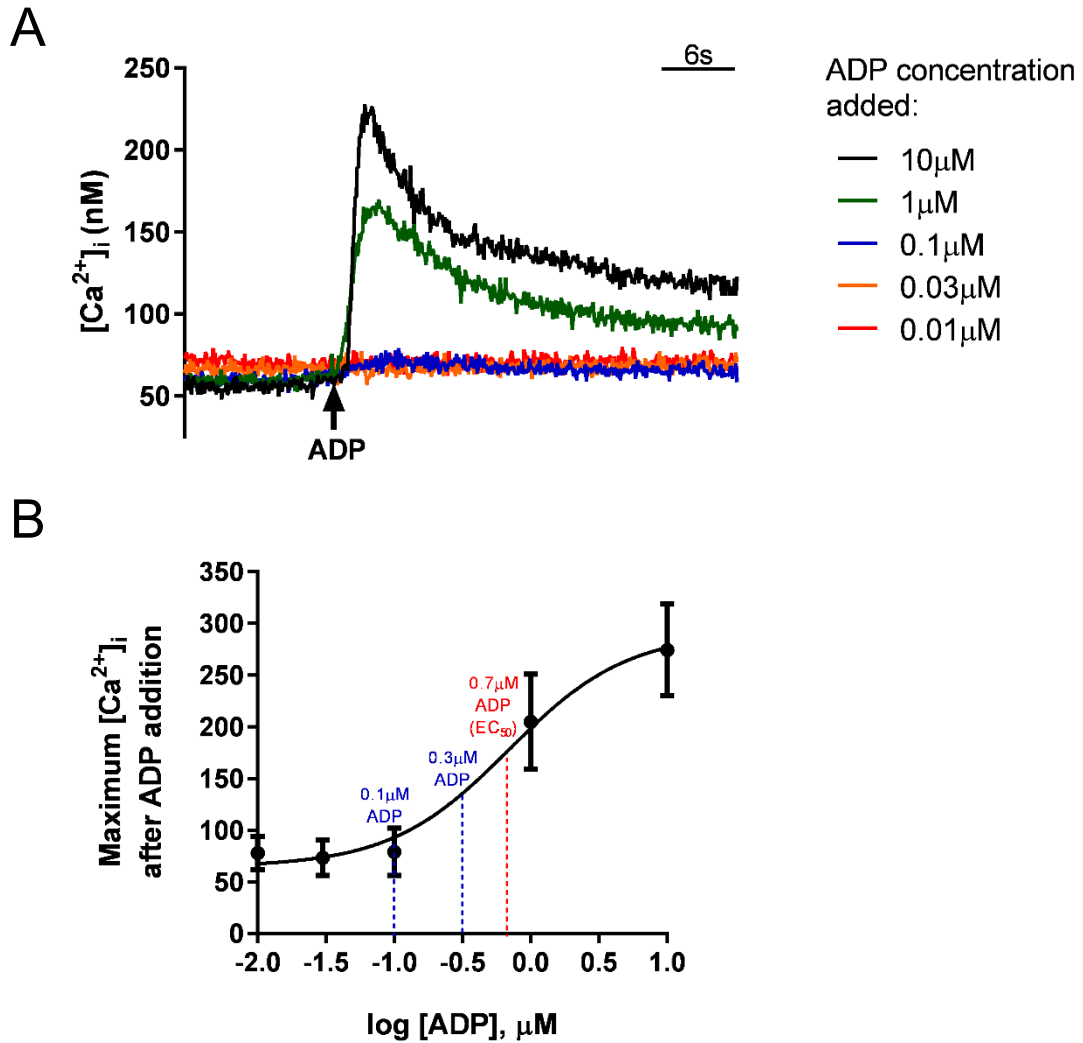


Figure 4.7 The effect of addition of a series of ADP concentrations on $[Ca^{2+}]_i$ in washed platelet suspensions. (A) Representative $[Ca^{2+}]_i$ responses obtained in Fura-2-loaded platelet suspensions following the addition of a range of ADP concentrations (0.01-10 μ M). (B) The concentration-effect relationship between ADP concentrations and corresponding maximum $[Ca^{2+}]_i$ obtained. The EC_{50} ADP concentration (0.7 μ M) is shown in red, and the concentrations chosen to achieve slight stimulation of P2Y receptors in shear stress assays (0.1 μ M and 0.3 μ M) are shown in blue. Data represent mean \pm SEM ($n=3$).

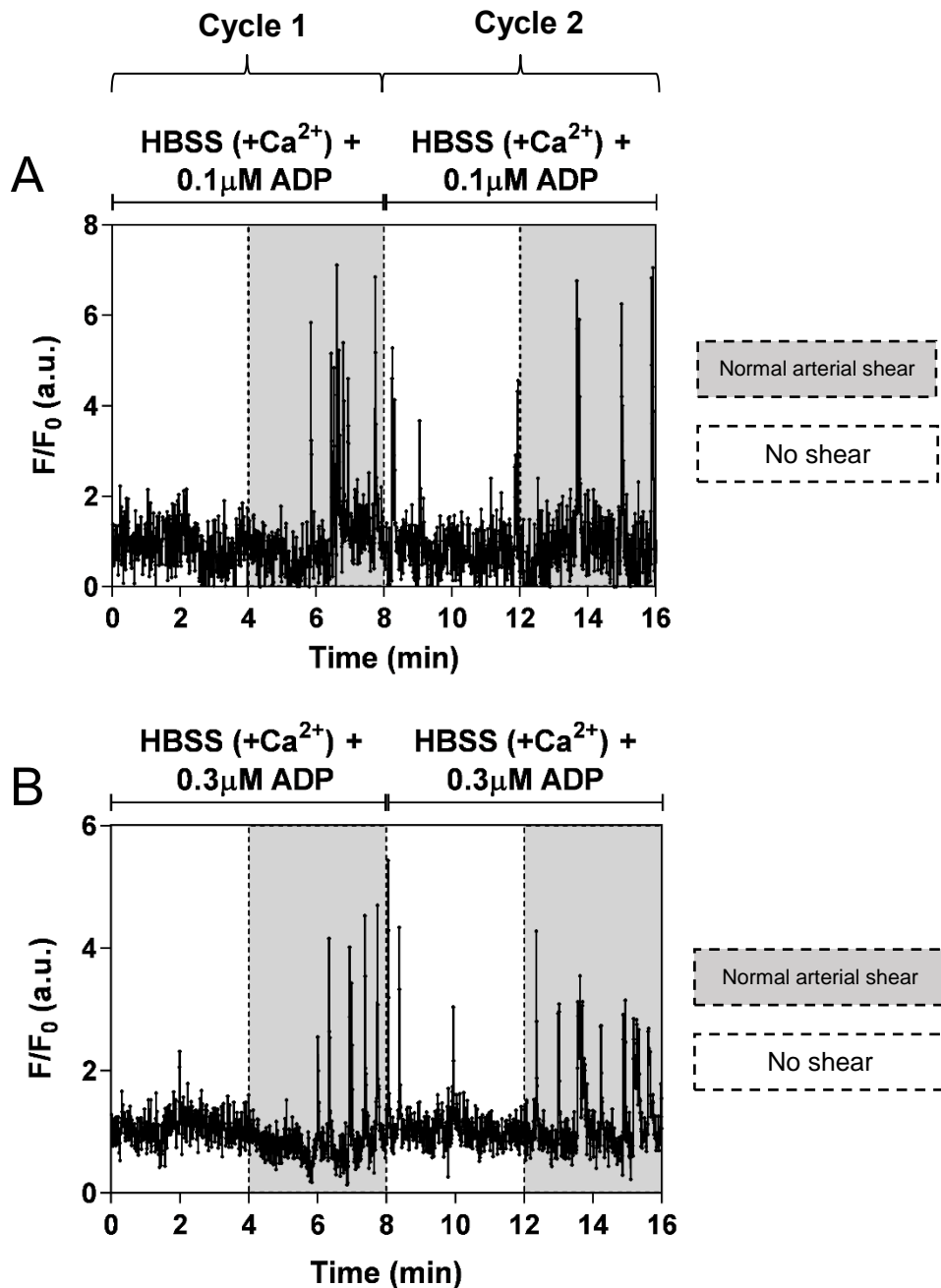
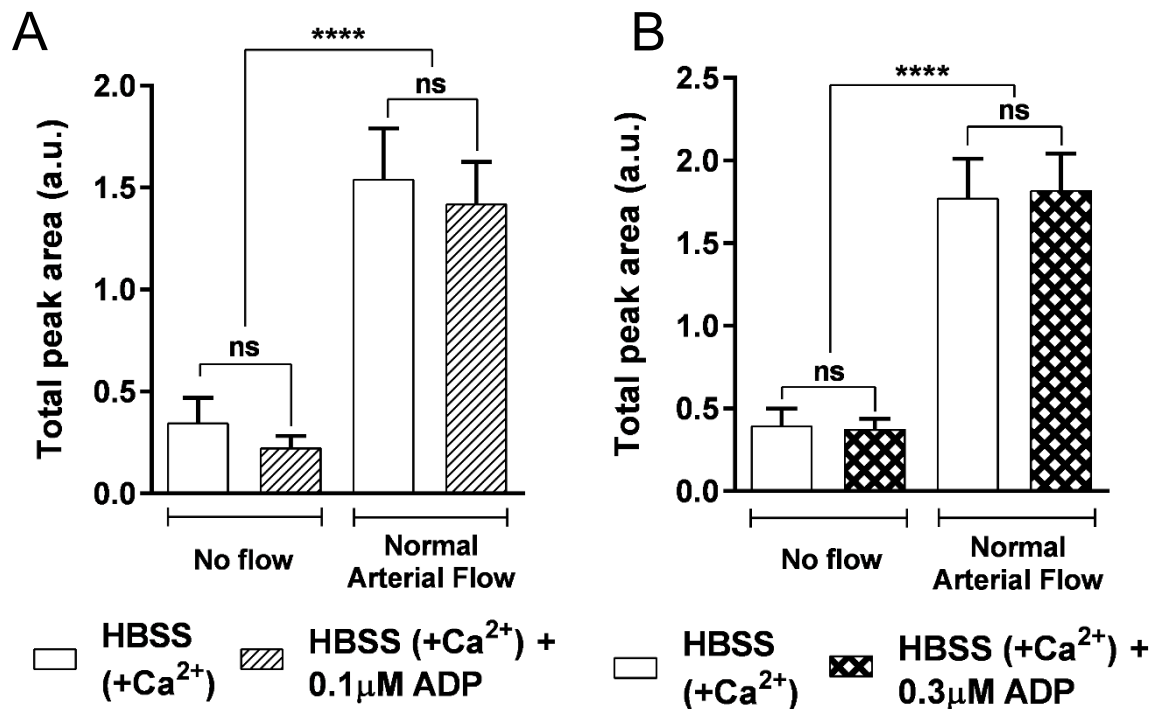


Figure 4.8 Stimulation of P2Y1 and P2Y12 receptors with a near-threshold concentration of ADP did not cause an observable change to the Ca^{2+} transient profile in singly attached platelets under shear. Representative F/F_0 Fluo-3 recordings in single platelets perfused with saline (HBSS+ Ca^{2+}) containing (A) $0.1 \mu\text{M}$ ADP, and (B) $0.3 \mu\text{M}$ ADP in both of the successive cycles of 4 minutes without shear followed by 4 minutes of arterial shear. Compared to control traces (Figure 4.1 B), there was no observable change when ADP was included in the extracellular saline. Apyrase was omitted from the extracellular saline to avoid P2X1 receptor responses.



*Figure 4.9 Fluid shear stress-induced average Ca^{2+} increases in single platelets remain unchanged by the inclusion of a low concentration of ADP in the extracellular saline. Average Ca^{2+} increases were calculated as the 4 min F/F_0 integral of all $[Ca^{2+}]_i$ transients. Responses in the absence of shear and during normal arterial shear, in the presence of extracellular Ca^{2+} , with and without (A) $0.1\mu M$ ADP, or (B) $0.3\mu M$ ADP [$n=36$ (control) and 30 (ADP-treated) cells, and 47 (control) and 37 (ATP-treated) cells in A and B, respectively]. **** $P<0.0001$; ns=not statistically significant. Data represent mean \pm SEM of 6 individual donors.*

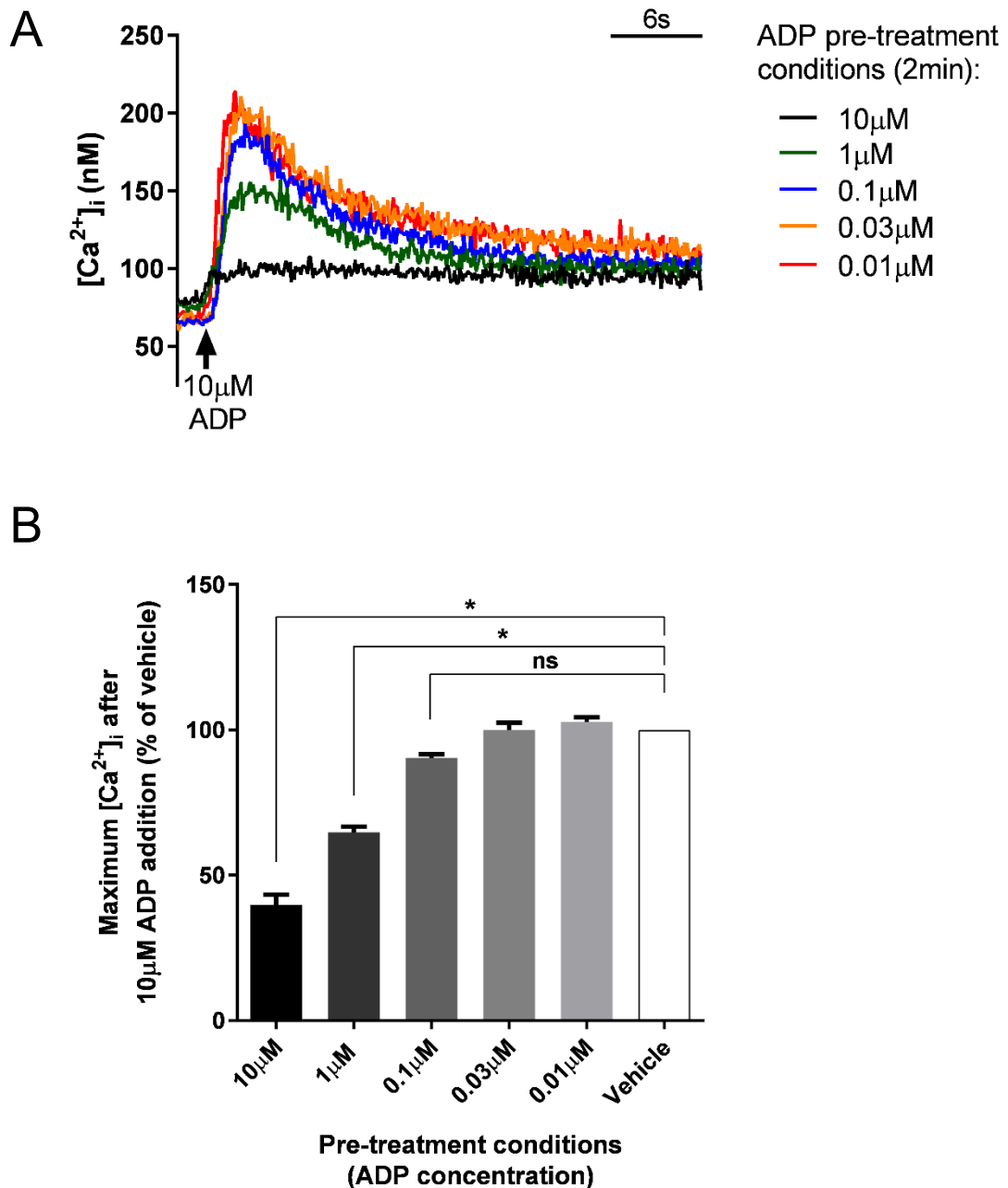


Figure 4.10 Pre-treatment with ADP concentrations higher than 0.1 μ M reduce maximum $[Ca^{2+}]_i$ responses to 10 μ M ADP. (A) Representative $[Ca^{2+}]_i$ traces recorded after the addition of 10 μ M ADP to platelet suspensions pre-exposed to a range of (0.01-10 μ M) ADP concentrations for 2 minutes. (B) Average maximum $[Ca^{2+}]_i$ responses to 10 μ M ADP, following pre-exposure to different ADP concentrations, compared to samples pre-treated with vehicle (saline). * $P < 0.05$; ns: not statistically significant. Data represent mean \pm SEM ($n=3$).

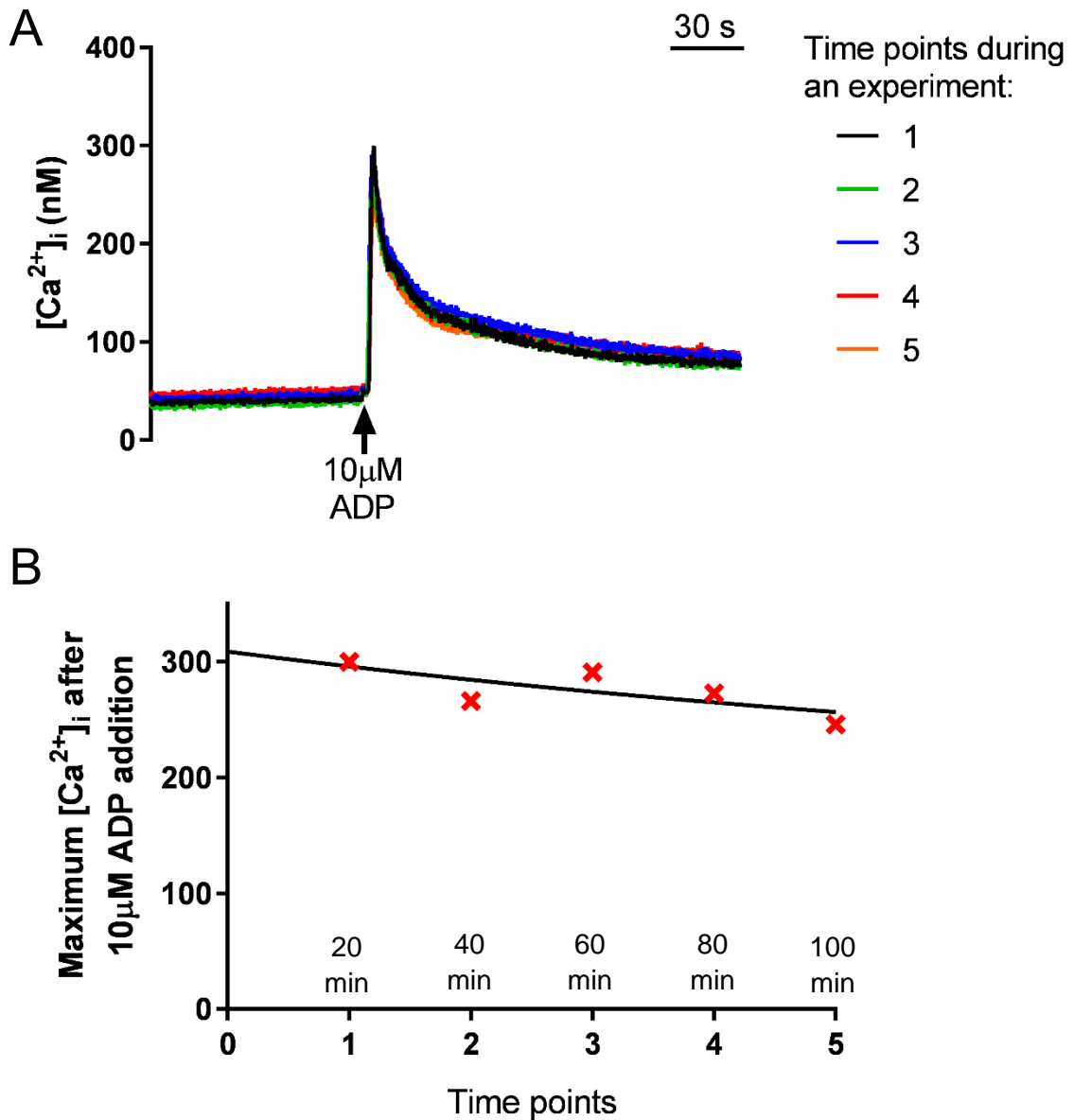


Figure 4.11 Monitoring of ADP-induced Ca²⁺ response activity over a period of 100 minutes. (A) Representative [Ca²⁺]_i responses obtained in each Fura-2-loaded platelet suspension following the addition of 10 μM ADP at regular time points throughout an experiment. (B) Representative line of best fit constructed using the maximum [Ca²⁺]_i attained at the regular time points in panel A, together with the corresponding approximate time of each recording, indicating P2Y1 and P2Y12 activity of a platelet sample over the course of an experiment.

4.2.3 Effect of GsMTx-4 on previously identified Ca^{2+} entry pathways of human platelets

GsMTx-4 is widely used as an inhibitor of MS ion channels, however its effects on well-established platelet Ca^{2+} entry pathways are unknown. Store-operated Ca^{2+} entry through Orai1 channels is a major Ca^{2+} entry pathway evoked by multiple agonists and can be selectively activated by depletion of intracellular Ca^{2+} stores with the SERCA inhibitor thapsigargin (Mahaut-Smith, 2012; Varga-Szabo *et al.*, 2009). GsMTx-4 had no significant effect on store-operated Ca^{2+} entry assessed from the peak increase in Ca^{2+} after addition of 1.26mM Ca^{2+} to platelets pre-treated with 1 μ M thapsigargin for 15 min in nominally Ca^{2+} -free saline (Figure 4.12 A). Furthermore, GsMTx-4 caused no inhibition of Ca^{2+} entry through the transient receptor potential cation channel subfamily C member 6 (TRPC6) ion channels directly activated using the diacylglycerol analogue 1-Oleoyl-2-acetyl-glycerol (OAG) (60 μ M) (Haddock *et al.*, 2002; Hofmann *et al.*, 1999) (Figure 4.12 B). A third Ca^{2+} -permeable pathway in platelets is the ATP-gated P2X1 channel, which can be selectively activated by α,β -meATP (Rolf *et al.*, 2001). Interestingly, a 30s pre-treatment with GsMTx-4 led to a 40% reduction in the peak Ca^{2+} response to a supramaximal concentration of α,β -meATP (10 μ M; a decrease from 296.1 ± 12.2 nM to 162.4 ± 20.7 nM; $P < 0.01$, $n=4$) (Rolf *et al.*, 2001) (Figure 4.12 C). In all ratiometric measurements in this section, P2X1 channel activity was monitored to make sure there was no time-dependent desensitisation (Figure 4.13). Loss of P2X1 receptor activity did not contribute to the inhibition of platelet shear-dependent Ca^{2+} responses by GsMTx-4 (Figure 4.2) since these experiments were carried out in the absence of apyrase, which leads to complete desensitisation of these ATP-gated cation channels (Rolf *et al.*, 2001) (Chapter 5, Figure 5.2 C). Similarly, in Chapter 3, Meg-01 shear-dependent Ca^{2+} responses were independent of P2X1 receptors because these receptors were not detected by Western blotting in this cell line (Chapter 3, Figure 3.4 A). To further confirm this, Fura-2-loaded Meg-01 suspensions were treated with the P2X1 receptor agonist α,β -meATP, following which no $[\text{Ca}^{2+}]_i$ response was obtained, as opposed to a strong response following P2Y receptor stimulation using ADP (Figure 4.14).

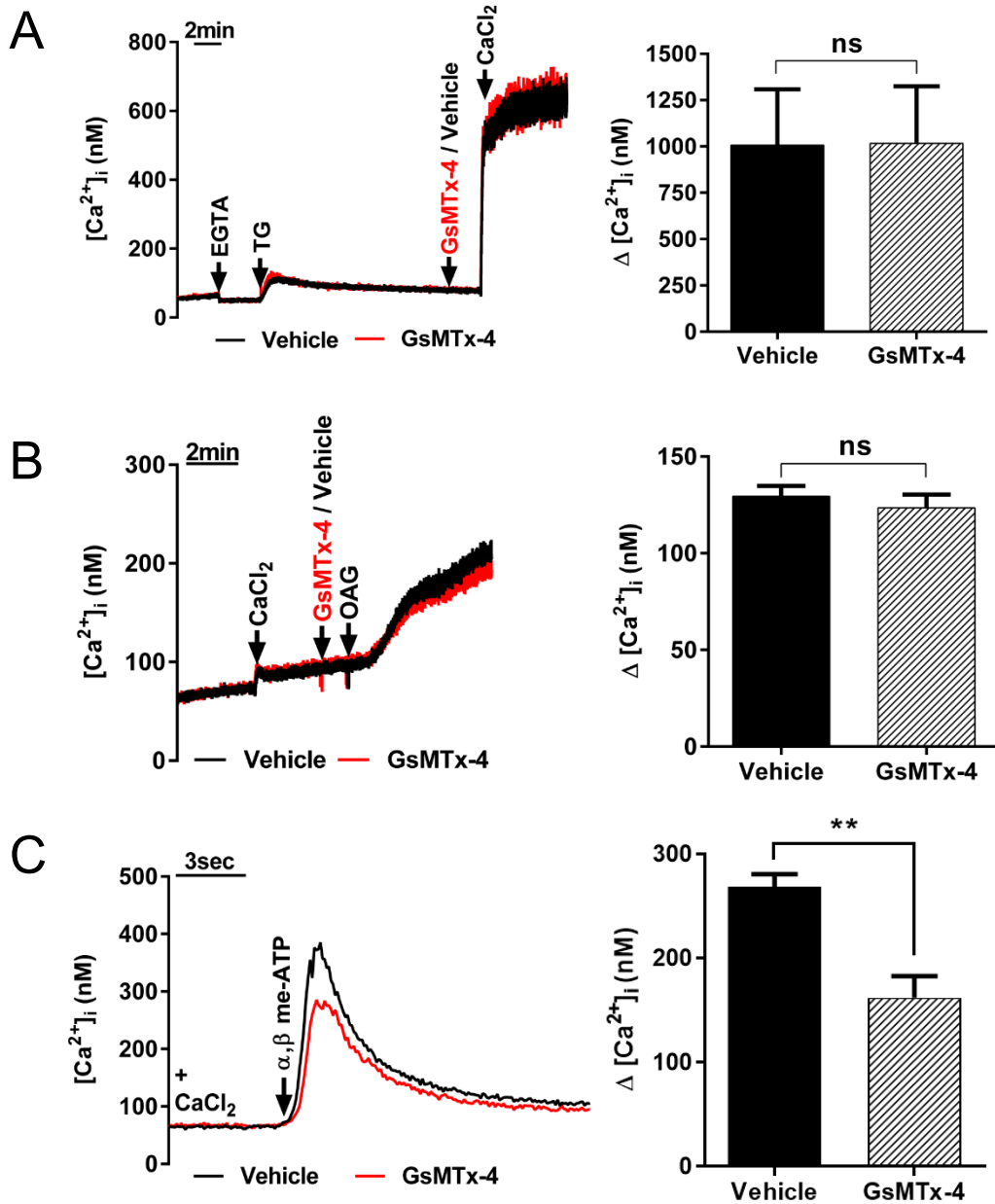


Figure 4.12 Effect of GsMTx-4 on Ca^{2+} entry via TRPC6, P2X1 and store-operated channels in platelets. Representative $[Ca^{2+}]_i$ recordings (left panels) and average peak $[Ca^{2+}]_i$ responses (right panels, $n=4$) for store-operated (A), TRPC6 (B) and P2X1 cation channels (C) in suspensions of platelets in the presence and absence of GsMTx-4. Store-operated Ca^{2+} entry was assessed by addition of 1.26mM $CaCl_2$ 15 minutes after treatment with the SERCA inhibitor thapsigargin (TG; 1 μ M). 0.2mM EGTA was added in the beginning to chelate any residual extracellular Ca^{2+} . TRPC6 was activated using the diacylglycerol analogue 1-oleoyl-2-acetyl-sn-glycerol (OAG; 60 μ M). P2X1 was activated with the non-hydrolysable ATP analogue α, β -meATP (10 μ M). ** $P < 0.01$; ns=not significant. Data represent mean \pm SEM. In all panels vehicle was ddH₂O.

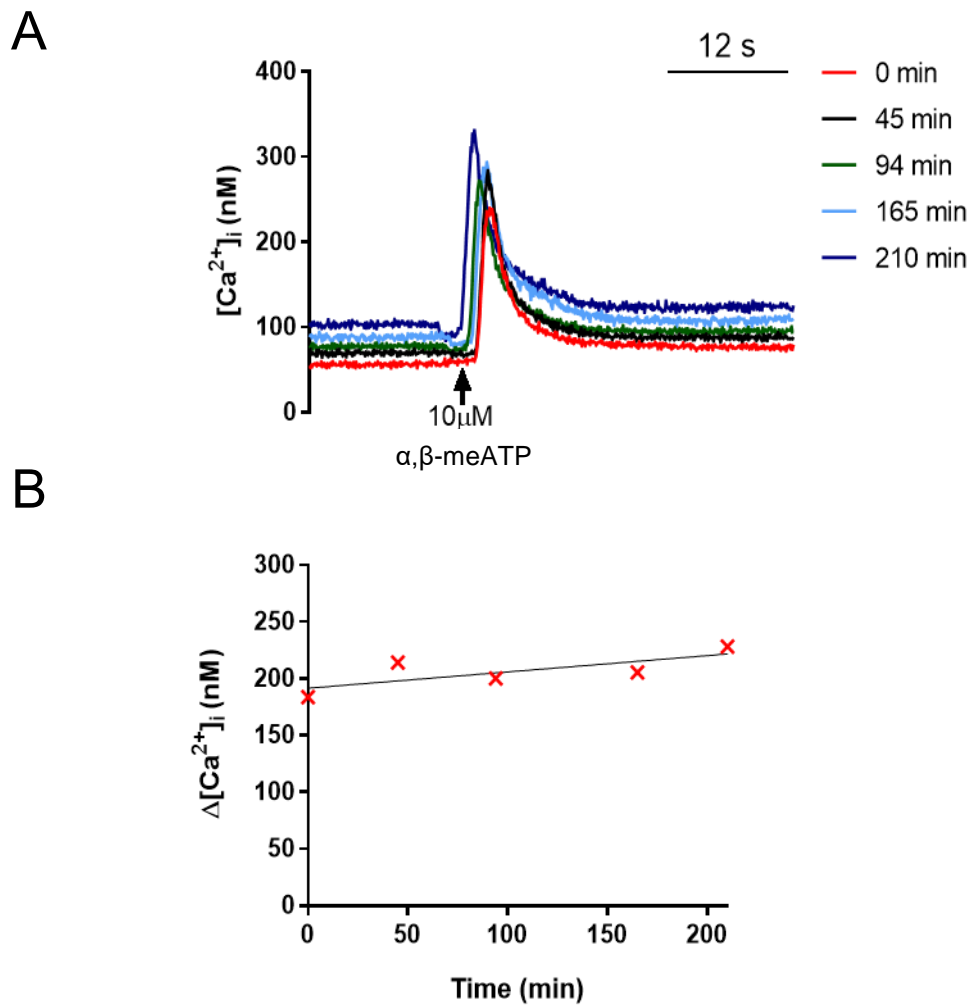


Figure 4.13 P2X1 activity was monitored throughout the experiments where P2X1 responses were measured. (A) Representative traces of maximum $[Ca^{2+}]_i$ responses following the stimulation of P2X1 channels using $10\mu M$ α, β -meATP, at several time points interspersed throughout the duration of an experiment. Maximum $\Delta[Ca^{2+}]_i$ at the different time points were calculated, and charts of P2X1 activity profiles were plotted with a line of best fit (B shows a representative profile), which were used to estimate the maximum P2X1 responses at the required time points during an experiment.

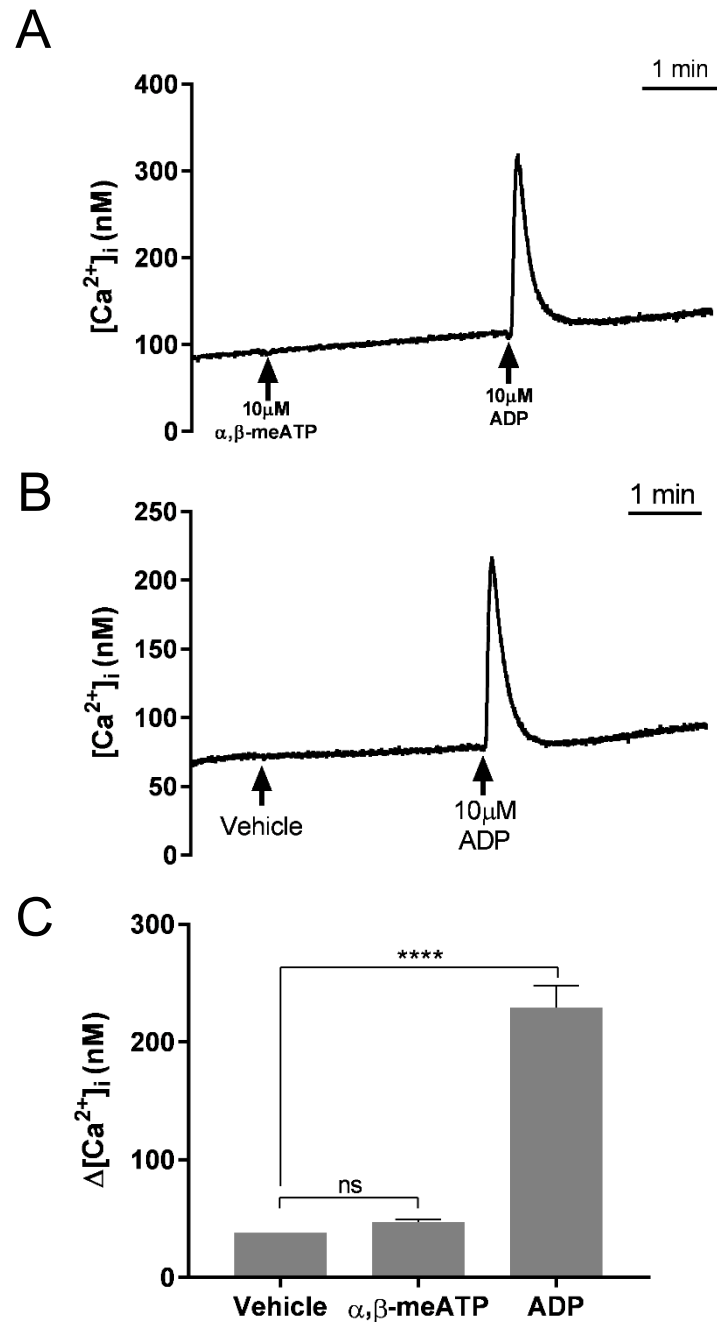


Figure 4.14 Fura-2-loaded Meg-01 suspensions do not display $[Ca^{2+}]_i$ increases following α,β -meATP treatment. Treatment of Meg-01 cells with the P2X1 channel agonist α,β -meATP (A), or vehicle (saline) (B), does not induce any elevation in $[Ca^{2+}]_i$, however stimulation of P2Y receptors with ADP leads to a sharp increase in $[Ca^{2+}]_i$. (C) Average increases in $[Ca^{2+}]_i$ following treatment with vehicle, 10 μ M α,β -meATP and 10 μ M ADP. **** $P < 0.0001$; ns=not statistically significant. Data represent mean \pm SEM ($n=3$).

4.2.4 Collagen-induced thrombus formation but not platelet aggregation is inhibited by GsMTx-4

Pre-treatment of whole blood with GsMTx-4 for 30s consistently resulted in a marked reduction in thrombus formation under normal arterial flow (1002.6s^{-1}) on a collagen surface (Figure 4.15 A). All three aspects of thrombus dimension analysed (height, volume and surface coverage) were reduced compared to control conditions; mean thrombus height by 48% ($1.2\pm 0.2\mu\text{m}$ to $0.6\pm 0.2\mu\text{m}$; $P<0.01$, $n=6$), mean thrombus volume by 48% ($48133\pm 7739\mu\text{m}^3$ to $25126\pm 6434\mu\text{m}^3$; $P<0.01$, $n=6$), and mean surface coverage by 38% ($26.4\pm 4.2\%$ to $16.3\pm 3.5\%$; $P<0.01$, $n=6$) (Figure 4.15 B). In contrast, GsMTx-4 had no effect on the aggregation response of platelets to $1\mu\text{g/mL}$ collagen measured in stirred suspensions, which induce minimal levels of shear (Figure 4.16). This suggests that the underlying GsMTx-4-sensitive pathway is crucially dependent upon application of shear stress for its activation.

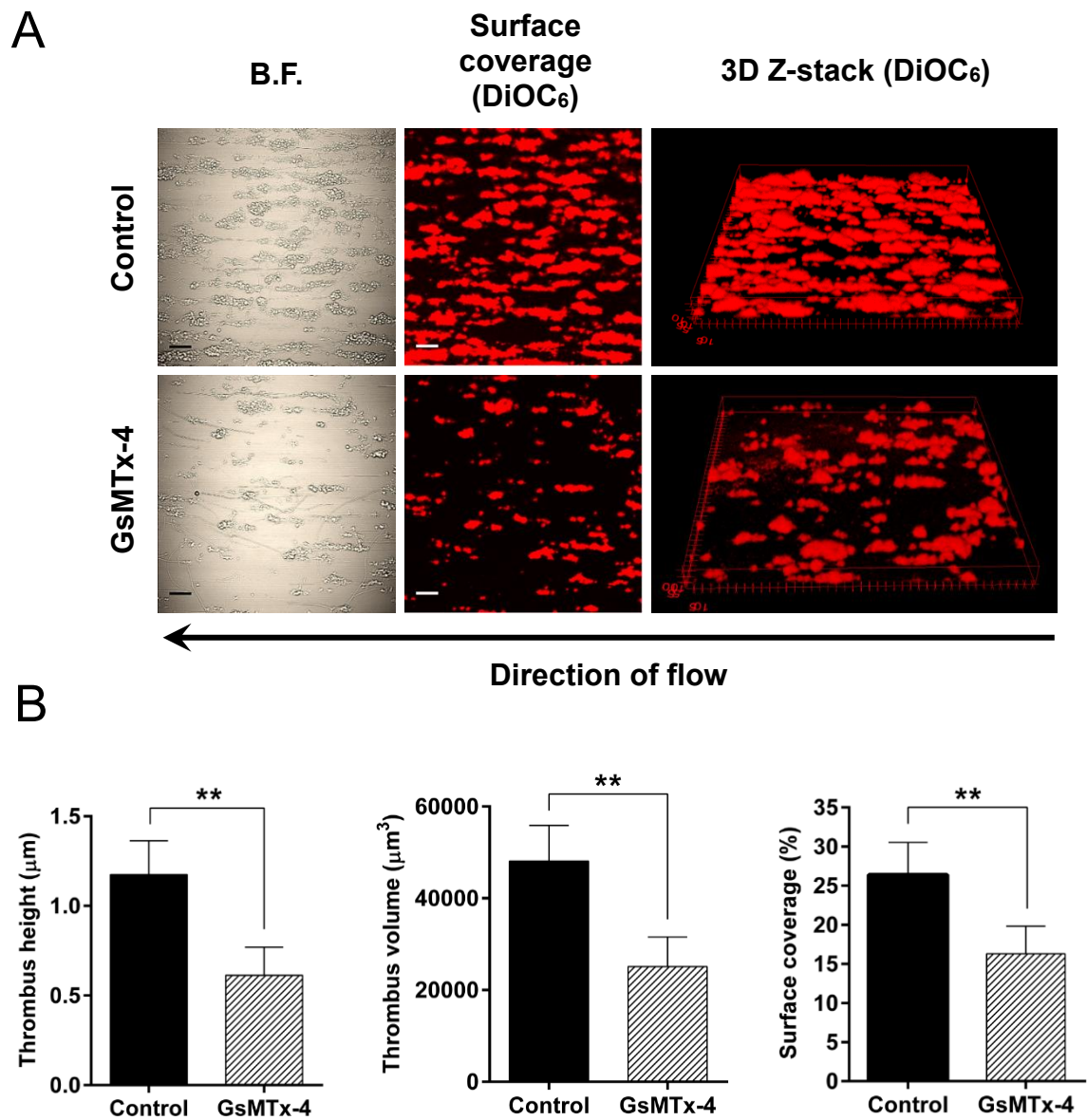


Figure 4.15 Collagen-induced thrombus formation is inhibited by GsMTx-4. (A) Representative images of surface coverage and 3D Z-stacks for thrombi formed by DiOC₆-stained platelets on a collagen surface under control and GsMTx-4 pre-treated conditions. Blood samples were perfused over collagen under normal arterial shear stress conditions (1002.6s^{-1}). The scale bars represent $20\mu\text{m}$. (B) Average figures for thrombus height, thrombus volume and surface coverage under control and GsMTx-4 treated conditions. $**P < 0.01$. Data represent mean \pm SEM ($n=6$ individual donors).

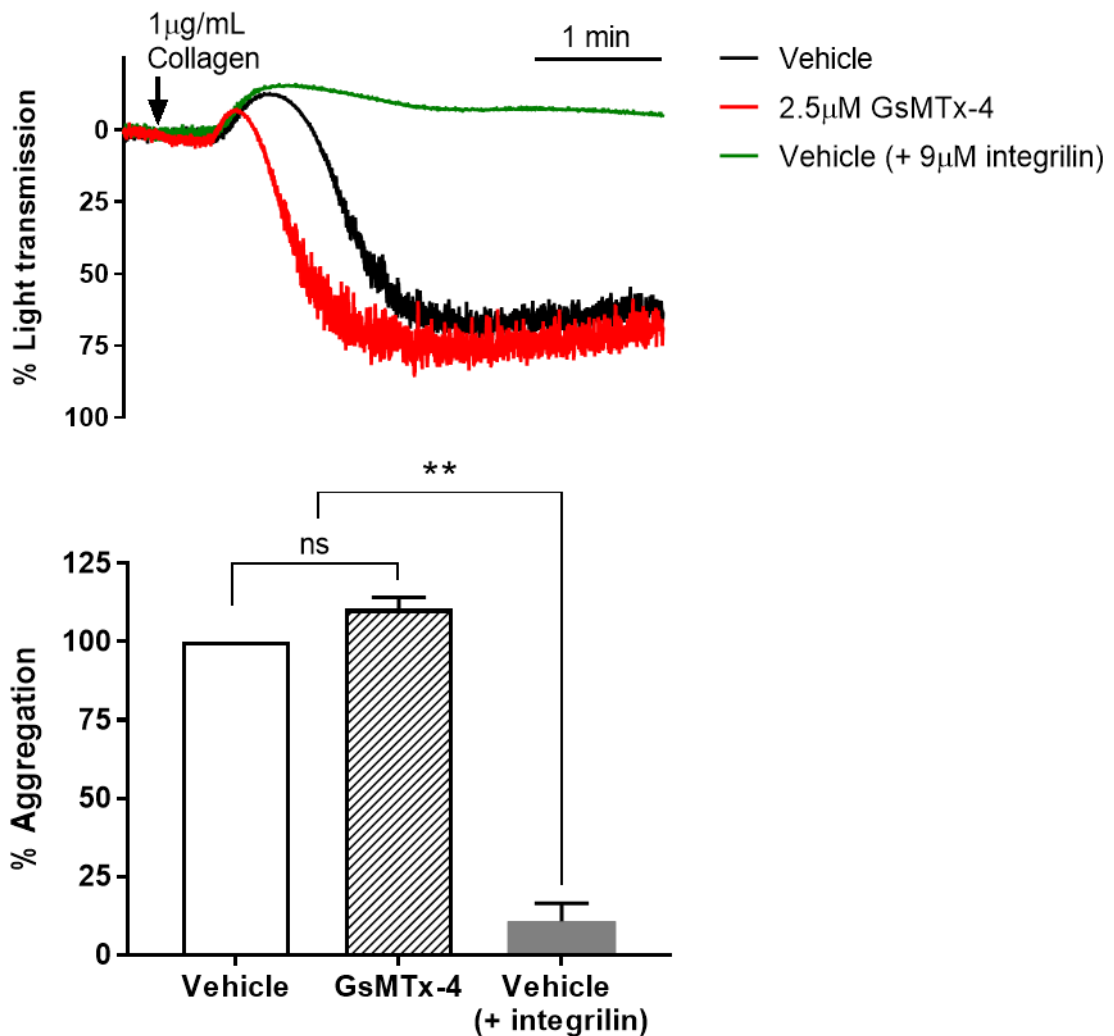


Figure 4.16 Collagen-induced platelet aggregation is not inhibited by GsMTx-4. Collagen (1 μg/mL)-evoked aggregation under control and GsMTx-4-treated conditions; integrilin treatment was performed as a control to demonstrate that aggregation in the samples can be blocked by the inhibition of $\alpha_{IIb}\beta_3$ integrin complex. Representative light transmission traces are shown in the upper panel and average maximal light transmission responses expressed as % aggregation in the lower panel (Data represent mean \pm SEM; $n=3$ individual donors); ** $P<0.01$; ns = not significant. Vehicle = ddH₂O.

4.2.5 *GsMTx-4 inhibits thrombus formation by blocking P2X1 as well as mechanosensitive cation channels*

In contrast to washed platelet suspensions where P2X1 receptors are desensitised unless apyrase is added to the extracellular saline, whole blood is known to contain sufficient ectonucleotidase activity that prevents purinergic receptor desensitisation (Jones *et al.*, 2014b; Cauwenberghs *et al.*, 2006; Glenn *et al.*, 2005; Hechler *et al.*, 2005). It is well established that P2X1 receptors contribute to thrombus formation at arterial levels of shear (Erhardt *et al.*, 2006; Oury *et al.*, 2003; Hechler *et al.*, 2003). Consequently, the inhibitory effect of GsMTx-4 on thrombus formation (Figure 4.15) could have resulted, at least in part, from a reduction of P2X1-induced $[Ca^{2+}]_i$ elevation (Figure 4.12 C). Therefore, the effect of GsMTx-4 on thrombus formation was assessed with and without the P2X1 antagonist NF449. 1 μ M NF449, which abolishes P2X1 activity (induced with a supramaximal concentration of α,β -meATP (Rolf *et al.*, 2001)) (Figure 4.17 A), caused a 37% reduction of thrombus volume (Figure 4.17 Bi), consistent with previous reports (Hechler *et al.*, 2005). Importantly, combined addition of GsMTx-4 and NF449 caused a more significant inhibition of thrombus formation compared with NF449 alone (Figure 4.17 B). Using NF449 alone, mean thrombus volume was reduced from $99856 \pm 11408 \mu\text{m}^3$ to $62678 \pm 10886 \mu\text{m}^3$ (by 37%; $P < 0.05$, $n=7$), whereas using GsMTx-4, and GsMTx-4 and NF449 combined, there were 69% (to $31290 \pm 18 \mu\text{m}^3$) and 75% (to $24889 \pm 2363 \mu\text{m}^3$) reductions in thrombus volume ($P < 0.0001$, $n=7$, for both), respectively (Figure 4.17 Bi). Similarly, mean % surface coverage was reduced from $46.9 \pm 2.9\%$ to $36.1 \pm 4.4\%$ using NF449 (not statistically significant), and to $24.6 \pm 1.7\%$ and $18.4 \pm 1.4\%$ using GsMTx-4 and both GsMTx-4 and NF449 ($P < 0.0001$, $n=7$, for both), respectively (Figure 4.17 Bii). Mean thrombus height decreased from $2.4 \pm 0.3 \mu\text{m}$ to $1.5 \pm 0.3 \mu\text{m}$ using NF449 ($P < 0.05$, $n=7$), and to $0.8 \pm 0.1 \mu\text{m}$ and $0.6 \pm 0.1 \mu\text{m}$ using GsMTx-4 and both GsMTx-4 and NF449 ($P < 0.0001$, $n=7$, for both), respectively (Figure 4.17 Biii). Together these results indicate that a pathway other than P2X1 receptors is also inhibited by GsMTx-4 during inhibition of thrombus formation.

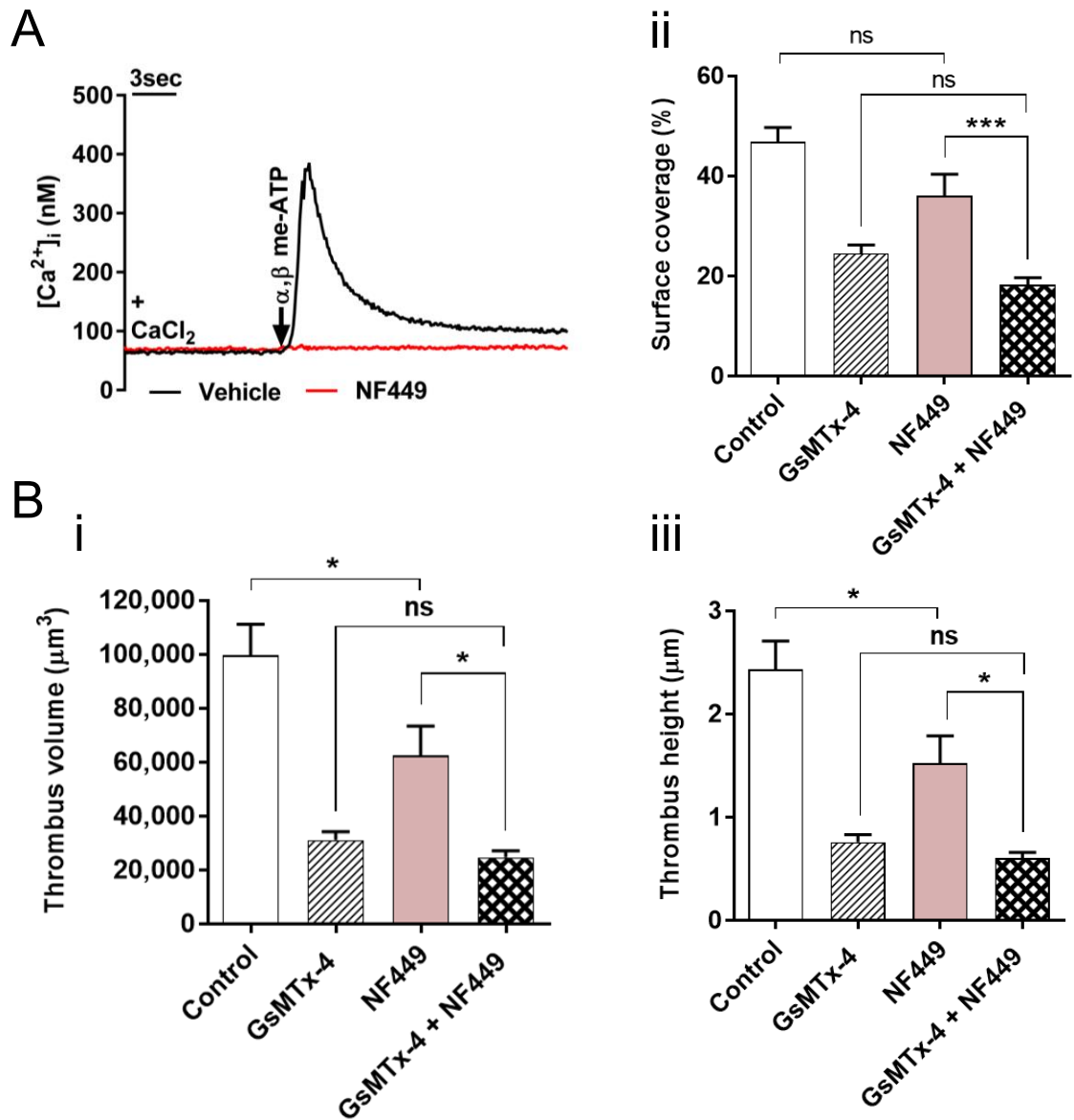


Figure 4.17 GsMTx-4 inhibits thrombus formation by blocking P2X1 as well as mechanosensitive cation channels. (A) P2X1-dependent Ca²⁺ entry (α,β-meATP, 10μM) in platelet suspensions is completely inhibited by 1μM NF449. (B) Effect of 2.5μM GsMTx-4 and 1μM NF449, individually and combined, on thrombi formed on a collagen surface; average values are shown for thrombus volume (i), surface coverage (ii), and thrombus height (iii). Blood samples were perfused over collagen under normal arterial shear stress conditions (1002.6s⁻¹). ***P<0.001; *P<0.05; ns=not statistically significant. Data represent mean ± SEM (n=7 individual donors).

4.3 Discussion

Data within this chapter provide evidence for MS Piezo1 ion channel activity in human platelets, which operate under normal and pathological arterial levels of shear stress and contribute to the elevation of $[Ca^{2+}]_i$ directly in a shear-dependent manner. The use of the MS cation channel inhibitor GsMTx-4 in thrombus formation assays provide a link between the observed physiological and functional responses.

Individual platelets that were attached to a surface without causing activation, displayed $[Ca^{2+}]_i$ responses upon exposure to arterial levels of shear that were inhibited by the MS channel blocker GsMTx-4 or removal of external Ca^{2+} , indicating MS cation channel activity in single cells under flow. Importantly, the Piezo1 agonist Yoda1 directly stimulated Ca^{2+} entry into both platelets and in the absence of shear and also potentiated shear-dependent Ca^{2+} transients in platelets, indicating Piezo1 channel activity. In agreement with these data, Patapoutian and colleagues demonstrated that Yoda1 can induce Piezo1 activation in the absence of mechanical stimulation and also increase its sensitivity to mechanical activation (Syeda *et al.*, 2015). Although GsMTx-4 is a generic MS ion channel blocker, it has been the main inhibitor used in study of Piezo1 function (Copp *et al.*, 2016; Li *et al.*, 2015; Pathak *et al.*, 2014; Bae *et al.*, 2011). The toxin acts through insertion into the lipid bilayer and modification of the lipid:channel interface (Suchyna *et al.*, 2004), hence may influence a number of ion channels. However, GsMTx-4 did not block TRPC6 or Orai1 store-operated Ca^{2+} entry in platelets (Figure 4.12). It has been shown that the molecular mechanism underlying either mechanical or chemical activation of TRPC6 channels is the same, and involves sensing tension along the phospholipid bilayer (Spassova *et al.*, 2006). Therefore, the lack of inhibitory effect of GsMTx-4 on OAG-induced Ca^{2+} mobilisation could potentially indicate that GsMTx-4 inhibits other MS channels in experiments carried out under shear stress. Although P2X1 channels were partially inhibited by GsMTx-4, these ATP-gated Ca^{2+} -permeable channels would have been desensitised in the ectonucleotidase (i.e. apyrase)-free conditions used to record shear-induced Ca^{2+} transients in this study (Rolf *et al.*, 2001). Furthermore, in the thrombus formation assay using whole blood, which retains significant ectonucleotidase activity and thus also P2X1 channel activity (Cauwenberghs *et al.*, 2006; Hechler *et al.*, 2005; Glenn *et al.*, 2005), the GsMTx-4 block of thrombus formation was still observed after abrogation of P2X1 channel responses with NF449. Figure 4.14 further demonstrates that P2X1

channels are not expressed in the Meg-01 cell line, and hence that the shear stress-dependent Ca^{2+} responses in Meg-01 cells (*see* Chapter 3: Figures 3.7 A and 3.8 A) also do not depend upon activation of this ATP-gated cation channel. Another evidence which could confirm MS cation channel activity in platelets is the different inhibitory action of this blocker in the presence and absence of shear stress (Section 4.2.4). Although thrombus formation under flow over collagen surfaces were reduced by GsMTx-4 pre-treatment, there was no reduction in collagen-induced platelet aggregation where there was no applied laminar flow. It is worth noting that intravital imaging studies have recently suggested that blood rheology is the primary factor driving thrombus formation *in vivo*, with less significant roles for classical diffusible platelet agonists (Nesbitt *et al.*, 2009; Miyazaki *et al.*, 1996). Ca^{2+} influx through Piezo1 channels certainly represents a candidate for transduction events directly influenced by rheological forces in the arterial circulation.

The presence of a MS pathway in platelets has been suggested in earlier studies, which hypothesised potential existence of MS cation channels which may be responsible for the shear-induced Ca^{2+} elevations observed (Chow *et al.*, 1992; Levenson *et al.*, 1990). Using a cone-and-plate viscometer, Kroll and colleagues demonstrated a transmembrane Ca^{2+} influx in response to arterial or higher levels of shear (Chow *et al.*, 1992). In addition, a link between transmembrane Ca^{2+} flux and hemodynamic shear stress from studies of hypertensive patients has also been reported (Levenson *et al.*, 1990). Piezo1 could account for these previously reported shear-dependent Ca^{2+} influx pathways, although further work is required to address this possibility.

Shear-induced Ca^{2+} responses took the form of Ca^{2+} spikes in singly attached platelets, as opposed to sustained elevations in Meg-01 cells. Similar Ca^{2+} spiking profiles were reported previously in single Fura-2-loaded platelets that were immobilised on fibrinogen, following stimulation with relatively high concentrations of thrombin (0.1-1U/mL) or ADP (10-40 μM), or simply by contact with a glass surface (Hussain & Mahaut-Smith, 1999; Ariyoshi & Salzman, 1995; Heemskerk *et al.*, 1993; Heemskerk *et al.*, 1992). A noticeable difference between the shear-dependent Ca^{2+} responses of Meg-01 cells and platelets was the more immediate nature of the cell line response compared to the delayed increase in platelets (Figures 3.8 and 4.1). A likely explanation is the very different cytoskeletal arrangement of platelets, which consists of a cortical cytoskeleton that is responsible for its discoid resting shape and also results in

a less flexible plasma membrane compared to other cell types, including its precursor and related cell lines (Mahaut-Smith, 2004; Hartwig & Italiano, 2003). Since Piezo1 is gated by tensions within the lipid bilayer of the membrane itself rather than via a link to the cytoskeleton (Cox *et al.*, 2016; Coste *et al.*, 2012; Coste *et al.*, 2010), platelets may need to undergo a greater deformation by the fluid shear compared to Meg-01 cells before channel activation. Although Piezo1 channels are gated by bilayer tension in cytoskeleton-free artificially generated blebs, Cox and co-workers have emphasised that cytoskeletal proteins or links to the extracellular matrix components can modify the tension experienced by the bilayer in intact cells (Cox *et al.*, 2016). This cytoskeletal ‘mechanoprotection’ effect is known to curb the activity of endogenous Piezo channels (Gnanasambandam *et al.*, 2015; Morris, 2001). Manipulating the cytoskeletal properties of cells has also been linked to changes in latency of channel activation and channel gating in general (Cox *et al.*, 2016; Suchyna & Sachs, 2007). In the experiments presented in this chapter, a second application of increased shear stimulated Ca²⁺ transients with reduced delay, similar to effects on stretch-activated K⁺ channels in *Lymnaea* neurons, where it has been suggested that application of repeated pressure causes cytoskeleton-dependent adaptation (Small & Morris, 1994).

The lack of change in shear-dependent Ca²⁺ spiking by low levels of stimulation of P2Y receptors in single platelets provide further evidence for the conclusion that Piezo1 channels are responsible for the MS Ca²⁺ events observed in platelets. Firstly, the observation that low levels of P2Y receptor stimulation does not modify the shear-induced Ca²⁺ spiking patterns observed in single platelets could potentially rule out the possibility that P2Y receptors perform MS roles or modulate MS ion channel responses leading to [Ca²⁺]_i elevations (Linan-Rico *et al.*, 2013; Anfinogenova *et al.*, 2011; Inoue *et al.*, 2009; Song *et al.*, 2009; Fernandes *et al.*, 2008; Leon *et al.*, 1999). Provided this is the case, the possibility that the delayed commencement of Ca²⁺ spiking under flow could represent the relatively longer time needed by the signalling pathways downstream of P2Y receptors can be eliminated. This potentially further confirms that the delayed commencement of Ca²⁺ spiking under flow is due to the mechanoprotection effect as described above.

In conclusion, this chapter shows that MS cation channels mediate Ca²⁺ entry into the human platelets under arterial shear stress *in vitro*. Piezo1 is the likely MS channel mediating the effects we have observed. Pharmacological inhibition of these channels demonstrate that they contribute to thrombus formation under arterial flow.

However, future work should develop an animal model lacking Piezo1 specifically in platelets and megakaryocytes to further support these conclusions and to extend to *in vivo* studies. MS cation channels, at pathologically high levels of shear stress that is generally experienced at the regions of vessel narrowing resulting from stenosis or atherosclerosis, could potentially enhance Ca²⁺ influx which can increase the risk of life-threatening thrombus formation.

Chapter 5

Role for P2X1 channels in FcγRIIa-induced calcium entry and functional responses in human platelets

5.1 Introduction

Recent advances in the characterisation of the role of FcγRIIa receptors as a mediator of human platelet immunogenic responses highlight the diversity of the biological processes platelets are involved in. Platelets are believed to accelerate the removal of the invading pathogens mediating pathogen-induced secretion of chemokines, cytokines and antimicrobial compounds (Cox *et al.*, 2011). Platelet FcγRIIa receptors contribute to this by binding to IgG-opsonised pathogens, resulting in platelet activation. Moreover, FcγRIIa receptors have been shown to contribute to IgG-independent responses, such as mediating $\alpha_{IIb}\beta_3$ -dependent spreading on fibrinogen and GPIIb-dependent signalling (Boylan *et al.*, 2008; Sullam *et al.*, 1998). Nevertheless, the IgG-dependent interactions of FcγRIIa receptors can contribute to diseases such as infective endocarditis (IE) in which streptococci or staphylococci infect areas of the endocardium, particularly the heart valves. Such infections can result in thrombus formation on the valves obstructing their movement, and can even lead to dangerous circulating embolisms. Arman and colleagues studied tyrosine phosphorylation, platelet aggregation, and ATP secretion responses to FcγRIIa receptor activation achieved by cross-linking the receptors using specific antibodies (IV.3 + F(ab')₂), and five different bacterial strains most commonly known to be involved in IE (Arman *et al.*, 2014). In control experiments, the anti-FcγRIIa (IV.3) antibody was shown that it does not interfere with activation of platelet function by standard haemostatic agonists (Tilley *et al.*, 2013). Further studies demonstrate the important role of FcγRIIa receptors in thrombus formation under shear stress *in vitro* and *in vivo*, through the inhibition of the receptors by the anti-FcγRIIa antibody (IV.3) (Tilley *et al.*, 2013; Zhi *et al.*, 2013; Kerrigan *et al.*, 2008). Consequently, FcγRIIa receptors have been indicated as novel therapeutic targets against infection-related cardiovascular diseases. Therefore, a wider understanding of FcγRIIa receptor activation is crucial, in order to help us identify potential therapeutic approaches.

Despite the growing evidence for FcγRIIIa receptor involvement in platelet function, our knowledge of the physiological effects leading up to platelet activation induced by FcγRIIIa receptor activation remains unclear. Three pieces of evidence support our hypothesis that P2X1 channels contribute to $[Ca^{2+}]_i$ increases following FcγRIIIa receptor activation. Firstly, FcγRIIIa receptor activation results in the activation of a signal transduction pathway through a single ITAM (Figure 1.7), in a similar manner to the signalling profile observed after the activation of collagen receptor GPVI which is known to synergise with P2X1 channels via ATP secretion (Fung *et al.*, 2012; Fung *et al.*, 2005; Watson & Gibbins, 1998). Secondly, the activation of TLR2/1, which play important roles in the innate immune system, was also demonstrated to induce Ca^{2+} entry through P2X1 channels and interestingly these responses were resistant to endothelium-derived inhibitors (Fung *et al.*, 2012). Thirdly, the possible co-operation between platelet FcγRIIIa and purinergic receptors were postulated by a study (Klarstrom Engstrom *et al.*, 2014), however such a synergy has not been extensively studied by this group.

This chapter will investigate the potential role of P2X1 channels in contributing to $[Ca^{2+}]_i$ elevations following FcγRIIIa receptor activation by antibodies or *S. sanguinis*. Furthermore, the molecular signalling mechanisms responsible for a possible co-operation between FcγRIIIa receptors and P2X1 channels, and the influence of physiological parameters, such as the presence of endothelium-derived inhibitors or arterial shear stress, on this mechanism will also be examined in this chapter.

5.2 Results

5.2.1 *FcγRIIa* receptor activation induces Ca^{2+} entry through P2X1 channels

FcγRIIa receptor stimulation by cross-linking the receptor-bound IV.3 antibody by IgG F(ab')₂ resulted in prominent elevations in $[Ca^{2+}]_i$. Platelets were first pre-incubated with a concentration of mAb IV.3 used in previous studies where the phosphorylation of the Fc receptor γ chain was successfully induced following stimulation by the addition of IgG F(ab')₂ (Gibbins *et al.*, 1996). This stimulation resulted in an $[Ca^{2+}]_i$ increase of 440.6 ± 33.2 nM in $[Ca^{2+}]_i$ within the first 1 minute after stimulation in all platelet samples tested (Figure 5.1 A, F). In order to assess the potential contribution of P2X1 channels to $[Ca^{2+}]_i$ increases induced by *FcγRIIa* receptor stimulation, the complete inhibition of P2X1 channel activity was achieved by three different approaches: pre-incubation of washed platelets for 1 minute with NF449 at a concentration (1 μ M) shown to be specific for P2X1 channels; exclusion of apyrase from the extracellular saline during platelet preparation to desensitise P2X1 channels; or desensitization using a low concentration (600 nM) of the stable ATP analogue α, β -meATP prior to addition of extracellular Ca^{2+} (Fung *et al.*, 2005) (Figure 5.2). All three approaches resulted in significant reductions in the peak $[Ca^{2+}]_i$ reached after *FcγRIIa* receptor stimulation to: 303.5 ± 31.5 nM ($P < 0.05$, $n = 3$), 307.7 ± 42.8 nM ($P < 0.05$, $n = 3$), and 291.1 ± 39.9 nM ($P < 0.01$, $n = 3$) after NF449, apyrase exclusion and α, β -meATP-induced desensitisation, respectively (Figure 5.1 A, B, E and F). The levels of inhibition achieved by all three approaches used to eliminate P2X1 channel activity were very similar ($31.7 \pm 1.1\%$) (Figure 5.1 F).

In order to determine the source(s) of Ca^{2+} responsible for the remaining Ca^{2+} response after *FcγRIIa* receptor stimulation when the P2X1 activity is inhibited, firstly Ca^{2+} was excluded from the extracellular saline, and then the intracellular Ca^{2+} stores were depleted by pre-treating the platelets with thapsigargin (TG) (in EGTA-containing saline) for 15 minutes (Authi *et al.*, 1993). Exclusion of extracellular Ca^{2+} resulted in a further reduction in *FcγRIIa* receptor-evoked $[Ca^{2+}]_i$ to 191.7 ± 30.5 nM (by $56.5 \pm 6.9\%$), compared to when P2X1 activity was inhibited, indicating a potential contribution from other Ca^{2+} influx pathways (Figure 5.1 C, F). Simultaneous depletion of intracellular Ca^{2+} stores and chelation of any residual extracellular Ca^{2+} using EGTA led to an even further reduction in the peak $[Ca^{2+}]_i$ to 108.6 ± 8.2 nM (by $75.4 \pm 1.9\%$) (Figure 5.1 D, F).

A range of *Streptococci* strains including *S. sanguinis* were previously used to induce platelet aggregation in washed platelet suspension (Arman *et al.*, 2014). As an alternative to antibody stimulation of the FcγRIIa receptors, this study also sought to use *S. sanguinis* as a more physiologically relevant method of receptor stimulation. Arman *et al* have observed that the absence of IgGs and fibrinogen from the washed platelets accounted for the lack of aggregation responses after the addition of bacterial suspensions to platelets. This was because, FcγRIIa activation can be achieved by IgG-opsonized pathogens, where IgG forms a link between the FcγRIIa receptors and the pathogen, clustering the receptors to induce activation (Figure 5.3 A). For this reason, 0.1mg/mL hIgGs and 100μg/mL fibrinogen were included in each cuvette before experimentation. Also, platelets were not treated with aspirin for the purposes of this experiment since aspirin treatment prevented bacteria-evoked Ca²⁺ responses (Figure 5.3 B). Over a period of 25 minutes after addition of bacterial suspensions, a steady increase in [Ca²⁺]_i levels compared to vehicle control was observed, and the maximal Ca²⁺ levels reached at the end of the experiment did not change when P2X1 channels were desensitized using α,β-meATP (341.5±36.5nM and 344.4±27.2nM, respectively) (Figure 5.3 C, D). Interestingly, within the first 3 minutes after the addition of bacteria, a small Ca²⁺ peak was observed, which was fully inhibited by P2X1 channel desensitization (Figure 5.3 C, E), reducing the overall [Ca²⁺]_i by 44% (P<0.01, n=3), from 69.2±3.2nM to 39.7±4.3nM. Thus, Ca²⁺ entry through P2X1 channels can be stimulated by cross-linking the FcγRIIa receptors using bacteria in addition to using antibodies.

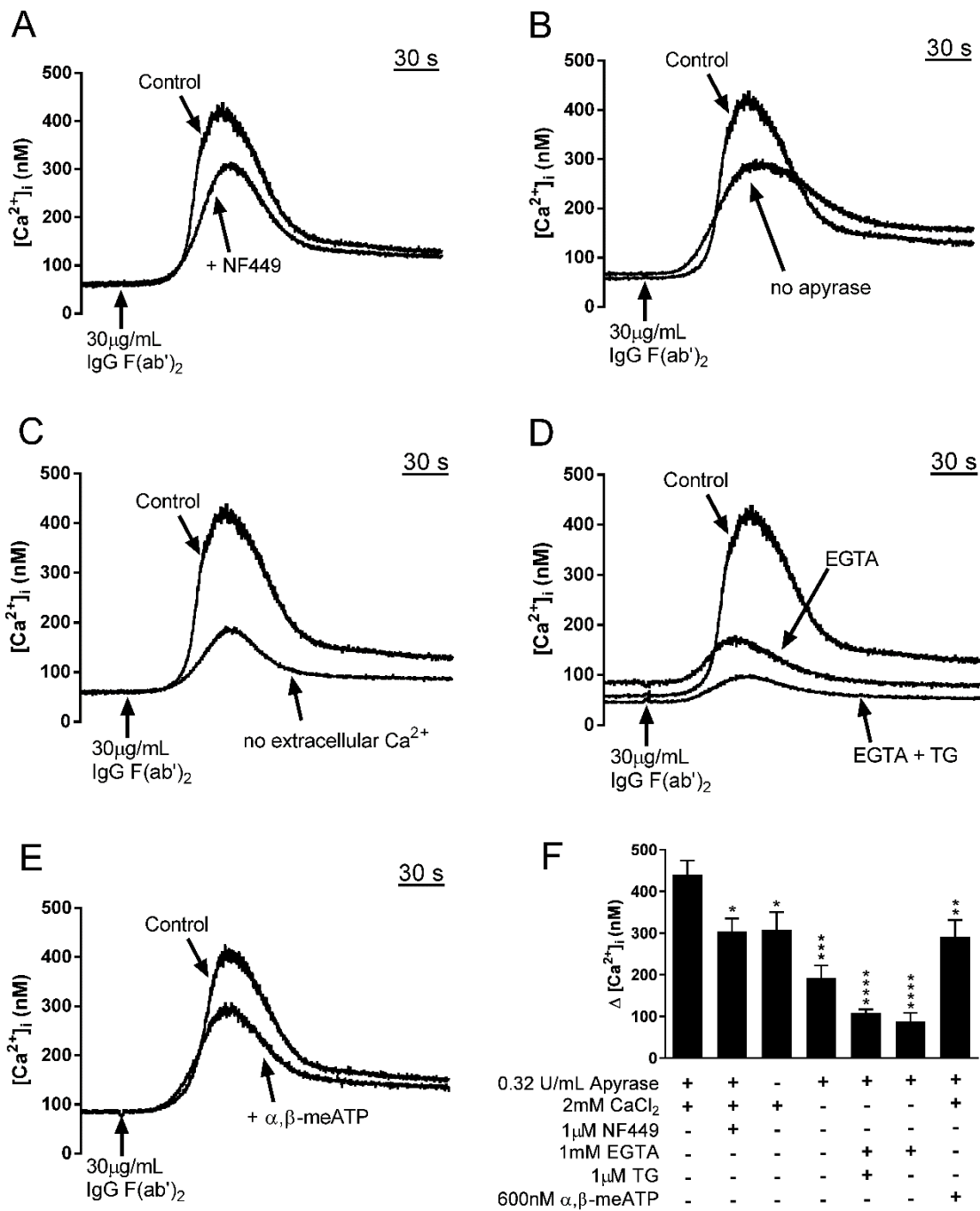


Figure 5.1 Cross-linked mAb IV.3-evoked $Fc\gamma RIIa$ receptor activation induces Ca^{2+} entry through P2X1 channels. Representative (A-E) and average (F) Ca^{2+} responses to $Fc\gamma RIIa$ receptor activation via cross-linking of the receptor-bound mAb IV.3 (1 μ g/mL), which was added 2 min prior to the cross-linker IgG F(ab')₂ antibody. The effects of the presence of NF449 (1 μ M), exclusion of extracellular apyrase and of Ca^{2+} , depletion of stores by TG and chelation of residual extracellular Ca^{2+} by EGTA, and addition of α,β -meATP (600nM) 90 sec prior to IgG F(ab')₂ were studied. Average peak $[Ca^{2+}]_i$ responses have been worked out as the difference in $[Ca^{2+}]_i$ before and after IgG F(ab')₂ addition ($\Delta[Ca^{2+}]_i$). Data represent mean \pm SEM (n=3) * P <0.05; ** P <0.01; *** P <0.001; **** P <0.0001.

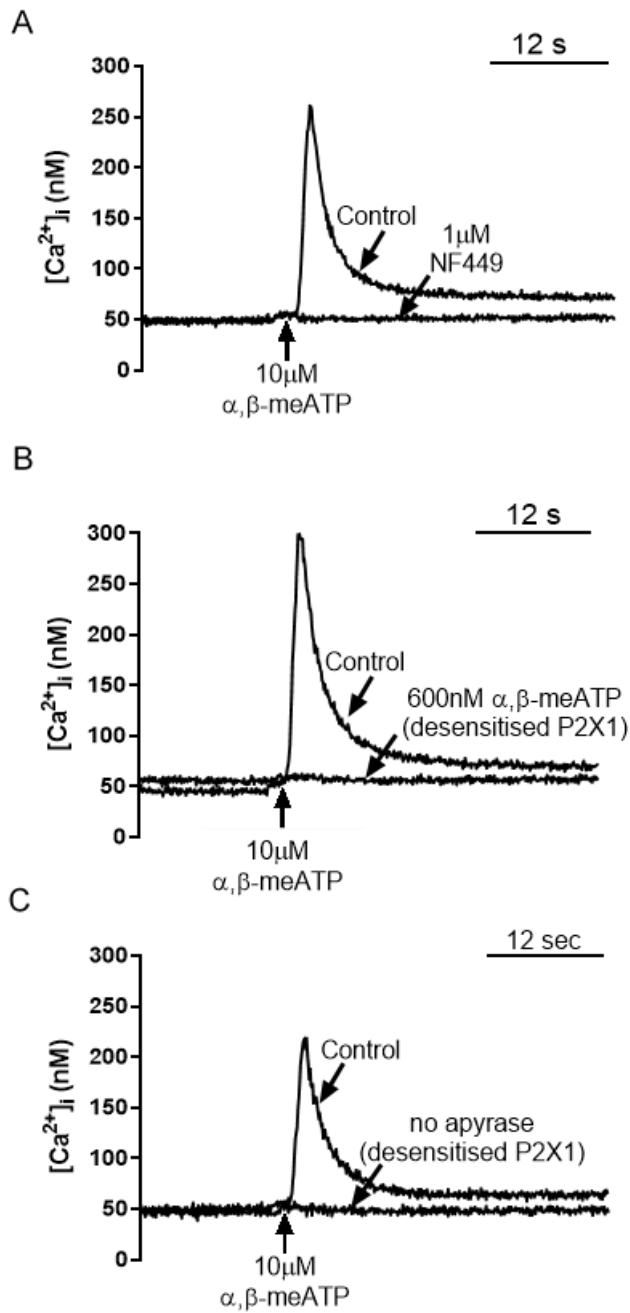


Figure 5.2 Ca^{2+} entry through P2X1 channels can be fully inhibited by the selective antagonist NF449 or by channel desensitization. Representative control traces ($n=3$) obtained from ratiometric Ca^{2+} measurements demonstrating that (A) pre-incubation with $1\mu M$ NF449 for 1 minute, (B) pre-incubation with $600nM$ α, β -meATP for 1.5 minutes, or (C) exclusion of $0.32U/mL$ apyrase from platelet suspensions result in full inhibition of Ca^{2+} entry through P2X1 channels induced by $10\mu M$ [supramaximal (Rolf et al., 2001)] α, β -meATP. In all experiments, control indicates vehicle-treated platelet samples.

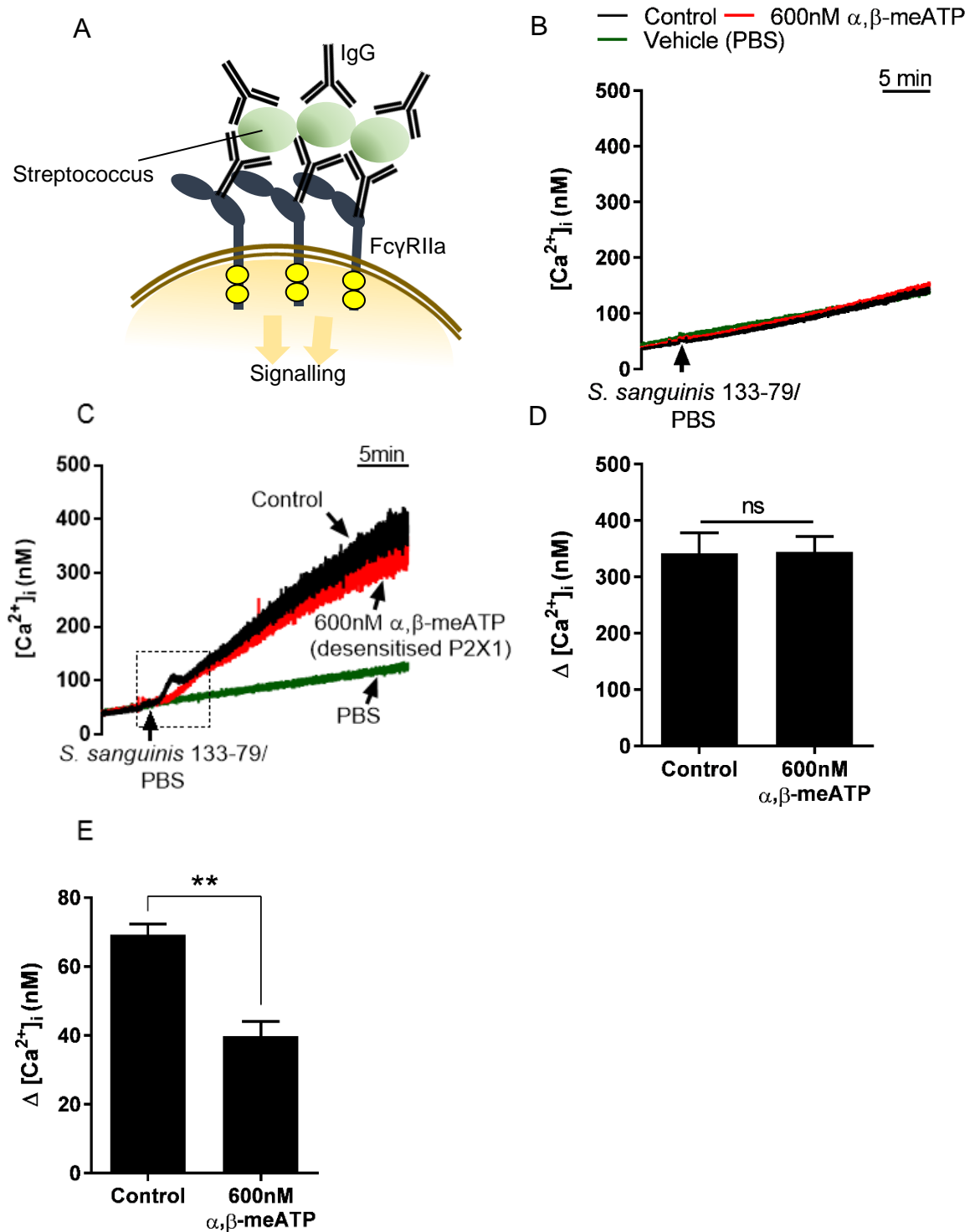


Figure 5.3 *FcγRIIa* receptor activation induced by *S. sanguinis* results in an early P2X1-dependent Ca²⁺ event. (A) Cartoon illustration of *FcγRIIa* activation by IgG-opsinized pathogens (*Streptococci*), where IgG forms a link between the *FcγRIIa* receptors and the pathogen, clustering the receptors to induce activation. (B) Representative Ca²⁺ traces showing lack of Ca²⁺ responses when *S. sanguinis* was ...

(...) added to Fura-2-loaded aspirin-treated platelet suspensions with and without (control) 600nM α,β -meATP pre-treatment (90 seconds), as opposed to the restored Ca^{2+} response when platelets were not treated with aspirin (C). No response was obtained when vehicle (PBS) was added instead of bacteria. α,β -meATP pre-treatment diminished the early small Ca^{2+} peak that occurred after bacterial stimulation (shown in dashed box). (D, E) Average peak $\Delta[Ca^{2+}]_i$ responses obtained within 25 min and 3 min after bacterial stimulation of non-aspirin-treated platelets, respectively, with and without α,β -meATP pre-treatment. All platelet suspensions were added 0.1mg/mL hIgGs and 100 μ g/mL fibrinogen prior to the experiments. Data represent mean \pm SEM (n=3). ** $P < 0.01$; ns: no statistical significance.

5.2.2 P2X1 channel desensitisation inhibits Ca^{2+} entry induced by a range of concentrations of the cross-linker IgG F(ab')₂ antibody

Using collagen to achieve GPVI-induced $[Ca^{2+}]_i$ elevations, it has been demonstrated that maximal effect of P2X1 channel desensitisation using 600nM α,β -meATP was observed at relatively lower collagen concentrations, which was supported by functional studies (Fung *et al.*, 2005; Hechler *et al.*, 2003; Oury *et al.*, 2001). It was reported that after P2X1 desensitisation, peak $[Ca^{2+}]_i$ were reduced by ~45%, 66%, 75% and 92% at 2, 1, 0.5 and 0.25 μ g/mL collagen, respectively (Fung *et al.*, 2005). In order to deduce whether a similar inhibition pattern exists when activating the Fc γ RIIa receptors, the effect of P2X1 desensitisation by pre-exposure to α,β -meATP on Ca^{2+} entry evoked by the different IgG F(ab')₂ concentrations (3.75-30 μ g/mL) was tested. In the presence of extracellular Ca^{2+} , concentration-dependent increases in $[Ca^{2+}]_i$ in platelet suspensions pre-incubated with mAb IV.3 were observed (Figure 5.4 A, B, C, D, E). After P2X1 desensitisation, peak $[Ca^{2+}]_i$ were reduced by 29.3 \pm 3.2% (from 435.4 \pm 62.8nM to 310.5 \pm 53.6nM; $P < 0.001$, n=4), 32.6 \pm 4.7% (324.0 \pm 38.6nM to 217.2 \pm 28.4nM; $P < 0.001$, n=4), 38.1 \pm 11.8% (249.9 \pm 56.8nM to 141.2 \pm 24.7nM; $P < 0.001$, n=4) and 35.5 \pm 14.7% (121.7 \pm 30.7nM to 65.4 \pm 4.7nM; $P < 0.05$, n=4), at 30, 15, 7.5 and 3.75 μ g/mL IgG F(ab')₂, respectively. The contribution of P2X1 to Fc γ RIIa was found to vary less (in comparison to what was found using collagen in the previous study), although it does increase as a percentage as the antibody concentration is reduced. However, at the lower concentrations, there was a marked inter-donor

variability (Figure 5.4 F), and at the lowest concentration (3.75 μ g/mL), the effect of P2X1 inhibition was less significant. For these reasons, a concentration of 15 μ g/mL was used in the subsequent experiments.

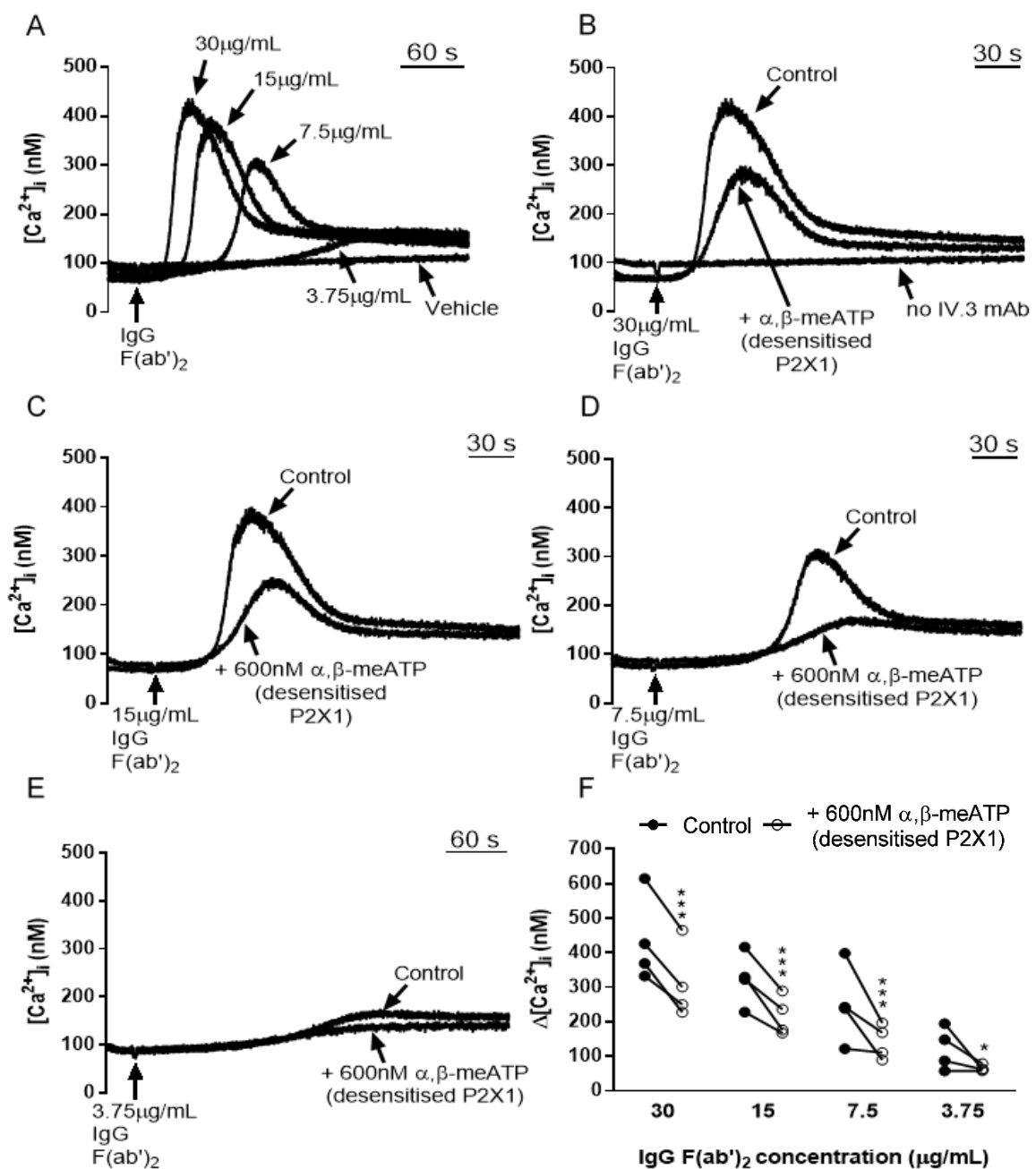


Figure 5.4 P2X1 receptor desensitization inhibits Ca^{2+} entry through P2X1 channels induced by a range of cross-linker IgG F(ab')₂ antibody concentrations. Representative Ca^{2+} responses (A-E) and individual $\Delta[Ca^{2+}]_i$ values (F) measured in Fura-2-loaded platelet suspensions. (A) Ca^{2+} responses obtained when a range of IgG F(ab')₂ concentrations were added to platelet suspensions which contained mAb IV.3 (1 μg/mL). (B-E) The effect of pre-treatment of platelet suspensions with 600 nM α,β-meATP for 90 seconds on Ca^{2+} entry, following the addition of different IgG F(ab')₂ concentrations. (F) Comparison of peak $[Ca^{2+}]_i$ increases following cross linking of mAb IV.3 with IgG F(ab')₂ concentrations with and without 600 nM α,β-meATP pre-treatment. Note the inter-donor variability at 7.5 μg/mL F(ab')₂. * $P < 0.05$; *** $P < 0.001$.

5.2.3 *FcγRIIa*-mediated Ca^{2+} responses are partially resistant to apyrase and NO, but are abolished by PGI_2

Platelets *in vivo* are constantly exposed to inhibitory molecules which regulate platelet function such as prostacyclin (PGI_2), the gasotransmitter NO, and the ectonucleotidase CD39 expressed on the endothelial cells. Elevating the levels of apyrase (from 0.32 to 3.2U/mL), which has been suggested to exhibit similar features to human CD39 (Handa & Guidotti, 1996), did not cause a reduction in the Ca^{2+} response evoked by $Fc\gamma RIIa$ receptor cross-linking achieved by 15 μ g/mL IgG F(ab')₂. In this series of experiments, P2X1 receptor desensitization achieved by pre-exposure to α,β -meATP in the presence of 3.2U/mL apyrase caused a 49% reduction in the Ca^{2+} response, from 345.3 \pm 35.3nM to 175.2 \pm 12.4nM ($P<0.001$, n=3) (Figure 5.5 A and Figure 5.6).

Pre-incubation of the platelet suspensions with the NO donor spermine NONOate (100 μ M) for 10 minutes caused a 69% reduction in the $Fc\gamma RIIa$ receptor-induced Ca^{2+} responses, from 345.3 \pm 35.3nM to 106.5 \pm 30.5nM ($P<0.0001$, n=3) (Figure 5.5 B and Figure 5.6). The trend observed in data from individual donors suggest that a significant proportion of the remaining NO-resistant Ca^{2+} responses were due to P2X1 receptors, indicated by a further reduction when the P2X1 channels were desensitized using α,β -meATP (to 60.0 \pm 12.4nM), although this reduction was not statistically significant (Figure 5.5 B and Figure 5.6).

500nM PGI_2 was sufficient to substantially inhibit the Ca^{2+} response induced by the 0.03 U/mL thrombin, as opposed to much higher PGI_2 concentrations previously used (Fung *et al.*, 2012) (Figure 5.5 C). In a series of optimisation experiments, PGI_2 concentrations within the range of 200-500nM fully inhibited thrombin-induced responses, provided that stock solutions were prepared fresh and used immediately (Figure 5.8). In contrast to previous reports which demonstrate that Ca^{2+} responses to collagen and TLR2/1 activation are resistant to 60 μ M PGI_2 (Fung *et al.*, 2012), $Fc\gamma RIIa$ -induced Ca^{2+} responses were reduced by 93% ($P<0.0001$, n=3) after a 90 second pre-incubation with 500nM PGI_2 , from 345.3 \pm 35.3nM to 23.0 \pm 2.0nM (Figure 5.5 D and Figure 5.6). In order to test the possibility that this substantial inhibition could be due to the inhibitory effect of PGI_2 on ATP secretion, $Fc\gamma RIIa$ -induced ATP release was monitored in the presence and absence of PGI_2 . It was observed that PGI_2 completely inhibits dense granule secretion, as indicated by the loss of ATP release (Figure 5.7).

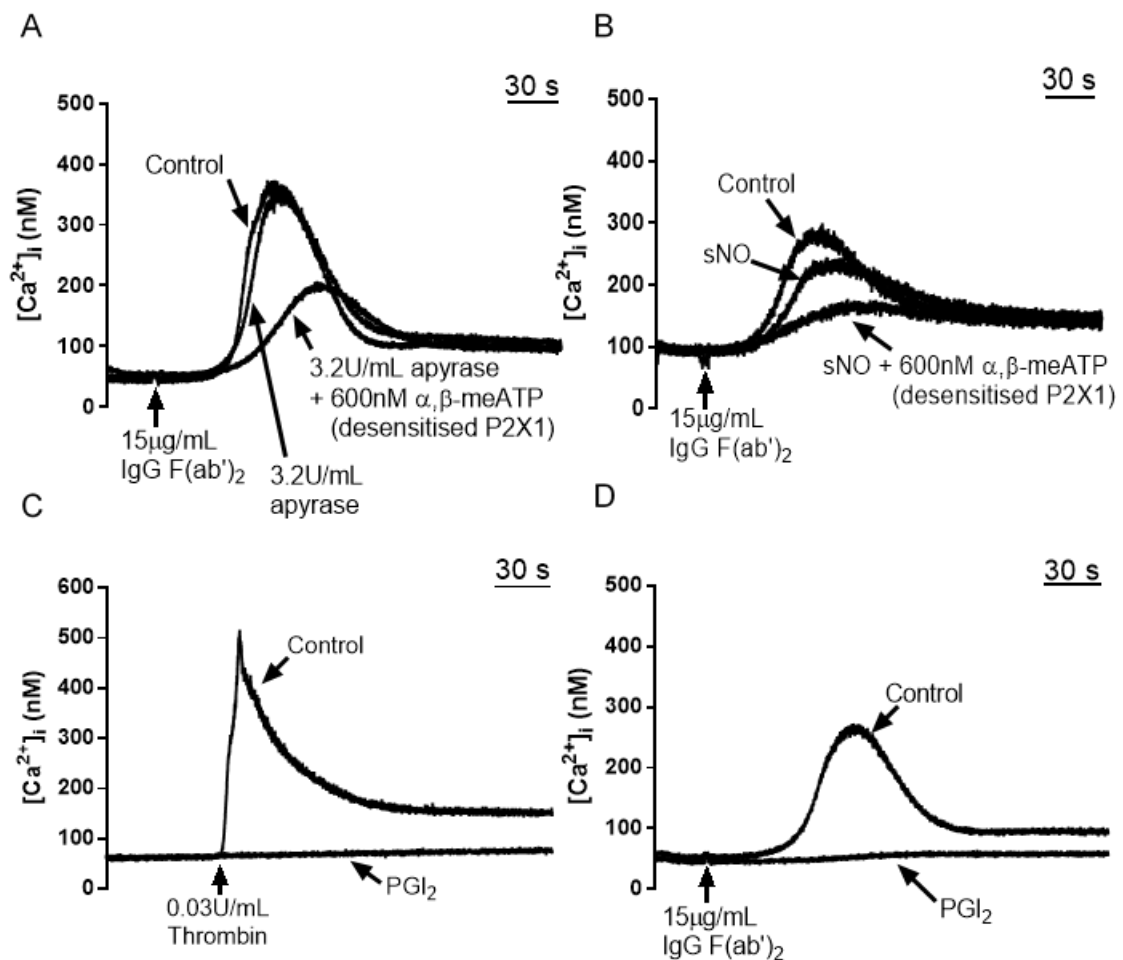


Figure 5.5 *P2X1*-mediated Ca^{2+} responses to $\text{Fc}\gamma\text{RIIa}$ receptor activation are resistant to NO and elevated apyrase levels, but are abolished by PGI_2 . Representative $[\text{Ca}^{2+}]_i$ responses (A, B, D) induced by $\text{Fc}\gamma\text{RIIa}$ receptor activation by cross-linking of mAb IV.3, in the presence of elevated apyrase levels (3.2U/mL), spermine NONOate pre-treatment for 10 minutes (sNO; 100 μM), and prostacyclin pre-treatment for 90 seconds (PGI_2 ; 500nM). (C) 500nM PGI_2 treatment completely abolished Ca^{2+} entry induced by thrombin. Control traces are representative of the vehicle-treated platelet samples in each panel (saline, 0.01M NaOH, ddH₂O and ddH₂O, respectively). In A and B, *P2X1* receptor desensitization was achieved by pre-treatment with 600nM α,β -meATP for 90 seconds.

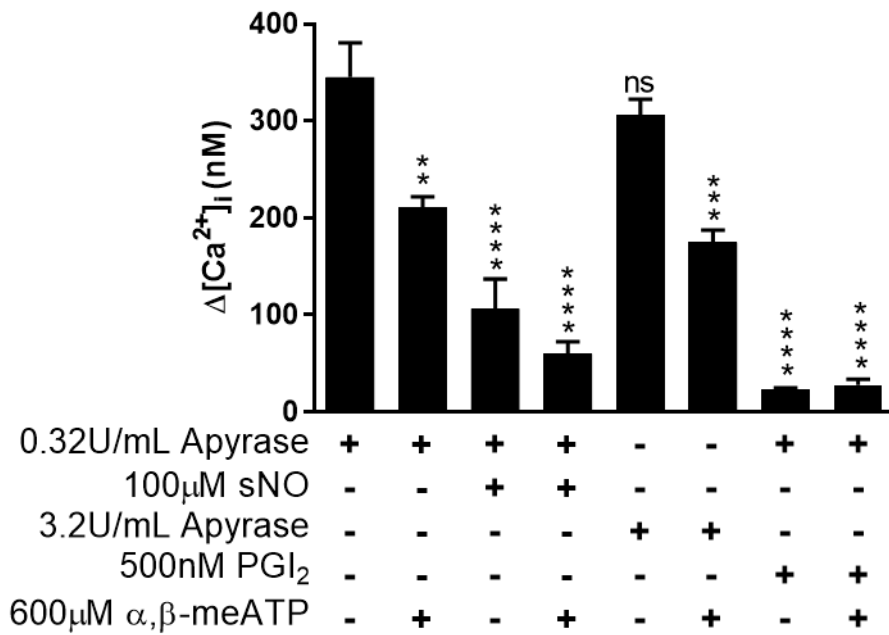


Figure 5.6 Average $\Delta[Ca^{2+}]_i$ responses to $Fc\gamma RIIIa$ receptor activation by cross-linking mAb IV.3, in the presence of endothelium-derived inhibitors. The presence of elevated apyrase levels (3.2U/mL), spermine NONOate pre-treatment for 10 minutes (sNO; 100μM), and prostacyclin pre-treatment for 90 seconds (PGI₂; 500nM) led to significant reductions in $Fc\gamma RIIIa$ -induced $[Ca^{2+}]_i$ increases, which were further reduced by P2X1 desensitisation, except in the presence of PGI₂ which abolished the Ca^{2+} responses. Data represent mean \pm SEM (n=3). ns: no statistical significance; **P<0.01; ***P<0.001; ****P<0.0001, compared to the first column.

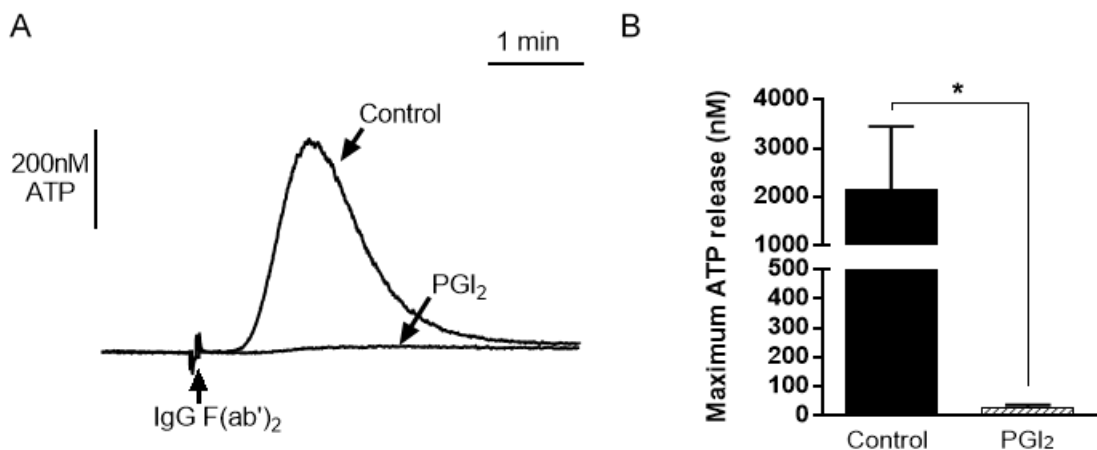


Figure 5.7 PGI₂ inhibits ATP secretion induced by $Fc\gamma RIIIa$ receptor activation. Representative ATP secretion traces (A) and average maximum ATP secretion (B), in the presence and absence of PGI₂ pre-treatment for 90 seconds (500nM). Control indicates vehicle (ddH₂O) addition instead of PGI₂. *P<0.05. Data represent mean \pm SEM (n=3).

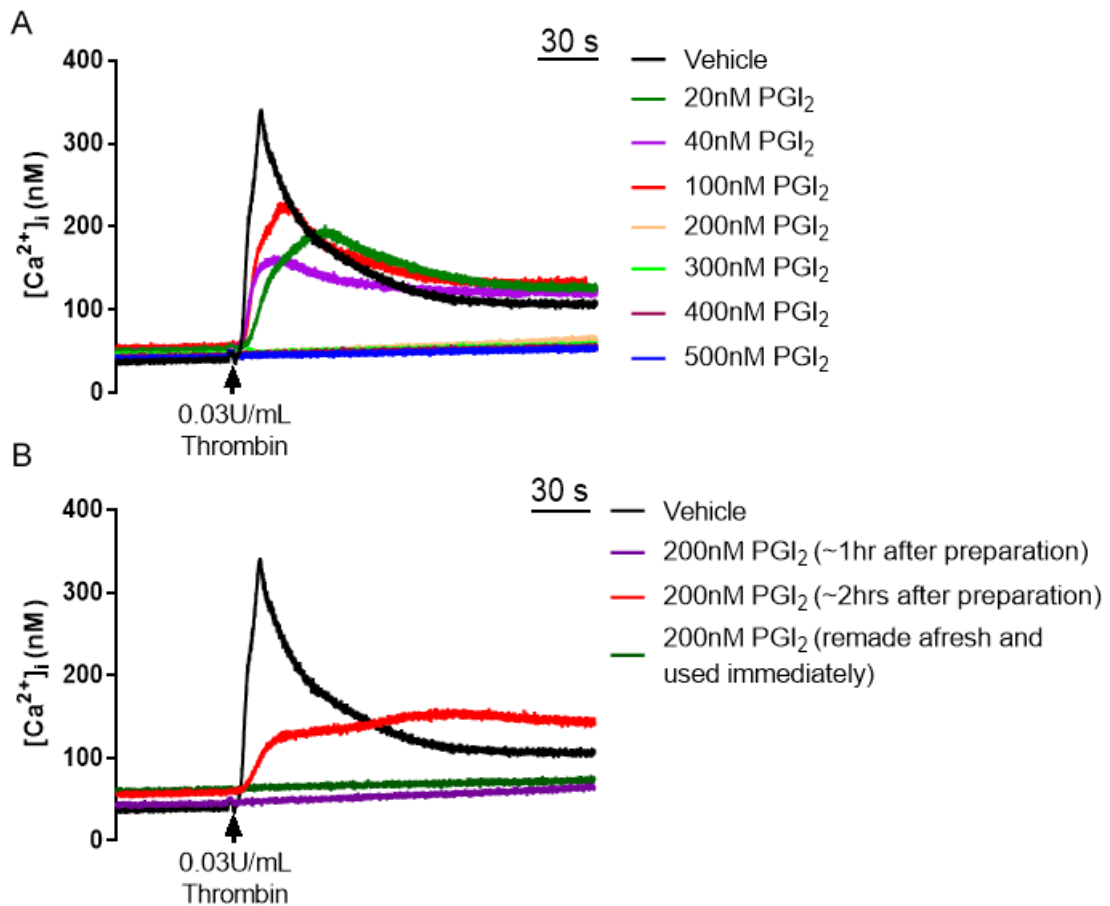


Figure 5.8 Optimisation of PGI₂ concentration and preparation conditions. (A) Representative $[Ca^{2+}]_i$ traces indicate that PGI₂ concentrations within the range of 200-500nM fully inhibit Ca^{2+} responses following the addition of 0.03U/mL thrombin (EC_{50}). (B) Pre-incubation of platelet samples with 200nM PGI₂ from a stock solution prepared 1 hour before the experiment fully inhibited the Ca^{2+} responses, however, effectiveness of the PGI₂ stock decreased after 2 hours of preparation. Following this, pre-incubation of platelets with a freshly prepared stock solution resulted in full inhibition of the Ca^{2+} response to 0.03U/mL thrombin.

5.2.4 Antibody or bacteria-induced FcγRIIIa activation causes ATP secretion, and platelet aggregation responses which are partially inhibited by P2X1 desensitisation

Data described in Section 5.2.1 indicates that P2X1 channels mediate Ca²⁺ entry when the platelet FcγRIIIa receptors are activated by cross-linking using either IgG F(ab')₂ and mAb IV.3, or IgG opsonized bacteria. In order to assess whether FcγRIIIa-induced Ca²⁺ entry through P2X1 contributes to platelet function, platelet aggregometry was performed using the antibody and bacterial stimulation approaches both in the presence and absence of P2X1 activity. Platelet aggregation was significantly inhibited by α,β-meATP (600nM) pre-treatment using the antibody or bacteria approach to induce aggregation [by 55% from 73.8±4.2% to 33.5±13.2% (P<0.05, n=5), and by 35% from 35.7±1.9% to 23.2±4.4% (P<0.05, n=5), respectively] (Figure 5.9 A, B, E). Simultaneous ATP luminescence measurements demonstrate that ATP release through dense granule secretion takes place upon FcγRIIIa receptor activation, independent of P2X1 channel activity (Figure 5.9 C, D, F). There was no significant difference in the ATP levels released from control samples and samples pre-treated with α,β-meATP. ATP release in the control and α,β-meATP pre-treated platelets was 2108.6±324.2nM and 1660.7±732.1nM (respectively) following antibody-induced FcγRIIIa activation; and 65.8±31.5nM and 18.6±9.6nM (respectively) following bacteria-induced FcγRIIIa activation (Figure 5.9 E, F).

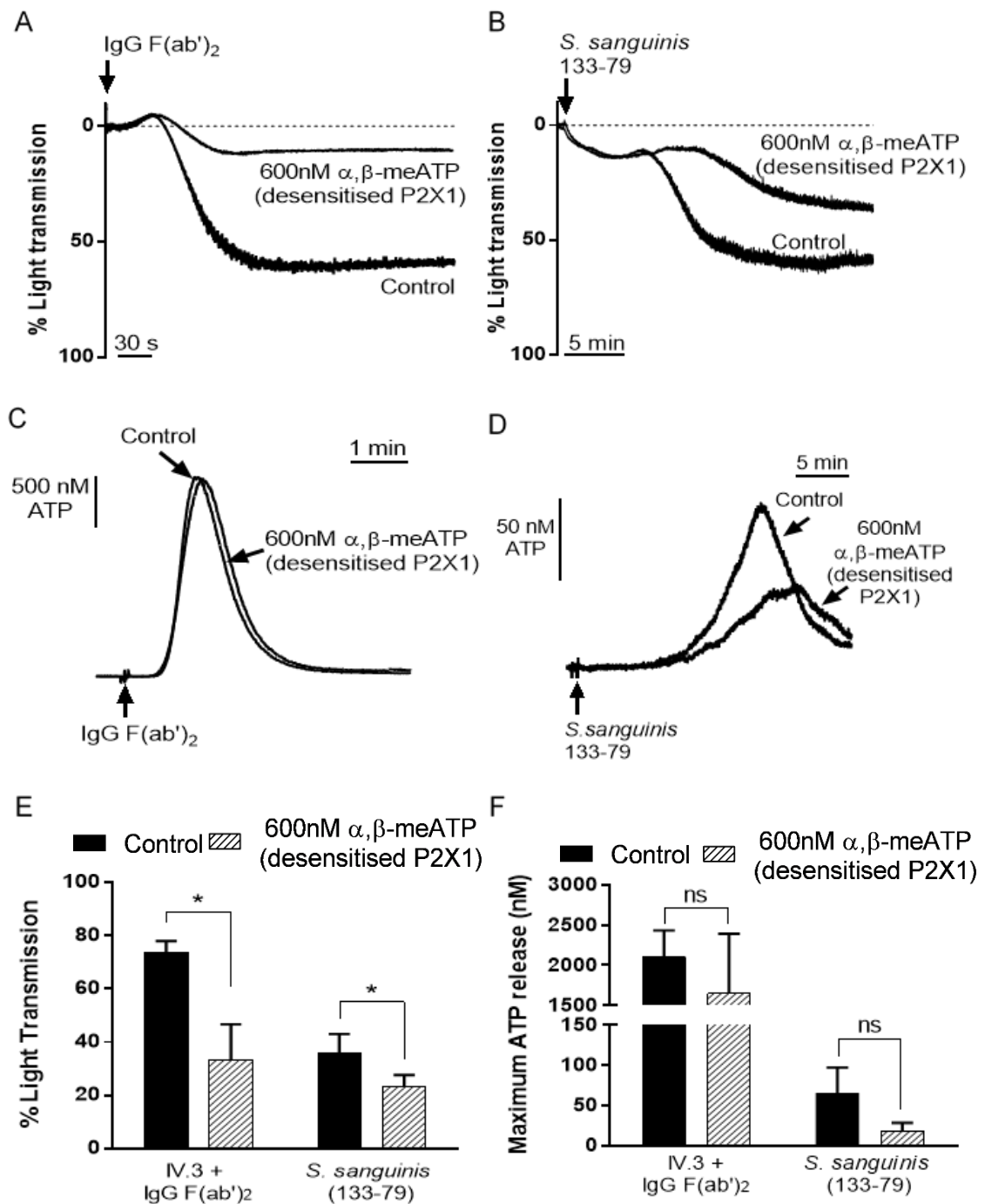


Figure 5.9 P2X1 channels contribute to FcγRIIa-induced platelet aggregation achieved by *S. sanguinis* or cross-linking of mAb IV.3 with IgG F(ab')₂ in washed platelets, accompanied by P2X1-independent dense granule secretion. Representative aggregation traces (A, B), extracellular ATP measurements (C, D), and average peak responses (E, F) obtained following FcγRIIa receptor activation, with and without 600nM α,β-meATP pre-treatment for 90 seconds. Platelet suspensions were added 0.1mg/mL hIgGs prior to stimulation when bacteria were used to activate FcγRIIa receptors. All samples contained 100μg/mL fibrinogen. Data represent mean ± SEM (n=5). *P<0.05; ns: no statistical significance.

5.2.5 *FcγRIIIa* receptor stimulation by antibody cross-linking induces P2X1-independent tyrosine phosphorylation events

Data shown in Section 5.2.4 indicates that inhibition of P2X1 channel activity significantly reduces platelet aggregation, while at the same time ATP release stays relatively unaffected. However, the mechanism by which Ca^{2+} entry through P2X1 contributes to functional responses remains unknown. Therefore, this section sought to investigate whether Ca^{2+} entry through P2X1 channels directly contributes to $[\text{Ca}^{2+}]_i$ elevations following *FcγRIIIa* activation, or an early P2X1-dependent signalling event underpins the ITAM-dependent *FcγRIIIa* signalling cascade. There are examples of GPCRs as well as tyrosine kinase-coupled receptors which were shown to be Ca^{2+} -dependent or modulated by changes in $[\text{Ca}^{2+}]_i$ (Jones *et al.*, 2014b; Vial *et al.*, 2002; Brinson *et al.*, 1998; Huckle *et al.*, 1992). To address this issue, tyrosine phosphorylation of the downstream elements of the *FcγRIIIa* signalling pathway (PLCγ2, Syk and LAT) 60 and 90 seconds after activation was assessed, with and without P2X1 desensitisation by pre-exposure to 600nM α,β -meATP. Compared to control platelet samples which have been lysed after vehicle treatment that induced no signalling events, in the samples where *FcγRIIIa* activation was achieved by cross-linking of the mAb IV.3 using IgG F(ab')₂, phosphorylation of all targets were detected by the anti-phosphotyrosine antibodies (Figure 5.10). There was no observable difference in the phosphorylation levels of these key targets in any of the platelet samples pre-treated with α,β -meATP, regardless of the duration of the time period allowed after *FcγRIIIa* receptor stimulation and before lysis (Figure 5.10). This argues against the possibility that an early Ca^{2+} entry event through P2X1 channels reinforces the tyrosine phosphorylation of the key downstream elements following *FcγRIIIa* activation.

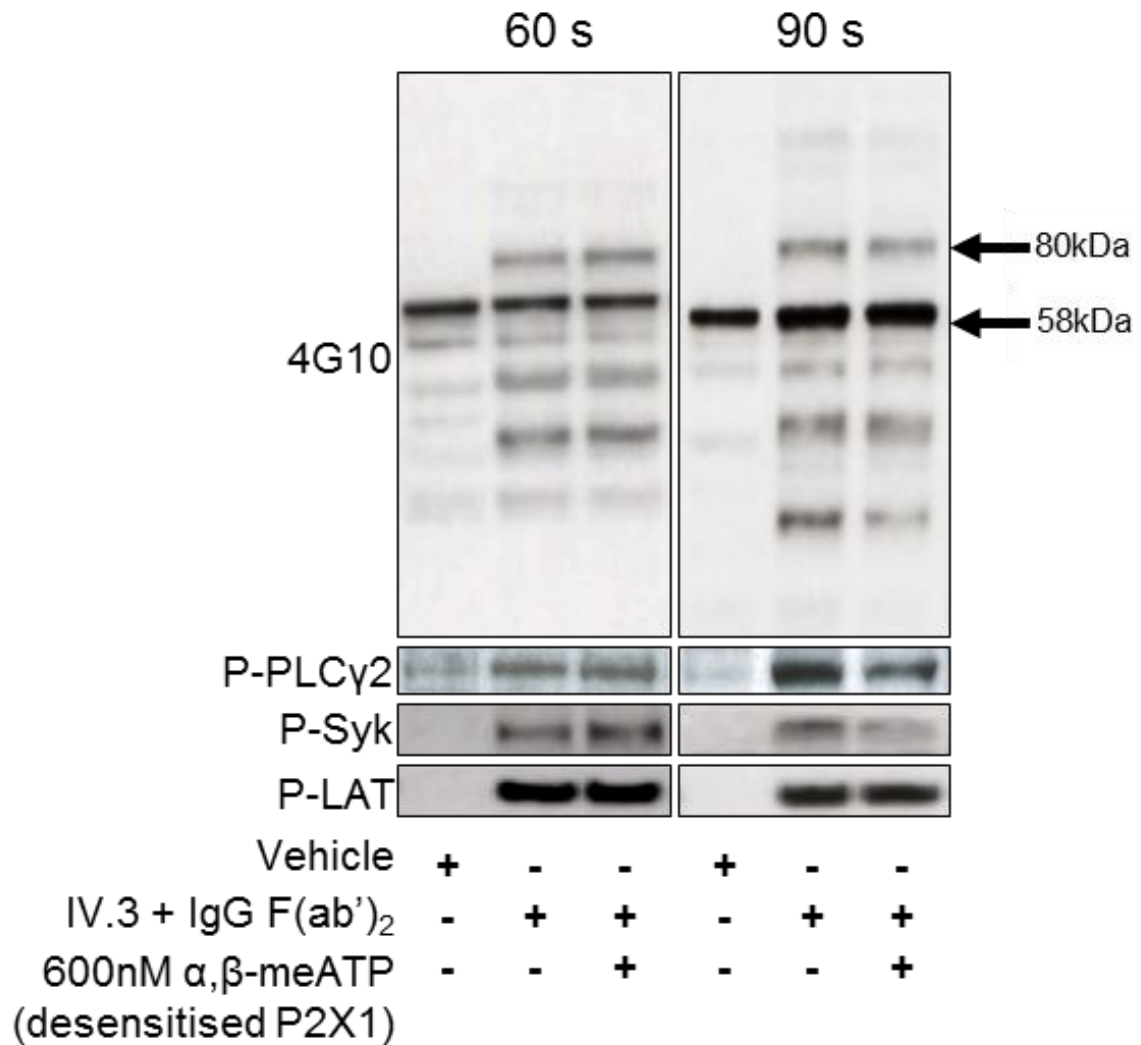


Figure 5.10 *Fc γ RIIa* receptor stimulation by cross-linking of mAb IV.3 induces phosphorylation events downstream of the *Fc γ RIIa* signalling pathway regardless of *P2X1* channel desensitization. Tyrosine phosphorylation of PLC γ 2 (150kDa), Syk (72 kDa) and LAT (28kDa), at 60 seconds and 90 seconds after vehicle (control) or IgG F(ab')₂ addition to cross-link mAb IV.3 were assessed using phospho-specific antibodies in platelets pre-treated with and without 600nM α,β -meATP for 90 seconds. The pan-phosphotyrosine antibody 4G10 was also used as a control, to assess all tyrosine phosphorylation events after *Fc γ RIIa* receptor stimulation.

5.2.6 Thrombus formation under normal arterial shear stress over *Streptococcus sanguinis* is independent of P2X1 channel activity

The contribution of P2X1 channels to platelet functional responses, such as thrombus formation, were shown to be modulated by arterial shear stress *in vitro* on a collagen surface, and *in vivo*, highlighting the critical role of P2X1 channels in arterial thrombosis under shear conditions (Erhardt *et al.*, 2006; Hechler *et al.*, 2003; Oury *et al.*, 2003). In addition, using fluorescently labelled platelets in whole blood from transgenic mice lacking FcγRIIa, it has been shown that FcγRIIa amplifies thrombus formation under both arterial and venous shear stress (Zhi *et al.*, 2013). Platelet aggregate formation under arterial shear stress conditions over *Streptococcus oralis*-coated surfaces in a parallel-plate flow chamber was also shown to be feasible (Tilley *et al.*, 2013). Furthermore, it was demonstrated that the interaction of platelets with bacteria under flow was dependent on the cross-linking of FcγRIIa receptors by IgG-opsonised *S. oralis* (Tilley *et al.*, 2013). Experiments therefore assessed whether P2X1 channels contribute to thrombus formation on immobilised *S. sanguinis* under arterial flow conditions.

Under normal arterial flow conditions, stable aggregate formation over uniformly coated *S. sanguinis* was observed (Figure 5.11 A, B). 2D and 3D images of the stable fluorescent thrombi formed indicate that the coverage and size of the uniformly spread aggregates formed under control conditions were unaffected by pre-treatment with 1μM NF449 (Figure 5.11 B). Quantification of thrombus height, thrombus volume and percentage surface coverage under control and P2X1 inhibitory conditions demonstrated that inhibition of P2X1 channels by NF449 does not alter thrombus formation on *S. sanguinis* under normal arterial shear stress (Figure 5.11 C).

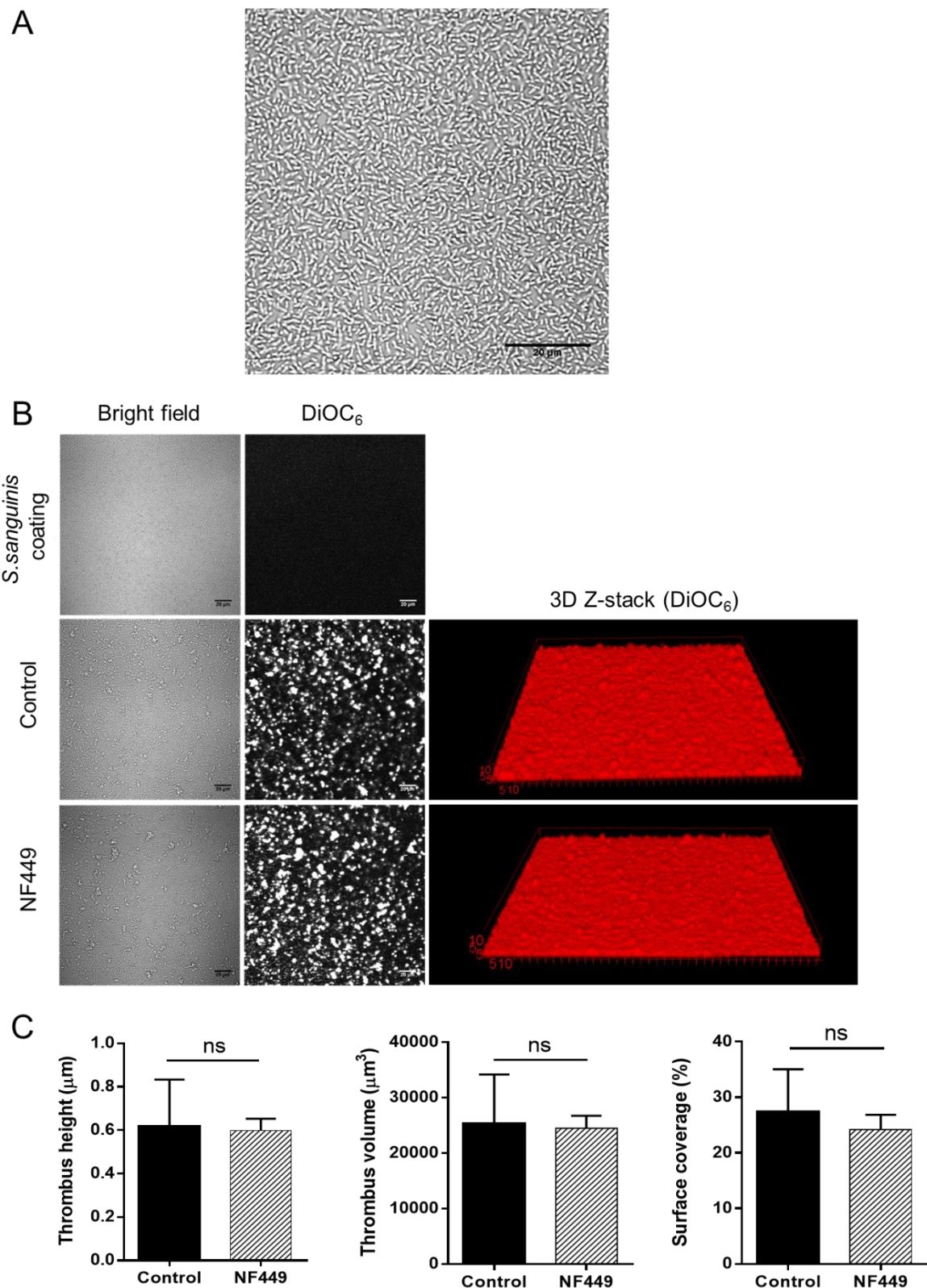


Figure 5.11 Inhibition of P2X1 channels with $1\mu\text{M}$ NF449 does not alter thrombus formation on immobilised *S. sanguinis* under normal arterial shear stress conditions (1002.6s^{-1}). (A) Representative $\times 2.5$ zoomed image of the *S. sanguinis* coating in bright field shown in B, illustrating uniform bacteria coating before the start of each thrombus formation experiment. (B) Representative bright field and DiOC₆ images showing ...

(...) *S. sanguinis* coating before the introduction of whole blood, and the stable thrombi formed after 5 minutes of perfusion of blood with or without NF449 pre-treatment for 1 minute. 3D reconstructions using Z-stack images of DiOC₆-stained thrombi indicate no observable difference in thrombus formation between control samples and those pre-treated with NF449. All scale bars represent 20µm. (C) Average thrombus height, thrombus volume and % surface coverage with or without (control) NF449 pre-treatment. Data represent mean ± SEM (n=6). ns: no statistical significance.

5.3 Discussion

Results presented within this chapter reveal a previously unknown mechanism whereby P2X1 channels amplify Ca^{2+} signalling and function of Fc γ RIIa receptors in response to immunogenic stimuli. The unique role of P2X1 channels in TLR2/1, GPVI, and GPCR-dependent Ca^{2+} signalling has been previously described (Fung *et al.*, 2012; FUNG *et al.*, 2007; Fung *et al.*, 2005). Using either an antibody against the Fc γ RIIa receptors or a previously described bacterial strain, *S. sanguinis*, to activate the receptors in the presence and absence of P2X1 channel activity, data in this chapter describes a new role for P2X1 channels in Ca^{2+} mobilisation which underlies Fc γ RIIa-induced platelet activation.

In addition to Ca^{2+} release from the endoplasmic reticulum, platelets can derive Ca^{2+} from the extracellular milieu through a number of ion channels. Of importance, the human platelet ATP-gated P2X1 channels provide the most efficient route for Ca^{2+} entry following ATP release from a vascular damage site (Mahaut-Smith, 2012; Wang *et al.*, 2003), and these channels have been shown to exacerbate thrombosis *in vivo* (Erhardt *et al.*, 2006; Hechler *et al.*, 2003; Oury *et al.*, 2003). Furthermore, ADP and thromboxane A₂ were demonstrated to contribute to P2X1-dependent $[\text{Ca}^{2+}]_i$ elevations (FUNG *et al.*, 2007). Despite their close apposition to the vessel walls under shear stress in circulation, which provides an enhanced exposure to endothelium-derived inhibitors, platelets are able to elevate their $[\text{Ca}^{2+}]_i$ through P2X1-mediated Ca^{2+} entry coupled to GPVI and TLR2/1 (Fung *et al.*, 2012). The activation of the immune receptor Fc γ RIIa has been shown to signal in a similar manner to GPVI, through the phosphorylation of the ITAM portion of the receptor, leading to platelet aggregation and thrombus formation under arterial shear stress *in vitro* (Arman *et al.*, 2014; Tilley *et al.*, 2013; Watson & Gibbins, 1998). Data presented here indicates that P2X1 channels become activated following the activation of the Fc γ RIIa receptors, through the release of ATP upon dense granule secretion.

The inhibition of P2X1 channels was achieved by three different approaches, all of which clearly demonstrate that P2X1 channels significantly contribute to Ca^{2+} entry into platelets upon Fc γ RIIa receptor activation. Using NF449 to maximally inhibit, or excluding the ectonucleotidase (apyrase) from the platelet suspensions or using a low concentration of α,β -meATP to desensitize the P2X1 channels, similar levels of inhibition of Ca^{2+} entry in response to Fc γ RIIa receptor activation were achieved.

Interestingly, the removal of extracellular Ca^{2+} , which resulted in greater inhibition of Ca^{2+} influx, demonstrates that other Ca^{2+} -permeable channels also play a role in elevating $[\text{Ca}^{2+}]_i$ following $\text{Fc}\gamma\text{RIIa}$ receptor activation. Furthermore, using TG to deplete intracellular Ca^{2+} stores in EGTA-containing medium before $\text{Fc}\gamma\text{RIIa}$ receptor activation, an even further reduction in $[\text{Ca}^{2+}]_i$ elevation was observed, confirming the contribution of inositol triphosphate (IP₃)-dependent Ca^{2+} release from the endoplasmic reticulum.

Using a range of collagen concentrations to stimulate platelet aggregation, studies have clearly shown that the most significant inhibitory effect of P2X1 desensitization is observed at lower collagen concentrations, implying involvement of other Ca^{2+} entry mechanisms (i.e. via signalling, from intracellular stores) which override P2X1 responses when high agonist concentrations are used (Fung *et al.*, 2005; Hechler *et al.*, 2003; Oury *et al.*, 2001). Data presented here indicate that no such significant correlation exists between the cross-linking IgG F(ab')₂ concentration and the inhibitory effect of P2X1 channel desensitisation. This potentially indicates that regardless of the strength of the stimulus, P2X1 channels remain as the major route for Ca^{2+} entry following $\text{Fc}\gamma\text{RIIa}$ receptor activation using the cross-linking antibody approach. Supporting this, when *S. sanguinis* in presence of hIgGs is used to activate the $\text{Fc}\gamma\text{RIIa}$ receptors, a characteristic $[\text{Ca}^{2+}]_i$ trace was obtained where a distinguishable early Ca^{2+} event within the first few minutes of stimulation was followed by a gradual elevation in $[\text{Ca}^{2+}]_i$. The early Ca^{2+} event was eliminated by α,β -meATP pre-treatment, indicating Ca^{2+} entry through P2X1 channels as the source, which was strong enough to persist the overriding effect of the global Ca^{2+} response.

It is important to note that GPVI and TLR2/1 dependent P2X1-mediated Ca^{2+} responses display resistance to the inhibitory effects of cyclic nucleotides such as cyclic AMP, and hence can still mediate Ca^{2+} mobilisation events in the presence of endothelium-derived negative regulators of platelet function, such as NO and PGI₂ (Fung *et al.*, 2012; Mahaut-Smith *et al.*, 2004; Sage *et al.*, 2000; Sage & Rink, 1987). This is despite the fact that PGI₂ at a nanomolar range was shown to inhibit dense granule secretion evoked by the main platelet agonists thrombin and collagen (Rink & Sanchez, 1984), indicating a crucial role for GPVI and TLR2/1 dependent Ca^{2+} entry through P2X1 channels under normal physiological conditions. Our observations demonstrate that NO and elevated apyrase levels-resistant portions of the $\text{Fc}\gamma\text{RIIa}$ -induced Ca^{2+} responses are mediated by P2X1 channels. However, PGI₂ completely

abolished the Ca^{2+} response, as well as secretion downstream of Fc γ RIIa receptors, which was also observed with GPCRs such as TxA₂Rs and PARs (Fung *et al.*, 2012) (e.g. thrombin in Figure 5.5 C). This is surprising because Fc γ RIIa receptors are tyrosine kinase-coupled, and other such receptors such as TLR2/1 and GPVI were shown to evoke PGI₂-resistant dense granule secretion responses. At present, the reason for this difference cannot be explained, however, a potential underlying reason could be that Fc γ RIIa stimulation possibly evokes different secretion mechanisms. Evidence shows that different modes of exocytosis exist in platelets, such as single and multigranular fusion events, which differentially take place during activation depending on factors such as the agonist, the extent of stimulation, and the time point after stimulation (Eckly *et al.*, 2016; Jonnalagadda *et al.*, 2012).

Previous studies by Arman and colleagues have demonstrated concentration-dependent “all-or-nothing” aggregation responses to gram-positive bacteria, with a distinctive lag phase (Watson *et al.*, 2016; Arman *et al.*, 2014). Similar aggregation profiles were obtained when *S. sanguinis* was used to induce aggregation, which were significantly reduced by desensitization of P2X1 channels, highlighting the important contribution of ATP-gated P2X1 channels to platelet function. Interestingly, even in the presence of ectonucleotidase activity in these assays, simultaneous elevations in extracellular ATP levels following dense granule secretion were observed, in line with previous reports (FUNG *et al.*, 2007). Although the ATP levels released upon bacterial stimulation was much lower compared to those attained by antibody stimulation, P2X1 channel activation and hence their contribution to aggregation responses were significant in both scenarios, possibly due to the fast activation kinetics of the P2X1 channel (Mahaut-Smith *et al.*, 2004; MacKenzie *et al.*, 1996). The levels of either bacteria or antibody-induced ATP release with and without P2X1 channel desensitization were not significantly different from each other, however, data from individual donors indicated potential donor-dependent variation in these two secretion responses. Also given the evidence for Ca^{2+} -dependent tyrosine kinase activity in previous studies (Brinson *et al.*, 1998; Huckle *et al.*, 1992), the possibility that an early P2X1 activity underpins the phosphorylation of the main signalling molecules downstream of the Fc γ RIIa receptors and hence vary the level of ATP secretion, was considered. The phosphorylation of the downstream signalling elements following Fc γ RIIa receptor stimulation were successfully visualised, however, the phosphorylation levels remained unaltered after P2X1 channel desensitization. This

indicates that P2X1 channels contribute to FcγRIIIa-induced responses via a direct Ca²⁺ influx, amplifying the activity of the subsequent Ca²⁺-dependent downstream effectors, rather than via a feedforward effect on early tyrosine phosphorylation events.

Although the results presented indicate that immobilised *S. sanguinis* is able to support thrombus formation under normal arterial levels of shear stress, P2X1 channels are not involved in this process, under the experimental conditions described. This observation is in line with previous reports which showed that, *in vitro*, P2X1 does not play a significant role in thrombus formation on collagen at normal levels of shear stress in large arteries (~800s⁻¹). Future studies would benefit from the use of much higher shear levels (equivalent to what is observed in the smaller arterioles (~6000s⁻¹)) where the contribution of P2X1 to thrombus formation was found to be highly significant (Hechler *et al.*, 2003). It is also important to remember that aggregate formation over bacteria will not be solely mediated by FcγRIIIa-IgG-opsonised bacteria interactions, and thus P2X1 would likely contribute to thrombus formation mediated by other immune receptors, such as TLR2/1 (Fung *et al.*, 2012; Garraud & Cognasse, 2010).

In conclusion, this section provides evidence that human platelet FcγRIIIa receptor activation triggers Ca²⁺ entry through ATP-gated P2X1 channels in addition to other Ca²⁺ entry routes. The data therefore suggest that P2X1-dependent Ca²⁺ entry is a significant underlying event that could potentially contribute to platelet activation in inflammatory situations such as IE.

Chapter 6

General discussion and future work

6.1 Recapitulation of main findings

This thesis identifies, for the first time, two distinct pathways of Ca^{2+} entry into human platelets which can contribute to Ca^{2+} influx during stimulation by arterial shear stress and $\text{Fc}\gamma\text{RIIa}$ receptor activation. Firstly, data from Chapters 3 and 4 provide evidence that human platelets express MS Piezo1 Ca^{2+} -permeable channels, which operate in response to different levels of arterial shear stress, and *in vitro* findings suggest that these channels contribute to thrombus formation. In addition, the outcomes of the experiments carried out using cells from the Meg-01 cell line indicate the possibility that such MS channels may also contribute to megakaryocyte development and function within the bone marrow. Previous studies which investigated the link between arterial levels of shear stress and platelet $[\text{Ca}^{2+}]_i$ suggested that possible “shear stress-regulated Ca^{2+} channels” of unknown identity may alter $[\text{Ca}^{2+}]_i$ and could exacerbate the pathogenesis of arterial disease (Chow *et al.*, 1992; Levenson *et al.*, 1990). Data presented in Chapters 3 and 4 suggest that Piezo1 could account for the shear-dependent physiological events reported by these earlier studies. Furthermore, these chapters describe the development of new technical approaches which permit the study of changes in $[\text{Ca}^{2+}]_i$ in Meg-01 cells under flow, and more importantly in singly attached resting human platelets under shear stress. Secondly, Chapter 5 reveals that Ca^{2+} -permeable P2X1 channels amplify Ca^{2+} signalling and the concomitant functional responses in human platelets during $\text{Fc}\gamma\text{RIIa}$ receptor stimulation. $\text{Fc}\gamma\text{RIIa}$ receptors are activated by natural stimuli such as bacteria (Arman *et al.*, 2014), suggesting that P2X1-mediated Ca^{2+} influx contributes to platelet activation in inflammatory diseases such as IE.

The most important outcomes of the experiments presented in Chapter 3 not only provide insights into the MS Ca^{2+} events in megakaryocytes and platelets, but also establish the foundations of the study of MS cation channels in human platelets (presented in Chapter 4) from a technical point of view. Primarily, Chapter 3 demonstrated that human platelets and the Meg-01 cell line express the MS cation channel Piezo1 at the protein level, confirming the findings of the previous transcriptomic and proteomic studies (Wright *et al.*, 2016; Burkhart *et al.*, 2012;

Boyanova *et al.*, 2012). Furthermore, it was observed that Fluo-3-loaded Meg-01 cells display shear-dependent elevations in $[Ca^{2+}]_i$ which can be diminished by the MS cation channel inhibitor GsMTx-4 in the presence of extracellular Ca^{2+} , or simply by the removal of extracellular Ca^{2+} (Figures 3.7, 3.8 and 3.9). Under similar experimental conditions, the inhibitory effect of GsMTx-4 treatment on MS Ca^{2+} entry was previously reported in cells which express functional Piezo1 channels (Li *et al.*, 2014; Miyamoto *et al.*, 2014; Coste *et al.*, 2012; Bae *et al.*, 2011; Coste *et al.*, 2010). This demonstrated that shear stress-operated Ca^{2+} -permeable channels on the Meg-01 plasma membrane mediate Ca^{2+} entry into the cytosol. In addition to its established inhibitory effect on Piezo1 channels, GsMTx-4 was reported to inhibit other MS cation channels (Gnanasambandam *et al.*, 2015; Coste *et al.*, 2012; Bae *et al.*, 2011; Coste *et al.*, 2010). The use of the selective Piezo1 agonist, Yoda1, which induced prominent Ca^{2+} responses in Meg-01 cell suspensions in ratiometric measurements, indicated presence of Piezo1 channels which could account for the MS Ca^{2+} responses observed in these cells (Syeda *et al.*, 2015; Cahalan *et al.*, 2015) (Figure 3.14). Moreover, Chapter 3 identified and optimised the most suitable assay which incorporates mechanical stimulation with $[Ca^{2+}]_i$ recordings in Meg-01 cells. Amongst the most commonly used mechanical stimulation methods for cell-based assays that have been performed (Figure 3.1) (Delmas *et al.*, 2011), application of fluid shear stress over cells attached to poly-D-lysine was preferred due to the relevance of this type of mechanical force to platelet function in the circulation and thrombus formation.

Using a modified version of the shear stress assay developed in Chapter 3, Chapter 4 provided evidence for MS Piezo1 ion channel activity in human platelets, which operate under normal and pathological arterial levels of shear stress and contribute to the elevation of $[Ca^{2+}]_i$ directly in a shear-dependent manner. Application of fluid shear stress resulted in repetitive Ca^{2+} transients in singly-attached Fluo-3 loaded platelets, occurrence of which increased more significantly under shear levels equivalent to pathological arterial levels (Figures 4.1 and 4.4 A). Nevertheless, shear-dependent Ca^{2+} spiking was diminished by GsMTx-4 or removal of extracellular Ca^{2+} at either level of shear, demonstrating that plasma membrane MS cation channels mediate Ca^{2+} entry under shear. An increase in Ca^{2+} spiking achieved by the inclusion of Yoda1 in the extracellular saline provided evidence that Piezo1 is possibly the ion channel responsible for the effects observed. The *in vitro* thrombus formation and aggregation assays revealed that Piezo1 channels likely contribute to platelet functional responses,

highlighting their potential contribution to the development of cardiovascular disease. Given the fact that GsMTx-4 is a non-selective inhibitor of MS cation channels and the evidence for the involvement of P2Y receptors in mechanosensation in various cell types (Linan-Rico *et al.*, 2013; Inoue *et al.*, 2009; Song *et al.*, 2009; Fernandes *et al.*, 2008; Leon *et al.*, 1999), further experiments were performed to take into account possible contribution of Ca²⁺ entry through other mechanisms. Slight stimulation of P2Y receptors with ADP did not change shear-induced Ca²⁺ responses in single platelets, and shear-induced Ca²⁺ responses were demonstrated to be independent of other Ca²⁺ entry pathways, such as P2X1 (Figures 4.8, 4.9 and 4.12).

Chapter 5 reveals that platelet P2X1 ion channels amplify the [Ca²⁺]_i response following the stimulation of the immune receptor FcγRIIa. FcγRIIa stimulation was achieved by cross-linking an antibody against the receptor (mAb IV.3), or by the more natural method of using IgG-opsonised bacteria, as previously published (Arman *et al.*, 2014). Inhibition or desensitisation of P2X1 channels in ratiometric Ca²⁺ measurements revealed that Ca²⁺ entry through P2X1 channels significantly amplify the FcγRIIa responses (Figure 5.1). Importantly, aggregation induced by FcγRIIa receptor stimulation was significantly reduced following P2X1 channel desensitisation, which highlights the importance of the FcγRIIa-P2X1 co-operation in platelet functional responses (Figure 5.9). Given the resistance of these P2X1-dependent Ca²⁺ responses to some endothelium-derived inhibitors, this route for amplifying platelet immune responses could be an important contributor to disease development *in vivo*. The studies of FcγRIIa-induced ATP release and ITAM-dependent phosphorylation events point towards an underlying mechanism whereby P2X1 channels contribute via direct Ca²⁺ influx and subsequent amplification of Ca²⁺-dependent downstream effectors, rather than via a feedforward effect on early tyrosine phosphorylation events.

6.2 Physiological and clinical implications

6.2.1 Potential roles for Piezo1 in haemostasis and thrombosis

Since their identification in 2010 by the Patapoutian group (Coste *et al.*, 2010), the MS Piezo ion channels have received considerable attention and been shown to contribute to functional responses across a range of cell types (Wang *et al.*, 2016; Allison, 2016; Cahalan *et al.*, 2015; Lukacs *et al.*, 2015; Li *et al.*, 2015; Cinar *et al.*, 2015; Ranade *et al.*, 2014a; Li *et al.*, 2014; Miyamoto *et al.*, 2014; Peyronnet *et al.*, 2013). Furthermore, disease conditions have been reported that result from both gain of function and loss of function mutations of these cation-permeable channels (Lukacs *et al.*, 2015; Albuissou *et al.*, 2013; Zarychanski *et al.*, 2012). Of relevance to the present work, Piezo1 channels play crucial mechanotransduction roles in the cardiovascular system, particularly in red blood cells and endothelial cells where they regulate cell volume homeostasis (Cahalan *et al.*, 2015) and vascular development (Ranade *et al.*, 2014a), respectively. In the circulation, the mechanical forces of shear have a well-established influence on platelet activation (Kroll *et al.*, 1996). For example, the ability of vWF to engage its receptors on the platelet surface is enhanced by increased shear (Siedlecki *et al.*, 1996). In addition, platelet membrane morphological events respond to physical influences in a PI3 kinase-dependent manner (Mountford *et al.*, 2015). However, mechanisms for more direct mechanical activation of platelet signalling events have not been previously identified (Kroll *et al.*, 1996). The findings presented in Chapters 3 and 4 indicate that platelet Piezo1 channels could mediate direct entry of Ca²⁺ into the cytosol from the extracellular milieu, under shear stress.

There are a number of ways via which Piezo1 channels could contribute to platelet function. Under normal physiological conditions *in vivo*, platelets constantly circulate throughout the cardiovascular system and hence are exposed to varying levels of fluid shear stress, depending on the type and the location of the vessels they pass through (White & Frangos, 2007; Shih-Hsin & Mcintire, 1998; Kroll *et al.*, 1996; Ku *et al.*, 1985). It is important to note that the experimental conditions under which shear-dependent Ca²⁺ transients were observed in singly attached platelets may not necessarily represent MS responses *in vivo* where platelets are not normally fixed to a surface. A role for Piezo1 in the activation of platelets as they circulate under normal conditions would not be a beneficial one anyway. It is, however, conceivable that platelets in resting state travelling through arteries may exhibit shear-operated opening of the

Piezo1 channels which would allow repetitive transient Ca^{2+} entry events as they travel. These Ca^{2+} influx events, which permit the entry of relatively small quantities of Ca^{2+} into the cytosol, could serve the purpose of priming platelets to fulfil their haemostatic function whenever necessary. Such a function for Piezo1 in platelets would be particularly interesting at the regions of arterial stenosis where elevated levels of arterial shear could lead to more significant Ca^{2+} spiking in individual platelets (Figure 4.4 A) (Bark & Ku, 2010; Shih-Hsin & McIntire, 1998; Kroll *et al.*, 1996). This may increase the chances of spontaneous platelet activation in susceptible patients. Alternatively, Piezo1 activity under shear could be another Ca^{2+} entry pathway contributing to the global $[\text{Ca}^{2+}]_i$ elevations in adherent, activating platelets. Ca^{2+} entry via Piezo1 channels may serve to enhance platelet responses in a growing thrombus at the distal end of an atherosclerotic plaque where pathological levels of shear stress are commonly experienced due to severe stenosis (Figure 1.4 B) (Wolberg *et al.*, 2012; Bark & Ku, 2010). It is also plausible to suggest that Ca^{2+} entry through platelet Piezo1 channels could account for the previously observed shear-dependent transmembrane Ca^{2+} fluxes, and/or could make a contribution to shear-induced platelet activation and aggregation responses (Holme *et al.*, 1997; Chow *et al.*, 1992; Levenson *et al.*, 1990; O'Brien, 1990). These candidate roles for Piezo1 in human platelets also demonstrate its potential role in increasing the risk of life-threatening thrombus formation. This could mean that local elevations in arterial shear stress levels, especially in individuals prone to thrombotic disorders, may render platelets pro-thrombotic. Nevertheless, further research is required to investigate the suitability of Piezo1 as a potential therapeutic target.

It is useful to emphasise the heterogeneity of the shear-induced Ca^{2+} responses in singly attached platelets, i.e. not all platelets responded to shear stress. There could be several explanations for this observation. The most likely reason could be that not all platelets in the circulation express Piezo1, resulting from the uneven distribution of plasma membrane proteins during fragmentation from megakaryocytes in the process of thrombopoiesis. This idea is supported by the findings of the Western blot experiments that platelets express much lower levels of Piezo1 protein than Meg-01 cells, and also a much bigger proportion of Meg-01 cells displayed shear stress-induced Ca^{2+} responses. Given these observations, it is also worth pointing out that Piezo1 channels display relatively higher permeability to Ca^{2+} compared to other ions (Coste *et al.*, 2010), and also very little Ca^{2+} permeability is required for a significant $[\text{Ca}^{2+}]_i$ elevation in a cell

the size of the platelet due to its high surface area:volume ratio (Tolhurst *et al.*, 2008). Therefore, low Piezo1 expression in platelets compared to cells such as Meg-01 or erythrocytes could still achieve effective $[Ca^{2+}]_i$ elevations.

As discussed in Section 3.3, the findings of this thesis also raise the possibility that Piezo1 may contribute to megakaryocyte function, although further experimental evidence is needed to address this possibility. Previous studies have indicated important roles for mechanical forces in megakaryocyte gene expression and in the interactions between megakaryocytes and osteoblasts in the regulation of bone mass (Soves *et al.*, 2014). Also considering the significance of shear forces during thrombopoiesis, Piezo1 certainly represents a possible candidate for the mechanosensors in these previous studies (Thon *et al.*, 2012; Junt *et al.*, 2007).

6.2.2 Novel role for P2X1 in platelet immune responses

Since the last decade, platelet P2X1 channels have also been gathering increasing attention due to the growing evidence for their unique roles in amplifying activation and aggregation responses to a broad range of agonists such as ADP, collagen and thrombin (Jones *et al.*, 2014b; Oury *et al.*, 2014; Fung *et al.*, 2012; FUNG *et al.*, 2007; Fung *et al.*, 2005). Furthermore, because of their critical involvement in thrombus formation under arterial shear stress and the persistence of thrombin-induced channel activity to aspirin, P2X1 channels are considered to be excellent candidates of future therapeutic targets (Grenegard *et al.*, 2008; Hechler *et al.*, 2003). More recent studies revealed roles for P2X1 channels in platelet immune responses mediated by TLR2/1 activation (Klarstrom Engstrom *et al.*, 2014; Fung *et al.*, 2012). As a new role for P2X1 channels in immunity, Chapter 5 demonstrated the significant contribution of P2X1 channels to Fc γ RIIa-induced platelet functional responses, through amplification of the $[Ca^{2+}]_i$ following receptor activation. This chapter also investigated the likely molecular mechanisms underlying the observations made, and the potential role of shear stress on Fc γ RIIa-driven thrombus formation.

The findings of this study support the theory that P2X1 channels contribute to Fc γ RIIa-induced platelet function on the basis of the idea that tyrosine kinase-coupled Fc γ RIIa receptors, and GPVI and TLR2/1 receptors share the same ITAM-dependent signalling pathway (Fung *et al.*, 2005; Oury *et al.*, 2001; Watson & Gibbins, 1998). As observed with TLR2/1, P2X1 was found to significantly amplify Fc γ RIIa-induced

platelet Ca^{2+} responses. Despite this, certain differences exist between GPVI- or TLR2/1-, and Fc γ RIIa-induced P2X1 activity under the experimental conditions employed. For instance, PGI₂ completely abolished the Fc γ RIIa-induced Ca^{2+} response and secretion, whereas GPVI and TLR2/1 were shown to evoke PGI₂-resistant dense granule secretion responses. A potential reason for this difference could be that Fc γ RIIa stimulation possibly evokes different secretion mechanisms that are known to be dependent on factors such as the agonist used, the extent of stimulation, and the time point after stimulation (Eckly *et al.*, 2016; Jonnalagadda *et al.*, 2012).

By revealing the contribution of P2X1 channels to Fc γ RIIa-mediated platelet activation, this study also helps better understand the contribution of Fc γ RIIa receptors to platelet function, and thus disease development, from a physiological perspective. Importantly, this work demonstrated that P2X1 channels contribute to Fc γ RIIa-mediated platelet responses via direct Ca^{2+} influx and subsequent amplification of Ca^{2+} -dependent downstream effectors. Although the inhibition of platelet P2X1 channels in whole blood did not significantly influence thrombus formation over *S. sanguinis* under normal arterial shear stress conditions, further research should investigate the effect of pathological levels of shear (*see* Section 6.3). With the aid of further study, this work could provide another way in which P2X1 channels could pose as potential therapeutic targets in reducing the risk of circulating thrombi caused by bacteria-induced platelet activation, or localised thrombi in conditions such as IE.

6.3 Limitations and future directions

Data presented in Chapters 3 and 4 provide evidence for MS cation channel expression and activity in the Meg-01 cell line and human platelets, and indicate that the likely identity of the channels is Piezo1. The assays performed to reach this conclusion relied heavily on the use of pharmacological tools, such as GsMTx-4 and Yoda1. Although many studies mostly relied on the use of GsMTx-4 to investigate Piezo1 function (Li *et al.*, 2014; Coste *et al.*, 2012; Bae *et al.*, 2011), it is a generic inhibitor of MS cation channels and may also target other channels or receptors of yet unknown function. Similarly, the recently identified Piezo1 agonist, Yoda1, is a synthetic molecule which has not yet been widely used despite its clearly demonstrated specificity for Piezo1 over related channels such as Piezo2 (Syeda *et al.*, 2015; Lukacs *et al.*, 2015). Global KO of Piezo1 in mice reportedly led to embryonic lethality,

however conditional KO of this gene in embryonic stem cells has been achieved (Ranade *et al.*, 2014a; Li *et al.*, 2014). Also, in a study of the role of Piezo1 in erythrocyte volume regulation, morpholino-mediated KO of this gene was successfully achieved in zebrafish embryos, which retained similar quantities of blood cells (including thrombocytes) compared to wild-type embryos (Faucherre *et al.*, 2014). However, thrombocyte physiology or function in these Piezo1 KO zebrafish models have not been studied. Therefore, future work using an animal model lacking Piezo1 specifically in platelets and megakaryocytes could provide further evidence for the conclusions drawn here and extend them to *in vivo* studies. It should be remembered that mouse platelets, which are smaller in size and are normally exposed to the relatively higher levels of normal arterial shear in rodent circulation, may not necessarily behave in an identical manner to human platelets. As a first step, it may be feasible to try to suppress Piezo1 expression in the Meg-01 cell line, which can then be used to repeat the shear stress assays described in Chapter 3 to demonstrate loss of responses. Several studies have successfully performed targeted gene knockdown by transfecting Meg-01 cells with siRNA or shRNA (Edelstein *et al.*, 2013; Lopez *et al.*, 2013; Khandoga *et al.*, 2011; Withey *et al.*, 2005).

It is very important to acknowledge that the novel shear stress assays developed to study MS channel function in Meg-01 cells and platelets would not precisely recreate the biophysical conditions that the cells are exposed to *in vivo*. These assays primarily provide a model for platelet activation under shear, following attachment to vessel wall components such as collagen. In the normal intact circulation, platelets constantly travel within the blood vessels, and the influence of shear stress on Piezo1 channels under such conditions may be different to the experimental situation in this study in which platelets are attached via PECAM1 to a glass coverslip. Nevertheless, given the limited availability of techniques which would allow the study of platelet $[Ca^{2+}]_i$ changes under fluid shear stress *per se*, this study describes the best possible approach to date.

Interesting questions still remain about Piezo1 channel function in platelets and Meg-01 cells, which should also be addressed by further research. It is worth noting that in addition to fluid shear stress, other types of mechanical stimuli such as shape change during platelet activation could also operate Piezo1 channels through bilayer tension. Additionally, the effect of Piezo1 channel inhibitors/agonists on platelet functional responses should be studied in greater detail, preferably with the help of *in vivo* assays such as measuring radiolabelled platelet thromboembolisms before and after

intravenous injection of the pharmacological tools (Tymvios *et al.*, 2008). In answering the following questions, future studies will help further confirm the identity of the MS Ca^{2+} channels responsible for the effects observed in this thesis, and discover additional aspects of the contribution by these channels to platelet or megakaryocyte function: What is the cause of the switch from Piezo2 to Piezo1 expression during thrombopoiesis? Is Piezo1 protein in platelets inherited from the megakaryocyte or is it synthesised *de novo*? How would MS Ca^{2+} responses vary under pulsatile or disturbed flow, or at vessel bifurcations? What is the relevance of stimuli other than collagen in thrombus formation under flow? Do platelet GPCRs other than P2Y receptors modulate mechanosensitivity?



Throughout Chapter 5, the use of specific antibodies (IV.3 + F(ab')₂) to stimulate FcγRIIIa receptors in a wide variety of assays as described previously (Arman *et al.*, 2014; Gibbins *et al.*, 1996), led to the discovery of the contribution P2X1 makes to FcγRIIIa-induced $[\text{Ca}^{2+}]_i$ increases. However, the physiological relevance of the concentrations of the antibodies used to bind and cross-link the receptors has not been reported by these studies. In an effort to achieve a more physiologically relevant receptor activation, one of the five bacterial strains previously reported to cause FcγRIIIa-induced platelet aggregation (*S. sanguinis*) (Arman *et al.*, 2014) were also used in the assays. Although the results obtained with either stimulation method were similar, it is important to realise that the interactions between bacteria and platelets are not limited to FcγRIIIa, despite this receptor was shown to be the chief mediator (Arman *et al.*, 2014; Cox *et al.*, 2011). Provided the fact that P2X1 contributes to immune receptor TLR2/1-induced Ca^{2+} responses, more controls are required to ensure the bacteria-induced effects observed are not mediated by TLR2/1 in the experiments presented (Fung *et al.*, 2012). Therefore, future studies should aim to confirm and improve the specificity of activation and optimise the strength of stimulation of the FcγRIIIa receptors.

In addition to the experiments performed to characterise the molecular mechanism underlying the contribution of P2X1 to FcγRIIIa-induced $[\text{Ca}^{2+}]_i$ responses, further ATP measurements should monitor dense granule secretion in the presence of sNO and 3.2U/mL apyrase levels to confirm that under such inhibitory conditions ATP

release still takes place. This would support the observation that P2X1 mediates the $[Ca^{2+}]_i$ elevations obtained under the influence of endothelium-derived inhibitors. An exploration of the possible different secretion events underlying the PGI₂-resistant secretion by GPVI or TLR2/1 stimulation and the PGI₂-sensitive FcγRIIIa-induced responses will also greatly enhance our knowledge of the molecular events responsible for the effects observed. Further research should also repeat *in vitro* thrombus formation assays at higher levels of shear stress that were studied before (Hechler *et al.*, 2003), and also using other strains of bacteria known to activate platelets, where P2X1 may also amplify signalling. In these studies, the use of the F(ab')₂ fragment of the anti-FcγRIIIa antibody (IV.3) to specifically block FcγRIIIa-bacteria interactions, can help demonstrate the specificity of these functional responses.

6.4 Conclusions

Data presented in this thesis reveal new information on two distinct Ca²⁺ entry mechanisms into human platelets, which have the potential to contribute to cardiovascular disease. Firstly, the MS cation channel Piezo1 was detected and identified in human platelets, which was demonstrated to elevate $[Ca^{2+}]_i$ under normal and pathological levels of arterial shear stress, in a shear rate-dependent manner. A new experimental approach was developed that allowed the visualisation of shear-induced Ca²⁺ transients in singly attached platelets, and to study MS channel function using the MS channel inhibitor GsMTx-4. The Piezo1 agonist, Yoda1, enhanced shear-induced Ca²⁺ spiking and elevated $[Ca^{2+}]_i$ in platelet suspensions, further suggesting the identity of the MS channel as Piezo1. The inhibitory effect of GsMTx-4 on thrombus formation and the more significant increase in Ca²⁺ spiking under pathological levels of arterial shear indicate a potential role for Piezo1 in the development of arterial thrombosis. Shear stress induced GsMTx-4-sensitive $[Ca^{2+}]_i$ elevations in Meg-01 cells also, which raised the possibility that megakaryocytic Piezo1 channels may participate in mechanosensation within the bone marrow or during thrombopoiesis. Secondly, the ATP-gated P2X1 channels were shown to amplify $[Ca^{2+}]_i$ elevations in FcγRIIIa-induced platelet immune responses. Selective inhibition or desensitisation of P2X1 channels significantly reduced $[Ca^{2+}]_i$ elevations and platelet aggregation following FcγRIIIa receptor activation by cross-linking FcγRIIIa-specific antibodies or IgG-coated *S. sanguinis*. Evidence shows that ATP secretion mediates FcγRIIIa-induced direct Ca²⁺

influx through P2X1, which would result in the subsequent amplification in the activity of Ca²⁺-dependent downstream effectors. This P2X1-mediated Ca²⁺ entry persisted in the presence of endothelium-derived inhibitors such as sNO, which may highlight the importance of this mechanism *in vivo*. Together, these findings suggest that P2X1 may contribute to the formation of bacteria-induced, FcγRIIa-mediated thromboembolisms or thrombosis in diseases such as IE.

Bibliography

- Aidley, D.J. & Stanfield, P.R. 1996, *Ion channels: Molecules in action*, Cambridge University Press, Cambridge, United Kingdom.
- Albuisson, J., Murthy, S.E., Bandell, M., Coste, B., Louis-Dit-Picard, H., Mathur, J., Feneant-Thibault, M., Tertian, G., de Jaureguiberry, J.P., Syfuss, P.Y., Cahalan, S., Garcon, L., Toutain, F., Simon Rohrlich, P., Delaunay, J., Picard, V., Jeunemaitre, X. & Patapoutian, A. 2013, Dehydrated hereditary stomatocytosis linked to gain-of-function mutations in mechanically activated PIEZO1 ion channels, *Nature communications*, (4), 1884.
- Allison, S.J. 2016, Hypertension: Mechanosensation by PIEZO1 in blood pressure control, *Nature reviews Nephrology*, 13(1):3.
- Amisten, S. 2012, A rapid and efficient platelet purification protocol for platelet gene expression studies. in *Platelets and Megakaryocytes Additional Protocols and Perspectives, Volume 3*, eds. J.M. Gibbins & M.P. Mahaut-Smith, 155-172.
- Andolfo, I., Alper, S.L., De Franceschi, L., Auriemma, C., Russo, R., De Falco, L., Vallefucio, F., Esposito, M.R., Vandorpe, D.H., Shmukler, B.E., Narayan, R., Montanaro, D., D'Armiento, M., Vetro, A., Limongelli, I., Zuffardi, O., Glader, B.E., Schrier, S.L., Brugnara, C., Stewart, G.W., Delaunay, J. & Iolascon, A. 2013, Multiple clinical forms of dehydrated hereditary stomatocytosis arise from mutations in PIEZO1, *Blood*, (121) 19, 3925-35, S1-12.
- Andrews, R.K. & Berndt, M.C. 2004, Platelet physiology and thrombosis, *Thrombosis research*, (114) 5-6, 447-453.
- Anfinogenova, Y., Brett, S.E., Walsh, M.P., Harraz, O.F. & Welsh, D.G. 2011, Do TRPC-like currents and G protein-coupled receptors interact to facilitate myogenic tone development? *American journal of physiology.Heart and circulatory physiology*, (301) 4, H1378-88.

-
- Ariyoshi, H. & Salzman, E.W. 1995, Spatial distribution and temporal change in cytosolic pH and $[Ca^{2+}]$ in resting and activated single human platelets, *Cell calcium*, (17) 5, 317-326.
- Arman, M. & Krauel, K. 2015, Human platelet IgG Fc receptor FcgammaRIIA in immunity and thrombosis, *Journal of thrombosis and haemostasis : JTH*, (13) 6, 893-908.
- Arman, M., Krauel, K., Tilley, D.O., Weber, C., Cox, D., Greinacher, A., Kerrigan, S.W. & Watson, S.P. 2014, Amplification of bacteria-induced platelet activation is triggered by FcgammaRIIA, integrin alphaIIb beta3, and platelet factor 4, *Blood*, (123) 20, 3166-3174.
- Authi, K.S., Bokkala, S., Patel, Y., Kakkar, V.V. & Munkonge, F. 1993, Ca^{2+} release from platelet intracellular stores by thapsigargin and 2,5-di-(t-butyl)-1,4-benzohydroquinone: relationship to Ca^{2+} pools and relevance in platelet activation, *The Biochemical journal*, (294) Pt 1, 119-126.
- Badimon, L., Padro, T. & Vilahur, G. 2012, Atherosclerosis, platelets and thrombosis in acute ischaemic heart disease, *European heart journal- Acute cardiovascular care*, (1) 1, 60-74.
- Bae, C., Sachs, F. & Gottlieb, P.A. 2011, The mechanosensitive ion channel Piezo1 is inhibited by the peptide GsMTx4, *Biochemistry*, (50) 29, 6295-6300.
- Bagal, S.K., Brown, A.D., Cox, P.J., Omoto, K., Owen, R.M., Pryde, D.C., Sidders, B., Skerratt, S.E., Stevens, E.B., Storer, R.I. & Swain, N.A. 2013, Ion channels as therapeutic targets: a drug discovery perspective, *Journal of medicinal chemistry*, (56) 3, 593-624.
- Ballermann, B.J., Dardik, A., Eng, E. & Liu, A. 1998, Shear stress and the endothelium, *Kidney international. Supplement*, (67), S100-8.
- Bark, D.L., Jr & Ku, D.N. 2010, Wall shear over high degree stenoses pertinent to atherothrombosis, *Journal of Biomechanics*, (43) 15, 2970-2977.

-
- Barrett, N.E., Holbrook, L., Jones, S., Kaiser, W.J., Moraes, L.A., Rana, R., Sage, T., Stanley, R.G., Tucker, K.L., Wright, B. & Gibbins, J.M. 2008, Future innovations in anti-platelet therapies, *British journal of pharmacology*, (154) 5, 918-939.
- Baurand, A., Raboisson, P., Freund, M., Leon, C., Cazenave, J.P., Bourguignon, J.J. & Gachet, C. 2001, Inhibition of platelet function by administration of MRS2179, a P2Y1 receptor antagonist, *European journal of pharmacology*, (412) 3, 213-221.
- Bergmeier, W. & Stefanini, L. 2009, Novel molecules in calcium signaling in platelets, *Journal of thrombosis and haemostasis : JTH*, (7 Suppl 1), 187-190.
- Berridge, M.J., Bootman, M.D. & Roderick, H.L. 2003, Calcium signalling: dynamics, homeostasis and remodelling, *Nature reviews - Molecular cell biology*, (4) 7, 517-529.
- Bird, R.B., Stewart, W.E. & Lightfoot E.N. 2002, *Transport Phenomena*, 2nd Edition edn, John Wiley & Sons, Inc, New York.
- Bizzozero, G. 1882, Ueber einen neuen Formbestandteil des Blutes und dessen Rolle bei der Thrombose und Blut gerinnung, *Virchows Arch Pathol Anat Physiol Klin Med*, (90), 261-332.
- Bizzozero, G. 1881, Su di un nuovo elemento morfologico del sangue dei mammiferi e sulla sua importanza nella trombosi e nella coagulazione. *Osservatore Gazzetta delle Cliniche*, (17), 785-787.
- Blake, R.A., Asselin, J., Walker, T. & Watson, S.P. 1994, Fc gamma receptor II stimulated formation of inositol phosphates in human platelets is blocked by tyrosine kinase inhibitors and associated with tyrosine phosphorylation of the receptor, *FEBS letters*, (342) 1, 15-18.
- Bluestein, D., Gutierrez, C., Londono, M. & Schoepfoerster, R.T. 1999, Vortex shedding in steady flow through a model of an arterial stenosis and its

relevance to mural platelet deposition, *Annals of Biomedical Engineering*, (27) 6, 763-773.

Bluestein, D., Niu, L., Schoephoerster, R.T. & Dewanjee, M.K. 1997, Fluid mechanics of arterial stenosis: relationship to the development of mural thrombus, *Annals of Biomedical Engineering*, (25) 2, 344-356.

Born, G.V. & Kratzer, M.A. 1984, Source and concentration of extracellular adenosine triphosphate during haemostasis in rats, rabbits and man, *The Journal of physiology*, (354), 419-429.

Boyanova, D., Nilla, S., Birschmann, I., Dandekar, T. & Dittrich, M. 2012, PlateletWeb: a systems biologic analysis of signaling networks in human platelets, *Blood*, (119) 3, e22-34.

Boylan, B., Gao, C., Rathore, V., Gill, J.C., Newman, D.K. & Newman, P.J. 2008, Identification of FcγRIIIa as the ITAM-bearing receptor mediating αIIbβ3 outside-in integrin signaling in human platelets, *Blood*, (112) 7, 2780-2786.

Braun, A., Varga-Szabo, D., Kleinschnitz, C., Pleines, I., Bender, M., Austinat, M., Bosl, M., Stoll, G. & Nieswandt, B. 2009, Orai1 (CRACM1) is the platelet SOC channel and essential for pathological thrombus formation, *Blood*, (113) 9, 2056-2063.

Brewer, D.B. 2006, Max Schultze (1865), G. Bizzozero (1882) and the discovery of the platelet, *British journal of haematology*, (133) 3, 251-258.

Brinson, A.E., Harding, T., Diliberto, P.A., He, Y., Li, X., Hunter, D., Herman, B., Earp, H.S. & Graves, L.M. 1998, Regulation of a calcium-dependent tyrosine kinase in vascular smooth muscle cells by angiotensin II and platelet-derived growth factor. Dependence on calcium and the actin cytoskeleton, *The Journal of biological chemistry*, (273) 3, 1711-1718.

Burkhart, J.M., Vaudel, M., Gambaryan, S., Radau, S., Walter, U., Martens, L., Geiger, J., Sickmann, A. & Zahedi, R.P. 2012, The first comprehensive

and quantitative analysis of human platelet protein composition allows the comparative analysis of structural and functional pathways, *Blood*, (120) 15, e73-82.

Cahalan, S.M., Lukacs, V., Ranade, S.S., Chien, S., Bandell, M. & Patapoutian, A. 2015, Piezo1 links mechanical forces to red blood cell volume, *eLife*, (4), 10.7554/eLife.07370.

Carlsson, R., Engvall, E., Freeman, A. & Ruoslahti, E. 1981, Laminin and fibronectin in cell adhesion: enhanced adhesion of cells from regenerating liver to laminin, *Proceedings of the National Academy of Sciences of the United States of America*, (78) 4, 2403-2406.

Cattaneo, M., Lombardi, R., Zighetti, M.L., Gachet, C., Ohlmann, P., Cazenave, J.P. & Mannucci, P.M. 1997, Deficiency of (33P)2MeS-ADP binding sites on platelets with secretion defect, normal granule stores and normal thromboxane A₂ production. Evidence that ADP potentiates platelet secretion independently of the formation of large platelet aggregates and thromboxane A₂ production, *Thrombosis and haemostasis*, (77) 5, 986-990.

Cauwenberghs, S., Feijge, M.A., Hageman, G., Hoylaerts, M., Akkerman, J.W., Curvers, J. & Heemskerk, J.W. 2006, Plasma ectonucleotidases prevent desensitization of purinergic receptors in stored platelets: importance for platelet activity during thrombus formation, *Transfusion*, (46) 6, 1018-1028.

Cesarman-Maus, G. & Hajjar, K.A. 2005, Molecular mechanisms of fibrinolysis, *British journal of haematology*, (129) 3, 307-321.

Chapin, J.C. & Hajjar, K.A. 2015, Fibrinolysis and the control of blood coagulation, *Blood reviews*, (29) 1, 17-24.

Chow, T.W., Hellums, J.D., Moake, J.L. & Kroll, M.H. 1992, Shear stress-induced von Willebrand factor binding to platelet glycoprotein Ib initiates calcium influx associated with aggregation, *Blood*, (80) 1, 113-120.

-
- Cinar, E., Zhou, S., DeCoursey, J., Wang, Y., Waugh, R.E. & Wan, J. 2015, Piezo1 regulates mechanotransductive release of ATP from human RBCs, *Proceedings of the National Academy of Sciences of the United States of America*, (112) 38, 11783-11788.
- Clare, J.J. 2010, Targeting ion channels for drug discovery, *Discovery medicine*, (9) 46, 253-260.
- Clemetson, K.J. 2012, Platelets and primary haemostasis, *Thrombosis research*, (129) 3, 220-224.
- Copp, S.W., Kim, J.S., Ruiz-Velasco, V. & Kaufman, M.P. 2016, The mechanogated channel inhibitor GsMTx4 reduces the exercise pressor reflex in decerebrate rats, *The Journal of physiology*, (594) 3, 641-655.
- Coppinger, J.A., Cagney, G., Toomey, S., Kislinger, T., Belton, O., McRedmond, J.P., Cahill, D.J., Emili, A., Fitzgerald, D.J. & Maguire, P.B. 2004, Characterization of the proteins released from activated platelets leads to localization of novel platelet proteins in human atherosclerotic lesions, *Blood*, (103) 6, 2096-2104.
- Coste, B., Mathur, J., Schmidt, M., Earley, T.J., Ranade, S., Petrus, M.J., Dubin, A.E. & Patapoutian, A. 2010, Piezo1 and Piezo2 are essential components of distinct mechanically activated cation channels, *Science (New York, N.Y.)*, (330) 6000, 55-60.
- Coste, B., Murthy, S.E., Mathur, J., Schmidt, M., Mechioukhi, Y., Delmas, P. & Patapoutian, A. 2015, Piezo1 ion channel pore properties are dictated by C-terminal region, *Nature communications*, (6), 7223.
- Coste, B., Xiao, B., Santos, J.S., Syeda, R., Grandl, J., Spencer, K.S., Kim, S.E., Schmidt, M., Mathur, J., Dubin, A.E., Montal, M. & Patapoutian, A. 2012, Piezo proteins are pore-forming subunits of mechanically activated channels, *Nature*, (483) 7388, 176-U72.

-
- Coughlin, S.R. 2000, Thrombin signalling and protease-activated receptors, *Nature*, (407) 6801, 258-264.
- Cox, C.D., Bae, C., Ziegler, L., Hartley, S., Nikolova-Krstevski, V., Rohde, P.R., Ng, C.A., Sachs, F., Gottlieb, P.A. & Martinac, B. 2016, Removal of the mechanoprotective influence of the cytoskeleton reveals PIEZO1 is gated by bilayer tension, *Nature communications*, (7), 10366.
- Cox, D., Kerrigan, S.W. & Watson, S.P. 2011, Platelets and the innate immune system: mechanisms of bacterial-induced platelet activation, *Journal of thrombosis and haemostasis : JTH*, (9) 6, 1097-1107.
- Crittenden, J.R., Bergmeier, W., Zhang, Y., Piffath, C.L., Liang, Y., Wagner, D.D., Housman, D.E. & Graybiel, A.M. 2004, CalDAG-GEFI integrates signaling for platelet aggregation and thrombus formation, *Nature medicine*, (10) 9, 982-986.
- Davi, G. & Patrono, C. 2007, Platelet activation and atherothrombosis, *The New England journal of medicine*, (357) 24, 2482-2494.
- De Meyer, S.F., Deckmyn, H. & Vanhoorelbeke, K. 2009, von Willebrand factor to the rescue, *Blood*, (113) 21, 5049-5057.
- Delmas, P., Hao, J. & Rodat-Despoix, L. 2011, Molecular mechanisms of mechanotransduction in mammalian sensory neurons, *Nature reviews.Neuroscience*, (12) 3, 139-153.
- Eckly, A., Rinckel, J.Y., Proamer, F., Ulas, N., Joshi, S., Whiteheart, S.W. & Gachet, C. 2016, Respective contributions of single and compound granule fusion to secretion by activated platelets, *Blood*, (128) 21, 2538-2549.
- Edelstein, L.C., Simon, L.M., Montoya, R.T., Holinstat, M., Chen, E.S., Bergeron, A., Kong, X., Nagalla, S., Mohandas, N., Cohen, D.E., Dong, J.F., Shaw, C. & Bray, P.F. 2013, Racial differences in human platelet PAR4 reactivity reflect expression of PCTP and miR-376c, *Nature medicine*, (19) 12, 1609-1616.

-
- Einav, S. & Bluestein, D. 2004, Dynamics of blood flow and platelet transport in pathological vessels, *Annals of the New York Academy of Sciences*, (1015), 351-366.
- Enyedi, A., Sarkadi, B., Foldes-Papp, Z., Monostory, S. & Gardos, G. 1986, Demonstration of two distinct calcium pumps in human platelet membrane vesicles, *The Journal of biological chemistry*, (261) 20, 9558-9563.
- Erhardt, J.A., Toomey, J.R., Douglas, S.A. & Johns, D.G. 2006, P2X1 stimulation promotes thrombin receptor-mediated platelet aggregation, *Journal of thrombosis and haemostasis : JTH*, (4) 4, 882-890.
- Escobar, G. & White, J.G. 1991, The platelet open canalicular system: a final common pathway, *Blood cells*, (17) 3, 467-85; discussion 486-95.
- Farrugia, A., Hughes, C., Douglas, S., Neal, M. & James, J. 1989, Microtitre plate measurement of platelet response to hypotonic stress, *Journal of clinical pathology*, (42) 12, 1298-1301.
- Faucherre, A., Kissa, K., Nargeot, J., Mangoni, M.E. & Jopling, C. 2014, Piezo1 plays a role in erythrocyte volume homeostasis, *Haematologica*, (99) 1, 70-75.
- Fernandes, J., Lorenzo, I.M., Andrade, Y.N., Garcia-Elias, A., Serra, S.A., Fernandez-Fernandez, J.M. & Valverde, M.A. 2008, IP3 sensitizes TRPV4 channel to the mechano- and osmotransducing messenger 5'-6'-epoxyeicosatrienoic acid, *The Journal of general physiology*, (131) 5, i2.
- Fernandez, K.S. & de Alarcon, P.A. 2013, Development of the hematopoietic system and disorders of hematopoiesis that present during infancy and early childhood, *Pediatric clinics of North America*, (60) 6, 1273-1289.
- Fitzgerald, J.R., Foster, T.J. & Cox, D. 2006, The interaction of bacterial pathogens with platelets, *Nature reviews.Microbiology*, (4) 6, 445-457.
- Fox, S.C., Behan, M.W. & Heptinstall, S. 2004, Inhibition of ADP-induced intracellular Ca²⁺ responses and platelet aggregation by the P2Y12 receptor

-
- antagonists AR-C69931MX and clopidogrel is enhanced by prostaglandin E1, *Cell calcium*, (35) 1, 39-46.
- Franconi, F., Miceli, M., De Montis, M.G., Crisafi, E.L., Bennardini, F. & Tagliamonte, A. 1996, NMDA receptors play an anti-aggregating role in human platelets, *Thrombosis and haemostasis*, (76) 1, 84-87.
- Freyssinet, J.M. & Toti, F. 2010, Formation of procoagulant microparticles and properties, *Thrombosis research*, (125 Suppl 1), S46-8.
- Fung, C.Y., Brearley, C.A., Farndale, R.W. & Mahaut-Smith, M.P. 2005, A major role for P2X1 receptors in the early collagen-evoked intracellular Ca²⁺ responses of human platelets, *Thrombosis and haemostasis*, (94) 1, 37-40.
- Fung, C.Y.E., Cendana, C., Farndale, R.W. & Mahaut-Smith, M.P. 2007, Primary and secondary agonists can use P2X1 receptors as a major pathway to increase intracellular Ca²⁺ in the human platelet, *Journal of Thrombosis and Haemostasis*, (5) 5, 910-917.
- Fung, C.Y.E., Jones, S., Ntrakwah, A., Naseem, K.M., Farndale, R.W. & Mahaut-Smith, M.P. 2012, Platelet Ca²⁺ responses coupled to glycoprotein VI and Toll-like receptors persist in the presence of endothelial-derived inhibitors: roles for secondary activation of P2X1 receptors and release from intracellular Ca²⁺ stores, *Blood*, (119) 15, 3613-3621.
- Gale, A.J. 2011, Current Understanding of Hemostasis, *Toxicologic pathology*, (39) 1, 273-280.
- Garraud, O. & Cognasse, F. 2010, Platelet Toll-like receptor expression: the link between "danger" ligands and inflammation, *Inflammation & allergy drug targets*, (9) 5, 322-333.
- Ge, J., Li, W., Zhao, Q., Li, N., Chen, M., Zhi, P., Li, R., Gao, N., Xiao, B. & Yang, M. 2015, Architecture of the mammalian mechanosensitive Piezo1 channel, *Nature*, (527) 7576, 64-69.

-
- Gibbins, J., Asselin, J., Farndale, R., Barnes, M., Law, C.L. & Watson, S.P. 1996, Tyrosine phosphorylation of the Fc receptor gamma-chain in collagen-stimulated platelets, *The Journal of biological chemistry*, (271) 30, 18095-18099.
- Gilio, K., Harper, M.T., Cosemans, J.M., Konopatskaya, O., Munnix, I.C., Prinzen, L., Leitges, M., Liu, Q., Molkenin, J.D., Heemskerk, J.W. & Poole, A.W. 2010, Functional divergence of platelet protein kinase C (PKC) isoforms in thrombus formation on collagen, *The Journal of biological chemistry*, (285) 30, 23410-23419.
- Gillespie, P.G. & Walker, R.G. 2001, Molecular basis of mechanosensory transduction, *Nature*, (413) 6852, 194-202.
- Gimbrone, M.A., Jr, Anderson, K.R., Topper, J.N., Langille, B.L., Clowes, A.W., Berce, S., Davies, M.G., Stenmark, K.R., Frid, M.G., Weiser-Evans, M.C., Aldashev, A.A., Nemenoff, R.A., Majesky, M.W., Landerholm, T.E., Lu, J., Ito, W.D., Arras, M., Scholz, D., Imhof, B., Aurrand-Lions, M., Schaper, W., Nagel, T.E., Resnick, N., Dewey, C.F., Gimbrone, M.A. & Davies, P.F. 1999, Special communication the critical role of mechanical forces in blood vessel development, physiology and pathology, *Journal of vascular surgery*, (29) 6, 1104-1151.
- Glenn, J.R., White, A.E., Johnson, A., Fox, S.C., Behan, M.W., Dolan, G. & Heptinstall, S. 2005, Leukocyte count and leukocyte ecto-nucleotidase are major determinants of the effects of adenosine triphosphate and adenosine diphosphate on platelet aggregation in human blood, *Platelets*, (16) 3-4, 159-170.
- Gnanasambandam, R., Bae, C., Gottlieb, P.A. & Sachs, F. 2015, Ionic Selectivity and Permeation Properties of Human PIEZO1 Channels, *PloS one*, (10) 5, e0125503.
- Grenegard, M., Vretenbrant-Oberg, K., Nylander, M., Desilets, S., Lindstrom, E.G., Larsson, A., Ramstrom, I., Ramstrom, S. & Lindahl, T.L. 2008, The ATP-gated P2X1 receptor plays a pivotal role in activation of aspirin-

-
- treated platelets by thrombin and epinephrine, *The Journal of biological chemistry*, (283) 27, 18493-18504.
- Grynkiewicz, G., Poenie, M. & Tsien, R.Y. 1985, A new generation of Ca²⁺ indicators with greatly improved fluorescence properties, *The Journal of biological chemistry*, (260) 6, 3440-3450.
- Hanasaki, K. & Arita, H. 1988, Characterization of thromboxane A₂/prostaglandin H₂ (TXA₂/PGH₂) receptors of rat platelets and their interaction with TXA₂/PGH₂ receptor antagonists, *Biochemical pharmacology*, (37) 20, 3923-3929.
- Handa, M. & Guidotti, G. 1996, Purification and cloning of a soluble ATP-diphosphohydrolase (apyrase) from potato tubers (*Solanum tuberosum*), *Biochemical and biophysical research communications*, (218) 3, 916-923.
- Hardy, A.R., Conley, P.B., Luo, J., Benovic, J.L., Poole, A.W. & Mundell, S.J. 2005, P₂Y₁ and P₂Y₁₂ receptors for ADP desensitize by distinct kinase-dependent mechanisms, *Blood*, (105) 9, 3552-3560.
- Hardy, A.R., Jones, M.L., Mundell, S.J. & Poole, A.W. 2004, Reciprocal cross-talk between P₂Y₁ and P₂Y₁₂ receptors at the level of calcium signaling in human platelets, *Blood*, (104) 6, 1745-1752.
- Harper, M.T. & Poole, A.W. 2011, Store-operated calcium entry and non-capacitative calcium entry have distinct roles in thrombin-induced calcium signalling in human platelets, *Cell calcium*, (50) 4, 351-358.
- Hartwig, J. & Italiano, J., Jr 2003, The birth of the platelet, *Journal of thrombosis and haemostasis : JTH*, (1) 7, 1580-1586.
- Hartwig, J.H. 1992, Mechanisms of actin rearrangements mediating platelet activation, *The Journal of cell biology*, (118) 6, 1421-1442.
- Hassock, S.R., Zhu, M.X., Trost, C., Flockerzi, V. & Authi, K.S. 2002, Expression and role of TRPC proteins in human platelets: evidence that TRPC6 forms the store-independent calcium entry channel, *Blood*, (100) 8, 2801-2811.

-
- Hathaway, D.R. & Adelstein, R.S. 1979, Human platelet myosin light chain kinase requires the calcium-binding protein calmodulin for activity, *Proceedings of the National Academy of Sciences of the United States of America*, (76) 4, 1653-1657.
- Hattori, M. & Gouaux, E. 2012, Molecular mechanism of ATP binding and ion channel activation in P2X receptors, *Nature*, (485) 7397, 207-212.
- Hechler, B., Lenain, N., Marchese, P., Vial, C., Heim, V., Freund, M., Cazenave, J.P., Cattaneo, M., Ruggeri, Z.M., Evans, R. & Gachet, C. 2003, A role of the fast ATP-gated P2X1 cation channel in thrombosis of small arteries in vivo, *The Journal of experimental medicine*, (198) 4, 661-667.
- Hechler, B., Magnenat, S., Zighetti, M.L., Kassack, M.U., Ullmann, H., Cazenave, J.P., Evans, R., Cattaneo, M. & Gachet, C. 2005, Inhibition of platelet functions and thrombosis through selective or nonselective inhibition of the platelet P2 receptors with increasing doses of NF449 [4,4',4'',4'''-(carbonylbis(imino-5,1,3-benzenetriylbis-(carbonylimino)))tetrakis - benzene-1,3-disulfonic acid octasodium salt, *The Journal of pharmacology and experimental therapeutics*, (314) 1, 232-243.
- Heemskerk, J.W., Hoyland, J., Mason, W.T. & Sage, S.O. 1992, Spiking in cytosolic calcium concentration in single fibrinogen-bound fura-2-loaded human platelets, *The Biochemical journal*, (283 (Pt 2)) Pt 2, 379-383.
- Heemskerk, J.W., Vis, P., Feijge, M.A., Hoyland, J., Mason, W.T. & Sage, S.O. 1993, Roles of phospholipase C and Ca²⁺-ATPase in calcium responses of single, fibrinogen-bound platelets, *The Journal of biological chemistry*, (268) 1, 356-363.
- Heino, J. 2007, The collagen family members as cell adhesion proteins, *BioEssays : news and reviews in molecular, cellular and developmental biology*, (29) 10, 1001-1010.

-
- Hofmann, T., Obukhov, A.G., Schaefer, M., Harteneck, C., Gudermann, T. & Schultz, G. 1999, Direct activation of human TRPC6 and TRPC3 channels by diacylglycerol, *Nature*, (397) 6716, 259-263.
- Holme, P.A., Orvim, U., Hamers, M.J., Solum, N.O., Brosstad, F.R., Barstad, R.M. & Sakariassen, K.S. 1997, Shear-induced platelet activation and platelet microparticle formation at blood flow conditions as in arteries with a severe stenosis, *Arteriosclerosis, Thrombosis, and Vascular Biology*, (17) 4, 646-653.
- Hu, H. & Hoylaerts, M.F. 2010, The P2X1 ion channel in platelet function, *Platelets*, (21) 3, 153-166.
- Huckle, W.R., Dy, R.C. & Earp, H.S. 1992, Calcium-dependent increase in tyrosine kinase activity stimulated by angiotensin II, *Proceedings of the National Academy of Sciences of the United States of America*, (89) 18, 8837-8841.
- Hussain, J.F. & Mahaut-Smith, M.P. 1999, Reversible and irreversible intracellular Ca²⁺ spiking in single isolated human platelets, *The Journal of physiology*, (514 (Pt 3)) Pt 3, 713-718.
- Inoue, R., Jensen, L.J., Jian, Z., Shi, J., Hai, L., Lurie, A.I., Henriksen, F.H., Salomonsson, M., Morita, H., Kawarabayashi, Y., Mori, M., Mori, Y. & Ito, Y. 2009, Synergistic activation of vascular TRPC6 channel by receptor and mechanical stimulation via phospholipase C/diacylglycerol and phospholipase A2/omega-hydroxylase/20-HETE pathways, *Circulation research*, (104) 12, 1399-1409.
- ISTH Steering Committee for World Thrombosis Day 2014, Thrombosis: a major contributor to global disease burden, *Thrombosis research*, (134) 5, 931-938.
- Iwasaki, Y.K., Nishida, K., Kato, T. & Nattel, S. 2011, Atrial fibrillation pathophysiology: implications for management, *Circulation*, (124) 20, 2264-2274.

-
- Jiang, J., Woulfe, D.S. & Papoutsakis, E.T. 2014, Shear enhances thrombopoiesis and formation of microparticles that induce megakaryocytic differentiation of stem cells, *Blood*, (124) 13, 2094-2103.
- Jin, J., Daniel, J.L. & Kunapuli, S.P. 1998, Molecular basis for ADP-induced platelet activation. II. The P2Y1 receptor mediates ADP-induced intracellular calcium mobilization and shape change in platelets, *The Journal of biological chemistry*, (273) 4, 2030-2034.
- Jones, C.I., Moraes, L.A. & Gibbins, J.M. 2012, Regulation of platelet biology by platelet endothelial cell adhesion molecule-1, *Platelets*, (23) 5, 331-335.
- Jones, C.I., Sage, T., Moraes, L.A., Vaiyapuri, S., Hussain, U., Tucker, K.L., Barrett, N.E. & Gibbins, J.M. 2014a, Platelet endothelial cell adhesion molecule-1 inhibits platelet response to thrombin and von Willebrand factor by regulating the internalization of glycoprotein Ib via AKT/glycogen synthase kinase-3/dynamin and integrin alphaIIb beta3, *Arteriosclerosis, Thrombosis, and Vascular Biology*, (34) 9, 1968-1976.
- Jones, S., Evans, R.J. & Mahaut-Smith, M.P. 2014b, Ca²⁺ influx through P2X1 receptors amplifies P2Y1 receptor-evoked Ca²⁺ signaling and ADP-evoked platelet aggregation, *Molecular pharmacology*, (86) 3, 243-251.
- Jonnalagadda, D., Izu, L.T. & Whiteheart, S.W. 2012, Platelet secretion is kinetically heterogeneous in an agonist-responsive manner, *Blood*, (120) 26, 5209-5216.
- Junt, T., Schulze, H., Chen, Z., Massberg, S., Goerge, T., Krueger, A., Wagner, D.D., Graf, T., Italiano, J.E., Jr, Shivdasani, R.A. & von Andrian, U.H. 2007, Dynamic visualization of thrombopoiesis within bone marrow, *Science (New York, N.Y.)*, (317) 5845, 1767-1770.
- Kauffmanstein, G., Laher, I., Matrougui, K., Guerineau, N.C. & Henrion, D. 2012, Emerging role of G protein-coupled receptors in microvascular myogenic tone, *Cardiovascular research*, (95) 2, 223-232.

-
- Kawashima, Y., Geleoc, G.S., Kurima, K., Labay, V., Lelli, A., Asai, Y., Makishima, T., Wu, D.K., Della Santina, C.C., Holt, J.R. & Griffith, A.J. 2011, Mechanotransduction in mouse inner ear hair cells requires transmembrane channel-like genes, *The Journal of clinical investigation*, (121) 12, 4796-4809.
- Kerrigan, S.W., Clarke, N., Loughman, A., Meade, G., Foster, T.J. & Cox, D. 2008, Molecular basis for *Staphylococcus aureus*-mediated platelet aggregate formation under arterial shear in vitro, *Arteriosclerosis, Thrombosis, and Vascular Biology*, (28) 2, 335-340.
- Khandoga, A.L., Pandey, D., Welsch, U., Brandl, R. & Siess, W. 2011, GPR92/LPA(5) lysophosphatidate receptor mediates megakaryocytic cell shape change induced by human atherosclerotic plaques, *Cardiovascular research*, (90) 1, 157-164.
- Kim, S.E., Coste, B., Chadha, A., Cook, B. & Patapoutian, A. 2012, The role of *Drosophila* Piezo in mechanical nociception, *Nature*, (483) 7388, 209-212.
- Klarstrom Engstrom, K., Brommesson, C., Kalvegren, H. & Bengtsson, T. 2014, Toll like receptor 2/1 mediated platelet adhesion and activation on bacterial mimetic surfaces is dependent on src/Syk-signaling and purinergic receptor P2X1 and P2Y12 activation, *Biointerphases*, (9) 4, 041003.
- Kroll, M.H., Harris, T.S., Moake, J.L., Handin, R.I. & Schafer, A.I. 1991, von Willebrand factor binding to platelet GpIb initiates signals for platelet activation, *The Journal of clinical investigation*, (88) 5, 1568-1573.
- Kroll, M.H., Hellums, J.D., McIntire, L.V., Schafer, A.I. & Moake, J.L. 1996, Platelets and shear stress, *Blood*, (88) 5, 1525-1541.
- Ku, D.N., Giddens, D.P., Zarins, C.K. & Glagov, S. 1985, Pulsatile flow and atherosclerosis in the human carotid bifurcation. Positive correlation between plaque location and low oscillating shear stress, *Arteriosclerosis (Dallas, Tex.)*, (5) 3, 293-302.

-
- Kumar, D.R., Hanlin, E., Glurich, I., Mazza, J.J. & Yale, S.H. 2010, Virchow's contribution to the understanding of thrombosis and cellular biology, *Clinical medicine & research*, (8) 3-4, 168-172.
- Lankhof, H., van Hoeij, M., Schiphorst, M.E., Bracke, M., Wu, Y.P., Ijsseldijk, M.J., Vink, T., de Groot, P.G. & Sixma, J.J. 1996, A3 domain is essential for interaction of von Willebrand factor with collagen type III, *Thrombosis and haemostasis*, (75) 6, 950-958.
- Lentz, B.R. 2003, Exposure of platelet membrane phosphatidylserine regulates blood coagulation, *Progress in lipid research*, (42) 5, 423-438.
- Leon, C., Hechler, B., Freund, M., Eckly, A., Vial, C., Ohlmann, P., Dierich, A., LeMeur, M., Cazenave, J.P. & Gachet, C. 1999, Defective platelet aggregation and increased resistance to thrombosis in purinergic P2Y(1) receptor-null mice, *The Journal of clinical investigation*, (104) 12, 1731-1737.
- Levenson, J., Devynck, M.A., Pithois-Merli, I., Le Quan Sang, K.H., Filitti, V. & Simon, A. 1990, Dynamic association between artery shear flow condition and platelet cytosolic free Ca²⁺ concentration in human hypertension, *Clinical science (London, England : 1979)*, (79) 6, 613-618.
- Li, C., Rezania, S., Kammerer, S., Sokolowski, A., Devaney, T., Gorischek, A., Jahn, S., Hackl, H., Groschner, K., Windpassinger, C., Malle, E., Bauernhofer, T. & Schreibmayer, W. 2015, Piezo1 forms mechanosensitive ion channels in the human MCF-7 breast cancer cell line, *Scientific reports*, (5), 8364.
- Li, J., Hou, B., Tumova, S., Muraki, K., Bruns, A., Ludlow, M.J., Sedo, A., Hyman, A.J., McKeown, L., Young, R.S., Yuldasheva, N.Y., Majeed, Y., Wilson, L.A., Rode, B., Bailey, M.A., Kim, H.R., Fu, Z., Carter, D.A., Bilton, J., Imrie, H., Ajuh, P., Dear, T.N., Cubbon, R.M., Kearney, M.T., Prasad, K.R., Evans, P.C., Ainscough, J.F. & Beech, D.J. 2014, Piezo1 integration of vascular architecture with physiological force, *Nature*, (515) 7526, 279-282.

-
- Li, M., Cui, T., Mills, D.K., Lvov, Y.M. & McShane, M.J. 2005, Comparison of selective attachment and growth of smooth muscle cells on gelatin- and fibronectin-coated micropatterns, *Journal of nanoscience and nanotechnology*, (5) 11, 1809-1815.
- Li, Z., Delaney, M.K., O'Brien, K.A. & Du, X. 2010, Signaling during platelet adhesion and activation, *Arteriosclerosis, Thrombosis, and Vascular Biology*, (30) 12, 2341-2349.
- Linan-Rico, A., Wunderlich, J.E., Grants, I.S., Frankel, W.L., Xue, J., Williams, K.C., Harzman, A.E., Enneking, J.T., Cooke, H.J. & Christofi, F.L. 2013, Purinergic autocrine regulation of mechanosensitivity and serotonin release in a human EC model: ATP-gated P2X3 channels in EC are downregulated in ulcerative colitis, *Inflammatory bowel diseases*, (19) 11, 2366-2379.
- Lopez, E., Berna-Erro, A., Salido, G.M., Rosado, J.A. & Redondo, P.C. 2013, FKBP52 is involved in the regulation of SOCE channels in the human platelets and MEG 01 cells, *Biochimica et biophysica acta*, (1833) 3, 652-662.
- Lukacs, V., Mathur, J., Mao, R., Bayrak-Toydemir, P., Procter, M., Cahalan, S.M., Kim, H.J., Bandell, M., Longo, N., Day, R.W., Stevenson, D.A., Patapoutian, A. & Krock, B.L. 2015, Impaired PIEZO1 function in patients with a novel autosomal recessive congenital lymphatic dysplasia, *Nature communications*, (6), 8329.
- Machlus, K.R. & Italiano, J.E., Jr 2013, The incredible journey: From megakaryocyte development to platelet formation, *The Journal of cell biology*, (201) 6, 785-796.
- MacKenzie, A.B., Mahaut-Smith, M.P. & Sage, S.O. 1996, Activation of receptor-operated cation channels via P2X1 not P2T purinoceptors in human platelets, *The Journal of biological chemistry*, (271) 6, 2879-2881.

-
- Mahaut-Smith, M.P. 2012, The unique contribution of ion channels to platelet and megakaryocyte function, *Journal of thrombosis and haemostasis : JTH*, (10) 9, 1722-1732.
- Mahaut-Smith, M.P. 2004, Patch-clamp recordings of electrophysiological events in the platelet and megakaryocyte, *Methods in molecular biology (Clifton, N.J.)*, (273), 277-300.
- Mahaut-Smith, M.P., Jones, S. & Evans, R.J. 2011, The P2X1 receptor and platelet function, *Purinergic signalling*, (7) 3, 341-356.
- Mahaut-Smith, M.P., Rink, T.J., Collins, S.C. & Sage, S.O. 1990, Voltage-gated potassium channels and the control of membrane potential in human platelets, *The Journal of physiology*, (428), 723-735.
- Mahaut-Smith, M.P., Tolhurst, G. & Evans, R.J. 2004, Emerging roles for P2X1 receptors in platelet activation, *Platelets*, (15) 3, 131-144.
- Martinac, B. 2012, Mechanosensitive ion channels: an evolutionary and scientific tour de force in mechanobiology, *Channels (Austin, Tex.)*, (6) 4, 211-213.
- Massberg, S., Brand, K., Gruner, S., Page, S., Muller, E., Muller, I., Bergmeier, W., Richter, T., Lorenz, M., Konrad, I., Nieswandt, B. & Gawaz, M. 2002, A critical role of platelet adhesion in the initiation of atherosclerotic lesion formation, *The Journal of experimental medicine*, (196) 7, 887-896.
- Mazia, D., Schatten, G. & Sale, W. 1975, Adhesion of cells to surfaces coated with polylysine. Applications to electron microscopy, *The Journal of cell biology*, (66) 1, 198-200.
- Mazzarello, P., Calligaro, A.L. & Calligaro, A. 2001, Giulio Bizzozero: a pioneer of cell biology, *Nature reviews.Molecular cell biology*, (2) 10, 776-781.
- Mazzucato, M., Pradella, P., Cozzi, M.R., De Marco, L. & Ruggeri, Z.M. 2002, Sequential cytoplasmic calcium signals in a 2-stage platelet activation process induced by the glycoprotein Iba1 mechanoreceptor, *Blood*, (100) 8, 2793-2800.

-
- McCloskey, C., Jones, S., Amisten, S., Snowden, R.T., Kaczmarek, L.K., Erlinge, D., Goodall, A.H., Forsythe, I.D. & Mahaut-Smith, M.P. 2010, Kv1.3 is the exclusive voltage-gated K⁺ channel of platelets and megakaryocytes: roles in membrane potential, Ca²⁺ signalling and platelet count, *The Journal of physiology*, (588) Pt 9, 1399-1406.
- McVey, J.H. 2016, The role of the tissue factor pathway in haemostasis and beyond, *Current opinion in hematology*, (23) 5, 453-461.
- Mederos y Schnitzler, M., Storch, U., Meibers, S., Nurwakagari, P., Breit, A., Essin, K., Gollasch, M. & Gudermann, T. 2008, Gq-coupled receptors as mechanosensors mediating myogenic vasoconstriction, *The EMBO journal*, (27) 23, 3092-3103.
- Migliacci, R., Becattini, C., Pesavento, R., Davi, G., Vedovati, M.C., Guglielmini, G., Falcinelli, E., Ciabattoni, G., Dalla Valle, F., Prandoni, P., Agnelli, G. & Gresele, P. 2007, Endothelial dysfunction in patients with spontaneous venous thromboembolism, *Haematologica*, (92) 6, 812-818.
- Miyamoto, T., Mochizuki, T., Nakagomi, H., Kira, S., Watanabe, M., Takayama, Y., Suzuki, Y., Koizumi, S., Takeda, M. & Tominaga, M. 2014, Functional role for Piezo1 in stretch-evoked Ca²⁺ influx and ATP release in urothelial cell cultures, *The Journal of biological chemistry*, 289(23):16565-75.
- Miyazaki, Y., Nomura, S., Miyake, T., Kagawa, H., Kitada, C., Taniguchi, H., Komiyama, Y., Fujimura, Y., Ikeda, Y. & Fukuhara, S. 1996, High shear stress can initiate both platelet aggregation and shedding of procoagulant containing microparticles, *Blood*, (88) 9, 3456-3464.
- Molica, F., Morel, S., Meens, M.J., Denis, J.F., Bradfield, P.F., Penuela, S., Zufferey, A., Monyer, H., Imhof, B.A., Chanson, M., Laird, D.W., Fontana, P. & Kwak, B.R. 2015, Functional role of a polymorphism in the Pannexin1 gene in collagen-induced platelet aggregation, *Thrombosis and haemostasis*, (114) 2, 325-336.

-
- Mongrain, R. & Rodes-Cabau, J. 2006, Role of shear stress in atherosclerosis and restenosis after coronary stent implantation, *Revista espanola de cardiologia*, (59) 1, 1-4.
- Morrell, C.N., Sun, H., Ikeda, M., Beique, J.C., Swaim, A.M., Mason, E., Martin, T.V., Thompson, L.E., Gozen, O., Ampagoomian, D., Sprengel, R., Rothstein, J., Faraday, N., Huganir, R. & Lowenstein, C.J. 2008, Glutamate mediates platelet activation through the AMPA receptor, *The Journal of experimental medicine*, (205) 3, 575-584.
- Morris, C.E. 2001, Mechanoprotection of the plasma membrane in neurons and other non-erythroid cells by the spectrin-based membrane skeleton, *Cellular & Molecular Biology Letters*, (6) 3, 703-720.
- Morris, C.E. 1990, Mechanosensitive ion channels, *The Journal of membrane biology*, (113) 2, 93-107.
- Mountford, J.K., Petitjean, C., Putra, H.W., McCafferty, J.A., Setiabakti, N.M., Lee, H., Tonnesen, L.L., McFadyen, J.D., Schoenwaelder, S.M., Eckly, A., Gachet, C., Ellis, S., Voss, A.K., Dickins, R.A., Hamilton, J.R. & Jackson, S.P. 2015, The class II PI 3-kinase, PI3KC2alpha, links platelet internal membrane structure to shear-dependent adhesive function, *Nature communications*, (6), 6535.
- Nakeff, A. & Maat, B. 1974, Separation of megakaryocytes from mouse bone marrow by velocity sedimentation, *Blood*, (43) 4, 591-595.
- Nesbitt, W.S., Kulkarni, S., Giuliano, S., Goncalves, I., Dopheide, S.M., Yap, C.L., Harper, I.S., Salem, H.H. & Jackson, S.P. 2002, Distinct glycoprotein Ib/V/IX and integrin alpha IIbeta 3-dependent calcium signals cooperatively regulate platelet adhesion under flow, *The Journal of biological chemistry*, (277) 4, 2965-2972.
- Nesbitt, W.S., Westein, E., Tovar-Lopez, F.J., Tolouei, E., Mitchell, A., Fu, J., Carberry, J., Fouras, A. & Jackson, S.P. 2009, A shear gradient-dependent

-
- platelet aggregation mechanism drives thrombus formation, *Nature medicine*, (15) 6, 665-673.
- North, R.A. 2002, Molecular physiology of P2X receptors, *Physiological Reviews*, (82) 4, 1013-1067.
- O'Brien, J.R. 1990, Shear-induced platelet aggregation, *Lancet (London, England)*, (335) 8691, 711-713.
- Offermanns, S. 2006, Activation of platelet function through G protein-coupled receptors, *Circulation research*, (99) 12, 1293-1304.
- Office for National Statistics 2013, , *Avoidable Mortality in England and Wales, 2013*. Available at: http://webarchive.nationalarchives.gov.uk/20160105160709/http://www.ons.gov.uk/ons/dcp171778_404337.pdf.
- Ogura, M., Morishima, Y., Ohno, R., Kato, Y., Hirabayashi, N., Nagura, H. & Saito, H. 1985, Establishment of a novel human megakaryoblastic leukemia cell line, MEG-01, with positive Philadelphia chromosome, *Blood*, (66) 6, 1384-1392.
- Oury, C., Daenens, K., Hu, H., Toth-Zsamboki, E., Bryckaert, M. & Hoylaerts, M.F. 2006a, ERK2 activation in arteriolar and venular murine thrombosis: platelet receptor GPIb vs. P2X, *Journal of thrombosis and haemostasis : JTH*, (4) 2, 443-452.
- Oury, C., Kuijpers, M.J., Toth-Zsamboki, E., Bonnefoy, A., Danloy, S., Vreys, I., Feijge, M.A., De Vos, R., Vermynen, J., Heemskerk, J.W. & Hoylaerts, M.F. 2003, Overexpression of the platelet P2X1 ion channel in transgenic mice generates a novel prothrombotic phenotype, *Blood*, (101) 10, 3969-3976.
- Oury, C., Lecut, C., Hego, A., WÃ©ra, O. & Delierneux, C. 2014, Purinergic control of inflammation and thrombosis: Role of P2X1 receptors, *Computational and Structural Biotechnology Journal*, (13), 106-110.

-
- Oury, C., Toth-Zsamboki, E., Thys, C., Tytgat, J., Vermylen, J. & Hoylaerts, M.F. 2001, The ATP-gated P2X1 ion channel acts as a positive regulator of platelet responses to collagen, *Thrombosis and haemostasis*, (86) 5, 1264-1271.
- Oury, C., Toth-Zsamboki, E., Vermylen, J. & Hoylaerts, M.F. 2006b, The platelet ATP and ADP receptors, *Current pharmaceutical design*, (12) 7, 859-875.
- Oury, C., Toth-Zsamboki, E., Vermylen, J. & Hoylaerts, M.F. 2002, P2X1-mediated activation of extracellular signal-regulated kinase 2 contributes to platelet secretion and aggregation induced by collagen, *Blood*, (100) 7, 2499-2505.
- Overington, J.P., Al-Lazikani, B. & Hopkins, A.L. 2006, How many drug targets are there? *Nature reviews. Drug discovery*, (5) 12, 993-996.
- Palta, S., Saroa, R. & Palta, A. 2014, Overview of the coagulation system, *Indian Journal of Anaesthesia*, (58) 5, 515-523.
- Papaioannou, T.G. & Stefanadis, C. 2005, Vascular wall shear stress: basic principles and methods, *Hellenic journal of cardiology : HJC = Hellenike kardiologike epitheorese*, (46) 1, 9-15.
- Pathak, M.M., Nourse, J.L., Tran, T., Hwe, J., Arulmoli, J., Le, D.T., Bernardis, E., Flanagan, L.A. & Tombola, F. 2014, Stretch-activated ion channel Piezo1 directs lineage choice in human neural stem cells, *Proceedings of the National Academy of Sciences of the United States of America*, (111) 45, 16148-16153.
- Pearson, W.R., Wood, T., Zhang, Z. & Miller, W. 1997, Comparison of DNA sequences with protein sequences, *Genomics*, (46) 1, 24-36.
- Pease, D.C. 1956, An electron microscopic study of red bone marrow, *Blood*, (11) 6, 501-526.
- Peyronnet, R., Martins, J.R., Duprat, F., Demolombe, S., Arhatte, M., Jodar, M., Tauc, M., Duranton, C., Paulais, M., Teulon, J., Honore, E. & Patel, A.

-
- 2013, Piezo1-dependent stretch-activated channels are inhibited by Polycystin-2 in renal tubular epithelial cells, *EMBO reports*, (14) 12, 1143-1148.
- Poenie, M. 1990, Alteration of intracellular Fura-2 fluorescence by viscosity: a simple correction, *Cell calcium*, (11) 2-3, 85-91.
- Prakash, Y.S., Smithson, K.G. & Sieck, G.C. 1994, Application of the Cavalieri principle in volume estimation using laser confocal microscopy, *NeuroImage*, (1) 4, 325-333.
- Prandoni, P. 2009, Venous and arterial thrombosis: two aspects of the same disease? *European journal of internal medicine*, (20) 6, 660-661.
- Pratico, D., Tillmann, C., Zhang, Z.B., Li, H. & FitzGerald, G.A. 2001, Acceleration of atherogenesis by COX-1-dependent prostanoid formation in low density lipoprotein receptor knockout mice, *Proceedings of the National Academy of Sciences of the United States of America*, (98) 6, 3358-3363.
- Previtali, E., Bucciarelli, P., Passamonti, S.M. & Martinelli, I. 2011, Risk factors for venous and arterial thrombosis, *Blood transfusion = Trasfusione del sangue*, (9) 2, 120-138.
- Pugh, N., Simpson, A.M., Smethurst, P.A., de Groot, P.G., Raynal, N. & Farndale, R.W. 2010, Synergism between platelet collagen receptors defined using receptor-specific collagen-mimetic peptide substrata in flowing blood, *Blood*, (115) 24, 5069-5079.
- Quinn, M., Deering, A., Stewart, M., Cox, D., Foley, B. & Fitzgerald, D. 1999, Quantifying GPIIb/IIIa receptor binding using 2 monoclonal antibodies: discriminating abciximab and small molecular weight antagonists, *Circulation*, (99) 17, 2231-2238.
- Ramos, C.L., Huo, Y., Jung, U., Ghosh, S., Manka, D.R., Sarembock, I.J. & Ley, K. 1999, Direct demonstration of P-selectin- and VCAM-1-dependent

mononuclear cell rolling in early atherosclerotic lesions of apolipoprotein E-deficient mice, *Circulation research*, (84) 11, 1237-1244.

Ramstrom, S., Ranby, M. & Lindahl, T.L. 2003, Platelet phosphatidylserine exposure and procoagulant activity in clotting whole blood - different effects of collagen, TRAP and calcium ionophore A23187, *Thrombosis and haemostasis*, (89) 1, 132-141.

Ranade, S.S., Qiu, Z., Woo, S.H., Hur, S.S., Murthy, S.E., Cahalan, S.M., Xu, J., Mathur, J., Bandell, M., Coste, B., Li, Y.S., Chien, S. & Patapoutian, A. 2014a, Piezo1, a mechanically activated ion channel, is required for vascular development in mice, *Proceedings of the National Academy of Sciences of the United States of America*, .

Ranade, S.S., Woo, S.H., Dubin, A.E., Moshourab, R.A., Wetzel, C., Petrus, M., Mathur, J., Begay, V., Coste, B., Mainquist, J., Wilson, A.J., Francisco, A.G., Reddy, K., Qiu, Z., Wood, J.N., Lewin, G.R. & Patapoutian, A. 2014b, Piezo2 is the major transducer of mechanical forces for touch sensation in mice, *Nature*, (516) 7529, 121-125.

Raz, S., Einav, S., Alemu, Y. & Bluestein, D. 2007, DPIV prediction of flow induced platelet activation-comparison to numerical predictions, *Annals of Biomedical Engineering*, (35) 4, 493-504.

Riley, W.W., Jr & Pfeiffer, D.R. 1986, Rapid and extensive release of Ca²⁺ from energized mitochondria induced by EGTA, *The Journal of biological chemistry*, (261) 1, 28-31.

Rink, T.J. & Sanchez, A. 1984, Effects of prostaglandin I₂ and forskolin on the secretion from platelets evoked at basal concentrations of cytoplasmic free calcium by thrombin, collagen, phorbol ester and exogenous diacylglycerol, *The Biochemical journal*, (222) 3, 833-836.

Roberts, D.E., McNicol, A. & Bose, R. 2004, Mechanism of collagen activation in human platelets, *The Journal of biological chemistry*, (279) 19, 19421-19430.

-
- Rolf, M.G., Brearley, C.A. & Mahaut-Smith, M.P. 2001, Platelet shape change evoked by selective activation of P2X1 purinoceptors with alpha,beta-methylene ATP, *Thrombosis and haemostasis*, (85) 2, 303-308.
- Ross, R. 1999, Atherosclerosis--an inflammatory disease, *The New England journal of medicine*, (340) 2, 115-126.
- Ruggeri, Z.M. 2007, The role of von Willebrand factor in thrombus formation, *Thrombosis research*, (120 Suppl 1), S5-9.
- Ruggeri, Z.M. 2002, Platelets in atherothrombosis, *Nature medicine*, (8) 11, 1227-1234.
- Sachs, F. & Morris, C.E. 1998, Mechanosensitive ion channels in nonspecialized cells, *Reviews of physiology, biochemistry and pharmacology*, (132), 1-77.
- Sage, S.O. & Rink, T.J. 1987, The kinetics of changes in intracellular calcium concentration in fura-2-loaded human platelets, *The Journal of biological chemistry*, (262) 34, 16364-16369.
- Sage, S.O., Yamoah, E.H. & Heemskerk, J.W. 2000, The roles of P2X1 and P2T AC receptors in ADP-evoked calcium signalling in human platelets, *Cell calcium*, (28) 2, 119-126.
- Schmidt, E.M., Munzer, P., Borst, O., Kraemer, B.F., Schmid, E., Urban, B., Lindemann, S., Ruth, P., Gawaz, M. & Lang, F. 2011, Ion channels in the regulation of platelet migration, *Biochemical and biophysical research communications*, (415) 1, 54-60.
- Schmitt, A., Guichard, J., Masse, J.M., Debili, N. & Cramer, E.M. 2001, Of mice and men: comparison of the ultrastructure of megakaryocytes and platelets, *Experimental hematology*, (29) 11, 1295-1302.
- Schneider, C.A., Rasband, W.S. & Eliceiri, K.W. 2012, NIH Image to ImageJ: 25 years of image analysis, *Nature methods*, (9) 7, 671-675.

-
- Schneider, E.R., Mastrotto, M., Laursen, W.J., Schulz, V.P., Goodman, J.B., Funk, O.H., Gallagher, P.G., Gracheva, E.O. & Bagriantsev, S.N. 2014, Neuronal mechanism for acute mechanosensitivity in tactile-foraging waterfowl, *Proceedings of the National Academy of Sciences of the United States of America*, (111) 41, 14941-14946.
- Schneider, S.W., Nuschele, S., Wixforth, A., Gorzelanny, C., Alexander-Katz, A., Netz, R.R. & Schneider, M.F. 2007, Shear-induced unfolding triggers adhesion of von Willebrand factor fibers, *Proceedings of the National Academy of Sciences of the United States of America*, (104) 19, 7899-7903.
- Scholz, N., Gehring, J., Guan, C., Ljaschenko, D., Fischer, R., Lakshmanan, V., Kittel, R.J. & Langenhan, T. 2015, The adhesion GPCR latrophilin/CIRL shapes mechanosensation, *Cell reports*, (11) 6, 866-874.
- Schrenk-Siemens, K., Wende, H., Prato, V., Song, K., Rostock, C., Loewer, A., Utikal, J., Lewin, G.R., Lechner, S.G. & Siemens, J. 2015, PIEZO2 is required for mechanotransduction in human stem cell-derived touch receptors, *Nature neuroscience*, (18) 1, 10-16.
- Shattil, S.J., Kim, C. & Ginsberg, M.H. 2010, The final steps of integrin activation: the end game, *Nature reviews.Molecular cell biology*, (11) 4, 288-300.
- Shattil, S.J. & Newman, P.J. 2004, Integrins: dynamic scaffolds for adhesion and signaling in platelets, *Blood*, (104) 6, 1606-1615.
- Shih-Hsin, K. & McIntire, L. 1998, Rheology in *Thrombosis and Hemorrhage*, eds. J. Loscalzo & A. Schafer, 2nd edn, Lippincott Williams and Wilkins, 295.
- Siedlecki, C.A., Lestini, B.J., Kottke-Marchant, K.K., Eppell, S.J., Wilson, D.L. & Marchant, R.E. 1996, Shear-dependent changes in the three-dimensional structure of human von Willebrand factor, *Blood*, (88) 8, 2939-2950.
- Small, D.L. & Morris, C.E. 1994, Delayed activation of single mechanosensitive channels in *Lymnaea* neurons, *The American Journal of Physiology*, (267) 2 Pt 1, C598-606.

-
- Smethurst, P.A., Onley, D.J., Jarvis, G.E., O'Connor, M.N., Knight, C.G., Herr, A.B., Ouwehand, W.H. & Farndale, R.W. 2007, Structural basis for the platelet-collagen interaction: the smallest motif within collagen that recognizes and activates platelet Glycoprotein VI contains two glycine-proline-hydroxyproline triplets, *The Journal of biological chemistry*, (282) 2, 1296-1304.
- Smolenski, A. 2012, Novel roles of cAMP/cGMP-dependent signaling in platelets, *Journal of thrombosis and haemostasis : JTH*, (10) 2, 167-176.
- Smyth, S.S., McEver, R.P., Weyrich, A.S., Morrell, C.N., Hoffman, M.R., Arepally, G.M., French, P.A., Dauerman, H.L., Becker, R.C. & 2009 Platelet Colloquium Participants 2009, Platelet functions beyond hemostasis, *Journal of thrombosis and haemostasis : JTH*, (7) 11, 1759-1766.
- Song, Z., Gomes, D.A. & Stevens, W. 2009, Role of purinergic P2Y1 receptors in regulation of vasopressin and oxytocin secretion, *American journal of physiology.Regulatory, integrative and comparative physiology*, (297) 2, R478-84.
- Soves, C.P., Miller, J.D., Begun, D.L., Taichman, R.S., Hankenson, K.D. & Goldstein, S.A. 2014, Megakaryocytes are mechanically responsive and influence osteoblast proliferation and differentiation, *Bone*, (66), 111-120.
- Spassova, M.A., Hewavitharana, T., Xu, W., Soboloff, J. & Gill, D.L. 2006, A common mechanism underlies stretch activation and receptor activation of TRPC6 channels, *Proceedings of the National Academy of Sciences of the United States of America*, (103) 44, 16586-16591.
- Stein, P.D. & Sabbah, H.N. 1974, Measured turbulence and its effect on thrombus formation, *Circulation research*, (35) 4, 608-614.
- Stiber, J.A., Seth, M. & Rosenberg, P.B. 2009, Mechanosensitive channels in striated muscle and the cardiovascular system: not quite a stretch anymore, *Journal of cardiovascular pharmacology*, (54) 2, 116-122.

-
- Storch, U., Mederos y Schnitzler, M. & Gudermann, T. 2012, G protein-mediated stretch reception, *American journal of physiology.Heart and circulatory physiology*, (302) 6, H1241-9.
- Suchyna, T.M. & Sachs, F. 2007, Mechanosensitive channel properties and membrane mechanics in mouse dystrophic myotubes, *The Journal of physiology*, (581) Pt 1, 369-387.
- Suchyna, T.M., Tape, S.E., Koeppe, R.E., 2nd, Andersen, O.S., Sachs, F. & Gottlieb, P.A. 2004, Bilayer-dependent inhibition of mechanosensitive channels by neuroactive peptide enantiomers, *Nature*, (430) 6996, 235-240.
- Sullam, P.M., Hyun, W.C., Szollosi, J., Dong, J., Foss, W.M. & Lopez, J.A. 1998, Physical proximity and functional interplay of the glycoprotein Ib-IX-V complex and the Fc receptor FcγRIIA on the platelet plasma membrane, *The Journal of biological chemistry*, (273) 9, 5331-5336.
- Sullivan, M.J., Sharma, R.V., Wachtel, R.E., Chapleau, M.W., Waite, L.J., Bhalla, R.C. & Abboud, F.M. 1997, Non-voltage-gated Ca²⁺ influx through mechanosensitive ion channels in aortic baroreceptor neurons, *Circulation research*, (80) 6, 861-867.
- Sun, H., Swaim, A., Herrera, J.E., Becker, D., Becker, L., Srivastava, K., Thompson, L.E., Shero, M.R., Perez-Tamayo, A., Suktitipat, B., Mathias, R., Contractor, A., Faraday, N. & Morrell, C.N. 2009, Platelet kainate receptor signaling promotes thrombosis by stimulating cyclooxygenase activation, *Circulation research*, (105) 6, 595-603.
- Sun, Q.H., DeLisser, H.M., Zukowski, M.M., Paddock, C., Albelda, S.M. & Newman, P.J. 1996, Individually distinct Ig homology domains in PECAM-1 regulate homophilic binding and modulate receptor affinity, *The Journal of biological chemistry*, (271) 19, 11090-11098.
- Suzuki-Inoue, K., Fuller, G.L., Garcia, A., Eble, J.A., Pohlmann, S., Inoue, O., Gartner, T.K., Hughan, S.C., Pearce, A.C., Laing, G.D., Theakston, R.D.,

-
- Schweighoffer, E., Zitzmann, N., Morita, T., Tybulewicz, V.L., Ozaki, Y. & Watson, S.P. 2006, A novel Syk-dependent mechanism of platelet activation by the C-type lectin receptor CLEC-2, *Blood*, (107) 2, 542-549.
- Syeda, R., Xu, J., Dubin, A.E., Coste, B., Mathur, J., Huynh, T., Matzen, J., Lao, J., Tully, D.C., Engels, I.H., Petrassi, H.M., Schumacher, A.M., Montal, M., Bandell, M. & Patapoutian, A. 2015, Chemical activation of the mechanotransduction channel Piezo1, *eLife*, (4), 10.7554/eLife.07369.
- Tangelder, G.J., Teirlinck, H.C., Slaaf, D.W. & Reneman, R.S. 1985, Distribution of blood platelets flowing in arterioles, *The American Journal of Physiology*, (248) 3 Pt 2, H318-23.
- Taylor, K.A., Wright, J.R., Vial, C., Evans, R.J. & Mahaut-Smith, M.P. 2014, Amplification of human platelet activation by surface pannexin-1 channels, *Journal of thrombosis and haemostasis : JTH*, (12) 6, 987-998.
- Thon, J.N., Macleod, H., Begonja, A.J., Zhu, J., Lee, K.C., Mogilner, A., Hartwig, J.H. & Italiano, J.E., Jr 2012, Microtubule and cortical forces determine platelet size during vascular platelet production, *Nature communications*, (3), 852.
- Tilley, D.O., Arman, M., Smolenski, A., Cox, D., O'Donnell, J.S., Douglas, C.W., Watson, S.P. & Kerrigan, S.W. 2013, Glycoprotein Iba1 and FcγRIIIa play key roles in platelet activation by the colonizing bacterium, *Streptococcus oralis*, *Journal of thrombosis and haemostasis : JTH*, (11) 5, 941-950.
- Tolhurst, G., Carter, R.N., Amisten, S., Holdich, J.P., Erlinge, D. & Mahaut-Smith, M.P. 2008, Expression profiling and electrophysiological studies suggest a major role for Orai1 in the store-operated Ca²⁺ influx pathway of platelets and megakaryocytes, *Platelets*, (19) 4, 308-313.
- Traub, O. & Berk, B.C. 1998, Laminar shear stress: mechanisms by which endothelial cells transduce an atheroprotective force, *Arteriosclerosis, Thrombosis, and Vascular Biology*, (18) 5, 677-685.

-
- Tymvios, C., Jones, S., Moore, C., Pitchford, S.C., Page, C.P. & Emerson, M. 2008, Real-time measurement of non-lethal platelet thromboembolic responses in the anaesthetized mouse, *Thrombosis and haemostasis*, (99) 2, 435-440.
- Uijttewaal, W.S., Nijhof, E.J., Bronkhorst, P.J., Den Hartog, E. & Heethaar, R.M. 1993, Near-wall excess of platelets induced by lateral migration of erythrocytes in flowing blood, *The American Journal of Physiology*, (264) 4 Pt 2, H1239-44.
- Vaiyapuri, S., Flora, G.D. & Gibbins, J.M. 2015, Gap junctions and connexin hemichannels in the regulation of haemostasis and thrombosis, *Biochemical Society transactions*, (43) 3, 489-494.
- Vaiyapuri, S., Jones, C.I., Sasikumar, P., Moraes, L.A., Munger, S.J., Wright, J.R., Ali, M.S., Sage, T., Kaiser, W.J., Tucker, K.L., Stain, C.J., Bye, A.P., Jones, S., Oviedo-Orta, E., Simon, A.M., Mahaut-Smith, M.P. & Gibbins, J.M. 2012, Gap junctions and connexin hemichannels underpin hemostasis and thrombosis, *Circulation*, (125) 20, 2479-2491.
- Valant, P.A., Adjei, P.N. & Haynes, D.H. 1992, Rapid Ca^{2+} extrusion via the $\text{Na}^+/\text{Ca}^{2+}$ exchanger of the human platelet, *The Journal of membrane biology*, (130) 1, 63-82.
- van Kruchten, R., Braun, A., Feijge, M.A., Kuijpers, M.J., Rivera-Galdos, R., Kraft, P., Stoll, G., Kleinschnitz, C., Bevers, E.M., Nieswandt, B. & Heemskerk, J.W. 2012, Antithrombotic potential of blockers of store-operated calcium channels in platelets, *Arteriosclerosis, Thrombosis, and Vascular Biology*, (32) 7, 1717-1723.
- Varga-Szabo, D., Braun, A. & Nieswandt, B. 2009, Calcium signaling in platelets, *Journal of thrombosis and haemostasis : JTH*, (7) 7, 1057-1066.
- Vial, C., Rolf, M.G., Mahaut-Smith, M.P. & Evans, R.J. 2002, A study of P2X1 receptor function in murine megakaryocytes and human platelets reveals

-
- synergy with P2Y receptors, *British journal of pharmacology*, (135) 2, 363-372.
- Vicari, A.M., Monzani, M.L., Pellegatta, F., Ronchi, P., Galli, L. & Folli, F. 1994, Platelet calcium homeostasis is abnormal in patients with severe arteriosclerosis, *Arteriosclerosis and Thrombosis : A Journal of Vascular Biology / American Heart Association*, (14) 9, 1420-1424.
- Vu, T.K., Hung, D.T., Wheaton, V.I. & Coughlin, S.R. 1991, Molecular cloning of a functional thrombin receptor reveals a novel proteolytic mechanism of receptor activation, *Cell*, (64) 6, 1057-1068.
- Wang, E.C., Lee, J.M., Ruiz, W.G., Balestreire, E.M., von Bodungen, M., Barrick, S., Cockayne, D.A., Birder, L.A. & Apodaca, G. 2005, ATP and purinergic receptor-dependent membrane traffic in bladder umbrella cells, *The Journal of clinical investigation*, (115) 9, 2412-2422.
- Wang, L., Ostberg, O., Wihlborg, A.K., Brogren, H., Jern, S. & Erlinge, D. 2003, Quantification of ADP and ATP receptor expression in human platelets, *Journal of thrombosis and haemostasis : JTH*, (1) 2, 330-336.
- Wang, S., Chennupati, R., Kaur, H., Iring, A., Wettschureck, N. & Offermanns, S. 2016, Endothelial cation channel PIEZO1 controls blood pressure by mediating flow-induced ATP release, *The Journal of clinical investigation*, 126(12):4527-4536.
- Watson, C.N., Kerrigan, S.W., Cox, D., Henderson, I.R., Watson, S.P. & Arman, M. 2016, Human platelet activation by *Escherichia coli*: roles for FcγRIIA and integrin αIIbβ3, *Platelets*, (27) 6, 535-540.
- Watson, S.P. & Gibbins, J. 1998, Collagen receptor signalling in platelets: extending the role of the ITAM, *Immunology today*, (19) 6, 260-264.
- Weyrich, A.S., Schwertz, H., Kraiss, L.W. & Zimmerman, G.A. 2009, Protein synthesis by platelets: historical and new perspectives, *Journal of thrombosis and haemostasis : JTH*, (7) 2, 241-246.

-
- White, C.R. & Frangos, J.A. 2007, The shear stress of it all: the cell membrane and mechanochemical transduction, *Philosophical transactions of the Royal Society of London. Series B, Biological sciences*, (362) 1484, 1459-1467.
- Whiteheart, S.W. 2011, Platelet granules: surprise packages, *Blood*, (118) 5, 1190-1191.
- Withey, J.M., Marley, S.B., Kaeda, J., Harvey, A.J., Crompton, M.R. & Gordon, M.Y. 2005, Targeting primary human leukaemia cells with RNA interference: Bcr-Abl targeting inhibits myeloid progenitor self-renewal in chronic myeloid leukaemia cells, *British journal of haematology*, (129) 3, 377-380.
- Wolberg, A.S., Aleman, M.M., Leiderman, K. & Machlus, K.R. 2012, Procoagulant activity in hemostasis and thrombosis: Virchow's triad revisited, *Anesthesia and Analgesia*, (114) 2, 275-285.
- Wolfs, J.L., Wielders, S.J., Comfurius, P., Lindhout, T., Giddings, J.C., Zwaal, R.F. & Bevers, E.M. 2006, Reversible inhibition of the platelet procoagulant response through manipulation of the Gardos channel, *Blood*, (108) 7, 2223-2228.
- World Health Organization 2014, , *The top 10 causes of death* [Homepage of World Health Organisation], [Online]. Available: <http://www.who.int/mediacentre/factsheets/fs310/en/>.
- Wright, J.R., Amisten, S., Goodall, A.H. & Mahaut-Smith, M.P. 2016, Transcriptomic analysis of the ion channelome of human platelets and megakaryocytic cell lines, *Thrombosis and haemostasis*, (116) 2.
- Yap, C.L., Anderson, K.E., Hughan, S.C., Dopheide, S.M., Salem, H.H. & Jackson, S.P. 2002, Essential role for phosphoinositide 3-kinase in shear-dependent signaling between platelet glycoprotein Ib/V/IX and integrin alpha(IIb)beta(3), *Blood*, (99) 1, 151-158.

-
- Yasuda, N., Miura, S., Akazawa, H., Tanaka, T., Qin, Y., Kiya, Y., Imaizumi, S., Fujino, M., Ito, K., Zou, Y., Fukuhara, S., Kunimoto, S., Fukuzaki, K., Sato, T., Ge, J., Mochizuki, N., Nakaya, H., Saku, K. & Komuro, I. 2008, Conformational switch of angiotensin II type 1 receptor underlying mechanical stress-induced activation, *EMBO reports*, (9) 2, 179-186.
- Zarychanski, R., Schulz, V.P., Houston, B.L., Maksimova, Y., Houston, D.S., Smith, B., Rinehart, J. & Gallagher, P.G. 2012, Mutations in the mechanotransduction protein PIEZO1 are associated with hereditary xerocytosis, *Blood*, (120) 9, 1908-1915.
- Zhi, H., Rauova, L., Hayes, V., Gao, C., Boylan, B., Newman, D.K., McKenzie, S.E., Cooley, B.C., Poncz, M. & Newman, P.J. 2013, Cooperative integrin/ITAM signaling in platelets enhances thrombus formation *in vitro* and *in vivo*, *Blood*, (121) 10, 1858-1867.
- Zou, Y., Akazawa, H., Qin, Y., Sano, M., Takano, H., Minamino, T., Makita, N., Iwanaga, K., Zhu, W., Kudoh, S., Toko, H., Tamura, K., Kihara, M., Nagai, T., Fukamizu, A., Umemura, S., Iiri, T., Fujita, T. & Komuro, I. 2004, Mechanical stress activates angiotensin II type 1 receptor without the involvement of angiotensin II, *Nature cell biology*, (6) 6, 499-506.